2003

Chemical coupling in wood-polymer composites

Ziqiang Lu
Louisiana State University and Agricultural and Mechanical College

CHEMICAL COUPLING IN WOOD-POLYMER COMPOSITES

A Dissertation

Submitted to the Graduate Faculty of the
Louisiana State University and
Agricultural and Mechanical College
in partial fulfillment of the
requirements for the degree of
Doctor in Philosophy

in

The School of Renewable Natural Resources

by
Ziqiang Lu
B.S., Nanjing Forestry University, 1983
M.S., Nanjing Forestry University, 1991
M.S., Iowa State University, 1997
December 2003

COPYRIGHT

ACKNOWLEDGEMENTS

I cordially appreciate my major professor, Dr. Qinglin Wu for his support, advice, and guidance for my PhD program. I greatly appreciate my committee members, Dr. William H. Daly, Dr. Ioan I. Negulescu, Dr. W. Ramsay Smith, Dr. Richard P. Vlosky, and Dr. Jonathan Y. Chen for their support and encouragement. A special thank you goes to Dr. Negulescu for all his advice during my dissertation Research. I also thank my former committee member, Dr. Timothy G. Rials, for his involvement in my PhD program. He moved out of Louisiana in 2001. Without their strong support and guidance, I would have not completed my PhD program.

I am grateful to my former major advisor, Dr. Harold S. McNabb, Jr., for his support before and after I transferred from Iowa State University to Louisiana State University. I want to thank Dr. Zhiyong Cai and the Temple Inland Company for offering wood fibers for my research. I am grateful to Mr. Travis J. Keener at the Eastman Chemical Company and Mrs. Jeri Pryla at the DuPont Canada Company for supplying a series of maleated polyethylene and polypropylene coupling agents.

I sincerely thank Dr. Cornelis DeHoop, Dr. Paul Y. Burns, Dr. Todd F. Shupe, Mrs. Pat Lefeaux, and Mrs. Joann Doucet in the School of Renewable Natural Resources for their support. I am grateful to Dr. Jiechao Jiang in the Department of Mechanical Engineering for his assistance on ESCA analysis. My appreciation is also expressed to Ms. Yin Xiao in the Department of Biological Sciences for her help in microscopy analysis.

I want to thank Mr. and Mrs. Ray and Sam Morris for their friendship and fellowship. They brought God's light and love to my family and myself and led me to a truly new life. I was baptized on March 1, 2002. Thank you, Ray and Sam. Thank you, my Lord! I also express my thanks to my host family Mr. and Mrs. Mark and Kim Johnson for their friendship and encouragement.

This dissertation is dedicated to my mother, Qiongzhen Cui and my father in heaven, Binwen Lu. Mom has been struggling from paralysis caused by cerebral hemorrhage since 1997 and then her thighbone of the left leg was unfortunately broken in 1999. Although she suffered great pain every day, she has continuously encouraged me to make great progress in my research and study. Mom, I am proud of you. I wish this dissertation were a releasing agent to make you feel more comfortable.

I am deeply indebted to my wife, Haiyun Hu, for her love, understanding, and encouragement. Thank you, my love. I greatly appreciate my elder sister and sister-in-law for their support and encouragement. I also appreciate my mother and father-in-law, my brothers, young sister, and sister-in-law for their love.

TABLE OF CONTENTS

LIST OF TABLES

LIST OF FIGURES

NOMENCLATURE

AA	acetic anhydride
AACA	2-diallylamino 4,6-dichloro-s-triazine
ABAC	abietic acid
AN	acrylonitrile
ANOVA	analysis of variance
ASA	alkyl succinic anhydride
BA	butyl acrylate
BaAc	barium acetate
BMI (or PDM)	N,N'-*m*-phenylene bismaleicimide
BO	butylene oxide
BPO	benzoyl peroxide
BPP	N,N'-*m*-phenylene bismaleicimide modified polypropylene
^{60}Co	Colbat-60 gamma radiation
CRD	completely randomized design
CTMP	chemithermomechanical pulp
DCA	dynamic contact angle analysis
DCP	dicumyl peroxide
DDSC	derivative differential scanning calorimetry
DMA	dynamic mechanical analysis
DMM	mono- and dimehtylolmelamine resin
DOP	dioctyl phthalate
DR	decay ratio
DR_h	decay ratio in height
DSC	differential scanning calorimetry
DSTP	distearyl thiodipropionate
DTBPO	di-*tert*-butyl peroxide
DTG	derivative thermogravimetric analysis
E′	storage modulus
E″	loss modulus
E*	complex modulus
EIC	ethyl isocyanate
EPMA	epoxylpropyl methacrylate
Epolene E-43 (or 47L)	maleated polypropylene with low-molecular weight (M_W=10,000)
E/VAC	ethyl/vinyl acetate
ESCA	electron spectroscopy for chemical analysis
FTIR	Fourier transform infrared analysis
GMA	glycidyl methacrylate
GMS	mono- and diglycerides of fatty acids
13H	maleated polypropylene with high-molecular weight (M_W=31,900)
63H	maleated polypropylene with high-molecular weight (M_W=40,000)

HDPE	high-density polyethelene
HEMA	hydroxyethyl methacrylate
Hercoprime G	maleated polypropylene with high-molecular weight (M_W=39,000)
HMDIC	hexamethylene diisocyanate
Ionol	a butylated hydroxy toluene
Irganox-1010	a tertiary butyl hydroxyhydrocinnamate
K_θ	material constant related to contact angle
K_{hR}	material constant related to decay ratio in height
$K_{\phi R}$	material constant related to spreading ratio in base-diameter
KR 138S	titanium di(dioctylpyrophosphate)oxyacetate
15L	maleated polypropylene with low-molecular weight (M_W=14,600)
47L	maleated polypropylene with low-molecular weight (M_W=10,000)
LAC	linoleic acid
LDPE	low-density polyethylene
LLDPE	linear low-density polyethylene
LPO	lauroyl peroxide
MA	maleic anhydride
MAA	methacrylic acid
MAA-CAAPE	methacrylic acid, 3-((4,6-dichloro-*s*-triazine-2-yl)amino)propyl ester
MAPE	maleated polyethylene (or maleic anhydride-modified-polyethylene)
MAPP	maleated polypropylene (or maleic anhydride-modified-polypropylene)
MC	moisture content
MDSC	modulated differential scanning calorimetry
MMA	methyl methacrylate
M_n	number average molar mass
M_W	average molecular weight (or weight average molar mass)
OACA	2-octylamino 4,6-dichloro-*s*-triazine
PDM	see BMI
PE	polyethylene
PEMA	poly(ethylene-maleic anhydride)
PEPPIC	poly[ethylene(polyphenyl isocyanate)]
PF	phenol-formaldehyde resin
PHA	phthalic anhydride
PMAA	polymethacrylic acid
PMPPIC	poly[methylene(polyphenyl isocyanate)]
PO	propylene oxide
PP	polypropylene
PS	polystyrene
PS201	high-heat crystal polystyrene

PS525	high-impact polystyrene
PS685D	general-purpose and high-heat polystyrene
PS-PMAA	polystyrene/polymethacrylic acid
PVAC	polyvinyl acetate
PVC	polyvinyl chloride
RGP	refiner ground pulp
RT	room temperature
SA	succinic anhydride
SEBS	styrene-ethylene-butylene-styrene copolymer
SEBS-MA	styrene-ethylene-butylene-styrene/maleic anhydride
SEM	scanning electron microscopy
Silane A-172	vinyltri(2-methoxyethoxy) silane
Silane A-174	γ-methacryloxypropyltrimethoxy silane
Silane A-186	β-(3,4-epoxy cyclohexyl)ethyltrimethoxy silane
Silane A-187	γ-glycidoxy propyltrimethoxy silane
Silane A-1100	γ-aminopropyltriethoxy silane
SMA	styrene/maleic anhydride
SR	spreading ratio
SR_ϕ	spreading ratio in base-diameter
tanδ	a ratio of the loss modulus to the storage modulus
TBPB	*tert*-butyl peroxy benzonate
TDIC	toluene 2,4-diisocyanate
T_g	glass transition
TGA	thermogravimetric analysis
T_m	melting temperature
TMP	thermomechnical pulp
Vazo	2,2'-azobisisobyturonitrile
WF	wood flour
WFPC	wood fiber and polymer composites
WPC	wood-polymer composites
WS	wetting slope
WS_{hR}	wetting slope of decay ratio in height
$WS_{\phi R}$	wetting slope of spreading ratio in base-diameter
WS_θ	wetting slope of contact angle

ABSTRACT

Chemical coupling plays an important role in improving interfacial bonding strength in wood-polymer composites. In this study, the effects of coupling agent type and structure, graft polymerization of coupling agents, interfacial wettability, coupling treatment and process, coupling agent distribution, and coupling agent performance on chemical coupling were investigated. Coupling mechanisms were established based on maleated polyethylene copolymers.

For maleated wood veneer, the relationship among graft rate, concentration, and retention of coupling agent followed three-dimensional *parabloid* models. Wettability of maleated wood surface was related to acid number, amount of free or ungrafted maleic anhydride groups, and coupling agent concentration. Dynamic contact angle of water droplets on maleated wood followed the natural decay process, whereas the spreading process of droplets fitted the *Boltzmann* sigmoid model. Compared with untreated composites, maleated composites had significant shifts in most TGA, DSC, and DMA spectra because of chemical coupling at the interface. For melt-blending process, the best interfacial bonding strength was achieved at short compounding time (e.g., 10 min), appropriate mixing temperature (e.g., 180^{o}C), and moderate rotation speed (e.g., 90 rpm). With FTIR, ESCA, and SEM analyses, the evidence of chemical bridges at the interface was proved. The interfacial morphology was illustrated with the *pinwheel* models. For wood-plastic laminates, interfacial adhesion followed the *monolayer* models, while *brush*, *switch*, and *amorphous* structures applied to melt-blended composites. Therefore, the interface was strengthened with covalent bonding (such as esterification and carbon-carbon bonding), strong secondary bonding (e.g., hydrogen bonding), macromolecular

chain entanglement, and mechanical interblocking. Coupling agent performance for maleated copolymers was mainly related to their acid number, molecular weight, backbone structure, and concentration. Coupling agents with large molecular weight, moderate acid number, and concentration were preferred to have better performance at the interface. Based on the experimental results, 226D, 100D, and C16 were the best coupling agents among seven maleated copolymers used in this study. Compared with untreated composites, maleated composites increased interfacial bonding strength by 140% and flexural modulus by 29% at the concentration level of 3%.

CHEMICAL COUPLING IN WOOD-POLYMER COMPOSITES

A Dissertation

Submitted to the Graduate Faculty of the
Louisiana State University and
Agricultural and Mechanical College
in partial fulfillment of the
requirements for the degree of
Doctor in Philosophy

in

The School of Renewable Natural Resources

by
Ziqiang Lu
B.S., Nanjing Forestry University, 1983
M.S., Nanjing Forestry University, 1991
M.S., Iowa State University, 1997
December 2003

COPYRIGHT

ACKNOWLEDGEMENTS

I cordially appreciate my major professor, Dr. Qinglin Wu for his support, advice, and guidance for my PhD program. I greatly appreciate my committee members, Dr. William H. Daly, Dr. Ioan I. Negulescu, Dr. W. Ramsay Smith, Dr. Richard P. Vlosky, and Dr. Jonathan Y. Chen for their support and encouragement. A special thank you goes to Dr. Negulescu for all his advice during my dissertation Research. I also thank my former committee member, Dr. Timothy G. Rials, for his involvement in my PhD program. He moved out of Louisiana in 2001. Without their strong support and guidance, I would have not completed my PhD program.

I am grateful to my former major advisor, Dr. Harold S. McNabb, Jr., for his support before and after I transferred from Iowa State University to Louisiana State University. I want to thank Dr. Zhiyong Cai and the Temple Inland Company for offering wood fibers for my research. I am grateful to Mr. Travis J. Keener at the Eastman Chemical Company and Mrs. Jeri Pryla at the DuPont Canada Company for supplying a series of maleated polyethylene and polypropylene coupling agents.

I sincerely thank Dr. Cornelis DeHoop, Dr. Paul Y. Burns, Dr. Todd F. Shupe, Mrs. Pat Lefeaux, and Mrs. Joann Doucet in the School of Renewable Natural Resources for their support. I am grateful to Dr. Jiechao Jiang in the Department of Mechanical Engineering for his assistance on ESCA analysis. My appreciation is also expressed to Ms. Yin Xiao in the Department of Biological Sciences for her help in microscopy analysis.

I want to thank Mr. and Mrs. Ray and Sam Morris for their friendship and fellowship. They brought God's light and love to my family and myself and led me to a truly new life. I was baptized on March 1, 2002. Thank you, Ray and Sam. Thank you, my Lord! I also express my thanks to my host family Mr. and Mrs. Mark and Kim Johnson for their friendship and encouragement.

This dissertation is dedicated to my mother, Qiongzhen Cui and my father in heaven, Binwen Lu. Mom has been struggling from paralysis caused by cerebral hemorrhage since 1997 and then her thighbone of the left leg was unfortunately broken in 1999. Although she suffered great pain every day, she has continuously encouraged me to make great progress in my research and study. Mom, I am proud of you. I wish this dissertation were a releasing agent to make you feel more comfortable.

I am deeply indebted to my wife, Haiyun Hu, for her love, understanding, and encouragement. Thank you, my love. I greatly appreciate my elder sister and sister-in-law for their support and encouragement. I also appreciate my mother and father-in-law, my brothers, young sister, and sister-in-law for their love.

TABLE OF CONTENTS

LIST OF TABLES

LIST OF FIGURES

NOMENCLATURE

AA	acetic anhydride
AACA	2-diallylamino 4,6-dichloro-s-triazine
ABAC	abietic acid
AN	acrylonitrile
ANOVA	analysis of variance
ASA	alkyl succinic anhydride
BA	butyl acrylate
BaAc	barium acetate
BMI (or PDM)	N,N'-*m*-phenylene bismaleicimide
BO	butylene oxide
BPO	benzoyl peroxide
BPP	N,N'-*m*-phenylene bismaleicimide modified polypropylene
^{60}Co	Colbat-60 gamma radiation
CRD	completely randomized design
CTMP	chemithermomechanical pulp
DCA	dynamic contact angle analysis
DCP	dicumyl peroxide
DDSC	derivative differential scanning calorimetry
DMA	dynamic mechanical analysis
DMM	mono- and dimehtylolmelamine resin
DOP	dioctyl phthalate
DR	decay ratio
DR_h	decay ratio in height
DSC	differential scanning calorimetry
DSTP	distearyl thiodipropionate
DTBPO	di-*tert*-butyl peroxide
DTG	derivative thermogravimetric analysis
E′	storage modulus
E″	loss modulus
E*	complex modulus
EIC	ethyl isocyanate
EPMA	epoxylpropyl methacrylate
Epolene E-43 (or 47L)	maleated polypropylene with low-molecular weight (M_W=10,000)
E/VAC	ethyl/vinyl acetate
ESCA	electron spectroscopy for chemical analysis
FTIR	Fourier transform infrared analysis
GMA	glycidyl methacrylate
GMS	mono- and diglycerides of fatty acids
13H	maleated polypropylene with high-molecular weight (M_W=31,900)
63H	maleated polypropylene with high-molecular weight (M_W=40,000)

HDPE	high-density polyethelene
HEMA	hydroxyethyl methacrylate
Hercoprime G	maleated polypropylene with high-molecular weight (M_W=39,000)
HMDIC	hexamethylene diisocyanate
Ionol	a butylated hydroxy toluene
Irganox-1010	a tertiary butyl hydroxyhydrocinnamate
K_θ	material constant related to contact angle
K_{hR}	material constant related to decay ratio in height
$K_{\phi R}$	material constant related to spreading ratio in base-diameter
KR 138S	titanium di(dioctylpyrophosphate)oxyacetate
15L	maleated polypropylene with low-molecular weight (M_W=14,600)
47L	maleated polypropylene with low-molecular weight (M_W=10,000)
LAC	linoleic acid
LDPE	low-density polyethylene
LLDPE	linear low-density polyethylene
LPO	lauroyl peroxide
MA	maleic anhydride
MAA	methacrylic acid
MAA-CAAPE	methacrylic acid, 3-((4,6-dichloro-*s*-triazine-2-yl)amino)propyl ester
MAPE	maleated polyethylene (or maleic anhydride-modified-polyethylene)
MAPP	maleated polypropylene (or maleic anhydride-modified-polypropylene)
MC	moisture content
MDSC	modulated differential scanning calorimetry
MMA	methyl methacrylate
M_n	number average molar mass
M_W	average molecular weight (or weight average molar mass)
OACA	2-octylamino 4,6-dichloro-*s*-triazine
PDM	see BMI
PE	polyethylene
PEMA	poly(ethylene-maleic anhydride)
PEPPIC	poly[ethylene(polyphenyl isocyanate)]
PF	phenol-formaldehyde resin
PHA	phthalic anhydride
PMAA	polymethacrylic acid
PMPPIC	poly[methylene(polyphenyl isocyanate)]
PO	propylene oxide
PP	polypropylene
PS	polystyrene
PS201	high-heat crystal polystyrene

PS525	high-impact polystyrene
PS685D	general-purpose and high-heat polystyrene
PS-PMAA	polystyrene/polymethacrylic acid
PVAC	polyvinyl acetate
PVC	polyvinyl chloride
RGP	refiner ground pulp
RT	room temperature
SA	succinic anhydride
SEBS	styrene-ethylene-butylene-styrene copolymer
SEBS-MA	styrene-ethylene-butylene-styrene/maleic anhydride
SEM	scanning electron microscopy
Silane A-172	vinyltri(2-methoxyethoxy) silane
Silane A-174	γ-methacryloxypropyltrimethoxy silane
Silane A-186	β-(3,4-epoxy cyclohexyl)ethyltrimethoxy silane
Silane A-187	γ-glycidoxy propyltrimethoxy silane
Silane A-1100	γ-aminopropyltriethoxy silane
SMA	styrene/maleic anhydride
SR	spreading ratio
SR_ϕ	spreading ratio in base-diameter
tanδ	a ratio of the loss modulus to the storage modulus
TBPB	*tert*-butyl peroxy benzonate
TDIC	toluene 2,4-diisocyanate
T_g	glass transition
TGA	thermogravimetric analysis
T_m	melting temperature
TMP	thermomechnical pulp
Vazo	2,2'-azobisisobyturonitrile
WF	wood flour
WFPC	wood fiber and polymer composites
WPC	wood-polymer composites
WS	wetting slope
WS_{hR}	wetting slope of decay ratio in height
$WS_{\phi R}$	wetting slope of spreading ratio in base-diameter
WS_θ	wetting slope of contact angle

ABSTRACT

Chemical coupling plays an important role in improving interfacial bonding strength in wood-polymer composites. In this study, the effects of coupling agent type and structure, graft polymerization of coupling agents, interfacial wettability, coupling treatment and process, coupling agent distribution, and coupling agent performance on chemical coupling were investigated. Coupling mechanisms were established based on maleated polyethylene copolymers.

For maleated wood veneer, the relationship among graft rate, concentration, and retention of coupling agent followed three-dimensional *parabloid* models. Wettability of maleated wood surface was related to acid number, amount of free or ungrafted maleic anhydride groups, and coupling agent concentration. Dynamic contact angle of water droplets on maleated wood followed the natural decay process, whereas the spreading process of droplets fitted the *Boltzmann* sigmoid model. Compared with untreated composites, maleated composites had significant shifts in most TGA, DSC, and DMA spectra because of chemical coupling at the interface. For melt-blending process, the best interfacial bonding strength was achieved at short compounding time (e.g., 10 min), appropriate mixing temperature (e.g., 180^{o}C), and moderate rotation speed (e.g., 90 rpm). With FTIR, ESCA, and SEM analyses, the evidence of chemical bridges at the interface was proved. The interfacial morphology was illustrated with the *pinwheel* models. For wood-plastic laminates, interfacial adhesion followed the *monolayer* models, while *brush*, *switch*, and *amorphous* structures applied to melt-blended composites. Therefore, the interface was strengthened with covalent bonding (such as esterification and carbon-carbon bonding), strong secondary bonding (e.g., hydrogen bonding), macromolecular

chain entanglement, and mechanical interblocking. Coupling agent performance for maleated copolymers was mainly related to their acid number, molecular weight, backbone structure, and concentration. Coupling agents with large molecular weight, moderate acid number, and concentration were preferred to have better performance at the interface. Based on the experimental results, 226D, 100D, and C16 were the best coupling agents among seven maleated copolymers used in this study. Compared with untreated composites, maleated composites increased interfacial bonding strength by 140% and flexural modulus by 29% at the concentration level of 3%.

CHAPTER 1. INTRODUCTION

Synthetic polymers (or macromolecules) have a tremendous impact on our life today. “We wear these man-made materials, eat and drink from them, sleep between them, sit and stand on them; turn knobs, pull switches, and grasp handles made of them; with their help we heard sounds and see sights remote from us in time and space; we live in houses and move about in vehicles that are increasingly made of them” (Morrison and Boyd 1992).

Since the invention of polyolefin polymerization with Ziegler-Natta catalysis in 1950s (Ziegler et al. 1955a, 1955b; Natta et al. 1955), thermoplastics products have been inevitable in our everyday life. According to the statistics by American Plastic Council (C&EN 2002), the annual output of plastics in the United States was 32.5 million tons in 2000. Thermoplastic polymers were 32.2 million tons. Among plastics, the “big four plastic products” [polyethylene (PE), polypropylene (PP), polyvinyl chloride (PVC), and polystyrene (PS)] were 30.2 million tons, accounted for over 92% by volume of the whole plastics consumption in the United States. The amount of plastics annually consumed in the United States is around 100 kilograms per person (Chenier 1992).

However, thermoplastics also bring a serious problem to the environment after service because of its decomposition difficulty under natural conditions. Accordingly, thermoplastic wastes cause serious environmental pollution nationally every year. Since the late 1980s, public concern and government administration regulations have accelerated industrial recycling of thermoplastic wastes (Thompson Publishing Group 2001; California Dept of Conversation; Selke 2002). According to the statistical data

(EPA 2000), recycled thermoplastics increased to about 50 million tons, which was 10% percent of municipal solid waste in the United States. Recycled thermoplastics, however, accounted for only one fifth of thermoplastic wastes generated in the United States (EPA 2000).

As early as in the 1950s, Immergut and Mark (1956), Gaylord (1957), Bridgeford (1963), and other pioneers tried to combine thermoplastics with wood materials. Initial efforts were made to improve dimensional stability and moisture resistance of solid wood products by graft copolymerization of vinyl monomers onto wood cell. The research led to a number of publications (Karpov et al. 1960; Schwab et al. 1961; Siau et al. 1965; Siau and Meyer 1966; Ogiwara et al. 1968; Beall and Witt 1972; Rowell et al. 1976; Rowell et al. 1978; Meyer 1981, 1982, 1984).

Compared with reinforced thermoplastic products, wood-polymer composites (WPC) have many advantages such as high specific strength and modulus, low cost, low density, and low friction during compounding (Lightsey 1981; Klason et al. 1984; Zadorecki and Michell 1989; Rievld and Simon 1992). Unlike wood composites, wood-polymer composites have excellent dimensional stability under moisture exposure (Klason et al. 1984; Maldas and Kokta 1991) and better fungi and termite resistance (Mankowski and Morrell 2000; Verhey et al. 2001). For wood-polymer composites, one of the most attractive features is that it can help recycle thermoplastic and wood wastes. Therefore, wood-polymer composites have developed quickly in the last two decades (Youngquist 1995). However, polar wood fiber and non-polar thermoplastics are not compatible, thus poor adhesion at the interface can result (Gaylord 1972; Coran and Patel 1982; Geottler 1983).

1.1 AREA OF CONCERN

WPC has been extensively investigated from chemical modification and treatment of wood and thermoplastics to production technologies and applications for various types of WPC (Ham and Coran 1978; Meyer 1981, 1982; Rowell and Konkol 1987; Schneider 1994; Gauthier et al. 1998). Chemical coupling is one of the most important topics in WPC (Xanthos 1983; Klason et al. 1984). Although a number of researches on chemical coupling in WPC have been published since the 1980s (Woodhams et al. 1984; Dalväg et al. 1985), chemical coupling mechanisms are not completely understood.

The most important issues in chemical coupling include **1)** coupling agent absorption and fixation mechanisms, **2)** optimum compounding conditions, **3)** characteristics of melt-blending conditions, **4)** characterization of interface and coupling agent distribution, **5)** interfacial bonding mechanisms and coupling agent performance, **6)** searching for new coupling agents with high graft efficiency, and **7)** multifunction and durability of coupling agent-treated wood-polymer composites.

A number of research topics are focused on coupling agent performance in WPC. Kokta and co-workers reported that coupling agents improve interfacial bonding at low concentration, but they were detrimental to graft copolymerization and interfacial bonding strength at high concentration (Maldas et al. 1989; Maldas and Kokta 1991). However, the relationship among coupling agent concentration, graft rate, and graft efficiency has not been well understood.

Compatibility between polar wood fiber and non-polar thermoplastics is a key to improve the interfacial adhesion in the resultant composites (Zadorecki and Michell 1989). However, the relationship among wettabilty, compatibility, and interfacial

bonding strength has not been completely investigated. It is also not well known whether molecular structure and concentration of coupling agents influence compatibility and wettabilty at the interface.

Most investigations on compounding conditions and coupling agent performance were based on trial and error (Xanthos 1983; Maldas et al. 1989; Rietveld and Simon 1992). Optimum compounding conditions and coupling agent performance were usually determined with average means. The main and the interaction effects of these factors have not been fully understood.

Since it is hard to separate individual wood fibers from the matrix (Liu et al. 1994), characterization of treated wood fiber at the interface presents significant technical difficulty. So far, there have been few reports on wettability of wood fiber at the interface. The bulk of thermoplastics matrix in WPC causes difficulty in thermal and chemical analysis of interface because most signals from treated wood fiber are blocked due to wrapping and coverage by thermoplastics. For melt-blended WPC, most publications on surface and interfacial characterization were focused on modified wood fibers (Filex and Gatenholm 1991), which are different from actual fibers at the interface.

Therefore, fundamental research is still needed to further advance our understanding of chemical coupling. The objective of this study is to elaborate chemical coupling in WPC through coupling treatments, compounding process, and manufacture. In particular, surface and interfacial characterizations of chemical coupling (such as graft copolymerization, thermal analysis, dynamic wettability, and coupling agent distribution) were explored to help better understand chemical coupling concepts, functions, mechanisms, and its applications in WPC.

1.2 ORGANIZATION OF DISSERTATION

Chemical coupling is the quintessence of this dissertation. This dissertation is divided into the following seven chapters. Chapter 1 (this chapter) provides an overall introduction for the study.

Chapter 2 provides a comprehensive review on coupling agents, pretreatment, and mixing technology for wood fiber and polymer currently used in the manufacture of wood fiber-polymer composites (WFPC).

In Chapter 3, the influence of maleation on polymer adsorption and graft polymerization, surface wettability of maleated wood specimens, and interfacial bonding strength of wood-PVC composites is presented.

Chapter 4 focuses on dynamic and static contact angles and wetting behavior in wood-PVC composites. Two wetting models are discussed for dynamic wetting processes. With these models, contact angle, decay ratio, and spreading ratio are analyzed to describe kinetics of wetting for wood veneer specimens treated with three maleic anhydride-containing coupling agents.

Chapter 5 deals with the influence of maleation on thermal and dynamic mechanical properties of wood-PVC composites. Thermal behaviors of modified wood veneer and the interface are discussed.

Chapter 6 presents the results on the influence of a series of maleated polyethylene polymers (MAPE) on mechanical properties of wood fiber-HDPE composites. Compounding characterizations of wood fiber and HDPE blends, coupling performance of these agents, and distribution of coupling agent at the interface are

discussed. These MAPEs are also compared with maleated polypropylene (MAPP) on coupling performance.

Finally, Chapter 7 provides overall conclusions and recommendations.

1.3 SIGNIFICANCE OF THE STUDY

This dissertation is a systematic study on chemical coupling in WPC. It details the basics of chemical coupling in WPC and brings a new insight to this field. Chemical coupling in WPC is highlighted from wood science, chemistry, physicochemistry, to plastic engineering. Several models are proposed to help better understand coupling action and mechanisms.

By reviewing the worldwide literature on chemical coupling in WPC in the last two decades, coupling agents and treatments are first time systematically classified in this study. This state-of-the art review provides a broad view of chemical coupling conceptions and applications in WPC.

In this dissertation, many fundamental approaches are made to investigate surface and interfacial characterization related to chemical coupling in WPC (e.g., graft polymerization, graft rate and efficiency, dynamic wettability, thermal and dynamic mechanical properties, and coupling agent performance). Graft copolymerization and graft efficiency of coupling agents are first time quantified. The three-dimensional relationship among coupling agent concentration, retention, graft rate, and efficiency is explored and modeled.

In this study, dynamic wettability of the interface is simulated through maleated veneer with heat treatment and fracture surfaces of wood-polymer laminates. Dynamic wetting process and dynamic contact angle are illustrated with dimensional ratios, which

help visually elaborate dynamic wetting process. Wetting models related to contact angle and profile dimensional changes are proposed. This method helps compare dynamic wettability of wood surfaces and wood-polymer interface treated with different coupling agents and better understand their wetting behaviors with kinetics of wetting.

With combination of advanced analytical devices (such as FTIR, ESCA, and SEM), interfacial characterization of maleated WPC is investigated. A preliminary approach to the location of coupling agent at the interface is conducted and several models are proposed to illustrate coupling agent distribution in WPC.

Based on the interfacial similarity rule, new coupling agents suitable for wood fiber-polyethylene composites are investigated, and best coupling agents are screened and identified from several maleated copolymers through tensile/shear test, dynamic mechanical analysis, and SEM analysis. As a result, a new evaluation system for coupling agents is built up to help distinguish different coupling agents and select the best coupling agents with these techniques.

In this dissertation, several statistical methods are effectively applied in experimental design and data analysis for graft copolymerization, compounding process, coupling agent performance, and coupling agent screening. Main and interaction effects of factors related to graft copolymerization, compounding process, and coupling agent performance are established.

1.4 REFERENCES

Anonymous. 2001. Environmental packaging: U.S. guide to green labeling, packaging, and recycling. Thompson Publishing Group, Washington, D.C.

Anonymous. 2002. Facts and figures for the chemical industry. C&EN 80(25): 42-82.

Beall, F. C., and A. E. Witt. 1972. Polymerization of methyl methacrylate by heat-catalyst and Gamma-irradiation methods. Wood and Fiber 4(3): 179-184.

Bridgeford, D. J. 1963. US Patent 3,083,118.

California Department of Conversation. http://www.consrv.ca.gov.

Chenier, P. J. 1992. Survey of industrial chemistry. Wiley-VCH, Inc., New York, 527 pp.

Coran, A. Y., and R. Patel. 1982. US Patent 4,323,625.

Dalväg, H., C. Klason, and H. –E. Strömvall. 1985. The efficiency of cellulosic fillers in common thermoplastics. Part II. Filling with processing aids and coupling agents. Intern. J. Polymeric Mater. 11: 9-38.

Environmental Protection Agency. 2000. Environmental fact sheet: Municipal solid waste generation, recycling, and disposal in the United States: Facts and figures for 1998, EPA530-F-00-024.

Filex, J. M., and P. Gatenholm. 1991. The nature of adhesion in composites of modified cellulose fibers and polypropylene. J. Appl. Polym. Sci. 42: 609-620.

Gauthier, R., C. Joy, A.C. Coupas, H. Gauthier, and M. Escoubes. 1998. Interfaces in polyolefin/cellulosic fiber composites: Chemical coupling, morphology, correlation with adhesion and aging in moisture. Polym. Comp. 19(3): 287-300.

Gaylord, N. 1956/1957. Interchem. Review 15: 91.

Gaylord, N. G. 1972. US Patent 3,645,939.

Geottler, L. A. 1983. US Patent 4,376,144.

Hamed, P., and A. Y. Coran. 1978. Reinforcement of polymers through short cellulose fibers. Pages 29-50 *in* R. B. Seymour, ed. Additives for plastics, vol. 1. State of the art. Academic Press, New York, NY.

Immergut, E. H., and H. Mark. 1956. Graft and block copolymer by synthetic and natural macromolecules. Makromol. Chem. 18/19: 322-341.

Klason, C., J. Kubát, and H. –E. Strömer. 1984. The efficiency of cellulosic fillers in common thermoplastics, Part I. Filling without processing aids or coupling agents. Int. Polym. Mater. 10: 159-187.

Karpov, V. L., Y. M. Malinsky, V. I. Serenkov, R. S. Klimanova, and A. S. Freidin. 1960. Radiation makes better wood and copolymers. Necleonics 18(3): 88-90.

Lightsey, G. R. 1981. Polymer Sci. Technol. 17: 193.

Liu, F. P., M. P. Wolcott, D. J. Gardner, and T. G. Rials. 1994. Characterization of the interface between cellulosic fibers and a thermoplastic matrix. Comp. Interfaces 2(6): 419-432.

Maldas, D., and B. V. Kokta. 1991. Surface modification of wood fibers using maleic anhydride and isocyanate as coating components and their performance in polystyrene composites. J. Adhesive Sci. Tech. 5(9): 727-740.

Maldas, D., B. V. Kokta, C. Danuealt. 1989. Influence of coupling agents and treatments on the mechanical properties of cellulose fiber-polystyrene composites. J. Appl. Polym. Sci. 37: 751-775.

Mankowski, M., and J. J. Morrell. 2000. Patterns of fungal attack in wood-plastic composites following exposure in a soil block test. Wood Fiber Sci. 32(3): 340-345.

Meyer, J. A. 1981. Wood-polymer materials: State of the art. Wood Sci. 14(2): 49-54.

Meyer, J. A. 1982. Industrial use of wood polymer materials: State of the art. Forest Prod. J. 32(1): 24-29.

Meyer, J. A. 1984. Wood polymer materials. Pages 257-289 *in* R. M. Rowell, ed. The Chemistry of Solid Wood, ACS Advances in Chemistry Series 207. American Chemical Society, Washington, D.C.

Morrison, R. T., and R. N. Boyd. 1992. Organic Chemistry. Prentice Hall, Englewood Cliffs, New Jersey.

Natta, G., P. Pino, P. Corradini, F. Danusso, E. Mantica, G. Mazzanti, and G. Moraglio. 1955. Crystalline high polymers of α–olefins. J. Am. Chem. Soc. 77: 1708.

Ogiwara, Y., Y. Ogiwara, H. Kubota. 1968. Studies of the initiation mechanism of ferric ion-Hydrogen peroxide systems in graft copolymerization on cellulose. J. Appl. Polym. Sci. 12, 2575-2581.

Rietveld, J. X., and M. J. Simon. 1992. Processability and properties of wood flour filled polypropylene. Inter. J. Polymeric Mater. 18: 213-235.

Rowell, R. M., and W. D. Ellis. 1978. Determination of dimensional stability of wood using the water-soak method. Wood Fiber 10: 104-111.

Rowell R. M., and P. Konkol 1987. Treatments that enhance physical properties of wood. U.S. Forest Products Laboratory General Technical Report FPL-GTR-55. 12 pp.

Rowell, R. M., D. I. Gutzmer, I. B. Sachs, and R. E. Kinney. 1976. Effects of alkylene oxide treatments on dimensional stability of wood. Wood Sci. 9(1): 51-54.

Schneider, M. H. 1994. Wood polymer composites. Wood Fiber Sci. 26(1): 142-151.

Schwab, E., V. Stannet, and J. J. Hermans. 1961. Grafting onto cellulose and cellulose fibers. TAPPI 44(4): 251-256.

Selke, S. E. 2002. Plastics recycling. Pages 693-757 *in* C. A. Harper, ed. Handbook of plastics, elastomers, and composites. 4th ed. McGraw-Hill, New York.

Siau, J. F., and J. A. Meyer. 1966. Comparison of the properties of heat and radiation cured wood-polymer combinations. Forest Prod. J. 16(8): 47-56.

Siau, J. F., J. A. Meyer, and C. Skaar. 1965. A review of developments in dimensional stabilization of wood. Forest Prod. J. 15(4): 162-166.

Verhey, S., P. Laks, and D. Richter. 2001. Laboratory decay resistance of woodfiber/thermoplastic composites. Forest Prod. J. 51(9): 44-49.

Woodhams, R. T., G. Thomas, and D. K. Rodgers. 1984. Wood fibers as reinforcing fillers for polyolefins. Polym. Eng. Sci. 24(15): 1166-1171.

Xanthos, M. 1983. Processing conditions and coupling agent effects in polypropylene/wood flour composites. Plast. Rubber Process. Appl. 3(3): 223-228.

Youngquist, J. A. 1995. The marriage of wood and nonwood materials. Forest Prod. J. 45(10): 25-30.

Zadorecki, P., and A. J. Michell. 1989. Future prospects for wood cellulose as reinforcement in organic polymer composites. Polymer Composites. 10(2): 69-77.

Ziegler, K., E. Holzkamp, H. Brell, and H. Martin. 1955a. Polymerisation von athylen und anderen olefinen. Angew. Chemie 67 (16): 426.

Ziegler, K., E. Holzkamp, H. Brell, and H. Martin, 1955b. Das Mulheimer normaldruck-polyathylen-verfahren. Angew. Chemie 67 (19/20): 541-547.

CHAPTER 2. A REVIEW OF COUPLING AGENTS AND TREATMENTS*

2.1 INTRODUCTION

Wood fiber and polymer composites (WFPC) are normally produced by mixing wood fiber with polymer, or by adding wood fiber as filler in a polymer matrix, and pressing or molding under high pressure and temperature. Most polymers, especially thermoplastics, are non-polar (hydrophobic) substances, which are not compatible with polar (hydrophilic) wood fibers and, therefore, poor adhesion between polymer and wood fiber in WFPC can result (Geottler 1983; Klason et al. 1984). In order to improve the affinity and adhesion between wood fibers and thermoplastic matrices in production, chemical coupling agents have been employed (Chun and Woodhams 1984; Woodhams et al. 1984; Dalväg et al. 1985; Schneider and Brebner 1985). Coupling agents are substances that are used in small quantities to treat a surface so that bonding occurs between it and other surfaces, e.g., wood and thermoplastics (Pritchard 1998).

Generally, coupling agents comprise bonding agents and surfactants (surface-active agents), including compatibilizers and dispersing agents (Štepek and Daoust 1983; Radian Corporation 1987; Clint 1998). Bonding agents act as bridges that link wood fibers and thermoplastic polymers by one or more of the following mechanisms: covalent bonding, polymer chain entanglement, and strong secondary interactions as in the case of

*Reprinted in part with permission from *Wood Fiber and Science*, 2000, Vol. 32, No. 1, Pages 88-104; J. Z. Lu; Q. Wu; and H. S. McNabb, Jr.; Chemical Coupling in Wood Fiber and Polymer Composites: A Review of Coupling Agents and Treatments. Society of Wood Science and Technology State-of-the-Art-Review.

hydrogen bonding (Raj et al. 1988; Maldas et al. 1989a). Compatibilizers are used to provide compatibility between otherwise immiscible polymers through reduction of the interfacial tension (Pritchard 1998). Some compatibilizers, such as acetic anhydride and methyl isocyanate, are monofunctional reactants. They lower the surface energy of the fiber, and make it non-polar, more similar to the plastic matrix. Some bonding agents, such as maleated polypropylene (MAPP), maleated styrene-ethylene/butylene-styrene (SEBS-MA) and styrene-maleic anhydride (SMA), also act as compatibilizers in WFPC (Oksman and Lindberg 1998; Oksman et al. 1998; Simonsen et al. 1998). Dispersing agents reduce the interfacial energy at the wood fiber-matrix interface to help uniform dispersion of wood fiber in a polymer matrix without aggregation and thereby facilitate the formation of new interfaces (Rosen 1978; Porter 1994). For example, stearic acid and its metallic salts are used to improve the dispersibility of wood fibers in the matrix. In general, compatibilizers and dispersing agents do not form strong adhesion at the fiber-matrix interface (Štepek and Daoust 1983). Thus, a functional distinction between bonding agents, compatibilizers, and dispersing agents should be noticed. In this paper, however, all bonding agents and surfactants are lumped together as coupling agents for the purpose of the review.

With the development of coupling agents, a number of pretreatment (i.e. fiber coating and graft co-polymerization) and mixing processes for improving mechanical properties of WFPC have been introduced. For example, Youngquist and colleagues (Krzysik et al. 1990; Krzysik and Youngquist 1991) conducted successful experiments on the bonding of air-formed wood fiber-polypropylene composites using MAPP as a coupling agent. They developed an excellent coating method to spray the emulsified

Epolene E-43 on wood fiber before formation. As a result of these efforts, WFPC have been developed very rapidly during the last decade.

Several review articles on wood-polymer composites have been published (e.g., Hamed and Coran 1978; Meyer 1981, 1982, 1984; Rowell and Konkol 1987; Schneider 1994; Youngquist 1995). These reviews cover from chemical modification and treatment of wood and plastics to production technologies and applications for various types of wood-polymer composites. However, none of these reviews systematically dealt with coupling agents and treatments currently used in this field. The objective of this work is to provide a state-of-the-art review on coupling agents, pretreatment of wood fiber and polymer, and mixing technology for the manufacture of WFPC. The adhesion mechanism and coupling performance of various coupling agents will be discussed in future publications.

2.2 COUPLING AGENTS

2.2.1 Historical Account

Bridgeford (1963) invented a method to graft olefinically unsaturated monomers onto wood fiber with a catalyst system containing ferrous cations and hydrogen peroxide to modify the compatibility between wood fiber and thermoplastic polymer. This method was further developed by other researchers (Gulina et al. 1965; Faessinger and Conte 1967; Dimov and Pavlov 1969; Kokta and Valade 1972; Hornof et al. 1976). Meyer (1968) was possibly the first person who suggested using a coupling agent (which he called a crosslinking agent) to improve the mechanical properties of wood-polymer materials. Gaylord (1972) patented maleic anhydride (MA) as a coupling agent to

combine cellulose and polyethylene (PE) or polyvinyl chloride (PVC) in the presence of a free radical initiator.

However, little attention had been paid to the applications of coupling agents in WFPC until the 1980s. From 1980 to 1985, a series of patents was issued for the application of isocyanate and MA coupling agents in WFPC (Coran and Patel 1982; Geottler 1983; Nakamura et al. 1983; Woodhams 1984). Xanthos (1983) introduced γ-methacryloxypropyltrimethoxy-silane (A-174) and N,N′-*m*-phenylene dimaleimide (BMI or PDM) as coupling agents to improve the mechanical properties of wood flour and polypropylene composites. Some coupling agents, such as silane A-174 and propylene oxide (PO), were also applied in wood and plastic composites (WPC) to improve their dimensional stability (Rowell et al. 1976; Rowell and Ellis 1978; Schneider and Brebner 1985).

As pioneers in the applications of coupling agents in WFPC, Klason and coworkers made an initial study on using MA as the coupling agent in the cellulose flour and polypropylene (PP) composites (Dalväg et al. 1985). Woodhams et al. (1984) successfully introduced Epolene E-43, a kind of MAPP with low-molecular weight, as a coupling agent in thermomechanical pulp (TMP) and isotactic PP composites. These two articles have been the important references for the research on chemical coupling in WFPC.

The Kokta group in Canada made a number of investigations on isocyanate, alkoxysilane, and anhydride coupling agents. Through their efforts, poly[methylene (polyphenyl isocyanate)] (PMPPIC) has been successfully used as an important coupling agent in melt-blended composites. Kokta (1988) patented PMPPIC for cellulose fiber and

PE composites. In Japan, the Shiraishi group focused on the application of MAPP with high-molecular weight (Kishi et al. 1988; Han et al. 1989). In the United States and Sweden, much work has been done on the application of MAPP and other coupling agents in the melt-blending process, such as injection molding, extrusion, and transfer molding (Myers et al. 1990, 1991, 1993; Olsen 1991; Liang et al. 1994; Gatenholm et al. 1995).

2.2.2 Classification and Action of Coupling Agents

Over forty coupling agents have been used in WFPC (Table 2.1). Coupling agents are classified into organic, inorganic, and organic-inorganic groups. Organic agents include isocyanates, anhydrides, amides, imides, acrylates, chlorotriazines, epoxides, organic acids, monomers, polymers, and copolymers. Only a few inorganic coupling agents, such as silicates, are used in WFPC. Organic-inorganic agents include silanes and titanates.

Organic coupling agents in WFPC normally have bi- or multifunctional groups in their molecular structure. These functional groups, such as (-N=C=O) of isocyanates, [-$(CO)_2$ O-] of maleic anhydrides, and (-Cl-) of diclorotriazine derivatives, interact with the polar groups [mainly hydroxyl groups (-OH)] of cellulose and lignin to form covalent or hydrogen bonding (Zadorecki and Flodin 1985; Raj et al. 1988; Maldas et al. 1989a; Raj and Kokta 1991; Chtourou et al. 1992). Alternatively, organic coupling agents can modify the polymer matrix by graft copolymerization, thus resulting in strong adhesion, even crosslinking, at the interface.

Inorganic coupling agents possibly act as dispersing agents to counteract the surface polarity of wood fiber and improve the compatibility between wood fiber and

Table 2.1. Coupling agents used in WFPC.

Coupling Agent	Additive [a]	Reference
Organic agents		
1. Acrylates		
Glycidyl methacrylate (GMA)	TBPB	Takase and Shiraishi 1989
Hydroxyethyl methacrylate (HEMA)	TBPB	Takase and Shiraishi 1989
2. Amides and imides		
N,N′-*m*-Phenylene bismaleicimide (BMI)	DCP	Xanthos 1983; Sain and Kokta 1994
3. Anhydrides		
Acetic anhydride (AA)	–	Chtourou et al. 1992
Alkyl succinic anhydride (ASA)	–	Gatenholm et al. 1992, 1993
Succinic anhydride (SA)	BPO, pyridine	Rozman et al. 1994
Phthalic anhydride (PHA)	–	Maldas and Kokta 1989, 1990c
Maleic anhydride (MA)	BPO or TBPB	Maldas and Kokta 1990d, 1991a, b
4. Chlorotriazines and derivatives		
2-Diallylamino 4,6-dichloro-*s*-triazine (AACA)	BPO	Zadorecki and Flodin 1985
2-Octylamino 4,6-dichloro-*s*-triazine (OACA)	BPO	Zadorecki and Flodin 1985
Methacrylic acid,3-((4,6-dichloro-*s*-triazine-2-yl) amino)propyl ester (MAA-CAAPE)	BPO	Zadorecki and Flodin 1985
5. Epoxides		
Butylene oxide (BO)	–	Rowell et al. 1982
Propylene oxide (PO)	–	Rowell et al. 1982
6. Isocyanates		
Ethyl isocyanate (EIC)	–	Raj et al. 1988; Maldas and Kokta 1991b
Hexamethylene diisocyanate (HMDIC)	–	Raj et al. 1988; Maldas and Kokta 1991b; Gatenholm et al. 1992
Poly[ehtylene(polyphenyl isocayanate)] (PEPPIC)	–	Selke et al. 1990
Poly[methylene(polyphenyl isocyanate)] (PMPPIC)	DCP	Maldas et al. 1989a, b; Maldas and Kokta 1989, 1990a, b, 1991a; Raj et al. 1988
Toluene 2,4-diisocyanate (TDIC)	–	Raj et al. 1988; Kokta et al. 1990a
7. Organic acids		
Abietic acid (ABAC)	–	Kokta et al. 1990b
Linoleic acid (LAC)	–	Kokta et al. 1990b
8. Monomers		
Acrylonitrile (AN)	Vazo/γ-ray	Kenaga et al. 1962; Kent et al. 1962;
Butyl acrylate (BA)	or	Ramalingam et al. 1963; Meyer 1965,

[a] BPO-benzoyl peroxide; DCP- dicumyl peroxide; LPO- lauroyl peroxide; TBPB- *tert*-butyl peroxide benzonate, DTBPO- di-*tert*-butyl peroxide.

Table 2.1. Continued.

Coupling Agent	Additive [a]	Reference
Epoxylpropyl mechacrylate (EPMA) Methacrylic acid (MAA) Methyl methacrylate (MMA) Styrene Vinyl compounds	$CS_2/H_2O_2/Fe^{2+}$ or $N_2/H_2O_2/(CH_3)_2SO_4$ or $K_2S_2O_5/H_2O_2$	1981; Ellwood et al. 1972; Maldas et al. 1988, 1989a; Maldas and Kokta 1990d; Daneault et al. 1989; Chen et al. 1995
9. Polymers and copolymers		
Ethyl/vinyl acetate (E/VAC)	–	Dalväg et al. 1985
Maleated polyethylene (MAPE)	–	Sanadi et al. 1992
Maleated polypropylene (MAPP)	DCP or TBPB, xylene	Dalväg et al. 1985; Kishi et al. 1988; Han et al. 1989; Takase and Shiraishi 1989; Myers et al. 1991, 1993; Olsen 1991
N,N'-*m*-Phenylene bismaleicimide modified polypropylene (BPP)	–	Sain et al. 1993
Polymethacrylic acid (PMAA)	–	Liang et al. 1994
Polystyrene/polymethacrylic acid (PS-PMAA)	–	Liang et al. 1994
Polyvinyl acetate (PVAC)	–	Liang et al. 1994
Mono- and dimethylolmelamine resin (DMM)	CH_2O, CH_3OH (or C_2H_5OH)	Hua et al. 1987
Phenol-formaldehyde resin (PF)	CH_3OH or H_2O	Coran and Patel 1982; Chtourou et al. 1992; Simonsen and Rials 1992, 1996
Styrene-ethylene-butylene-styrene/maleic anhydride (SEBS-MA)	–	Gatenholm et al. 1995; Hedenberg and Gatenholm 1995; Oksman et al.1998
Styrene/maleic anhydride (SMA)	–	Simonsen et al. 1998
Inorganic agents		
1. Sodium silicate (Na_2SiO_3)	MA or PMPPIC	Maldas and Kokta 1990a, d
Organic-inorganic agents		
1. Silanes		
Vinyltri(2-methoxyethoxy) silane (A-172)	CCl_4, DCP	Beshay et al. 1985; Maldas et al. 1988, 1989a; Raj et al. 1989, 1990; Kokta et al. 1990c
γ-Methacryloxypropyltrimethoxy silane (A-174)	CCl_4, DCP, CH_3OH	Xanthos 1983; Beshay et al. 1985; Bataille et al. 1989; Maldas et al. 1989a; Raj et al. 1988, 1989; Kokta et al. 1990c
β-(3,4-Epoxy cyclohexyl)ethyltrimethoxy silane (A-186)	LPO or DTBPO	Kokta et al. 1990c
γ-Glycidoxy propyltrimethoxy silane (A-187)	LPO or DTBPO	Kokta et al. 1990c
γ-Aminopropyltriethoxy silane (A-1100)	DCP or BPO, MA, *p*-xylene	Maldas et al. 1988, 1989a; Bataille et al. 1989; Raj et al. 1989; Kokta et al. 1990c
2. Titanates		
Titanium di(dioctylpyrophosphate)oxyacetate (KR 138S)	CH_2Cl_2	Dalväg et al. 1985

[a] BPO- benzoyl peroxide; DCP- dicumyl peroxide; LPO- lauroyl peroxide; TBPB- *tert*-butyl peroxide benzonate, DTBPO- di-*tert*-butyl peroxide.

polymer (Dalväg et al. 1985; Maldas and Kokta 1990a, b). Organic-inorganic agents are hybrid compounds in structure. For example, titanates usually contain a titanium center and an organic part surrounding this inorganic atom. The functionality of the organic part in these agents determines their coupling effectiveness in WFPC. Organic-inorganic coupling agents are between organic and inorganic agents in function.

Anhydrides such as MA, AA, SA and PHA are popular coupling agents in WFPC. AA, SA and PHA have two functional groups, i.e., carboxylate groups (-COO-), which can link wood fiber through esterification or hydrogen bonding. But MA is an α, β-unsaturated carbonyl compound, containing one carbon-carbon double bond (C=C) and two carboxylate groups (-COO-). This conjugated structure greatly increases the graft reactivity of the carbon-carbon double bond on the heterocyclic ring with the polymer matrix through the conjugate addition under a radical initiator (Morrison and Boyd 1992), resulting in crosslinking or strong adhesion at the interface. However, the molecular chain of MA is much shorter than that of polymer matrix and wood fibers. This discrete nature makes MA not so effective to improve the interfacial adhesion (Maldas et al. 1988, Maldas and Kokta 1990d). Accordingly, MA is usually used to modify the polymer matrix by graft copolymerization. The formed copolymers, e.g., MAPE, MAPP, SEBS-MA and SMA, are used as coupling agents (Raj et al. 1990; Olsen 1991; Sanadi et al. 1992; Sain et al. 1993; Hedenberg and Gatenholm 1995; Oksman et al. 1998; Simonsen et al. 1998).

Isocyanate links wood fiber through the urethane structure (or a carbamate), which is more stable to hydrolysis than esterification (John 1982; Maldas and Kokta 1990c). Due to the difference in molecular structure, the reactivity of isocyanate

decreases in the following order: PMPPIC, TDIC, HMDIC, EIC (Kokta et al. 1990a). The delocalized π-electrons of the benzene rings in PMPPIC and TDIC lead to the stronger interaction with PS and other polymer matrices compared with HMDIC and EIC without π -electrons. Moreover, the cellulose phase and the polymer phase (PS or PVC) are continuously linked by PMPPIC at the interface, while the discrete nature of TDIC, HMDIC and EIC makes them inferior in this respect (Maldas et al. 1988). A comparison of the performance of these coupling agents is shown in Figure 2.1. As shown, composites with PMPPIC as a coupling agent had the highest tensile strength, compared with those made with other types of coupling agents. Thus, PMPPIC is the best coupling agent in these isocyanates, while TDIC has better coupling effectiveness than HMDIC and EIC.

Silanes, represented as R-Si(OR′)$_3$, have better performance in organic-inorganic coupling agents recently used in WFPC, because the attachment of silanes to hydroxy groups of cellulose or lignin is accomplished either directly to the alkoxy group (-OR′) attached to silicon or via its hydrolyzed products (i.e. silanol) by the hydrogen bonds or ether linkage (Kokta et al. 1990c). The functional group (R-) in silanes also influences the coupling action. Silane A-172 and A-174 both contain a vinyl group; silane A-186 and A-187, an epoxy group; while silane A-1100, an amino group. When in contact with PVC, polar methacryloxy groups in silane A-174 form a polar chain that is more hydrophilic than that of A-172, resulting in poor adhesion. But for other matrices, the α, β-unsaturated carbonyl structure of acrylic groups in A-174 may help form strong adhesion, even crosslinking, at the interface. Silane A-186 and A-187 with an epoxy

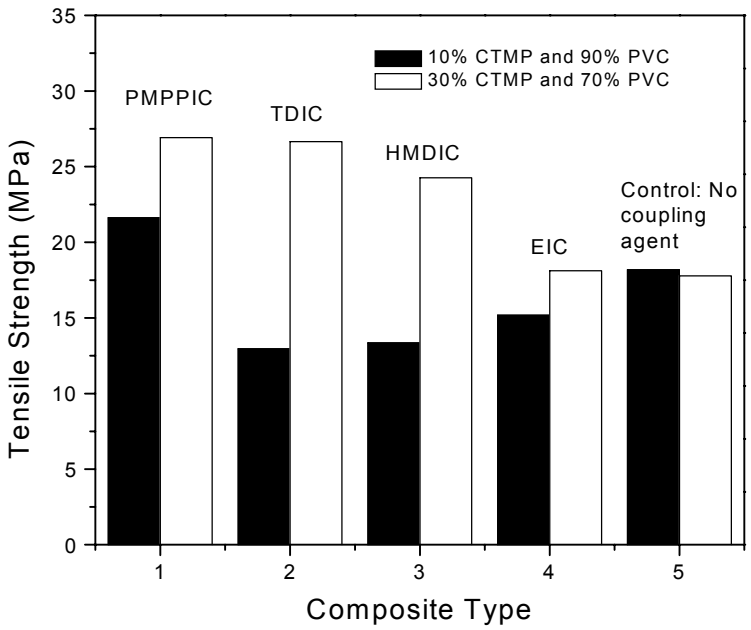

Figure 2.1. Comparison of coupling effectiveness for different isocyanate coupling agents in PVC and CTMP (aspen) composites (plot made with test data published by Kokta et al. 1990a). Coupling agent used was: 1- PMPPIC, 2- TDIC, 3- HMDIC, 4- EIC, and 5- no coupling agent (control). Concentration of coupling agents was 0.5% based on weight of the polymer matrix.

group link cellulose and lignin by ether linkages, whereas NH_2 groups of A-1100 offer mostly hydrogen bonding, which is a weaker force (Kokta et al. 1990c).

Dichlorotriazines and derivatives have multi-functional groups in their molecular structure. These groups have different functions in the coupling reaction (Zadorecki and Flodin 1985). On the heterocyclic ring, the reactive chlorines react with the hydroxyl group (-OH) of wood fiber and give rise to the ether linkage between the cellulose phase and the coupling agent. The electronegative nitrogen may link the hydroxyl group through hydrogen bonding. On the alkyl chain, the carbon-carbon double bonds (C=C) form covalent bonds with the polymer matrix by grafting. At the same time, the electronegative nitrogen in the amino groups and oxygen in the carboxylate groups also link the cellulose phase through hydrogen bonding.

Some thermosetting resin adhesives, such as phenol-formaldehyde resin (PF) and mono- or dimethylolmelamine resin (DMM), have been introduced as a bonding agent in WFPC (Coran and Patel 1982; Hua et al. 1987; Simonsen and Rials 1992, 1996). PF and DMM resins can crosslink wood fibers with the methylene ($-CH_2-$) linkage resulting from the condensation reaction between their reactive methylol groups ($-CH_2OH$) and the hydroxyl groups (-OH) of wood fiber. Although these methylol groups can not react with the thermoplastic matrix, PF and DMM improve the interfacial adhesion through molecular entanglement with the matrix (Simonsen and Rials 1992, 1996).

Similar to MA, acrylic acids and methacrylates (e.g., MAA, MMA, EPMA, and GMA) also contain the α, β-unsaturated carbonyl structure, which may lead to crosslinking or strong interfacial adhesion. Organic acids such as abietic acid (ABAC) and linoleic acid (LAC) contain dienes and carboxylate groups in their molecular

structure, which are helpful to form strong adhesion in the interfacial region. In addition, the reactive allylic group (-CH_2-) in LAC might graft to the polymer matrix (Kokta et al. 1990b). Lacking chemical bonding at the interface, KR 138S and Na_2SiO_3 perform poorly in WFPC (Dalväg et al. 1985; Maldas and Kokta 1990a, b). Na_2SiO_3 is usually required to mix with organic coupling agents.

2.3. PRETREATMENT OF WOOD FIBER AND POLYMER

Pretreatment of wood fiber and polymer with coupling agents is extensively applied before mixing to increase the mechanical properties of WFPC. There are two pretreatment methods: 1) coating coupling agents on wood fiber, and 2) modifying wood fiber and polymer by graft co-polymerization (Maldas et al. 1988, 1989a).

2.3.1 Coating Treatment

The compatibility between wood fiber and polymer is enhanced by coating wood fibers with coupling agents. This process can either cause the polar hydroxyl groups (-OH) of wood fibers to react with coupling agents (such as PMPPIC), which have a linear molecular structure similar to the polymer matrix, or create a chemical interaction between coupling agents (such as MA) and the matrix (Maldas et al. 1989a; Kokta et al. 1990a).

Four kinds of coating methods have been used in WFPC production: compounding, blending, soaking, and spraying. The compounding method mixes coupling agents at high temperature with wood fibers and polymers in an extruder (Dalväg et al. 1985; Myers et al. 1991). This method is mostly used in the melt-blending process. For the blending method, a coupling agent is coated on the surface of wood fiber, polymer or both in a roll mill or a magnetic stirrer at low or high temperature

(Maldas et al. 1988). For the soaking method, wood fiber (such as cellulose fiber) can be first impregnated in the form of sheets of paper with a coupling agent solution containing initiators or other additives. Then the impregnated paper is removed from the solution and placed between two pieces of polymer release film for molding (Zadorecki and Flodin 1985; Sanadi et al. 1992). In the spraying process, coupling agents are emulsified and sprayed on to the surface of wood fibers (Krzysik et al. 1990; Krzysik and Youngquist 1991). Both blending and spraying are suitable for the precoating of wood fiber and polymer before mixing. Spraying and soaking are better than compounding and blending for coating processes because coupling agents are distributed at the interface more evenly and efficiently in the former two cases. However, it is difficult to accurately control the impregnating amount of coupling agents for the soaking method.

2.3.2 Graft Co-polymerization

During graft co-polymerization, coupling agents either crosslink part of the polymer matrix to the wood surface to form a non-polar copolymer or modify the polarity of the polymer matrix by grafting it with polar monomers to form a graft copolymer. This results in the improvement of the interfacial adhesion. Recently, several graft methods have been used in WFPC: 1) xanthation, 2) radiation, 3) maleation, 4) methacrylate graft co-polymerization, 5) acetylation, and 6) others.

In the xanthation process, wood fibers are first kept under carbon disulfide (CS_2) vapor in a peroxide-ferrous-ion initiation system for a certain period of time. Xanthated fibers are then mixed with monomers, such as styrene, butyl acrylate, or epoxy compounds, to form graft copolymers (Maldas et al. 1988, 1989a; Maldas and Kokta

1990d; Daneault et al. 1989). This method has been widely used for pretreating wood fiber in WFPC.

Another conventional method of grafting monomers on to wood cells is by using high-energy radiation sources (such as beta (β) and gamma (γ) rays) with or without a free radical catalyst. For example, the polymerization of vinyl or styrene monomers with wood components was generated by using Cobalt-60 (^{60}Co) gamma radiation (Kenaga et al. 1962; Kent et al. 1962; Ramalingam et al. 1963; Meyer 1965, 1981, 1984; Ellwood et al. 1972). Usually, at least 500,000 to 1,000,000 curies of Cobalt-60 are required for a production source (Meyer 1981).

In the maleation method, MA is used to modify the polymer matrix in the presence of a free radical initiator. It is then grafted on to wood fibers by a succinic half-ester bridge (Gaylord 1972; Chun and Woodhams 1984; De Vito et al. 1984; Kishi et al. 1988; Maldas and Kokta 1990d). Besides the graft application of MA in the PS matrix (Maldas and Kokta 1990d, 1991b), MA can modify PE, PP, and SEBS to form graft copolymers (Maldas et al. 1989b; Gatenholm et al. 1992). Recently, maleic-anhydride-modified polypropylene or maleated polypropylene (MAPP) is a popular coupling agent for WFPC (Gaylord 1972; Chun and Woodhams 1984; Olsen 1991; Maldas and Kokta 1994). As mentioned before, two kinds of MAPP are used in WFPC. One is the MAPP with a high-molecular weight (M_W>30,000) (Kishi et al. 1988; Han et al. 1989; Takase and Shiraishi 1989), such as 63H, 13H, and Hercoprime G (Olsen 1991; Gatenholm et al. 1992). The other type, such as Epolene E-43 (or 47L) and 15L, has a low-molecular weight (M_W<20,000) (Woodhams et al. 1984; Olsen 1991; Myers et al. 1990, 1991, 1993). Maleated polymers are usually coated on to wood fiber before mixing.

The acid number, which represents the amount of functionality in a coupling agent, and molecular weight are two important properties influencing the coupling effectiveness of MAPP in WFPC (Olsen 1991). Generally, MAPP with a high molecular weight and high acid number effectively improves the mechanical properties of WFPC. It was suggested that the Epolene E-43 probably acts as a dispersing agent instead of a true coupling agent in melt-blending formation because of its low molecular weight (Wegner et al. 1992). Krzysik and coworkers (Krzysik et al. 1990; Krzysik and Youngquist 1991), however, reported that Epolene E-43 greatly improved the bonding of air-formed wood fiber and propylene composites.

Methacrylates can be used in graft reactions. For example, GMA and HEMA have been used to modify wood fiber and polymer (Maldas et al. 1989a; Takase and Shiraishi 1989). In a previous study, RGP was pretreated with an acetylating agent containing AA before mixing with MAPP (Kishi et al. 1988). For WPC, some epoxides [e.g., propylene oxide (PO) or butylene oxide (BO)] are grafted onto the cell wall before the impregnation of MMA into the cell lumen (Rowell et al. 1982). Other coupling agents, such as BMI (or PDM) and SA, are also applied in the graft copolymerization for PP matrix and TMP (Rozman et al. 1994; Sain and Kokta 1994).

2.4 MIXING TECHNOLOGY

2.4.1 Mixing Processes

Based on the coating and grafting methods in WFPC, coupling treatments are generally divided into three basic processes (Figure 2.2). Coupling agents can be directly coated on wood fiber and polymer during mixing (Woodhams et al. 1984; Takase and Shiraishi 1989; Maldas et al. 1989a; Myers et al. 1991). This process (one-step process)

is quite simple and cheap (Figure 2.2a). In the two-step process, coating or grafting is carried out before mixing (Figure 2.2b, c). Coupling agents are coated or grafted on the surface of wood fiber, polymer or both before mixing in the second process (Maldas et al. 1988; Krzysik et al. 1990; Maldas and Kokta 1990d; Krzysik and Youngquist 1991). In the third process, part of the polymer and wood fiber furnish is treated with a coupling agent, then mixed with untreated wood fiber and polymer (Maldas et al. 1989b; Kokta et al. 1990a). In the two-step process, the resulting mixtures are usually ground to mesh size 20 for melt-blending formation (Maldas et al. 1988, 1989b; Maldas and Kokta 1989, 1990a). All three processes are suitable for melt-blended composites. The second process (Figure 2.2b) is preferred for air-formed composites.

It has been suggested that a two-step process is better than a one-step process (Štepek and Daoust 1983). In the former case, less coupling agent and less mixing time are required to obtain good adhesion between wood fibers and polymers. Moreover, the two-step process helps increase the interface area (De Ruvo and Alfthan 1978; Maldas et al. 1989a), thus resulting in improving the mechanical properties of WFPC.

2.4.2 Mixing Ratios

Coupling agents usually account for 2-8% by weight of wood fibers for melt-blending formation (wood fiber-to-matrix weight ratio is 50:50); and 1-4% for air-forming processes (wood fiber-to-matrix weight ratio is 70:30) (Maldas et al. 1989a, b; Krzysik et al. 1990; Krzysik and Youngquist 1991; Myers et al. 1991, 1993). Accordingly, a coupling agent accounts for only 1-3% of the total weight of a composite in WFPC. The mixing ratios of coupling agents, wood fibers, and thermoplastic polymers optimum to the mechanical properties of WFPC are shown in Table 2.2.

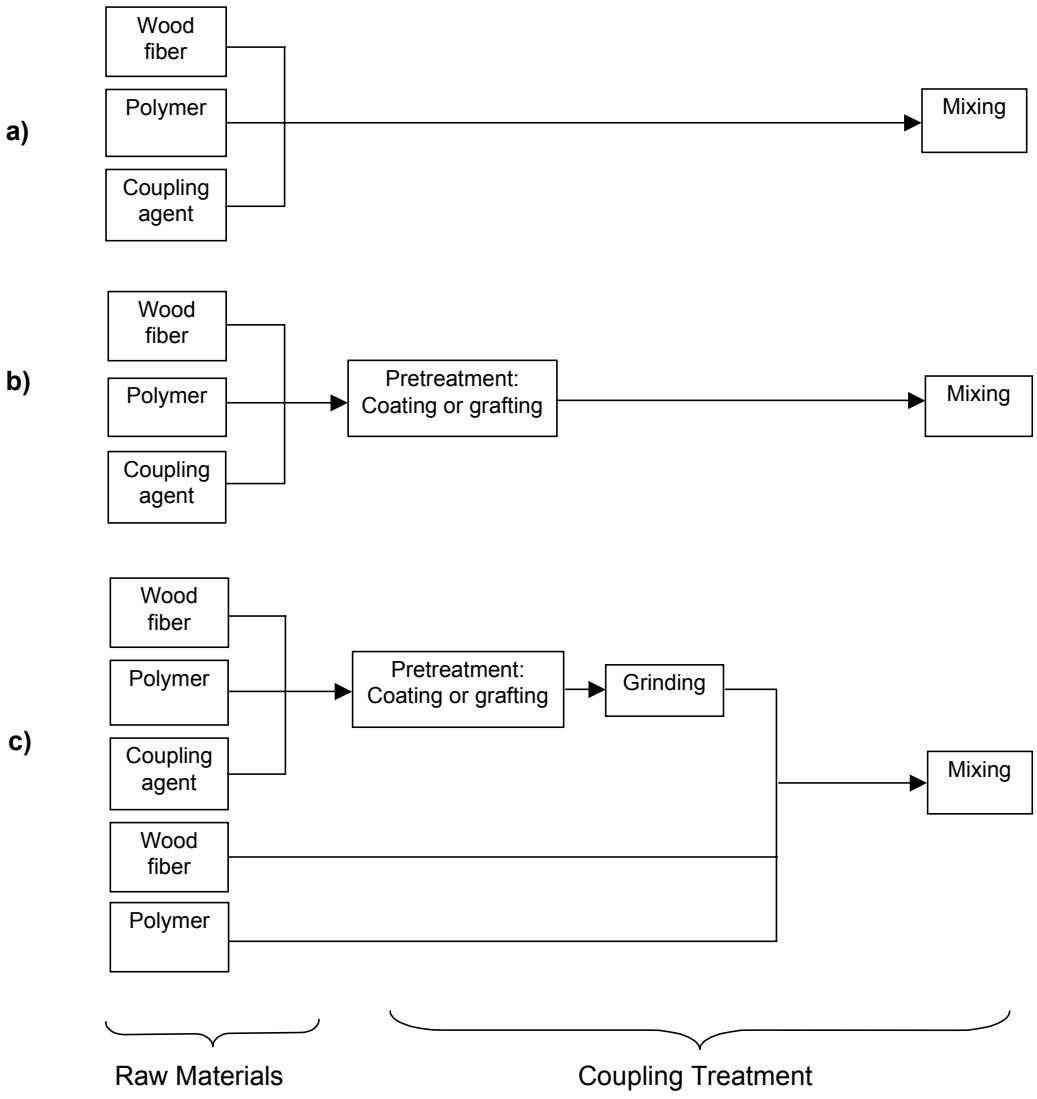

Figure 2.2. Three basic coupling treatments in WFPC: a) directly coating during mixing, b) and c) pretreating before mixing. In (a) wood fiber, polymer, or both is coated or grafted with a coupling agent, but in (c) only part of fiber and polymer is pretreated by a coupling agent, then mixed with untreated fiber and polymer.

The concentration of coupling agents determines the coupling effectiveness in the composite. Generally, mechanical properties increase with increased concentration of a coupling agent (e.g., PMPPIC, MA, PHA, and MAPP) up to a certain limit, and then decline or level off at higher concentrations (Figure 2.3). The reason that higher coupling agent concentrations result in lower mechanical properties of the composite possibly lies in 1) the formation of different by-products, 2) increase in concentration of unreacting or ungrafting coupling agents, and 3) interference with coupling reaction (John 1982; Beshay et al. 1985; Maldas et al. 1989a; Maldas and Kokta 1990d, 1991a, b). Consequently, an excess of a coupling agent is detrimental to the coupling reaction and may act as an inhibitor rather than a promoter of adhesion.

2.4.3 Additives

Initiators are usually required with coupling agents during the coupling treatment, especially in graft copolymerization. The most widely used initiators are organic peroxides, including dicumyl peroxide (DCP), benzoyl peroxide (BPO), lauroyl peroxide (LPO), *tert*-butyl peroxy benzonate (TBPB) and di-*tert*-butyl peroxide (DTBPO) (Table 2.1). DCP is usually used with BMI, MAPP, PMPPIC, and silanes; and BPO with MA, SA, silane A-1100, and chlorotriazines. TBPB is used as a free radical initiator of MA and acrylates. LPO and DTBPO can be used in the silane coupling agents. In graft reactions, the concentration of peroxide is usually between 0.5-1% by weight. Excess peroxide may adversely affect the mechanical properties of the composite because molecular chain scission of the polymer and cellulose occurs when peroxide is too abundant (Maldas and Kokta 1991a). DCP has also been found to be a better initiator for

Table 2.2. Optimum ratios of coupling agent, polymer and wood fiber in WFPC [a].

Polymer	Wood fiber	Coupling agent [b]	Coating and mixing temperature [c]	Fabrication method	Reference
PP 70%	WF 30%	MAPP 6%	-	injection molding	Dalväg et al. 1985
PS685D 70%	CTMP (aspen) 30%	A-172, A-174 4%	145-225°C (70-75 C)	Carver press	Maldas et al. 1989a
PP 50%	WF 50%	MAPP (E-43) 5%	215°C (200°C)	injection molding	Myers et al. 1991, 1993
PP 12-15% or 27-30%	CTMP (hemlock) 70% or 85%	MAPP (E-43) 1-4%	RT	air-forming, hot press	Krzysik et al. 1990; Krzysik and Youngquist 1991
PP 50%	RGP (radiata pine) 50%	MAPP 5%	170°C (200°C)	hot press	Takase and Shiraishi 1989
PS201 70-80%	CTMP (75% black spruce +20% balsam +5% aspen) 20-30%	PMPPIC 8%	175°C (175°C)	Carver press	Maldas et al. 1989b
PS201 65%	CTMP (aspen) 35%	PHA 10%	175°C	molding	Maldas and Kokta 1989, 1990c
PVC 70-80%	CTMP (aspen) 20-30%	PMPPIC 1-5%	145-150°C	Carver press	Kokta et al. 1990a
PS685D 75%	TMP (aspen) 25%	PMAA 4%	180-200°C	Transfer molding	Liang et al. 1994
HDPE 70%	CTMP (aspen) 30%	PMPPIC 7%	130-160°C (RT)	Carver press	Raj et al. 1989

[a] RT- room temperature, PP-polypropylene, PS-polystyrene, PVC-polyvinyl chloride, HDPE-high density polypropylene, WF-wood fiber, TMP- thermomechanical pulp, CTMP- chemithermomechanical pulp, RGP- refiner ground pulp, A-172-vinyltri(2-methoxyethoxy) silane, A-174-γ-methacryloxy-propyltrimethoxy silane, MAPP-maleated polypropylene, PHA-phthalic anhydride, PMAA-polymethacrylic acid, and PMPPIC-poly[methylene(polyphenyl isocyanate)].

[b] By weight of wood fiber.

[c] Values in the parentheses are coating temperature.

MA compared with BPO because the free radicals of DCP have superior thermal stability that leads to better graft performance (Maldas and Kokta 1991c). The free-radical initiator, 2,2'-azobisisiobytaronitrile (also called Vazo), is usually combined with gamma radiation for graft reaction of styrene and vinyl monomers (Meyer 1981).

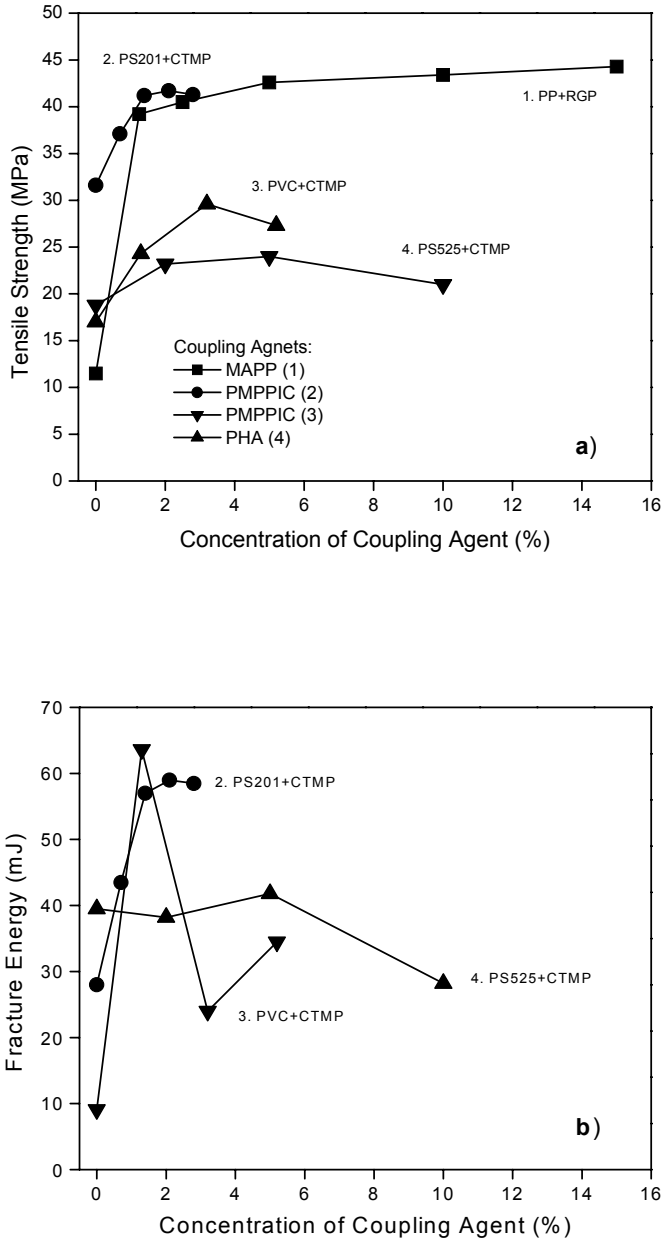

Figure 2.3. Influence of concentration of coupling agents on the mechanical properties of WFPC: (a) tensile strength and (b) fracture energy (plots made with test data published by Han et al. 1989; Maldas et al. 1989a; Maldas and Kokta 1990c; Kokta et al. 1990a). Concentration of coupling agents was based on weight of the composite. Concentration of MA was 1.85 weight percent of MAPP. Composite type: 1. PP:RGP (radiata)=50%:50%, 2. PS201: CTMP (aspen)=70%:30%, 3. PVC:CTMP (aspen)=70%:30%, and 4. PS525:CTMP (aspen)=65%:35%.

Organic solvents may be required with certain coupling agents. For example, carbon tetrachloride (CCl_4) is used in silanes A-172 and A-174 (Maldas et al. 1989a; Maldas and Kokta 1990c), while methylene dichloride (CH_2Cl_2) is a solvent of titanate coupling agents such as KR 138S (Dalväg et al. 1985). Other solvents include xylene, pyridine, methanol, and ethanol (Xanthos 1983; Hau et al. 1987; Han et al. 1989, Myers et al. 1990, 1991; Gatenholm et al. 1993; Simonsen and Rials 1996).

During the coupling treatment, antioxidants, stabilizers, plasticizers, and other processing aids are also added to the blends to improve the physical and mechanical properties of a composite. For example, alumina trihydrate [$Al(OH)_3$], magnesium oxide (MgO), boric acid ($H_2B_4O_7$), or borax ($Na_2B_4O_7$) provides flame retardation to the composite (Kishi et al. 1988; Han et al. 1989; Maldas and Kokta 1991a; Sain et al. 1993). The addition of magnesium oxide and boron compounds can protect wood fiber from thermal decomposition and degradation during high-temperature composite processing (Han et al. 1989; Sain et al. 1993). In addition, adding a moderate amount of MgO can improve the performance of MA because MgO reacts with water and the acid group to yield carboxylate ions ($-COO^-$). Concurrently, Mg^{2+} interacts with two carboxylate ions as a crosslinking agent and yields ionomer systems (Han et al. 1989). Organic additives primarily used in coupling treatments are dioctyl phthalte (DOP), barium acetate (BaAc), Irganox-1010, Ionol, mono- and diglycerides of fatty acids (GMS), and distearyl thiodipropionate (DSTP) (Han et al. 1989; Krzysik et al. 1990; Myers et al. 1991).

2.4.4 Mixing Conditions

Mixing conditions, i.e. temperature, time, and rotation speed, directly influence the coating quality and coupling agent performance (Takase and Shiraishi 1989; Maldas

and Kokta 1990d; Chen et al. 1995). Usually, mixing temperature is controlled at less than 200°C for most coupling treatments to avoid decomposition and degradation of wood fibers and some thermoplastic matrices (Woodhams et al. 1984; Maldas et al. 1989a; Takase and Shiraishi 1989; Myers et al. 1993). For refiner ground pulp (RGP) and PP composites, the optimum mixing conditions are 10 minutes under a mixing temperature of 180ºC and a rotation speed of 50 rpm (Takase and Shiraishi 1989). Maldas and Kokta (1990d) reported that the maximum improvement in mechanical properties of chemithermomechanical pulp (CTMP) and PS composites was achieved when the mixing time was 15 min at 175ºC. For melt-blended composites, the blends are required to re-mix 5-10 times (about 6-8 min) during compounding to achieve a better distribution of coupling agents at the interface, when directly mixing coupling agents with polymer and wood fiber (Maldas et al. 1989a; Maldas and Kokta 1990a, b, c). Rotation speed has similar influence on the coupling effectiveness as does mixing time. It was reported that moderate mixing speeds were preferred for better fiber length distribution and coupling effectiveness (Takase and Shiraishi 1989).

2.5 CONCLUSIONS

Coupling agents in WFPC play a very important role in improving compatibility and adhesion between polar wood fibers and non-polar polymer matrices. So far, more than forty coupling agents have been used in production and research. Organic coupling agents are better than inorganic coupling agents, because stronger adhesion is produced at the interface. Although a number of coupling agents are used or have been tested in production and research, the most popular are isocyanates, anhydrides, silanes, and anhydride-modified copolymers, such as PMPPIC and MAPP.

Coupling agents are usually coated on the surface of wood fiber, polymer or both by compounding, blending, soaking, spraying, or other coating methods. There are three basic mixing processes in production and research. Coupling agents can be directly mixed with wood fiber and polymer in the melt-blending formation, such as injection molding, extrusion, and transfer molding. They can also be coated or grafted on the surface of wood fiber, polymer, or both. Then the pretreated and untreated wood fiber and polymer are kneaded. Usually, pretreatment of wood fiber and polymer by coating or grafting helps enhance the mechanical properties of WFPC.

Some of the important considerations in choosing coupling treatments are concentration and chemical structure of coupling agents, choice of wood fiber and matrix (e.g. shape, size and species), ratio of wood fiber to total matrix weight, formation methods, and end-use requirements of the finished product. Future publications in this series will discuss the adhesion mechanism and coupling performance of different coupling agents.

2.6 REFERENCES

Bataille, P., L. Ricard, and S. Sapieha. 1989. Effects of cellulose fibers in polypropylene composites. Polym. Comp. 10(2): 103-108.

Beshay, A. D., B. V. Kokta, and C. Daneault. 1985. Use of wood fibers in thermoplastic composites II: Polyethylene. Polym. Comp. 6(4): 261-271.

Bridgeford, D. J. 1963. US Patent 3,083,118.

Chen, M. –J., J. J. Meister, D. W. Gunnells, and D. J. Gardner. 1995. A process for coupling wood to thermoplastic using graft copolymers. Adv. Polym. Technol. 14(2): 97-109.

Chtourou, H., B. Riedl, and A. Ait-Kadi. 1992. Reinforcement of recycled polyolefins with wood fibers. J. Reinf. Plast. Comp. 11: 372-394.

Chun, I., and R. T. Woodhams. 1984. Use of processing aids and coupling agents in mica-reinforced polypropylene. Polym. Comp. 5(4): 250-257.

Clint, J. H. 1998. Surfactants: applications in plastics. Pages 604-612 *in* G. Pritchard, ed. Plastics Additives: An A-Z Reference. Chapman and Hall, New York, NY.

Coran, A. Y., and R. Patel. 1982. US Patent 4,323,625.

Dalväg, H., C. Klason, and H. –E. Strömvall. 1985. The efficiency of cellulosic fillers in common thermoplastics. Part II. Filling with processing aids and coupling agents. Intern. J. Polymeric Mater. 11: 9-38.

Danuealt, C., B. V. Kokta, and D. Maldas. 1989. The xanthate method of grafting. XII. Effect of operating conditions on the grafting of vinyl monomers onto wood pulp. J. Appl. Polym. Sci. 38: 841-848.

De Ruvo, A., and E. Alfthan. 1978. Shifts in glass transition temperatures of synthetic polymers filled with microcrystalline cellulose. Polymer 19(8): 872-874.

De Vito, G., N. Lanzetta, G. Maglio, M. Malinconico, P. Musto, and R. Palumbo. 1984. Functionalization of an amorphous ethylene-propylene copolymer by free radical initiated grafting of unsaturated molecules. J. Polym. Sci. 22: 1335-1347.

Dimov, K., and P. Pavlov. 1969. Grafting with acrylonitrile with the redox system cellulose xanthogenate-hydrogen peroxide. J. Polym. Sci. 7: 2775-2792.

Ellwood, E. L., R. C. Gilmore, and A. J. Stamm. 1972. Dimensional stabilization of wood with vinyl monomers. Wood Sci. 4(3): 137-141.

Faessinger, R. W., and J. S. Conte. 1967. US Patent 3,359,224.

Gatenholm, P., J. Felix, C. Klason, and J. Kubát. 1992. Cellulose-polymer composites with improved properties. Pages 75-82 *in* J. C. Salamone, and J. S. Riffle, eds. Contemporary Topics in Polymer Science: Advances in New Materials. Vol. 7. Plenum Press, New York, NY.

Gatenholm, P., J. Felix, C. Klason, and J. Kubát. 1993. Methods for improvement of properties of cellulose-polymer composites. Pages 20-24 *in* M. P. Wolcott, ed. Wood Fiber/Polymer Composites: Fundamental Concepts, Processes, and Materials Options. Proc. of the 1st Wood Fiber-Plastic Composite Conference in Madison, WI.

Gatenholm, P., P. Hendenberg, and C. Klason. 1995. Recycling of mixed plastics using cellulosic reinforcement. Pages 367-377 *in* C.P. Rader, S. D. Baldwin, D.D. Cornell, G. D. Salder and R. F. Stockel, eds. Plastics, Rubber, and Paper

Recycling: A Pragmatic Approach. ACS Symposium Series 609. American Chemical Society, Washington, D. C. Chapter 30.

Gaylord, N. 1972. US Patent 3,645,939.

Geottler, L. A. 1983. US Patent 4,376,144.

Gulina, A. A., R. M. Livshits, and Z. A. Rogovin. 1965. Synthesis of cellulose-polyacrylonitrile graft copolymers in the presence of the oxidation-reduction system cellulose Fe^{2+}-H_2O_2. II. Investigation of the effect of initiation conditions on the polymerization coefficient of polyacrylonitrile and the degree of conversion of cellulose. Vysokomol. Soyed. **7**(9): 1529-1534.

Hamed, P., and A.Y. Coran. 1978. Reinforcement of polymers through short cellulose fibers. Pages 29-50 *in* R. B. Seymour, ed. Additives for Plastics, vol. I. State of the art. Academic Press, New York, NY.

Han, G. –S., H. Ichinose, S. Takase, and N. Shiraish. 1989. Composites of wood and polypropylene III. Mokuzai Gakkaishi 35(12): 1100-1104.

Hedenberg, P., and P. Gatenholm. 1995. Conversion of plastic/cellulose waste into composites. I. Model of interphase. J. Appl. Polym. Sci. 56: 641-651.

Hornof, V., B. V. Kokta, and J. L. Valade. 1976. The xanthate method of grafting. IV. Grafting of acrylonitrile onto high-yield pulp. J. Appl. Polym. Sci. 20: 1543-1554.

Hua, L., P. Zadorecki, and P. Flodin. 1987. Cellulose fiber-polyester composites with reduced water sensitivity. I. Chemical treatment and mechanical properties. Polym. Comp. 8(3): 199-202.

John, W. E. 1982. Isocyanate as wood binders: A review. J. Adhesion 15:59-67.

Kenaga, D. L., J. P. Fennessey, and V. I. Stannett. 1962. Radiation grafting of vinyl monomers to wood. Forest Prod. J. 12(4): 161-168.

Kent, J. A., R. W. Winston, W. R. Boyle, and L. W. Harmison. 1962. Preparation of wood-plastic combinations using gamma radiation to induce polymerization: Effect of gamma radiation of wood. Annual Report ORO-600, U.S. Atomic Energy Commission, Washington, D.C., Oct 31-Nov. 1, 1961.

Kishi, H., M. Yoshioka, A. Yamanoi, and N. Shiraishi. 1988. Composites of wood and polypropylenes I. Mokuzai Gakkaishi 34(2): 133-139.

Klason, C., J. Kubát, and H. –E. Strömvall. 1984. The efficiency of cellulosic fillers in common thermoplastics. Part I. Filling without processing aids or coupling agents. Intern. J. Polymeric Mater. 10: 159-187.

Kokta, B. V. 1988. US Patent 4,791,020.

Kokta, B. V., and J. L. Valade. 1972. Effect of acrylonitrile on grafting of styrene with the redox system cellulose xanthate-hydrogen peroxide. TAPPI 55(3): 366-369.

Kokta, B. V., D. Maldas, C. Daneault, and P. Béland. 1990a. Composites of polyvinyl chloride-wood fibers. I. Effect of isocyanate as a bonding agent. Polym. -Plast. Technol. Eng. 29(1&2): 87-118.

Kokta, B. V., D. Maldas, C. Daneault, and P. Béland. 1990b. Composites of poly(vinyl chloride) and wood fibers. Part II: Effect of chemical treatment. Polym. Comp. 11(2): 84-89.

Kokta, B. V., D. Maldas, C. Daneault, and P. Béland. 1990c. Composites of polyvinyl chloride-wood fibers. III: Effect of silane as coupling agent. J. Vinyl Technol. 12(3): 146-153.

Krzysik, A. M., and J. A. Youngquist. 1991. Bonding of air-formed wood fiber/polypropylene fiber composites. Intern. J. Adhes. Adhesives 11(4): 235-240.

Krzysik, A. M., J. A. Youngquist, G. E. Myers, I. S. Chahyadi, and P. C. Kolosick. 1990. Wood-polymer bonding in extruded and nonwoven web composites panels. Pages 183-189 *in* A. H. Conner, A. W. Christiansen, G. E. Myers, B. H. River, C. B. Vick, and H. N. Spelter, eds. Wood Adhesives 1990. Symp. of USDA Forest Service, Forest Products Laboratory and the Forest Products Research Society, Madison, WI.

Liang, B. –H., L. Mott, S. M. Shaler, and G. T. Caneba. 1994. Properties of transfer-molded wood-fiber/polystyrene composites. Wood Fiber Sci. 26(3): 382-389.

Maldas, D., and B. V. Kokta. 1989. Improving adhesion of wood fiber with polystyrene by the chemical treatment of fiber with a coupling agent and the influence on the mechanical properties of composites. J. Adhes. Sci. Technol. 3(7): 529-539.

Maldas, D., and B. V. Kokta. 1990a. Effects of coating treatments on the mechanical behavior of wood fiber-filled polystyrene composites. II. Use of inorganic salt/polyvinyl chloride and isocyanate as coating components. J. Reinf. Plast. Comp. 8: 2-12.

Maldas, D., and B. V. Kokta. 1990b. Effects of coating treatments on the mechanical behavior of wood-fiber-filled polystyrene composites. I. Use of polyethylene and isocyanate as coating components. J. Appl. Polym. Sci. 40: 917-928.

Maldas, D., and B. V. Kokta. 1990c. Influence of phthalic anhydride as a coupling agent on the mechanical behavior of wood fiber-polystyrene composites. J. Appl. Polym. Sci. 41: 185-194.

Maldas, D., and B. V. Kokta. 1990d. Influence of polar monomers on the performance of wood fiber reinforced polystyrene composites. I. Evaluation of critical conditions. Int. J. Polym. Mater. 14(3-4): 165-189.

Maldas, D., and B. V. Kokta. 1991a. Surface modification of wood fibers using maleic anhydride and isocyanate as coating components and their performance in polystyrene composites. J. Adhesion Sci. Technol. 5(9): 727-740.

Maldas, D., and B. V. Kokta. 1991b. Influence of maleic anhydride as a coupling agent on the performance of wood fiber-polystyrene composites. Polym. Eng. Sci. 31(18): 1351-1357.

Maldas, D., and B. V. Kokta. 1991c. Influence of organic peroxide on the performance of maleic anhydride coated cellulose fiber-filled thermoplastic composites. Polym. J. 23(10): 1163-1171.

Maldas, D., and B. V. Kokta. 1994. An investigation of the interfacial adhesion between reclaimed newspaper and recycled polypropylene composites through the investigation of their mechanical properties. J. Adhes. Sci. Technol. 8(12): 1439-1451.

Maldas, D., B. V. Kokta, and C. Daneault. 1989a. Influence of coupling agents and treatments on the mechanical properties of cellulose fiber-polystyrene composites. J. Appl. Polym. Sci. 37: 751-775.

Maldas, D., B. V. Kokta, and C. Daneault. 1989b. Thermoplastic composites of polystyrene: Effect of different wood species on mechanical properties. J. Appl. Polym. Sci. 38: 413-439.

Maldas, D., B. V. Kokta, R. G. Raj, and C. Daneault. 1988. Improvement of the mechanical properties of sawdust wood fiber-polystyrene composites by chemical treatment. Polymer 29: 1255-1265.

Meyer, J. A. 1965. Treatment of wood-polymer systems using catalyst-heat techniques. Forest Prod. J. 15(9): 362-364.

Meyer, J. A. 1968. Crosslinking affects sanding properties of wood-plastic. Forest Prod. J. 18(5): 89.

Meyer, J. A. 1981. Wood-polymer materials: State of the art. Wood Sci. 14(2): 49-54.

Meyer, J. A. 1982. Industrial use of wood polymer materials: State of the art. Forest Prod. J. 32(1): 24-29.

Meyer, J. A. 1984. Wood polymer materials. Pages 257-289 *in* R. M. Rowell, ed. The Chemistry of Solid Wood. ACS Advances in Chemistry Series 207. American Chemical Society, Washington, D.C.

Morrison, R. T., and R. N. Boyd. 1992. Organic Chemistry. Sixth Edition. Prentice-Hall, Inc., Englewood Cliffs, New Jersey. 971-985 pp.

Myers, G. E., I. S. Chahyadi, C. A. Coberly, and D. S. Ermer. 1991. Wood flour/polypropylene composites: Influence of maleated polypropylene and process and composition variables on mechanical properties. Intern. J. Polymeric Mater. 15: 21-44.

Myers, G. E., I. S. Chahyadi, C. Gonzalez, and C. A. Coberly. 1993. Wood flour and polypropylene or high-density polyethylene composites: Influence of maleated polypropylene concentration and extrusion temperature on properties. Pages 49-56 *in* M. P. Wolcott, ed. Wood Fiber/Polymer Composites: Fundamental Concepts, Processes, and Materials Options. Proc. of the 1st Wood Fiber-Plastic Composite Conference in Madison, WI.

Myers, G. E., P. C. Kolosick, I. S. Chahydi, C. A. Coberly, J. A. Koutsky, and D. S. Ermer. 1990. Extruded wood-flour polypropylene composites: Effect of a maleated polypropylene coupling agent on filler-matrix bonding and properties. Pages 67-76 *in* D. F. Caulfield, J. D. Passaretti, and S. F. Sobczynski, eds. Materials Interactions Relevant to the Pulp, Paper, and Wood Industries. Vol. 197. Materials Research Society, Pittsburgh, PA.

Nakamura, T., M. Okamura, Y. Moriguchi, and T. Hayase. 1983. US Patent 4,404,437.

Oksman, K., and H. Lindberg. 1998. Influence of thermoplastics elastomers on adhesion in polyethylene-wood flour composites. J. Appl. Polym. Sci. 68: 1845-1855.

Oksman, K., and H. Lindberg, and A. Holmgren. 1998. The nature and location of SEBS-MA compatibilizer in polyethylene-wood flour composites. J. Appl. Polym. Sci. 69: 201-209.

Olsen, D. J. 1991. Effectiveness of maleated polypropylenes as coupling agents for wood flour/polypropylene composites. Pages 1886-1891 *in* ANTEC, Proc. of the 49th

Annual Technical Conference, Montreal, Canada, May 5-9, 1991. Society of Plastics Engineers, Brookfield, CT.

Porter, M. R. 1994. Handbook of Surfactants. Blackie Academic & Professional, Glasgow G64 2NZ, UK. p. 80.

Pritchard, G. 1998. Quick reference guide. Page 12 *in* Plastics additives: An A-Z reference. G. Pritchard, ed. Chapman and Hall, New York, NY.

Radian Corporation. 1987. Chemical Additives for the Plastics Industry: Properties, Applications and Toxicologies. Noyes Data Corporation, Park Ridge, NJ. pp. 55-59.

Raj, R. G., and B.V. Kokta,. 1991. Improving the mechanical properties of HDPE-wood fiber composites with additives/coupling agents. Pages 1883-1885 *in* ANTEC, Proc. of the 49th Annual Technical Conference, Montreal, Canada, May 5-9, 1991. Society of Plastics Engineers, Brookfield, CT.

Raj, R. G., B.V. Kokta, D. Maldas, and C. Daneault. 1988. Use of wood fibers in thermoplastic composites: VI. Isocyanate as a bonding agent for polyethylene-wood fiber composites. Polym. Comp. 9(6): 404-411.

Raj, R. G., B.V. Kokta, D. Maldas, and C. Daneault. 1989. Use of wood fibers in thermoplastics. VII. The effect of coupling agents in polyethylene-wood fiber composites. J. Appl. Polym. Sci. 37: 1089-1103.

Raj, R. G., B.V. Kokta, G. Grouleau, and C. Daneault. 1990. The influence of coupling agents on mechanical properties of composites containing cellulosic fillers. Polym. Plast. Technol. Eng. 29(4): 339-353.

Ramalingam, K. V., G. N. Werezak, and J. W. Hodgins. 1963. Radiation-induced graft polymerization of styrene in wood. J. Polymer Sci. Part C 2: 153-167.

Rosen, M. J. 1978. Surfactants and Interfacial Phenomena. John Wiley & Sons, New York, NY. p. 266.

Rowell, R. M., and W. D. Ellis. 1978. Determination of dimensional stability of wood using the water-soak method. Wood Fiber 10: 104-111.

Rowell, R. M., and P. Konkol. 1987. Treatments that enhance physical properties of wood. U.S. Forest Products Laboratory General Technical Report FPL-GTR-55. 12 pp.

Rowell, R. M., R. Moisuk, and J. A. Meyer. 1982. Wood-polymer composites: cell wall grafting with alkylene oxides and lumen treatments with methyl methacrylate. Wood Sci. 15(2): 90-96.

Rowell, R. M., D. I. Gutzmer, I. B. Sachs, and R. E. Kinney. 1976. Effects of alkylene oxide treatments on dimensional stability of wood. Wood Sci. 9(1): 51-54.

Rozman, H. D., W. B. Banks, and M. L. Lawther. 1994. Improvements of fiberboard properties through fiber activation and subsequent copolymerization with vinyl monomer. J. Appl. Polym. Sci. 54: 191-200.

Sain, M. M., B. V. Kokta, and D. Maldas. 1993. Effect of reactive additives on the performance of cellulose fiber-filled polypropylene composites. J. Adhesion Sci. Technol. 7(1): 49-61.

Sain, M. M., and B. V. Kokta. 1994. Polyolefin-wood filler composites. I. Performance of *m*-phenylene bismaleimide-modified wood fiber in polypropylene composite. J. Appl. Polym. Sci. 54: 1545-1559.

Sanadi, A. R., R. M. Rowell, and R. A. Young. 1992. Estimation of fiber-matrix interfacial shear strengths in lignocellulosic-thermoplastic composites. Pages 81-92 *in* R. M. Rowell, T. L. Laufenberg, and J. K. Rowell, eds. Materials Interactions Relevant to Recycling of Wood-Based Materials. Vol. 266. Materials Research Society, Pittsburgh, PA.

Schneider, M. H. 1994. Wood polymer composites. Wood Fiber Sci. 26(1): 142-151.

Schneider, M. H., and K. I. Brebner. 1985. Wood-polymer combinations: The chemical modification of wood by alkoxysilane coupling agents. Wood Sci. Technol. 19(1): 67-73.

Selke, S. E., K. Nieman, J. Childress, M. Kel, and R. Bimpson. 1990. Use of eastern hardwoods in wood fiber/plastic composites. Pages 35-42 *in* Advanced Technology Applications to Eastern Hardwood Utilization. Michigan State University, East Lansing, MI.

Simonsen, J., and T. Rials. 1992. Enhancing the interfacial bond strength of lignocellulosic fiber dispersed in synthetic polymer matrices. Pages 105-111 *in* R. M. Rowell, T. L. Laufenberg, and J. K. Rowell, eds. Materials Interactions Relevant to Recycling of Wood-Based Materials. Vol. 266. Materials Research Society, Pittsburgh, PA.

Simonsen, J., and T. Rials. 1996. Morphology and properties of wood-fiber reinforced blends of recycles polystyrene and polyethylene. J. Thermoplastic Comp. Mater. 9: 292-302.

Simonsen, J., R. Jacobsen, and R. Rowell. 1998. Wood-fiber reinforcement of styrene-maleic anhydride copolymers. J. Appl. Polym. Sci. 68: 1567-1573.

Štepek, J., and H. Daoust. 1983. Additives for Plastics. Polymer/Properties and Applications 5. Springer-Verlag, New York. p. 84.

Takase, S., and N. Shiraishi. 1989. Studies on composites from wood and polypropylene. II. J. Appl. Polym. Sci. 37: 645-659.

Wegner, T. H., J. A. Youngquist, AND R. M. Rowell. 1992. Opportunities for composites from recycled wood based resources. Pages 3-15 *in* R. M. Rowell, T. L. Laufenberg, and J. K. Rowell, eds. Materials Interactions Relevant to Recycling of Wood-Based Materials. Vol. 266. Materials Research Society, Pittsburgh, PA.

Woodhams, R. T. 1984. US Patent 4,442,243.

Woodhams, R. T., G. Thomas, and D. K. Rodgers. 1984. Wood fibers as reinforcing fillers for polyolefins. Polym. Eng. Sci. 24(15): 1166-1171.

Xanthos, M. 1983. Processing conditions and coupling agent effects in polypropylene/wood flour composites. Plast. Rubber Process. Appl. 3(3): 223-228.

Youngquist, J. A. 1995. Unlikely partners? The marriage of wood and non-wood materials. Forest Prod. J. 45(10): 25-30.

Zadorecki, P., and P. Flodin. 1985. Surface modification of cellulose fibers. II. The effect of cellulose fiber treatment on the performance of cellulose-polyester composites. J. Appl. Polym. Sci. 30:3971-3983.

CHAPTER 3. THE INFLUENCE OF MALEATION ON POLYMER ADSORPTION AND FIXATION, WOOD SURFACE WETTABILITY, AND INTERFACIAL BONDING STRENGTH IN WOOD-PVC COMPOSITES*

3.1 INTRODUCTION

Coupling agents played a very important role in improving compatibility and bonding strength between polar wood fibers and non-polar thermoplastics in wood fiber and polymer composites (Chun and Woodhams 1984; Woodhams et al. 1984; Dalväg et al. 1985). Although exact mechanisms of interfacial bonding between wood and polymer are still not fully understood, several hypotheses and schematic models have been proposed to elucidate the interfacial behavior and performance improvement (Chun and Woodhams 1984; Kishi et al. 1988; Maldas et al. 1988; Gatenholm and Felix 1993; Sanadi et al. 1995). The maleation method uses maleic acid (MA) to modify the polymer matrix in the presence of a free radical initiator. The maleated polymer is grafted on to wood fibers by a succinic half-ester bridge. MA can modify a number of polyolefin to form maleated polymers. Maleated polypropylene (MAPP) has been extensively used in wood fiber and polymer composites (Lu et al. 2000). A number of investigations on maleated polypropylene have been done (Maldas et al. 1988; Maldas and Kokta 1989; Felix and Gatenholm 1991; Olsen 1991). However, very limited data are available on the relationship among coupling treatment, surface wettability, and interfacial bonding strength of wood and polymer systems.

Contact angle data have been widely used to evaluate compatibility between wood and polymer at the interface (Felix and Gatenholm 1991; Chen et al. 1995). Non-polar polymers generally have a larger contact angle compared with polar wood. The coupling treatment of wood helps increase contact angle and thus improve the compatibility at the interface. Felix and Gatenholm (1991) reported that the contact angle of cellulose fibers treated with MAPP was in the range of 130° and 140°. There was no significant difference of contact angle between specimens extracted and non-extracted with toluene before coupling treatments. Chen et al. (1995) studied adhesion properties of styrene-lignin graft copolymers using a Cahn dynamic contact angle analyzer. The contact angle data measured with distilled water on grafted lignin were close to those of polystyrene (i.e., 105°), indicating an improved compatibility at the interface. More recently, Matuana and coworkers (1998) used four different coupling agents to treat wood veneer and investigated the wettability of treated wood specimens with a contact angle meter. For wood veneer specimens treated with anhydride-based coupling agents (such as Epolene E-43 and phthalate anhydride), static contact angle of glycerol sessile drops on treated wood specimens was in a range from 100° to 110° (Matuana et al. 1998). However, few investigations have directly dealt with the influence of different coupling agents on the wettability (measured by contact angle) of treated wood and the correlations among contact angle, retention, and graft rate of coupling agents.

Bonding strength provides a direct measure of the interfacial adhesion between wood and thermoplastics. The strength is greatly influenced by properties of wood, polymer, and degree of coupling between them. Several test methods, including pullout, microbond, peel, tension (parallel and perpendicular to the fiber), and planar shear tests,

have been used to evaluate interfacial bonding strength of wood and polymer composites. The pullout and microbond tests are usually used to evaluate the bonding strength of a single fiber within the thermoplastic matrix (Sanadi et al. 1992; Liu et al. 1994). In these techniques, individual wood fibers are embedded in a plastic matrix. The fibers are pulled out during testing to indicate the interfacial bonding strength. Preparation of proper test specimens is often a difficult task for these tests. Also, it is difficult to test the interfacial bonding strength of very short fibers in the matrix, especially with poor interfaces (Liu et al. 1994). The tension, peel, and planar shear tests are suitable for evaluation of larger specimens. The tension tests (both parallel and perpendicular to the fiber) are the most popular method to evaluate the bonding strength of wood-plastic composites (Xanthos 1983; Woodhams et al. 1984; Dalväg et al. 1985; Maldas and Kokta 1989; Krzysik and Youngquist 1991; Olsen 1991; Chow et al. 1996). In peel tests, a 90° peel device is used to separate wood substrate and plastic film with a peeling force (Kolosick et al. 1992). In planar shear tests, the shear stress between laminated planar samples is directly measured under an in-plane shear load. The glue-joint strength of wood and polypropylene/modified polypropylene laminates was investigated by use of a planar shear test method (Goto et al. 1982). Humphrey (1993) developed an automatic device to bond specimens with adhesives under hot pressing and to perform a shear strength test sequentially.

Interfacial adhesion in PVC and wood veneer laminates has been studied with a shear testing method (Matuana et al. 1998). It was reported that the interfacial adhesion in PVC and wood veneer laminates was significantly improved when wood veneers were treated with amino-silane, while no improvement was observed for E-43 and other

coupling agents (Matuana et al. 1998). Snijder and Bos (2000) investigated the coupling efficiency of nine different MAPPs in agrofiber and polypropylene (PP) composites by injection molding. It was found that the molecular weight of MAPP was a more important parameter than MA content in MAPP for coupling efficiency. The backbone structure of MAPP influenced the interfacial adhesion in resultant composites because of miscibility in the PP matrix (Snijder and Bos 2000). In another paper (Snijder et al. 1997), they reported that the mechanical properties of resultant composites increased with the amount of MAPP, but the effect leveled off or decreased at high MAPP content levels. More recently, MAPP was also used as a coupling agent for kudzu fiber-reinforced polypropylene composites (Kit et al. 2001). Through an extruder, 23% of MAPP (weight percent of the composite) were blended with PP and kudzu fiber. Compared with that of untreated kudzu fiber-polypropylene composites, tensile strength of kudzu fiber-polypropylene composites treated with MAPP increased by 52%.

It is often believed that bonding strength is influenced by the compatibility between wood and thermoplastics. However, it is not clear whether larger contact angles of wood materials treated with coupling agents would always result in higher interfacial bonding strength of wood and polymer composites (i.e., compatibility determines interfacial bonding). It was reported that an excess of coupling agent at the interface is detrimental to the coupling action and may act as an inhibitor rather than a promoter of adhesion (Maldas and Kokta 1989). However, this phenomenon has not been further studied on compatibility (from chemical coupling) or surface wettability. Most studies on wettability did not include bonding strength. Therefore, it is necessary to further investigate the relationship between wettability and interfacial bonding.

The objectives of this study were to investigate the effects of maleation treatment on polymer adsorption and fixation, wood surface wettability, and interfacial bonding strength of wood-PVC composites, and to examine the correlations among concentration, retention, and graft rate and between surface wettability and interfacial bonding strength.

3.2 MATERIALS AND METHODS

3.2.1 Test Materials and Sample Preparation

Two MAPPs (Epolene E-43 and G-3015, Eastman Chemical Company) were used as coupling agents in this study. Epolene E-43 has an average weight molar mass (M_w) of 9,100 and its acid number is between 40 and 55. Epolene G-3015 has a high molecular weight (i.e., 47,000), but has a low acid number (between 12 and 18). E-43 contains more maleic anhydride groups [-$(CO)_2O$-] in its molecular chains than G-3015. Benzoyl peroxide (BPO, Aldrich) was used as initiator, and toluene (Fisher Scientific) was used as solvent for both MAPPs. Clear and rigid polyvinyl chloride (PVC, Curbell Plastics) polymer sheets (508 mm x 1270 mm x 0.0762 mm) were purchased commercially. The melting and glass transition temperatures of the PVC are 175°C and 81°C, respectively. The density of the PVC is 1,390 kg/m^3. It has a tensile strength of 55 MPa and a tensile modulus of 2,800 MPa (Delassus and Whiteman 1999).

Sheets of commercial yellow poplar (*Liriodendron tulipifera*) veneer (610 mm x 610 mm x 0.889 mm) were obtained from a wood veneer retailer. The veneer was kept in plastic bags to prevent large moisture content (MC) changes and potential surface damage. A total of 692 samples (50.8 mm x 25.4 mm x thickness) were cut from the veneer sheets for this study. The 692 samples were randomly divided into two equal groups. Samples in one group were designated for Soxhlet extraction and those in another

group were designated as unextracted controls. The samples in both groups were further divided for initiating and coupling treatments as shown in Figure 1. Prior to the coupling treatment, all veneer samples were conditioned to 5% MC in a conditioning chamber. All samples were numbered and kept in separate plastic bags before testing.

3.2.2 Soxhlet Extraction

Soxhlet extraction was conducted on the 346 prepared wood veneer samples according to the ASTM standard (ASTM D1105-96) to reduce the influence of extractives on the coupling process. The wood samples were first extracted with a solution of toluene (52 ml) and ethyl alcohol (68 ml) for 4 hours. The samples were then taken out of the solution and rinsed with ethyl alcohol in a Büchner-type filtering funnel. The cleaned samples were placed in the Soxhlet thimble again and underwent the second extraction with 120 ml of ethyl alcohol for 4 hours. The extracted wood samples were finally oven-dried at 70°C for 24 hours to reach a constant weight. The oven-dry weight of each sample was measured.

To determine graft rate and graft efficiency for MAPP-treated specimens, secondary Soxhlet extraction was conducted after coupling treatment. All treated specimens were continuously extracted with toluene (120 ml) for 24 hours. The extracted specimens were then oven-dried at 70°C for 24 hours to reach a constant weight. The oven-dry weight of each sample after extraction was measured.

3.2.3 Initiating Experiments with Toluene and BPO

Three completely randomized designs (CRD) factorial experiments were conducted as blank tests to investigate the influence of toluene and BPO on wood specimen weight changes (**A-** Figure3.1). In the first test (**A1**- 72 samples), the influence

of toluene on sample weight loss was investigated. There were two sample types (extracted and unextracted) and six dipping times. In the second (**A2-** 60 samples) and the third (**A3-** 72 samples) tests, the effects of BPO at five concentration levels in toluene solution and at six dipping times on sample weight change were studied, respectively. All these blank tests were done with six replications at each condition.

3.2.4 Coupling Treatments with MAPP

Coupling treatments with MAPPs followed the procedures developed by Felix and Gatenholm (1991). Three CRD factorial experiments (**B-** Figure 3.1) were conducted for coupling treatments. In the first experiment (**B1-** 200 specimens), the influence of MAPP type, sample condition, MAPP concentration level on retention of MAPP was investigated. Five MAPP concentration levels (i.e., 0 – control, 12.5, 25, 50, and 75 g/L) at the same dipping time of 5 min were used to treat extracted and unextracted specimens with two types of coupling agents. The relationship between dipping time and MAPP retention for extracted and unextracted specimens was investigated in the second experiment (**B2-** 144 specimens). Dipping times were 30, 100, 300, 600, 1200, and 2400 seconds. The concentration of E-43 and G-3015 in coupling agent solution was 25 g/L. In the third experiment (**B3-** 144 specimens), the influence of dipping time in MAPP solution, treating solution concentration level, MAPP type, and BPO on retention of MAPP in wood was investigated. Two coupling agent concentration levels (12.5 and 50 g/L) with and without BPO were used to treat extracted wood specimens. The dipping times were 30, 100, and 300 seconds.

For each treatment, a specified amount of MAPP pellets, based on the required concentration level, was added into the 150-ml toluene solution in a 600-ml glass beaker.

The amount of powder BPO (if added) was calculated based on a weight ratio of 0.5 between BPO and MAPP. The required BPO was weighed and added to the solution. The solution was heated on a hot plate with a magnetic stirrer until it started boiling. The temperature of the solution was kept at 100°C. After all MAPP pellets and BPO powder were dissolved in toluene, the prepared wood samples at each concentration level were placed into the solution for 5 minutes under continuous stirring with a magnetic stirrer. The treated specimens were then taken out of the beaker and cooled down to room temperature. All treated specimens were finally oven-dried at 70°C for 24 hours to reach a constant weight. The oven-dry weight of each sample was re-measured. For determination of graft rate and graft efficiency, 48 treated specimens from the 2×2×5 CRD experiment (**B11-** Figure 3.1) underwent the secondary Soxhlet extraction for 24 hours as mentioned in the above section.

Retention of coupling agent, graft rate, and graft efficiency for treated specimens were calculated as follows:

$$Rt(\%) = \frac{W_1 - W_0 - W_{BPO}}{W_0} \times 100\% \quad (3.1)$$

$$Gr(\%) = \frac{W_2 - W_0}{W_0} \times 100\% \quad (3.2)$$

$$Ge(\%) = \frac{W_2 - W_0}{W_1 - W_0 - W_{BPO}} \times 100\% \quad (3.3)$$

where, Rt = retention of coupling agent in a specimen (%);
Gr = graft rate of coupling agent in a specimen (%);
Ge = graft efficiency of coupling agent in a specimen (%);
W_0 = oven-dry sample weight after extraction and before coupling treatment (g);

W_1 = oven-dry sample weight after coupling treatment (g);
W_2 = oven-dry sample weight after coupling treatment and secondary extraction (g); and
W_{BPO} = oven-dry weight of residual BPO on a wood sample after initiating experiment (g).

The amount of residual BPO on treated specimens was calculated based on the weight change data from the second blank experiment (**A2-** Figure 3.1).

3.2.5 Contact Angle Measurement

A Kernco (Model G-1) contact angle meter was used to measure static contact angle of treated and untreated wood veneer samples. The contact angle meter consists of focusing lens, a light source, light prisms and filter slots, a goniometer inserted in the microscope, a cuvette and its adjusting system, and a body and its leveling system. With cuvette positioners, a specimen on the cuvette mounting plate can be moved horizontally and vertically to an appropriate position. The contact angle value is read after adjusting the movable scale of the goniometer to the tangent at the point of contact. The precision of measured angles in the range of 10° to 90° is within ±1% of the actual reading. Distilled water was dropped on one specimen surface through a microburette during measurement. The sessile droplet was controlled to be 0.05 ml by a micro adjuster. Three contact angle measurements were taken at each longitudinal edge on each strip (one on each end and one in the center). Twelve contact angle data points were obtained for each treatment. It took 2 to 3 seconds to complete each contact angle measurement. In this experiment, 44 specimens (including 32 treated and 12 untreated specimens) from the 2×2×5 CRD factorial experiment with coupling treatment were measured for contact angle data (**B12**- Figure 3.1).

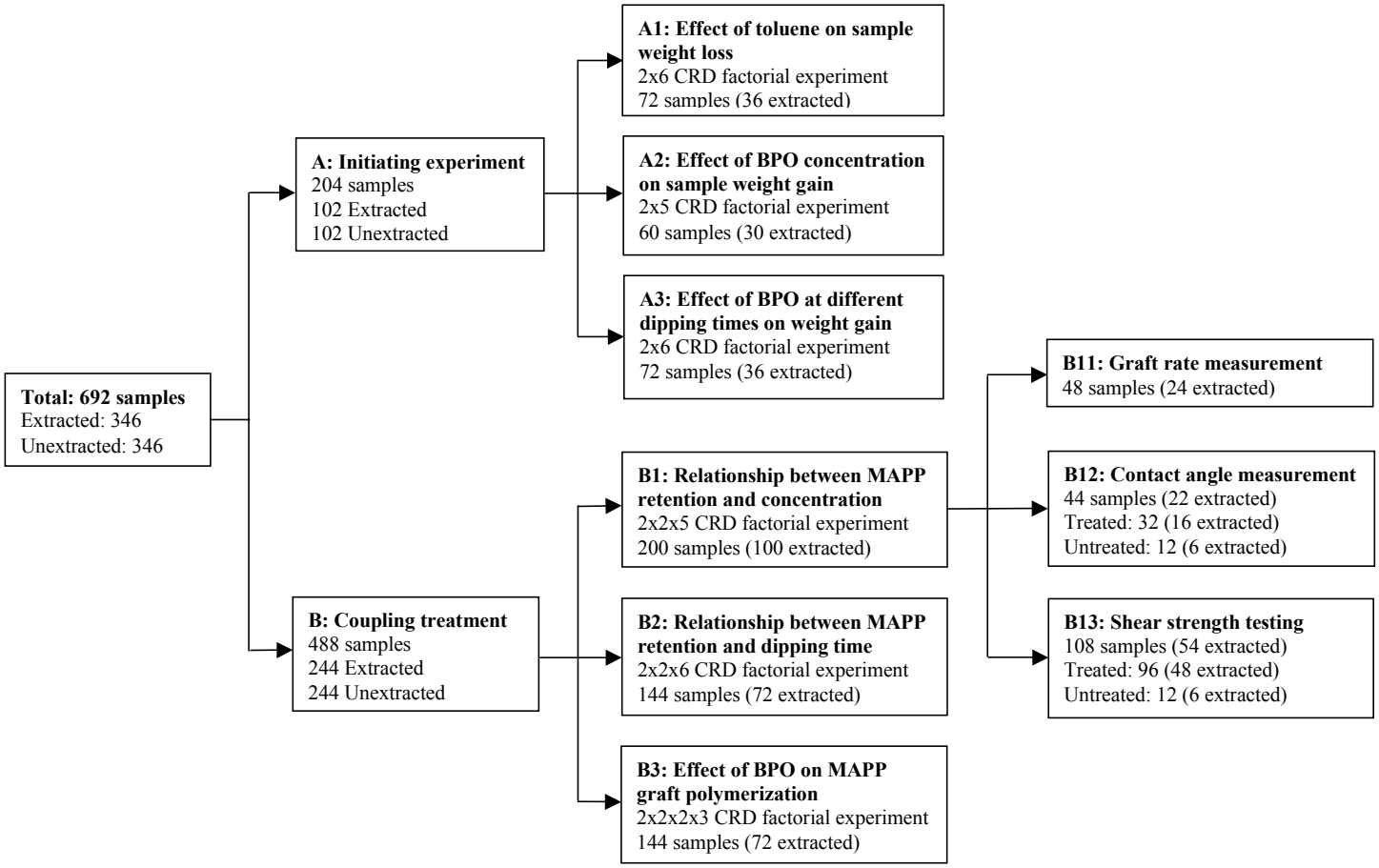

Figure 3.1. Experimental design and sample assignments. For the graft rate measurement (**B11**), all specimens underwent the secondary extraction with toluene for 24 h.

3.2.6 Interfacial Bonding Strength Measurements

Single-lap joints were created using a small-scale bonding machine to evaluate interfacial bonding strength of the wood-PVC system. The machine performs three basic functions: pressing, heating, and cooling. The pressing unit consists of two aluminum platens, two double-acting air cylinders, air pressure regulating valves, and regulated air supply. One platen is mounted on each cylinder. The double-acting cylinders allow opening and closing of the platens during pressing under controlled pressures. The heating unit consists of four 250-Watt cartridge heaters (two in each platen), two Micromega® PID temperature controllers (one controlling each platen), two solid-state relays, and two temperature sensors which provide in-process temperatures to the controllers. A separate control unit for each platen allows controlling each platen temperature within ±1°C around the set point. The cooling unit for each platen consists of unregulated water supply, water flow control valves, inlet and outlet water-lines (stainless steel tubes) connected directly to the platen. During the cooling process, the heating elements remained on and the water flow rate was adjusted to achieve desired platen temperature.

To create each wood-PVC lap joint, two prepared wood veneer samples were first selected. One line was drawn at the position of 12.7 mm from one end of each sample. One PVC sheet (12.7- by 25.4- by 0.0762-mm) was cut and placed on top of the marked end of one wood sample. The second wood sample was then placed on top of the PVC sheet with its marked end overlapping the PVC sample to create a 12.7-mm-long lap joint with a total bonding area of 323 mm^2. The lay-up was secured with two pieces of narrow Scotch tape (one placed on each side). The assembly was then inserted into the gap

between the two preheated platens in the bonding machine. It was hot-pressed under a pressure of 0.276 MPa. The pressing cycle for each specimen consisted of a three-minute heating period and a one-minute cooling period under pressure (Figure 3.2). The heating temperature was 178°C, which is 3°C higher than the melting temperature of rigid PVC. At the end of the heating period, the press platens were cooled with running tap water to 70°C, which is about 11°C less than the glass transition temperature of rigid PVC. The press was then opened and the wood-PVC laminate was removed. The laminate was allowed to cool to room temperature. Before the shear test, all manufactured laminates were conditioned to about 5% MC.

Shear tests were conducted with a Model 1125 INSTRON machine according to ASTM standards D3163 and D3165. Two mechanical tensile grips were used to clamp the sample to the loading frame. The span between the two clamps was 50.8 mm. Each sample was tested to failure at a loading speed of 2.54 mm/minute. Shear strength (Pa) was calculated as a ratio of the maximum failure load (N) to the bonding area (m^2). A total of 108 shear specimens were tested, including 12 untreated specimens used as controls (**B13-** Figure 1).

3.2.7 Data Analysis

Statistical comparisons based on analysis of variance (ANOVA) were done to test the effects of coupling agent type, initiator, dipping time, concentration, extractives, and their interaction on measured MAPP retention. A regression analysis was performed to establish the correlation between coupling agent retention and concentration of the treating solution (Wozniak and Geaghan 1994). Paraboloid regression models were used

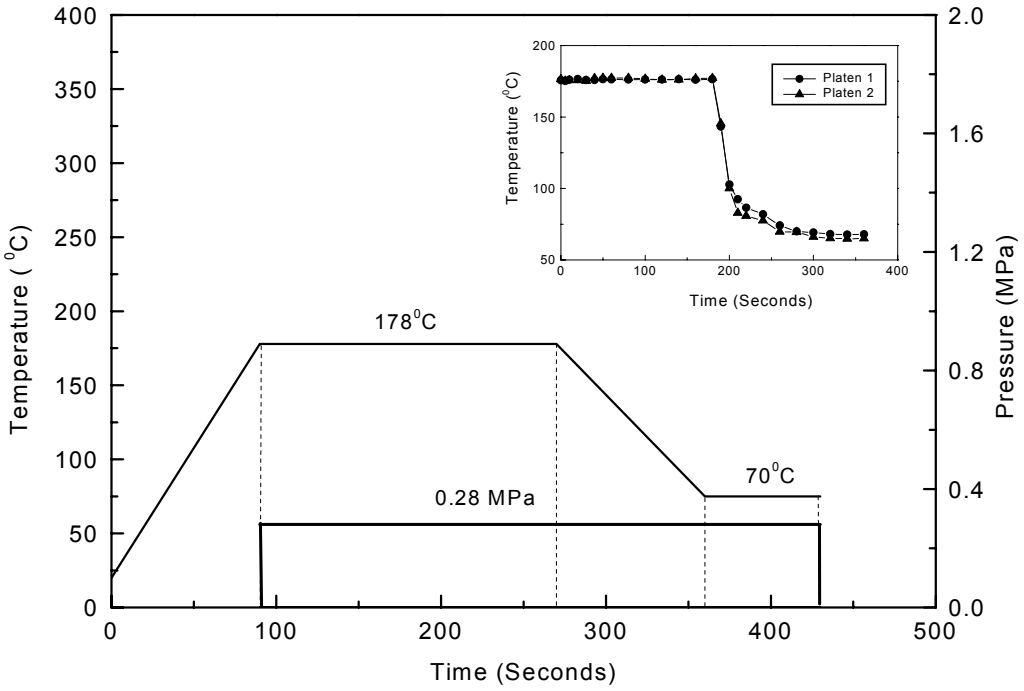

Figure 3.2. A schematic of heating, cooling and pressing procedures for manufacturing wood-PVC laminates. The inserted graph (top right) shows typical platen temperature measured during a given run.

to establish a three-dimensional relationship among graft rate, concentration, and retention for MAPP treated specimens.

3.3 RESULTS AND DISCUSSION

The extractive composition and the primary color component of yellow poplar were listed in Table 3.1. Experimental results on coupling agent retention, graft rate, contact angle, and shear strength of wood-PVC composites are summarized in Table 3.2. Results of ANOVA for the effects of coupling agent type, concentration levels, dipping time, initiator, Soxhlet extraction, and their interactions on retention are shown in Tables 3.3 and 3.4, respectively.

Table 3.1. Extractive composition in yellow poplar veneer.

Lumber	Physical appearance	Extractives by Soxhlet extraction		Liriodenine (wt%) [b, c]	Estimated liriodenine in extractives (%) [d]
		(mg/g) [a]	(wt%) [a, b]		
Sapwood	Pale yellow or white	7.37 (6.66)	1.74 (1.70)	0.13-0.27	7.98-16.57
Heartwood	Light or bright yellow	29.43 (6.05)	5.56 (1.32)	0.43-0.58	8.04-10.85

[a] The values in the parenthesis are standard deviations.
[b] wt% indicates the weight percentage of oven-dried wood specimens.
[c] The data are cited from the results by Mutton (1962).
[d] The values are calculated on average according to the data in columns 3 and 5. The average oven-dried weight of wood specimens was 0.551 g.

3.3.1 Adsorption of MAPP on Wood Surface

Weight losses of wood specimens occurred for specimens treated with toluene, because extractives, including resin acids, fatty acids, waxes, tannins, and coloring

Table 3.2. Experimental results for retention of coupling agent, contact angle data, and shear strength in wood-PVC systems [a,b].

Coupling Agent	Concentration (g/L)	Retention of MAPP (wt%) [c]		Graft rate (wt%) [c]		Initial contact angle (Degree) [d]		Shear strength (kPa) [d]	
		Unextracted	Extracted	Unextracted	Extracted	Unextracted	Extracted	Unextracted	Extracted
E-43	0.0	0	0	0	0	83.8 (10.3) [e]	63.6 (6.3) [e]	2977 (157)	3141 (376)
	12.5	2.16 (0.24)	2.95 (0.15)	2.06 (0.54)	1.96 (0.24)	112.6 (3.0)	102.4 (2.6)	3061 (90)	2902 (290)
	25.0	3.64 (0.51)	4.12 (0.94)	2.49 (0.20)	2.42 (0.21)	97.5 (2.4)	94.9 (2.6)	3040 (186)	3033 (221)
	50.0	7.14 (1.07)	6.83 (1.08)	3.25 (0.12)	2.86 (0.36)	92.1 (2.4)	85.0 (5.2)	3597 (160)	3316 (290)
	75.0	8.05 (1.14)	7.41 (1.16)	1.85 (0.07)	2.75 (0.21)	87.1 (2.3)	79.1 (3.6)	3572 (179)	3710 (103)
G-3015	0.0	0	0	0	0	83.8 (10.3) [e]	63.6 (6.3) [e]	2977 (157)	3141 (376)
	12.5	1.89 (0.43)	2.17 (0.07)	1.74 (0.34)	2.06 (0.18)	120.8 (3.2)	124.0 (2.6)	3123 (248)	2903 (207)
	25.0	3.49 (0.20)	3.64 (0.81)	2.15 (0.35)	2.63 (0.35)	121.1 (1.9)	122.1 (1.6)	3261 (283)	2937 (110)
	50.0	6.02 (1.34)	6.35 (1.03)	2.60 (0.70)	3.08 (0.78)	122.0 (1.7)	123.0 (2.1)	3723 (131)	3606 (227)
	75.0	9.48 (1.52)	10.54 (1.06)	1.77 (0.57)	2.74 (0.62)	122.1 (2.3)	123.3 (2.9)	3847 (159)	3847 (296)

[a] Un-extracted and Extracted indicate Non-Soxhlet extracted and Soxhlet extracted before coating.
[b] The values in parentheses are standard deviations.
[c] Weight percentage of oven-dried wood samples.
[d] Moisture content of all specimens was between 4% and 6%.
[e] Contact angle of distilled water on untreated yellow poplar veneer.

matters (Fengel and Wegener 1984), were removed easily from wood under high temperatures by toluene (Figure 3.3). For unextracted specimens, sample weight loss increased with increases of dipping time. However, the curve leveled off after dipping time increased beyond 10 min. The weight loss for Soxhlet -extracted specimens was in the range of 0.3-0.4%, independent of dipping time.

As the dipping time increased, BPO was precipitated on the sample surface, which resulted in a weight increase for treated wood specimens. Under short dipping times, weight change was less than 0.5 weight percent of the oven-dried wood specimens (Figure 3.4a). For instance, there was little BPO deposition on unextracted and extracted wood specimens when dipping time was less than 5 min. Accordingly, the weight change caused by solvent and BPO can be neglected when dipping time was less than 5 min. However, weight gain resulted from BPO deposition greatly increased under long dipping periods for both extracted and unextracted specimens. The amount of BPO was larger than 1% when dipping time was over 10 min. The weight increase resulting from BPO deposition increased with the increase of BPO concentration in toluene for both extracted and unextracted wood specimens (Figure 3.4b). The percentage of weight gain was larger than 1% when the concentration level was larger than 20 g/L. Thus, an adjustment for coupling agent retention was required to reduce the influence of residual BPO. In this study, Figure 3.4b was used as a reference to adjust the retention of MAPP.

The initiator, BPO, acted differently on MAPP adsorption at different treating solution concentration levels (Figure 3.5). At the low concentration level (i.e., 12.5 g/L), the coupling treatment with BPO did not significantly increase MAPP retention on wood surface. For both MAPPs, the retention level difference between specimens with BPO

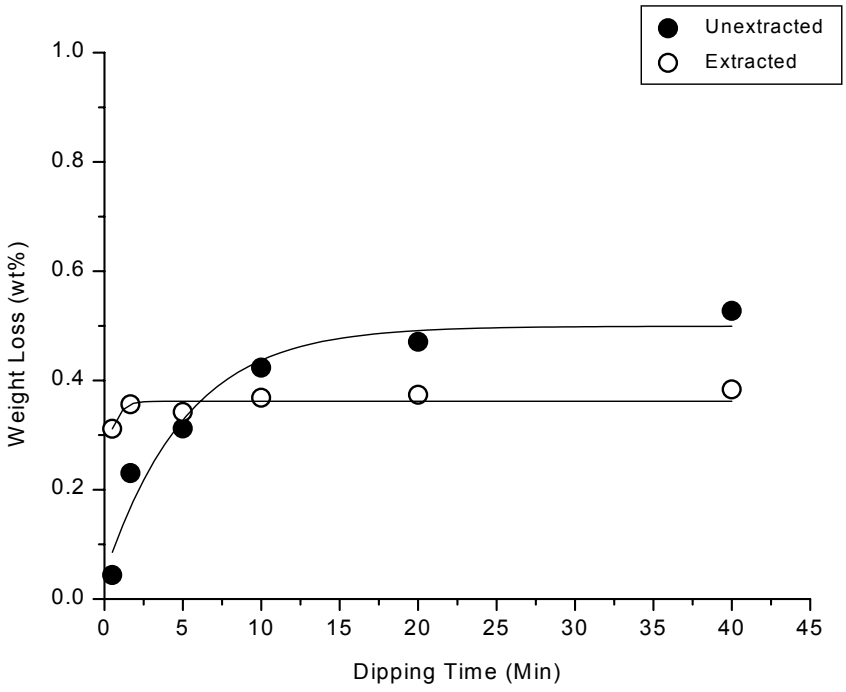

Figure 3.3. Effect of toluene on weight change of treated wood specimens at different dipping time.

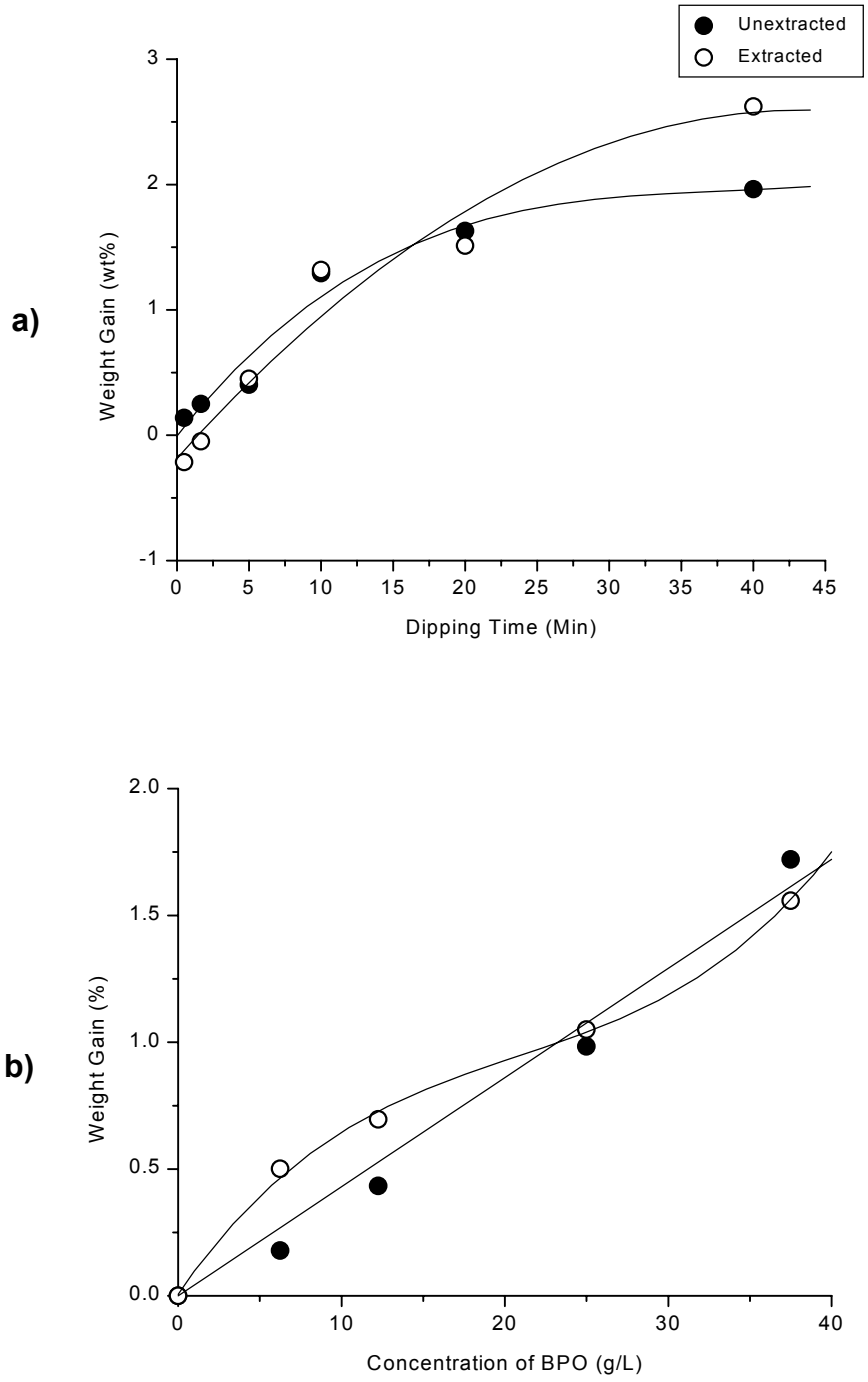

Figure 3.4. Effect of BPO solution on weight change of treated wood specimens at a) different dipping time (The concentration level of BPO was 30 g/L in toluene solution) and b) different concentration levels (Dipping time was 5 min).

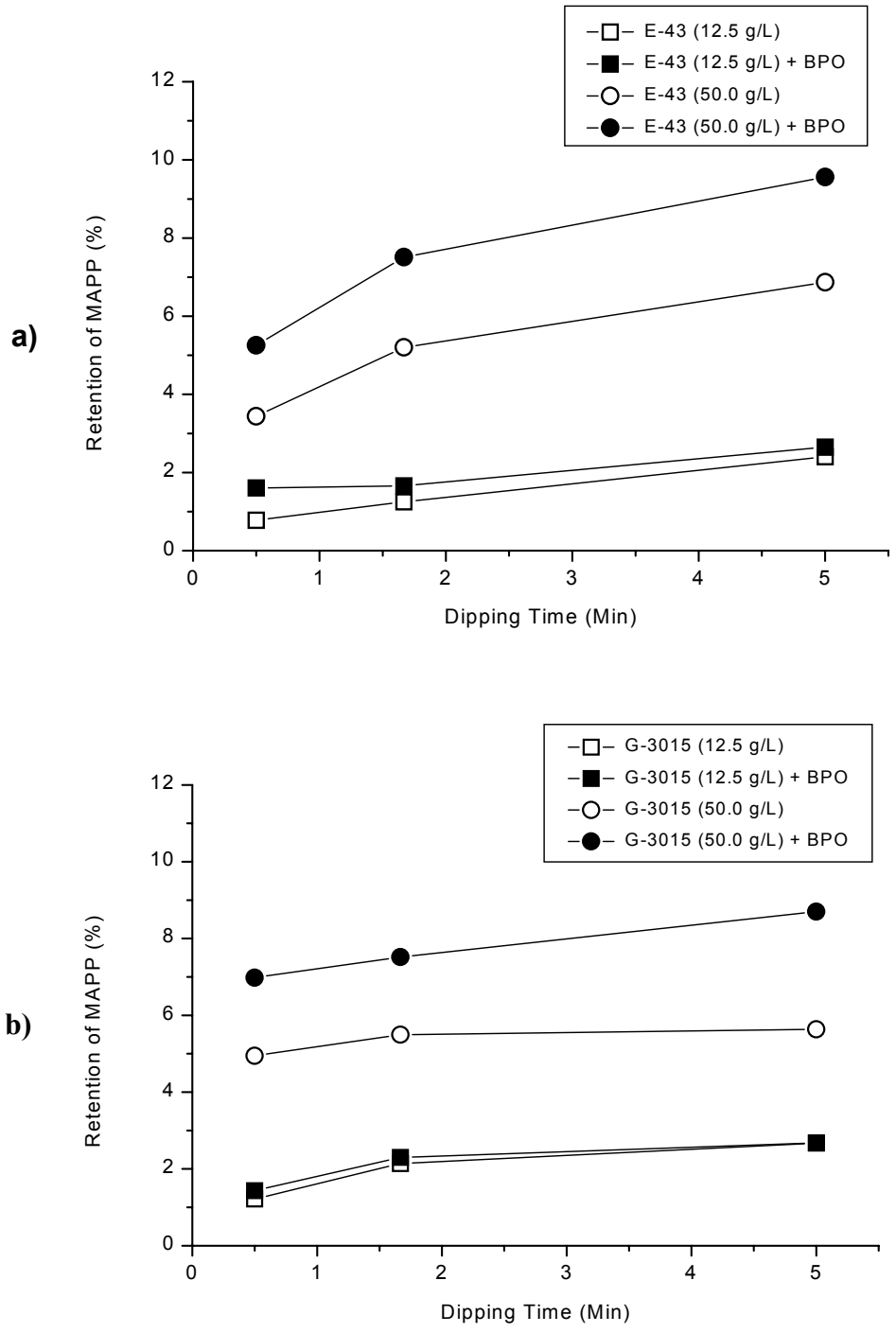

Figure 3.5. Effect of BPO and dipping time on retention for extracted wood specimens treated with different MAPPs. a) E-43 and b) G-3015. All wood specimens were Soxhlet-extracted before coupling treatment.

and without BPO increased with increases of dipping times (Figures 3.5a and 3.5b). At the high MAPP concentration level (i.e., 50 g/L), the retention level difference increased with increases of dipping times. It reached the maximum value (2 weight percent) at the dipping time of 5 min. Therefore, BPO helped improve the adsorption of MAPP by wood under high concentration levels and long dipping times.

The relationship between dipping time and MAPP retention in wood specimens is shown in Figure 3.6. At the concentration level of 25 g/L MAPP, MAPP retention increased with the increase of dipping time. The effect leveled off after dipping time was longer than 20 min (Figure 3.6). The retention on extracted specimens was larger than that of unextracted specimens at the same dipping time. At short dipping times, there was no significant retention difference between extracted and unextracted specimens. However, retention on extracted specimens was larger than that of unextracted specimens for long dipping periods. For example, the retention difference between extracted and unextracted specimens was over 1.5% when dipping time was over 10 min. This implied that extractives in yellow poplar influenced the adsorption of MAPP on wood specimens. According to the four-way ANOVA (Table 3.3), the main effects of coupling agent type, treating solution concentration, BPO, and dipping time were significant on adsorption of MAPP at the 5% significance level. The interaction effects between coupling agent and dipping time, between BPO and concentration, between concentration and dipping time, and among coupling agent, BPO, and dipping time were also significant. However, other interaction effects were not significant.

The retention of MAPP on wood samples was proportional to the concentration levels in the solution for both coupling agents (Table 3.2). For G-3015, there was a linear

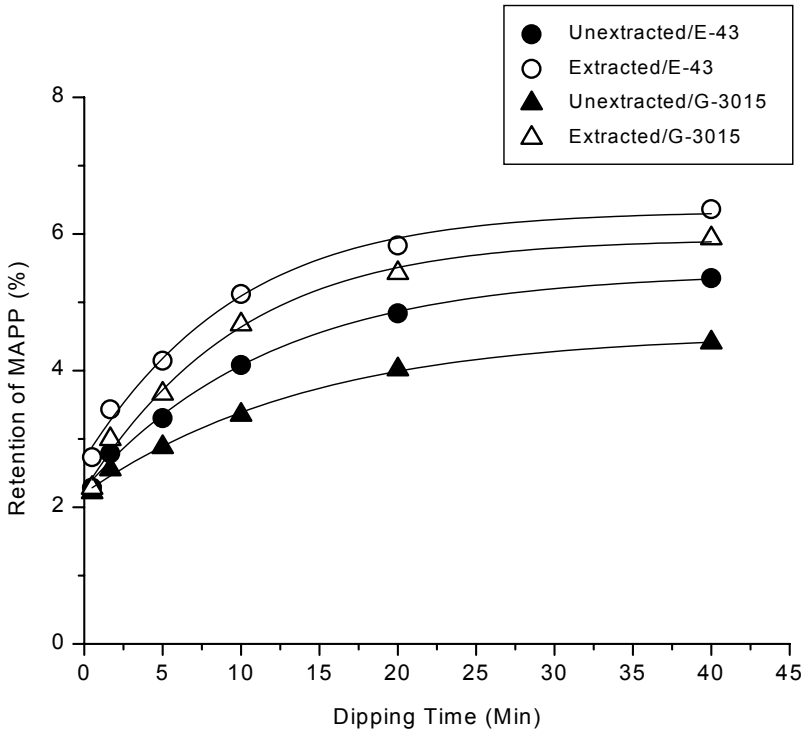

Figure 3.6. Relationship between dipping time and retention for MAPP-treated wood specimens. The concentration level of MAPP was 25 g/L.

Table 3.3. Four-way ANOVA for MAPP adsorption on wood specimens [a].

Source	DF	Sum of squares	Mean square	F Value	Pr>F
Model	23	962.9673564	41.8681459	61.54	0.0001
MAPP	1	3.4727565	3.4727565	5.10	0.0257
BPO	1	64.5665816	64.5665816	94.90	0.0001
MAPP*BPO	1	0.2452065	0.2452065	0.36	0.5494
Concentration	1	730.5542275	730.5542275	1073.77	0.0001
MAPP*Concentration	1	0.0501835	0.0501835	0.07	0.7864
BPO*Concentration	1	38.0641698	38.0641698	55.95	0.0001
MAPP*BPO*Concentration	1	0.3618424	0.3618424	0.53	0.4673
Time	2	90.2981282	45.1490641	66.36	0.0001
MAPP*Time	2	11.2037347	5.6018673	8.23	0.0004
BPO*Time	2	0.5086661	0.2543267	0.37	0.6889
MAPP*BPO*Time	2	0.2953047	0.1476523	0.22	0.8052
Concentration*Time	2	8.5649901	4.28284951	6.29	0.0025
MAPP*Concentration*Time	2	11.5708903	5.7854451	8.50	0.0004
BPO*Concentration*Time	2	2.7397087	1.3698543	2.01	0.1380
MAPP*BPO*Concentration*Time	2	0.470967	0.2354883	0.35	0.7081
Error	120	81.6434216	0.6803618		

[a] MAPP-maleated polypropylene; BPO-Benzoyl peroxide; Concentration-Concentration of MAPP; Time-Dipping time.

relationship between concentration and retention for unextracted and extracted veneer samples (Figure 3.7a). Retention of E-43, however, followed a polynomial relationship with treating solution concentration (Figure 3.7b). The E-43 retention was larger than that of G-3015 at low concentration levels, but it was lower than that of G-3015 as the concentration levels increased.

The retention of MAPP on wood samples was related to physical adsorption and graft rate. For E-43, a larger number of maleic anhydride groups provided more opportunities for graft reaction. This led to a relatively rapid deposition of the coupling agents on wood surfaces through graft copolymerization. This graft reaction may be

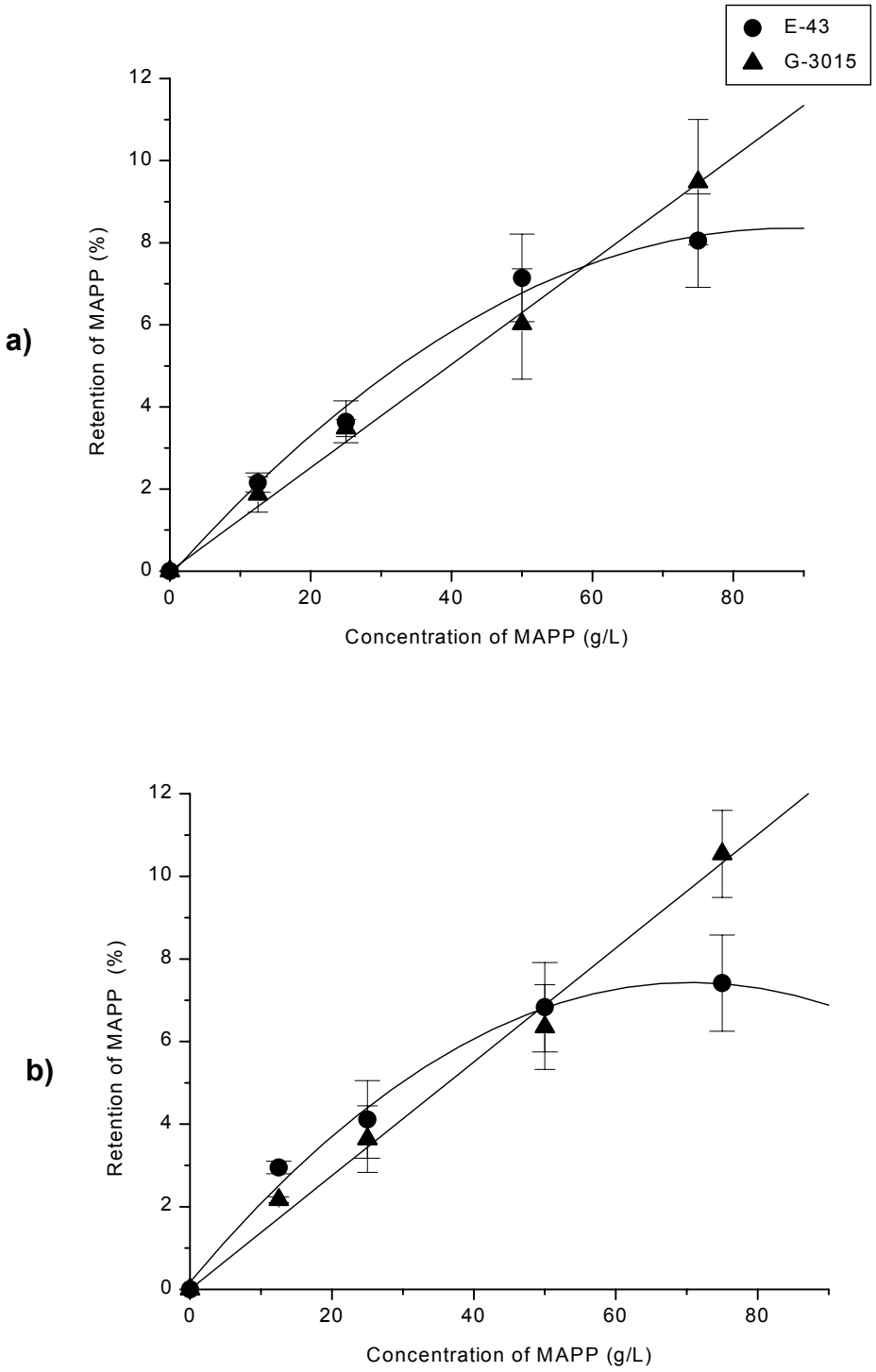

Figure 3.7. Retention of MAPP on treated yellow-poplar veneer samples. a) Wood specimens were not Soxhlet-extracted before coupling treatment and b) Wood specimens were Soxhlet-extracted before coupling treatment. Dipping time was 5 min.

dominant at low concentration levels. However, graft sites on wood surfaces are limited for MAPP even at high treating solution concentrations. Excessive ungrafted or non-reacted maleic anhydride (MA) groups interfered with the graft reaction, thus resulting in a negative retention rate at high concentration levels. For G-3015, there was a relatively constant retention rate throughout the whole concentration range. This shows that yellow poplar veneer absorbed G-3015 well. Accordingly, maleated polymer with high molecular weight and small acid number can be easily absorbed by wood.

There was about 4 weight percent of extractives on average as determined by Soxhlet extraction (Table 3.1). The ether-soluble extractives (mainly liriodenine) are the primary color element of yellow poplar (Buchanan and Dickey 1960). The weight percentage of liriodenine in yellow poplar sapwood and heartwood is about 0.13-0.27% and 0.43-0.58% respectively (Mutton 1962). Hence, liriodenine accounts for 10-12% of the total extractives on average (Table 3.1). These extractives had different effects on the adsorption of MAPP on wood veneer for different coupling agents. At low concentration, the retention of E-43 on unextracted veneers was lower than that on extracted veneer. For G-3015, Soxhlet extraction helped improve the coupling agent retention on wood samples (Table 3.2).

According to the three-way ANOVA (Table 3.4), the main effects of concentration and Soxhlet extraction were significant on retention of the coupling agent at the 5% significance level. The interaction effects between Soxhlet extraction and coupling agent and between concentration and coupling agent were also significant. The main effect of coupling agent and all other interaction effects were, however, not significant (Table 3.4). The regression analysis provided excellent fits between coupling

agent and treating solution concentration for both E-43 and G-3015 (Table 3.5 and Figure 3.7).

Table 3.4. Three-way ANOVA for retention of coupling agent MAPP [a].

Source	DF	Sum of squares	Mean square	F value	Pr > F
Model	19	1739.2375	91.5388	107.79	0.0001
MAPP	1	1.6224	1.6224	1.91	0.1708
Concentration	4	1608.3816	402.0954	473.76	0.0001
MAPP*Concentration	4	101.5068	25.3767	29.88	0.0001
Extraction	1	3.6291	3.6291	4.27	0.0420
MAPP*Extraction	1	4.7609	4.7609	5.61	0.0203
Concentration*Extraction	4	4.3677	1.0919	1.29	0.2826
MAPP*Concentration*Extraction	4	3.6839	0.9210	1.08	0.3699
Error	80	67.9412	0.8493		

[a] MAPP-Maleated polypropylene; Concentration-Concentration of MAPP; Extraction-Soxhlet extraction before coating.

3.3.2 Graft Rate and Graft Efficiency

The fixation of coupling agent on wood materials is mainly related to graft rate and graft efficiency. In general, the graft rate increased with concentration and retention, and it decreased after reaching its maximum value for both MAPPs. Graft efficiency decreased with the increase of the concentration and retention (Figures 3.8 and 3.9). Due to large differences of MA contents in the MAPP backbone, E-43 acted as an anionic polymer in toluene solution and G-3015 worked more like a nonionic polymer. Therefore, they had different graft reactions on wood.

For unextracted wood specimens, E-43 had higher graft rate and efficiency than G-3015 at most concentration levels (Figures 3.8a and 3.8c). It was due to the fact that E-

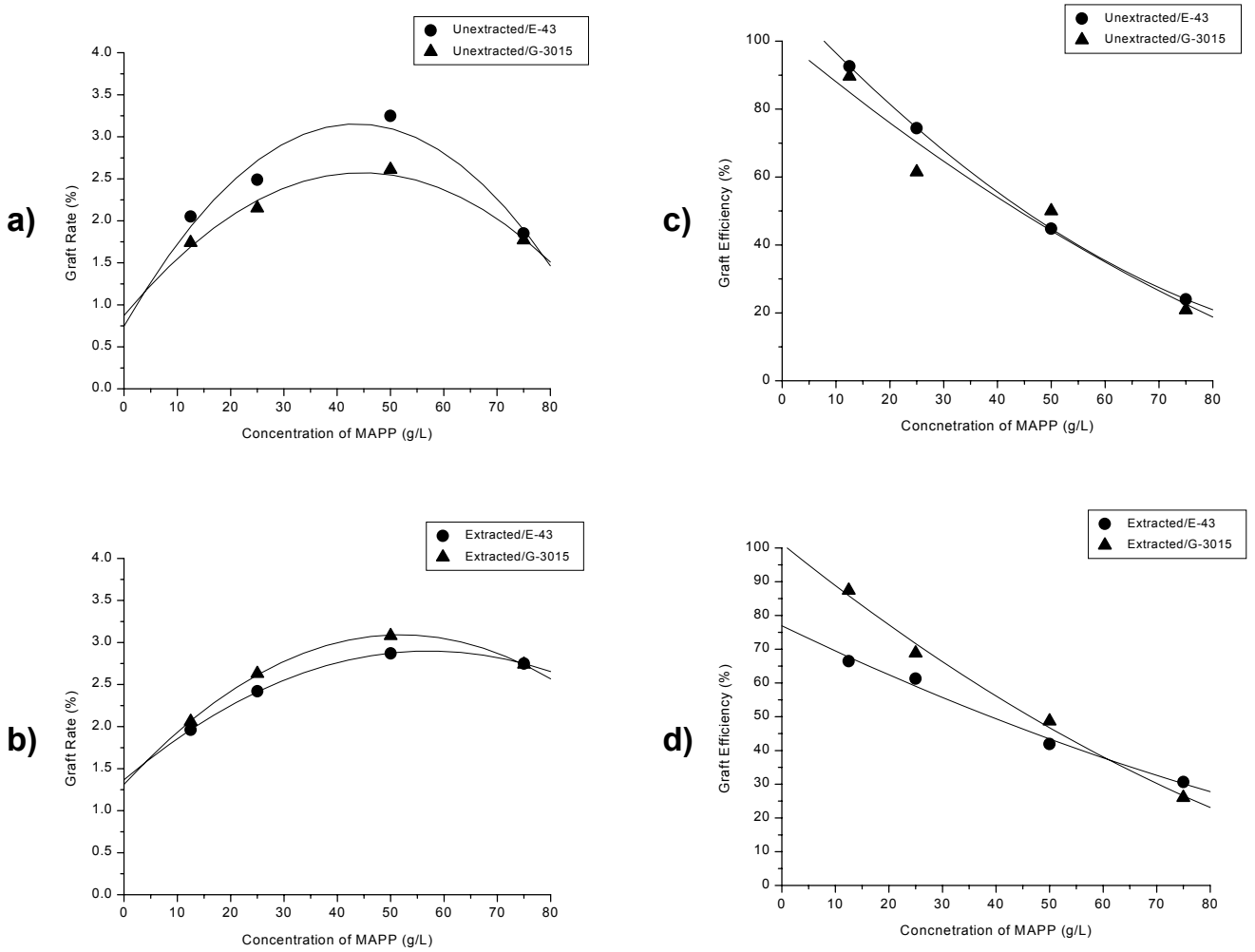

Figure 3.8. Relationships of concentration with graft rate and graft efficiency of MAPP. The dipping time was 5 min.

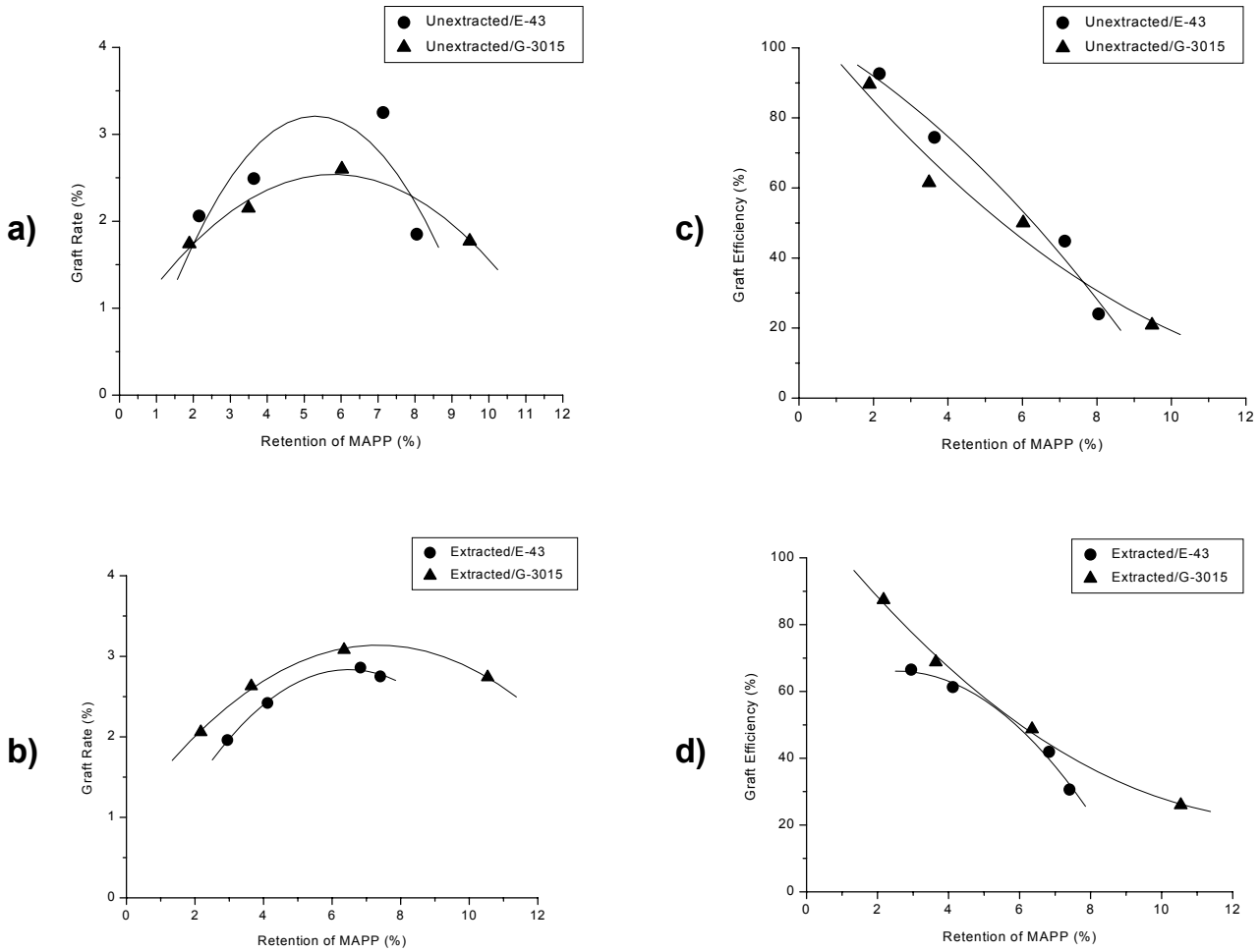

Figure 3.9. Relationships of retention with graft rate and graft efficiency. The dipping time was 5 min.

43 has a higher acid number than G-3015 (i.e., E-43 contains more MA groups in its molecular chains), which is helpful for graft reaction. Under the initiator BPO, more graft sites on wood reacted with E-43. However, it was different for extracted wood specimens. G-3015 had higher graft rate and graft efficiency than E-43 at most

Table 3.5. Relationship between concentration and retention of coupling agent [a]

MAPP	Extraction before coating	Regression for MAPP retention [b]	R-value	Standard deviation
E-43	Unextracted	$Rt(\%) = -0.1083 + 0.1926C - 0.0011C^2$	0.996	0.3893
	Extracted	$Rt(\%) = 0.1744 + 0.2056C - 0.0014C^2$	0.996	0.3893
G-3015	Unextracted	$Rt(\%) = 0.12602C$	0.999	0.2630
	Extracted	$Rt(\%) = 0.1377C$	0.998	0.3780

[a] Dipping time was 5 min.
[b] Rt- Retention of coupling agent, wt% and C – Concentration of coupling agent, g/L.

concentration levels (Figures 3.8b and 3.8d). Although more hydroxyl groups were exposed on wood surfaces after Soxhlet extraction, the electrostatic blocking effect (Tanaka et al. 1999) significantly resisted the graft reaction for E-43. It was also attributed to the inhibitor effect of coupling agent at high concentration (Maldas and Kokta 1989; Lu et al. 2000). The relationships of retention with graft rate and graft efficiency were similar to those of concentration with graft rate and graft efficiency (Figure 3.9).

The relationship among graft rate, concentration, and retention followed paraboloid regression models for both MAPPs (Figure 3.10). The shapes of distributions with these three factors for E-43 and G-3015 were similar. Graft rate was proportional to concentration and retention of MAPP at low concentration and low retention levels and reached its maximum value, and then decreased at high concentration and high retention levels. Graft rate had a parabolic relationship with concentration and retention for both MAPPs. Retention had a linear relationship with G-3015 and polynomial with E-43. The curved surfaces for extracted wood specimens had a smaller curvature than that for unextracted specimens. All these features are illustrated with the two-dimensional relationships between retention and concentration, between graft rate and concentration, and between graft rate and retention, respectively (Figures 3.7, 3.8, and 3.9). The paraboloid models used in this study provided excellent fits among graft rate, concentration, and MAPP retention for treated wood specimens (Figure 3.10 and Table 3.6).

3.3.3 Wettability

For untreated wood veneers, both extracted and unextracted specimens showed a similar wetting behavior (Table 3.7 and Figure 3.11). After being dropped on a wood surface, water droplets spread and penetrated into a porous wood surface. Thus, contact angles gradually decreased with the increase of wetting time until wood surface was completely wetted. Compared with unextracted samples, extracted yellow poplar had a smaller initial contact angle, but the contact angle was almost the same at 60 seconds. Extracted specimens had a smaller difference between the initial contact angle and the contact angle at 60 seconds than unextracted samples. Also, initial contact angles on

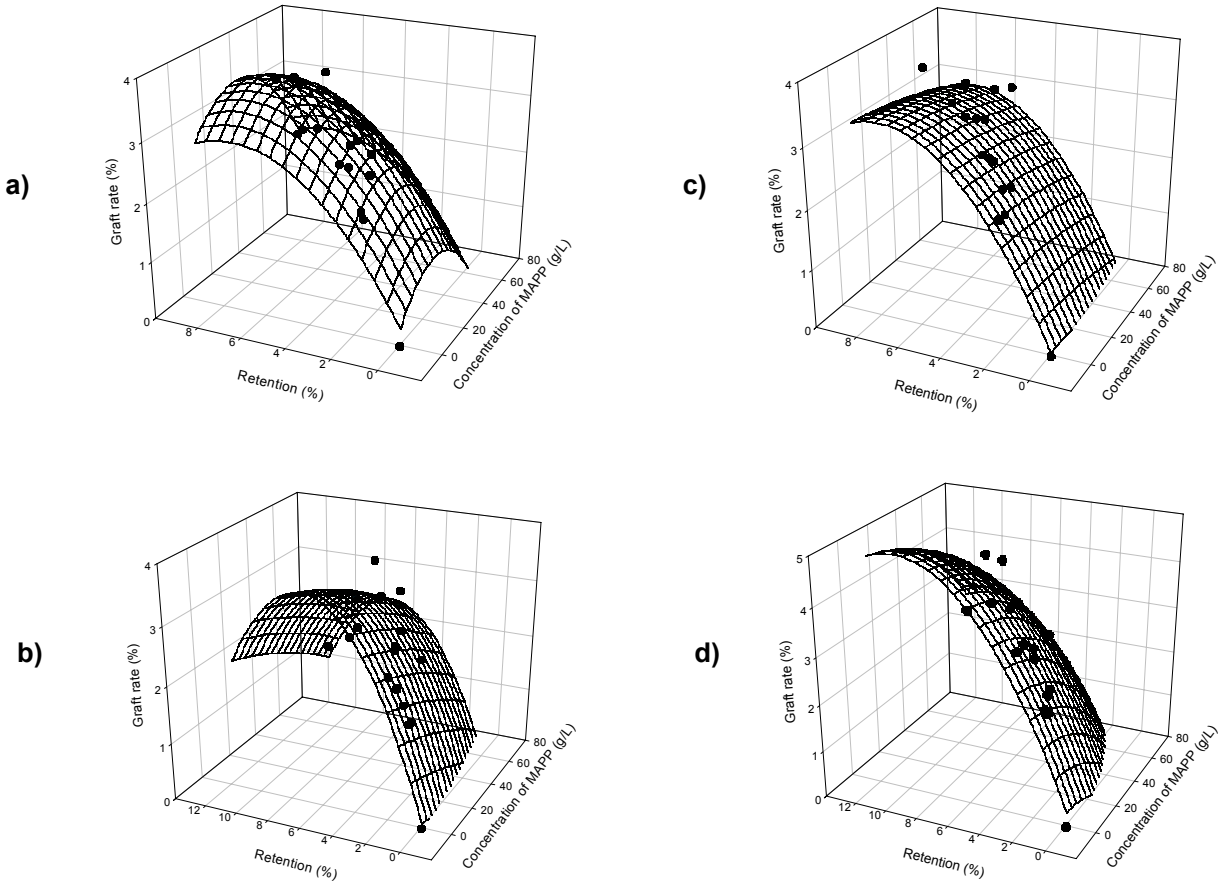

Figure 3.10. Relationship among graft rate, concentration, and retention of MAPP. a) E-43/Untreated, b) G-3015/Untreated, c) E-43/Extracted, and d) G-3015/Extracted. The dipping time was 5 min.

Table 3.6. Relationship among graft rate, concentration, and retention of coupling agent [a]

MAPP	Extraction before coating	Regression for MAPP graft rate [b]	R-value	Standard deviation
E-43	Unextracted	$Gr(\%) = 0.3096+0.0422C+0.6986Rt-0.0007C^2-0.0472Rt^2$	0.877	0.4694
	Extracted	$Gr(\%) = 0.0545-0.0018C+0.8079Rt+0.0001C^2-0.0510Rt^2$	0.959	0.2470
G-3015	Unextracted	$Gr(\%) = 0.0746-0.0107C+0.9713Rt-0.0001C^2-0.0674Rt^2$	0.920	0.3400
	Extracted	$Gr(\%) = 0.03026-0.0048C+0.8677Rt-0.0003C^2-0.0409Rt^2$	0.887	0.4631

[a] Dipping time was 5 min.
[b] Gr-Graft rate of coupling agent, wt%, Rt- Retention of coupling agent, wt %, and C – Concentration of coupling agent, g/L.

extracted yellow poplar had smaller standard deviations than that on unextracted (Table 3.7). This behavior indicated that wood surface chemical composition and structure (e.g., polarity and roughness) influenced the wettability of yellow poplar veneer.

Compared with untreated specimens, samples treated with MAPP had more uniform contact angles with smaller standard deviations (Table 3.7). Since the rough and void wood surfaces were covered with a thin and uniform polymer film, wetting variations caused by extractives, annual rings, heartwood and sapwood, grain orientations, and other macroscopic characters of wood were decreased. Accordingly, extractives did not have significant influence on initial contact angles and dynamic contact angles for MAPP-treated specimens (Table 3.7). This agreed with the results reported by Felix and Gatenholm (1991).

Table 3.7. Contact angle of distilled water on modified wood specimens with different treatments [a].

MAPP	Soxhlet extraction before coupling treatment	Retention of MAPP (wt%) [b]	Graft rate (wt%) [b]	Contact angle (Degree)			
				After coupling treatment		After secondary Soxhlet extraction [c]	
				0 second	60 seconds	0 second	60 seconds
E-43	Unextracted	0	0	83.8 (10.3)	56.6 (13.2)	83.8 (10.3)	56.6 (13.2)
		2.16 (0.24)	2.06 (0.54)	112.6 (3.0)	50.4 (7.6)	125.1 (2.2)	105.0 (4.2)
		3.64 (0.51)	2.49 (0.20)	97.5 (2.4)	30.9 (3.4)	121.1 (1.9)	87.1 (10.5)
		7.14 (1.07)	3.25 (0.12)	92.1 (2.4)	29.0 (4.4)	119.5 (3.3)	70.9 (10.0)
		8.05 (1.14)	1.85 (0.07)	87.1 (2.3)	27.5 (6.8)	122.6 (2.3)	73.1 (11.7)
	Extracted	0	0	63.6 (6.3)	56.0 (8.2)	63.6 (6.3)	56.0 (8.2)
		2.95 (0.15)	1.96 (0.24)	102.4 (2.6)	55.9 (8.1)	125.0 (2.4)	115.0 (2.6)
		4.12 (0.94)	2.42 (0.21)	94.9 (2.6)	44.3 (3.8)	126.0 (1.9)	98.1 (9.2)
		6.83 (1.08)	2.86 (0.36)	85.0 (5.2)	34.9 (4.3)	122.9 (3.4)	76.3 (8.1)
		7.41 (1.16)	2.75 (0.21)	79.1 (3.6)	34.0 (5.6)	121.9 (4.6)	63.3 (9.1)
G-3015	Unextracted	0	0	83.8 (10.3)	56.6 (13.2)	83.8 (10.3)	56.6 (13.2)
		1.89 (0.43)	1.74 (0.34)	120.8 (3.2)	116.9 (4.9)	129.6 (0.6)	124.0 (0.9)
		3.49 (0.20)	2.15 (0.35)	121.1 (1.9)	117.6 (2.1)	128.5 (0.9)	122.8 (1.0)
		6.02 (1.34)	2.60 (0.70)	122.0 (1.7)	119.0 (1.4)	129.1 (1.5)	122.4 (1.4)
		9.48 (1.52)	1.77 (0.57)	122.1 (2.3)	120.1 (2.5)	125.0 (2.4)	122.9 (1.6)
	Extracted	0	0	63.6 (6.3)	56.0 (8.2)	63.6 (6.3)	56.0 (8.2)
		2.17 (0.07)	2.06 (0.18)	124.0 (2.6)	121.1 (2.6)	123.1 (3.0)	118.8 (2.1)
		3.64 (0.81)	2.63 (0.35)	122.1 (1.6)	118.6 (1.3)	123.1 (2.6)	115.6 (3.9)
		6.35 (1.03)	3.08 (0.78)	123.0 (2.1)	119.0 (2.2)	123.6 (3.1)	117.8 (5.4)
		10.54 (1.06)	2.74 (0.62)	123.3 (2.9)	119.1 (3.3)	125.1 (3.2)	120.0 (3.6)

[a] The values in parentheses are standard deviation.
[b] Weight percentage of the oven-dried wood specimen.
[c] All MAPP treated specimens were extracted with toluene for 24 hours.

The initial contact angles on specimens treated with E-43 were smaller than those treated with G-3015. For specimens treated with E-43, initial contact angles decreased with increases of E-43 retention for both extracted and unextracted specimens (Figures 3.11a and 3.11b). Similar to the case of untreated specimens, contact angles on unextracted specimens had a large drop (about 60°) in 60 seconds, while there was a smaller drop (about 50°) on extracted specimens over the same wetting period. As a result, specimens treated with E-43 had a wetting behavior similar to untreated wood.

For G-3015, measured contact angles on treated samples were independent of the retention levels of the coupling agent. The contact angles were 122° on average for both extracted and unextracted samples. Wood samples treated with G-3015 showed good compatibility with PVC even at low concentrations. Water droplets did not spread on treated wood surfaces and did not wet them. For both extracted and unextracted specimens, there were little changes on initial contact angle at each retention level after the wetting time increased to 60 seconds (Figures 3.11a and 3.11b). Therefore, veneers treated with G-3015 acted more like thermoplastics.

For specimens treated with E-43, initial contact angles were reduced to less than 110° in 2 to 3 seconds, and the contact angle drop increased with the increase of E-43 retention, especially at the high retention levels (Figures 3.11a and 3.11b). However, G-3015 treated specimens had stable contact angles. In 60 seconds, contact angles on G-3015-treated specimens decreased only by 3-5° on average (Table 3.7). Hence, water droplets had a low wetting speed on G-3015 treated specimens, while they had a high wetting speed on E-43-treated specimens, which was related to the surface polarity of treated specimens. Increases of E-43 retention resulted in the wetting acceleration on

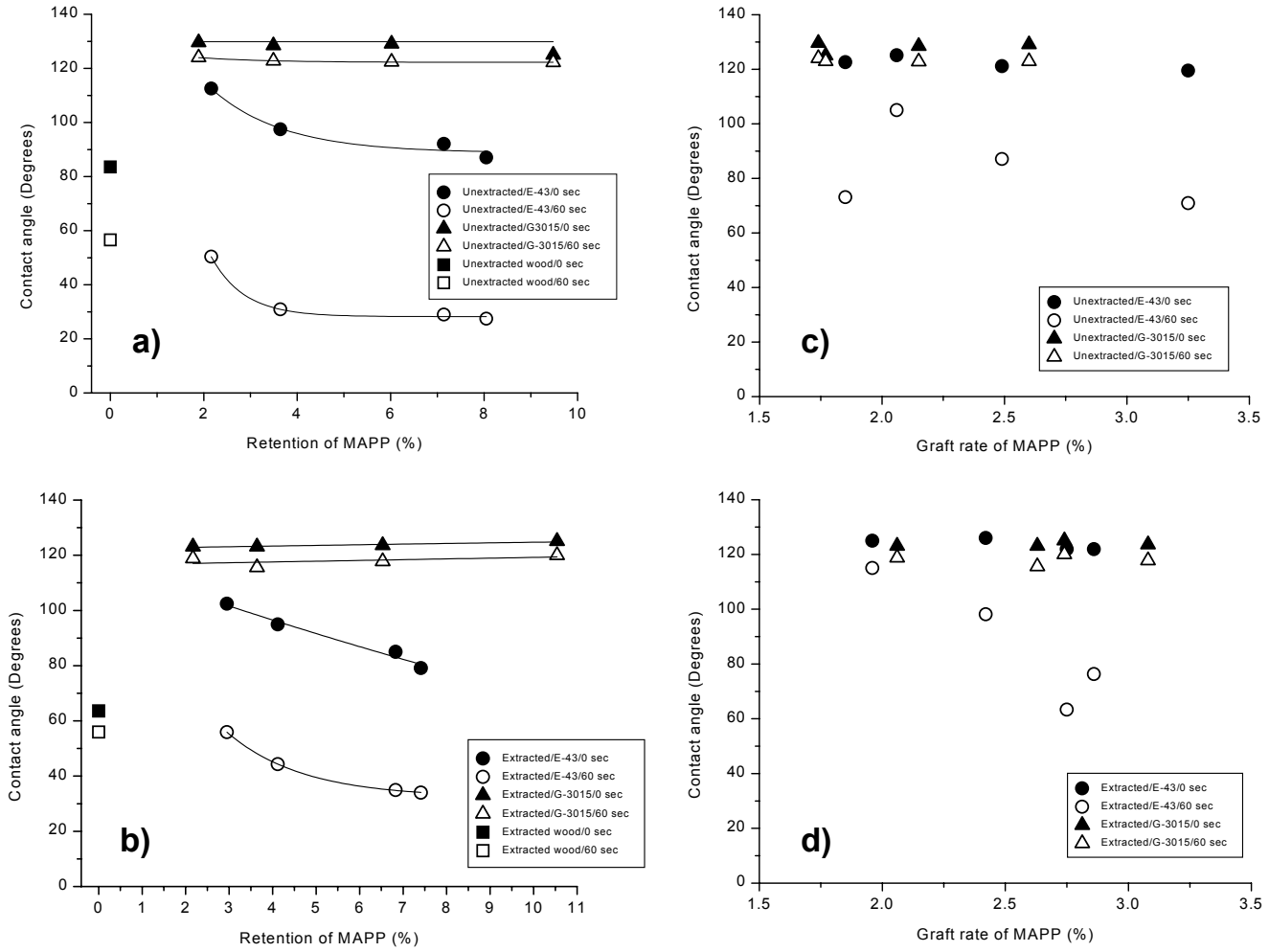

Figure 3.11. Relationships of contact angle with retention and graft rate of MAPP.

treated specimens. However, the wetting speed on G-3015-treated specimens was almost constant and independent of G-3015 retention. Compared with the results by Felix and Gatenholm (1991), measured initial contact angles on E-43-treated specimens might be less than actual contact angles. Initial contact angles on specimens treated with E-43 would be independent of the retention level, similar to the case of G-3015.

After removing the ungrafted MAPP from wood by secondary Sohxlet extraction, initial contact angles were over 120° on average and independent of graft rate for E-43- and G-3015-treated specimens (Table 3.7). For G-3015 treated specimens, the contact angles at 60 seconds were over 120° on average and independent of graft rate. In the case of E-43, however, contact angles at 60 seconds decreased with the increase of graft rate (Figures 3.11c and 3.11d). Therefore, grafted E-43 contained ungrafted MA groups in its molecular chains and the amount of ungrafted MA groups increased with the increase of graft rate. Some ungrafted MA groups may exist as the free MA groups in the succinic half-ester structure (Kishi et al. 1988; Felix and Gatenholm 1991).

In summary, samples treated with E-43 and G-3015 had different wetting behaviors. Contact angles on E-43-treated veneer samples decreased with increases of retention and wetting time; whereas contact angles on G-3015-treated specimens were independent of retention and wetting time (Table 3.7). The hydrolyzed products of ungrafted MA groups in E-43, double or single carboxylic acids, were released and freely exposed on the wood surface. Thus, these hydrolyzed products increased the surface energy of wetted wood specimens. The polarity of treated specimens increased with E-43 retention and led to a large contact angle drop in a short time. Veneer samples treated with G-3015, however, had fewer polar surfaces because there are less MA groups in its

molecular chains and some ungrafted MA groups may be buried in its larger molecular chains after coating. Therefore, these different wetting behaviors of MAPP treated specimens were mainly related to the acid number of MAPP, the amount of ungrafted or non-reacted MA groups on wood surface, and the polarity of treated specimens.

3.3.4 Interfacial Bonding Strength

Shear strength of all resultant wood-PVC laminates made of wood treated with both coupling agents increased with increase of coupling agent retention for both extracted and unextracted wood samples (Figure 3.12). Thus, both maleated polypropylenes provided excellent improvement on interfacial bonding strength of resultant wood-PVC laminates compared with those without coupling treatment. With Soxhlet extraction, the maximum shear strength of wood-PVC laminates treated with E-43 and G-3015 was 3.71 MPa and 3.85 MPa, respectively. Without Soxhlet extraction, the shear strength of the composites treated with E-43 and G-3015 was 3.57 MPa and 3.85 MPa, respectively. Shear strength of untreated wood-PVC composites was 3.14 MPa for extracted samples and 2.98 MPa for unextracted samples (Table 3.2 and Figure 3.12). Compared with untreated wood-PVC laminates, there was an 18.2% (extracted) and 20.8% (unextracted) increase in shear strength for E-43 treated laminates. For G-3015 treated laminates, the corresponding shear strength increase was 22.6% (extracted) and 29.2% (unextracted). Thus, shear strength of wood-PVC laminates with MAPP treated wood increased over 20% on average. For the extracted wood samples, E-43 provided higher interfacial bonding strength than G-3015 at low concentration levels. Shear strength of resultant composites increased with retention and reached a similar level at high retention for both coupling agents (Figure 3.12b).

a)

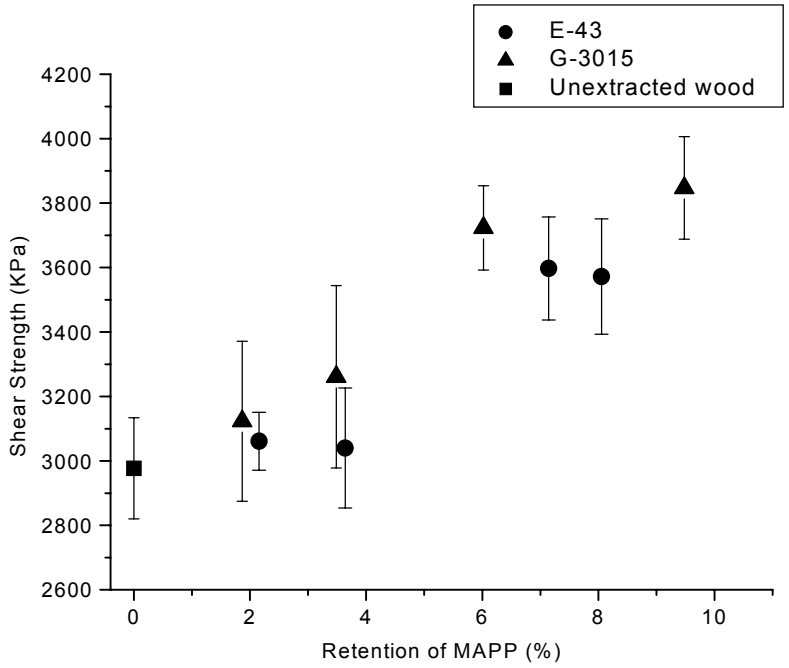

b)

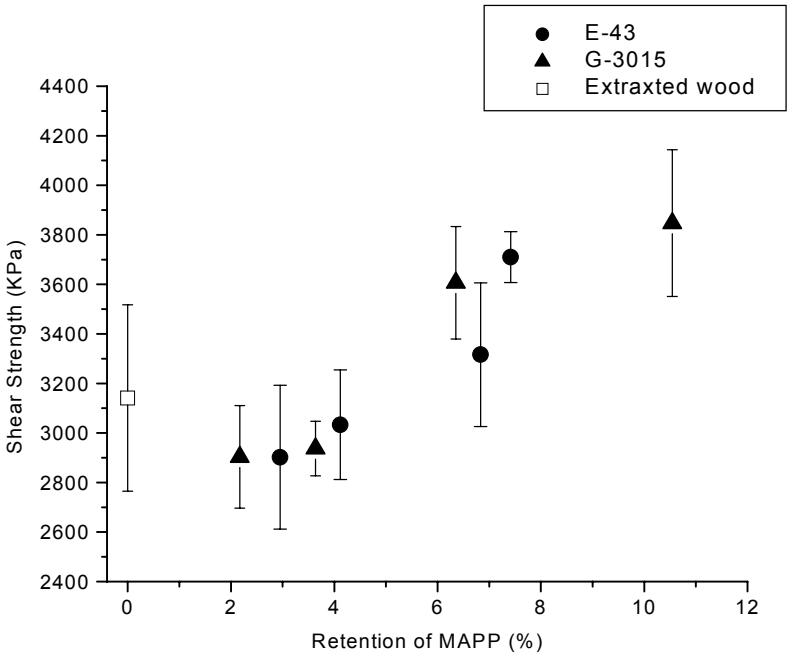

Figure 3.12. Shear strength of yellow-poplar and PVC composites treated with MAPP. a) Non-Soxhlet extracted before coupling treatment and b) Soxhlet extracted before coupling treatment.

The following *monolayer* models (Figure 3.13) are proposed to explain the adhesion mechanism at the interface. *Monolayers*, formed by MAPP, are located at the interface and serve as bridges to link wood and PVC. The coupling performance of MAPP in wood and PVC laminate composites is mainly due to the coupling structures of MAPP at the interface. Mode I represents the interfacial structure with low MAPP retention (<3%), while Model II indicates the interfacial structure with high MAPP retention (>6%). In model I, over 90 weight percent of MAPP molecular chains were grafted on the wood surface. In model II, however, less than 30 weight percent of MAPP were grafted on wood and most MAPP molecules were physically fixed on the wood surface (Figure 3.9).

For Model I, the interfacial area consists of four interphases, including wood-polymer, wood-MAPP, polymer-MAPP, and wood-MAPP-polymer interphases (Figure 3.13a). In Model I, the *monolayer* is decretive and randomly distributed. For Model II, there are three interphases except the wood-polymer interphase because wood and PVC are completely separated with a continuous and compact microfilm, *monolayers* (Figure 3.13b). Within a *monolayer* and between *monolayers* of these two models, the primary bonding force includes secondary bonding (such as van der Waals's forces and hydrogen bonding) and polymer chain entanglement. At the interface between wood and coupling agent, some MAPP may penetrate into wood by capillary action, thus resulting in mechanical interlocking. Esterification links, hydrogen bonding, and polymer chain entanglement also exist at this interface. Secondary bonding and polymer chain entanglement may be dominant between PVC film and the *monolayer(s)*. The *monolayer(s)* may form estrification links with PVC under an initiator during hot

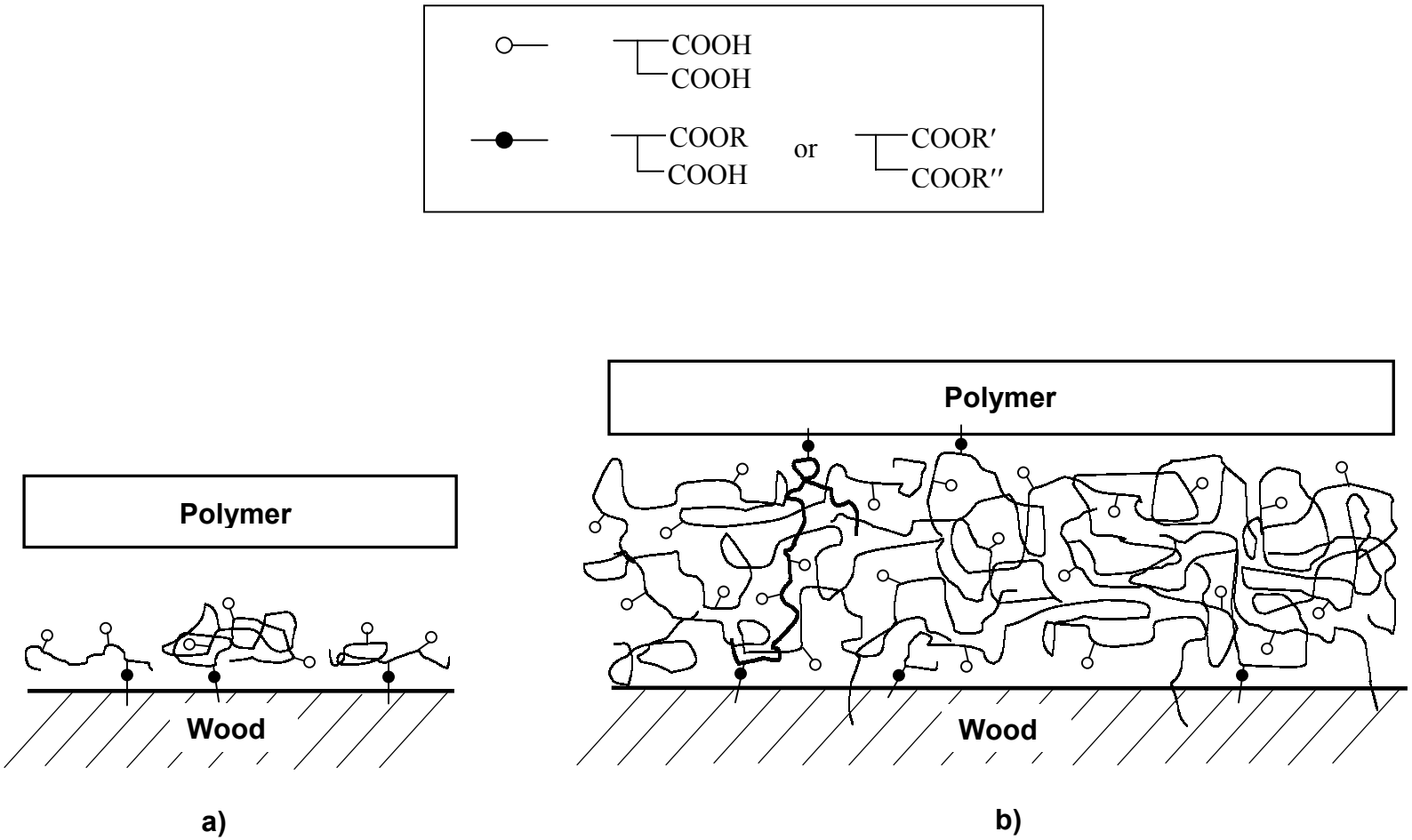

Figure 3.13. Hypothetical models for interfacial adhesion in wood-PVC composites. a) Model I and b) Model II.

pressing. The succinic half-ester links at the interface are possibly limited in an area within one or two *monolayers* close to wood surface and PVC film. Also, wood and PVC would be cross-linked by MAPP molecules across these *monolayers* (Figure 3.13).

For G-3015, the *monolayer(s)* close to the wood surface has a switch-like structure with a head-tail configuration (Sanadi et al. 1995). In this structure, one side of these MAPP molecules was grafted on the wood surface like an anchor. On the other side, these long flexible molecular chains would be helpful to form entanglement with other MAPP molecular chains. The morphological structure of E-43 may form a brush-like interface at the *monolayer(s)* close to the wood surface (Gateholmn and Felix 1993). This brush-like structure may restrict the mobility of grafted MAPP and offer a compact contact between MAPP and the polymer matrix at the wood-coupling agent interphase, thus effectively improving the interfacial adhesion.

Compared with wood fiber, wood veneer is smooth and continuous. The *monolayers* easily produce a microfilm on wood surface. This microfilm fills the gaps between wood and thermoplastics and decreases the contact distance between the wood-coupling agent interphase and between the polymer-coupling agent interphase, thus effectively transferring stresses at the interface. The microfilm thickness, δ (μm), is calculated with the following equation (Khroulev 1965):

$$\delta = \frac{Q}{\rho} \tag{3.4}$$

where Q is the quantity of adhesive in g/m^2, and ρ is the density of adhesive solution in kg/m^3. For phenolic formaldehyde (PF) resins with about 40% solid content, the PF quantity was 250-300 g/m^2 in order to achieve the optimum bonding strength on wood. Accordingly, the optimum microfilm thickness for PF was estimated to be 200-250 μm

(Khroulev 1965). In this study, MAPP solution has a low solid content (<10%) and it contained a very small amount of water (<1%). The average density of MAPP solution was 910 kg/m^3. Referenced to PF, the optimum coating quantity for MAPP was estimated to be 50-70 g/m^2. Based on the above equation, the Khroulev thickness of MAPP was estimated to be 60-80 μm. At low retentions (e.g., 1-2%), the MAPP microfilm thickness was about 10 μm, while it was about 40 μm at high retentions (e.g., 9-10%). As a result, the MAPP microfilm thickness was close to the Khroulev value at high retention. However, the thickness at low retention was only one fourth of that at high retention.

It was reported that E-43 was not effective in improving interfacial bonding strength in wood veneer and PVC laminates (Matuana et al. 1998). Based on the above-proposed *monolayer* models, MAPP at low retention levels formed a decretive and thin microfilm (much less than the Khroulev thickness) on the wood surface and could not significantly improve the interfacial adhesion. According to our experimental results, the shear strength of wood-PVC laminates treated with MAPP was lower or close to that of wood-PVC laminates when MAPP retention was less than 5%. However, there was a significant improvement on interfacial adhesion when MAPP retention levels were larger than 5% (Figure 3.12). The interface between PVC and smooth wood veneer seemed to be less sensitive to retention levels and graft rate of MAPP than the interface between PVC and relatively rough wood fiber. Therefore, even at high MAPP retention levels (e.g., 10%), shear strength of resultant wood-PVC laminates was still increasing as the retention levels increased.

Acid number significantly influenced the graft reaction of MAPP with wood components. It directly affected bonding strength of resultant composites. In general,

MAPP with a larger acid number is helpful to improve interfacial bonding strength and compatibility (Olsen 1991). Although the molecular weight of E-43 is smaller than that of G-3015, the shear strength of wood veneer and PVC laminates treated by E-43 was higher than or close to that by G-3015 when MAPP retention levels were less than 5% (Figure 3.12). At low retention, E-43 had more MA groups grafted by esterification links and even generated more cross-linking sites at the interface than G-3015. As a result, a low molecular weight coupling agent can compete with a high molecular weight coupling agent at low retention levels.

Extractives did not significantly influence shear strength of resultant wood-PVC laminate composites (Table 3.2 and Figure 3.12). Liriodenine in extractives may interfere with the graft reaction between MA groups of MAPP and hydroxyl groups of cellulose and lignin. Since carboxylic acid products from liriodenine by oxidation might react with MA groups of MAPP during coupling treatment (Buchanan and Dickey 1960; Taylor 1961), this reaction would reduce the number of MA groups and coupling effect of MAPP. However, the amount of liriodenine was so small that it did not interfere with the graft reaction. As shown in Figure 3.12, the shear strength of wood and PVC laminate composites with extraction was close to those without extraction at most retention levels. Therefore, shear strength of resultant laminate composites was not so sensitive to extractives in yellow poplar veneer.

3.3.5 Wettability versus Interfacial Bonding Strength

In this study, wettability was evaluated based on measured contact angle data. According to the experimental results, it appears that there is no obvious relationship between contact angles of treated wood samples and bonding strength of resultant

composites (Table 3.2). For example, shear strength increased with increases of coupling agent retention. However, contact angle values on treated veneer were almost identical at all G-3015 retention levels. For E-43, contact angle values seemed to decrease with the increase of coupling agent retention, but the shear strength increased.

Larger contact angle values on treated veneer samples did not necessarily result in higher bonding strength of the resultant laminates. For example, the contact angle values of wood samples treated with G-3015 were as large as 120° at low concentration levels (Table 3.7), which means that the treated wood samples were compatible to PVC. However, the shear strength of wood-PVC composites was close to and even less than that of untreated wood composites. Shear strength of E-43 treated composites at low retention levels (e.g., 2-4%) was smaller than that at high levels (e.g., 7-8%), even though treated wood samples at low retention levels were less polar than that at high levels (Table 3.2). As a result, large contact angles (or good surface compatibility between treated wood and thermoplastics) did not necessarily ensure improvement of bonding strength at the interface.

3.4 SUMMARY AND CONCLUSIONS

During coupling treatment, adsorption and fixation of MAPP were influenced by many factors such as solvent, initiator, dipping time, concentration, extractives and extraction, acid number, and molecular weight of MAPP. Adsorption and fixation of MAPP influenced the wettability of treated wood specimens and finally influenced the compatibility and bonding strength at the interface in wood and PVC laminates. Based on the above discussions, the following conclusions can be drawn.

1. Retention of coupling agent on wood samples increased with the increase of coupling solution concentration. The shape of the retention and concentration curves varied with coupling agents. For G-3015, the relationship between retention and concentration was linear. However, a polynomial pattern was followed for E-43.

2. The relationship among graft rate, concentration, and retention of MAPP followed three-dimensional parabloid models. Graft efficiency decreased with the increase of concentration and retention. This indicates that there was a limit to graft MAPP on wood surface. At low concentration levels and low retention, coupling agent molecules were mainly fixed on wood by esterification. At high concentration levels, however, most coupling agent molecules were deposited on wood by physical adsorption (such as capillary adsorption), accompanied with graft copolymerization.

3. Wettablity of MAPP-treated wood specimens was mainly influenced by the acid number of MAPP, the amount of ungrafted or non-reacted MA groups, and the surface polarity. Coupling treatment with G-3015 led to large and stable contact angles (115-130°), independent of wetting time, retention, and graft rate. Contact angles of wood samples treated with E-43 decreased with the increase of E-43 retention and wetting time, due to the deposit of ungrafted or non-reacted MA groups on wood surface. After removing the ungrafted E-43, contact angles decreased with the increase of graft rate and wetting time because many hydrolyzed products of ungrafted MA groups (double or single carboxylic acids)

in the grafted E-43 molecular chains were released and freely exposed on wood surfaces during wetting.

4. Adhesion took place within *monolayers* formed by MAPP and between these *monolayers* and the adherends (wood and PVC). Interfacial bonding consisted of covalent bonding, secondary bonding (such as hydrogen bonding and van der Waals's forces), polymer molecular entanglement, and mechanical interblocking. Esterification was limited on the *monolayer(s)* close to wood surface and PVC film. All these bonding forms may concurrently exist across the interface.

5. Shear strength of the resultant composites increased with the increase of MAPP retention in the wood. Increases of graft rate improved the coupling performance of MAPP at the interface. However, shear strength seemed not so sensitive to the change of graft rate at high retention levels. The acid number of MAPP had a significant influence on interfacial bonding of wood-PVC composites. There was no direct correlation between measured contact angle and shear strength.

6. Wood extractives had negative effects on MAPP retention in most cases. Soxhlet extraction helped improve retention of G-3015. However, it only worked at low concentration levels for E-43. Extractives did not significantly influence contact angles on MAPP-treated specimens and interfacial bonding strength of resultant wood and PVC composites.

3.5 REFERENCES

American Society for Testing and Materials (ASTM). 1993a. Standard test method for determining strength of adhesively bonded rigid plastic lap-shear joints in shear by tension loading. ASTM Standard D3163-91. ASTM, Philadelphia, PA.

American Society for Testing and Materials (ASTM). 1993b. Standard test method for strength properties of adhesives in shear by tension loading of single-lap-joint laminated assemblies. ASTM Standard D3165-91. ASTM, Philadelphia, PA.

American Society for Testing and Materials (ASTM). 1998. Standard test method for preparation of extractive-free wood. Annual book of ASTM standards. Section 4. ASTM Standard D1105-96. ASTM, West Conshohocken, PA. pp. 171-172.

Buchanan, M.A., and E. E. Dickey. 1960. Liriodenine, a nitrogen-containing pigment of yellow poplar heartwood. J. Org. Chem. 25: 1389-1391.

Chen, M. –J., J. J. Meister, D. W. Gunnells, and D. J. Gardner. 1995. A process for coupling wood to thermoplastic using graft copolymers. Adv. Polym. Technol. 14(2): 97-109.

Chow, P., Z. Bao, J. A. Youngquist, R. M. Rowell, J. H. Muehl, and A. M. Krzysik. 1996. Properties of hardboards made from acetylated aspen and southern pine. Wood Fiber Sci. 28(2): 252-258.

Chun, I, and R. T. Woodhams. 1984. Use of processing aids and coupling agents in mica-reinforced polypropylene. Polym. Comp. 5(4): 250-257.

Dalväg, H., C. Klason, and H. –E. Strömvall. 1985. The efficiency of cellulosic fillers in common thermoplastics, part II. Filling with processing aids and coupling agents. Int. J. Polym. Mater. 11: 9-38.

Delassus, P. T., and N. F. Whiteman. 1999. Physical and mechanical properties of some important polymers. Pages V159-V169 *in* J. Brandrup, E. H. Immergut, E. A. Grulke, A. Abe, and D. R. Bloch, eds. Polymer handbook. 4th ed. John Wiley & Sons, Inc., New York, NY.

Felix, J. M., and P. Gatenholm. 1991. The nature of adhesion in composites of modified cellulose fibers and polypropylene. J. Appl. Polym. Sci. 42: 609-620.

Fengel, D., and G. Wegener. 1984. Wood: Chemistry, ultrastructure, reactions. Walter de Gruyter, New York, NY. 613 pp.

Gatenholm, P., and J. M. Felix. 1993. Interphase design in cellulose fiber/polypropylene composites. Pages 237-244 *in* T. C. Chung, ed. New advances in polyolefins. Plenum Press, New York, NY.

Goto, T., H. Saiki, and H. Onishi. 1982. Studies on wood gluing XIII: Gluability and scanning electron microscopic study of wood-polypropylene bonding. Wood Sci. Technol. 16: 293-303.

Humphrey, P. E. 1993. A device to test adhesive bonds. U.S. Patent 5,176,028.

Khroulev, V. M. 1965. Surface roughness and rheological properties of adhesives as factors determining optimum thickness of glue line. Mekh. Polim. (6): 103-107.

Kishi, H., M. Yoshioka, A. Yamanoi, and N. Shiraishi. 1988. Composites of wood and polypropylenes I. Mokuzai Gakkaishi 34(2): 133-139.

Kit, K. M., R. S. Benson, M. Dever, and X. Luo. 2002. Kudzu fiber-reinforced polypropylene composites. Proceedings of the 6th International Conference on Woodfiber-Plastic Composites. May 15-16, 2001, Madison, WI. Forest Products Society, Madison, WI. In press.

Kolosick, P. C., G. E. Myers, and J. A. Koutsky. 1992. Polypropylene crystallization on maleated polypropylene-treated wood surface: Effects on interfacial adhesion in wood polypropylene composites. Pages 137-154 *in* R. M. Rowell, T. L. Laufenberg, and J. K. Rowell, eds. Materials interactions relevant to recycling of wood-based materials, vol. 266. Materials Research Society, Pittsburgh, PA.

Krzysik, A. M., and J. A. Youngquist. 1991. Bonding of air-formed wood fiber/polypropylene fiber composites. Int. J. Adhes. Adhesives 11(4): 235-240.

Liu, F. P., M. P. Wolcott, D. J. Gardner, and T. G. Rials. 1994. Characterization of the interface between cellulosic fibers and a thermoplastic matrix. Comp. Interfaces 2(6): 419-432.

Lu, J. Z., Q. Wu, and H. S. McNabb, Jr. 2000. Chemical coupling in wood fiber and polymer composites: A review of coupling agents and treatments. Wood Fiber Sci. 32(1): 88-104.

Maldas, D., and B.V. Kokta. 1989. Improving adhesion of wood fiber with polystyrene by the chemical treatment of fiber with a coupling agent and the influence on the mechanical properties of composites. J. Adhes. Sci. Technol. 3(7): 529-539.

Maldas, D., B. V. Kokta, R. G. Raj, and C. Daneault. 1988. Improvement of the mechanical properties of sawdust wood fiber-polystyrene composites by chemical treatment. Polymer 29: 1255-1265.

Matuana, L. M., J. J. Balantinecz, and C. B. Park. 1998. Effect of surface properties on the adhesion between PVC and wood veneer laminates. Polym. Eng. Sci. 38(5): 765-773.

Mutton, D. B. 1962. Wood resin. Pages 331 and 363 *in* W. E. Hillis, ed. Wood extractives and their significance to the pulp and paper industries. Academic Press, New York, NY.

Olsen, D. J. 1991. Effectiveness of maleated polypropylenes as coupling agents for wood flour/polypropylene composites. Pages 1886-1891 *in* ANTEC, Proc. 49th Annual Technical Conference, Montreal, Canada, May 5-9, 1991, Society of Plastics Engineers, Brookfield, CT.

Sanadi, A. R., R. M. Rowell, and R. A. Young. 1992. Estimation of fiber-matrix interfacial shear strengths in lignocellulosic-thermoplastic composites. Pages 81-92 *in* R. M. Rowell, T. L. Laufenberg, and J. K. Rowell, eds. Materials interactions relevant to recycling of wood-based materials, vol. 266. Materials Research Society, Pittsburgh, PA.

Sanadi, A. R., D. F. Caulfield, R. E. Jacobson, and R.M. Rowell. 1995. Renewable agricultural fibers as reinforcing fillers in plastics: Mechanical properties of kenaf fiber-polypropylene composites. Ind. Eng. Chem. Res. 34: 1889-1896.

Snijder, M. H. B., and H. L. Bos. 2000. Reinforcement of polypropylene by annual plant fibers: Optimisation of the coupling agent efficiency. Comp. Interfaces 7(2): 69-75.

Snijder, M. H. B., E. Wissing, and J. F. Modder. 1997. Polyolefins and engineering plastics reinforced with annual plant fibers. Pages 181-191 *in* Proceedings of the Fourth International Conference on Woodfiber-Plastic Composites, Forest Products Society, Madison, WI.

Tanaka, H., A. Swerin, L. Odberg, and S. –B. Park. 1999. Competitive adsorption of cationic polyacrylamides with different charge densities onto polystyrene latex, cellulose beads and cellulose fibers. J. Pulp Paper Sci. 25(8): 283-288.

Taylor, W. I. 1961. The structure and synthesis of liriodenine, a new type of isoquinoline alkaloid. Tetrahedron 14:42-45.

Woodhams, R. T., G. Thomas, and D. K. Rodgers. 1984. Wood fiber as reinforcing fillers for polyolefins. Polym. Eng. Sci. 24(15): 1166-1171.

Wozniak, P. J., and J. P. Geaghan. 1994. An introduction to the SAS® system for DOS and Windows. Department of Experimental Statistics, Louisiana State University. 167 pp.

Xanthos, M. 1983. Processing conditions and coupling agent effects in polypropylene/wood flour composites. Plast. Rubber Process. Appl. 3(3): 223-228.

CHAPTER 4. SURFACE AND INTERFACIAL CHARACTERIZATION OF WOOD-PVC COMPOSITES. PART I. DYNAMIC AND STATIC CONTACT ANGLES AND WETTING BEHAVIOR

4.1 INTRODUCTION

Wettability is an essential property to wood adhesion (Gray 1962). Wettability of wood materials is usually evaluated with contact angle, which provides an adverse measure of wettability (Zisman 1976). Wetting quality of wood is influenced by many factors including wood macroscopic characteristics (e.g., porosity, surface roughness, wood surface polarity, pH value, moisture content, grain orientation, and extractives), surface quality of wood (e.g., virgin, aging, and contamination), processing temperature, and properties of adhesives (e.g., acidity, rheology, and viscosity) (Bryant 1968; Lee and Luner 1972; Jordan and Wellons 1977; Scheikl and Dunky 1998).

There are several kinds of devices for static contact angle measurements. For a traditional device, the contact angle data were manually measured with a microscope eyepiece combined with a separate protractor or goniometer (Freeman 1959; Herczeg 1965). Since the late 1970s, static contact angle analyzers (such as Kernco G-1, Krüss G1/G40, Rame-Hart, Zeiss) have been equipped with an inserted goniometer in the microscope eyepiece. These improved optical apparatuses were relatively easy to use and accurate to measure static contact angles on wood surface. The profile of sessile drops on wood surfaces can be captured with a camera attached to the microscope. However, it is difficult to use this optical technique for determining dynamic contact angle data on surfaces with high polarity, because the measurement of a contact angle is usually accomplished in several seconds and lagged to the actual contact angle (Lu et al. 2002).

In the early 1970s, Elliott and Ford (1972) proposed a photography technique for dynamic contact angle measurements. This photography technique was later successfully combined with a microscope for convenient observation of liquid droplets on a substrate (Jordan and Wellons 1977). Skinner and colleagues (1989) applied two sets of microscopes and video cameras horizontally and vertically arranged to observe the instantaneous time-elapsed profiles of a droplet on a subject in three dimensions. Kalnins et al. (1988) used a video camera to record dynamic contact angle data to a video tape.

The operation with these early devices was laborious because most contact angle data were manually measured. The limitation for dynamic contact angle measurement was reduced by using a computer in combination with a video camera (Scheikl and Dunky 1996). A CCD (charged couple device) type video camera connected to a computer is directly equipped on a Krüss G1/G40 contact angle meter. The image of a droplet on a specimen is captured with the video camera and processed by the computer during measurements. A number of publications on dynamic contact angles are attributed to the applications of these techniques (Skinner et al. 1989; Scheikl and Dunky 1998).

Static contact angle measurement techniques have been extensively used to characterize water repellency, weathering, and durability of solid wood (Nussbaum 1999), bondability and adhesion of wood composites (Jordan and Wellons 1977), gluability of preservative-treated wood materials (Zhang et al. 1997), adsorption, printing, and recycling of paper products (Oye and Okayama 1989), and coatability of wood materials for paints (Feist 1977; Kleive 1986), surface energy and wettability for wood and wood products (Lee and Luner 1972; Hodgson and Berg 1988). Recently, contact angle measurement methods have been applied to evaluate compatibility of

chemically modified wood fibers in wood-polymer composites (Felix and Gatenholm 1991; Chen et al. 1995).

In general, interfacial wettability requirement in WPC is opposite to that for traditional wood composites. In WPC, modified wood surfaces are required to have smaller surface energy (i.e., larger contact angles) in order to improve their compatibility with thermoplastics. In wood composites, adhesive resins should have smaller contact angles on wood for better wetting and adhesion. Although a number of researches on wettability and interfacial bonding of wood-polymer composites have been published (Felix and Gatenholm 1991), there are few reports on characteristics of wettability at the wood-polymer interface. This was due to the difficulty in separating individual wood fibers from the polymer matrix in wood-polymer composites (Liu et al. 1994). To overcome these obstacles, wood-polymer laminates can be used as a substitute because interfacial layers in the laminates can be more easily separated and used for contact angle analysis.

In this study, the characteristics of dynamic wetting process for maleated wood surface and wood-polymer interface were investigated with an imaging system. Contact angle and water droplet morphology on maleated surface and wood-PVC interface were studied as a function of time. The objective of this work was to investigate wetting behavior and kinetics of wetting of maleated wood surfaces and wood-polymer interface. The wettability characteristics at the interface were simulated with maleated wood surface after heat treatment and wood-PVC interface. In particular, dynamic contact angle of water droplets and time-dependent changes in their profile dimension (e.g., base-diameter and height) on maleated wood surfaces were measured and modeled.

4.2 BACKGROUND

4.2.1 Contact Angle Analysis in Wood-Polymer Composites

Swanson and Becher (1966) studied the compatibility of handsheets and machine-made paper with polyethylene by different treatments. Compared with untreated handsheets and paper, stearic acid-treated specimens had larger water contact angles (107º on average). The results indicated that adhesion was governed by the critical surface tension for paper and handsheets. Using the Wilhelmy technique (Wilhelmy 1863), Young (1976) investigated the wettability of wood pulp fibers grafted with styrene and acrylonitrile monomers. The modified fibers presented different wetting characteristics. Acrylonitrile-grafted fiber had a wetting behavior similar to untreated fibers. However, the styrene-grafted fiber had a reduced wettability (i.e., larger contact angle and smaller surface energy) compared with the ungrafted fiber (Young 1976).

Little attention had been paid to wettability at the interface in wood-polymer composites until the 1990s. Felix and Gatenholm (1991) investigated the wettability of wood fibers treated with maleated polypropylene (MAPP). They reported that contact angle of cellulose fibers treated with MAPP was in the range of 130º and 140º. There was no significant difference of contact angle between specimens extracted and unextracted with toluene before coupling treatment. Chen et al. (1995) studied adhesion properties of styrene-lignin graft copolymers using a Cahn dynamic contact angle (DCA) analyzer. The contact angle data measured with distilled water on grafted lignin were close to those of polystyrene (i.e., 105º). Gardner et al. (1994) used the DCA and micro-bond technique to evaluate the interfacial adhesion in wood fiber-polystyrene composites. They reported that water contact angles on wood fibers treated with styrene-maleic anhydride (SMA)

copolymers increased with the grafting weight percent gain. However, the increase of SMA acid number resulted in the decrease of contact angle for SMA-treated specimens.

Matuana et al. (1998) used four different coupling agents to treat wood veneer and investigated the wettability of treated wood specimens. For specimens treated with anhydride-based coupling agents (such as Epolene E-43 and phthalate anhydride), initial contact angles of glycerol sessile drops on treated wood were in the range from 100º to 110º. Based on the relationship between exposure time and contact angles, the wetting behaviors of chemically modified specimens showed that coupling treatment helped improve the compatibility at the interface (Matuana et al. 1998).

More recently, the influence of maleation on polymer adsorption and fixation, wood surface wettability, and interfacial bonding strength in wood-PVC composites was studied (Lu et al. 2002). Veneer specimens treated with two MAPPs (Epolene G-3015 and Epolene E-43) presented different wetting behaviors. For G-3015-treated specimens, measured contact angles varied from 115º-130º, independent of retention, graft rate, and wetting time. For E-43-treated samples, retention, graft rate, and wetting time had a significant influence on the contact angle. After removing ungrafted or non-acted maleic anhydride groups in grafted E-43 on wood, contact angles decreased with the increase of graft rate and wetting time because many hydrolyzed products of ungrafted MA groups (double or single carboxylic groups) on grafted E-43 molecular chains were released and freely exposed on wood surfaces during wetting. Consequently, wettability of maleated wood specimens was mainly influenced by the acid number of coupling agent, the amount of ungrafted or non-reacted MA groups, and the surface polarity.

4.2.2 Theoretical Modeling of Dynamic Wetting Process

When a liquid droplet (e.g., water, urea formaldehyde resin, or phenol formaldehyde resin) is placed on wood surface, it simultaneously spreads on the surface. Concurrently, it penetrates into wood and is gradually absorbed by wood through capillary action (Figure 4.1). During the spreading process, the droplet expands in contact area and perimeter under surface tension, whereas it shrinks in height and volume by adsorption and spreading. These spreading and absorbing processes are not completed until the wood substrate is completely wetted.

Several models have been proposed to describe the dynamic wetting process (Wolstenholme and Schulman 1950; Elliot and Ford 1972; Wilkinson and Elliott 1974; Skinner et al. 1989; Liptáková and Kúdela 1994; Liu et al. 1995; Shi and Gardner 2001). Among these models, a natural decay model (Halliday et al. 1997) was used to model the decaying process for a sessile water droplet. The model has the following form:

$$\theta = \theta_0 + a \cdot \exp(-K_\theta t) \tag{4.1}$$

where, θ_0 = Initial contact angle, degrees,
θ = Contact angle at time t, degrees,
t = Wetting time, seconds, and
a and K_θ = Constants.

Shi and Gardner (2001) used constant K (K value) to evaluate the adhesive wetting process of wood. They suggested that K value was related to the rate of the liquid penetration and spreading rate on wood surface. In this study, a material constant (K_θ) is used to specify the rate of change in contact angle.

Equation 4.1 can be expressed in the natural logarithmic form (Elliott and Ford 1972) as:

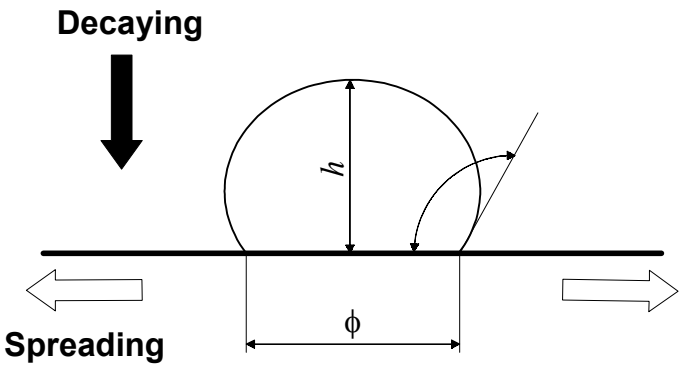

Figure 4.1. Profile of a water droplet on modified wood veneer during dynamic wetting.

$$-\ln(\theta_0 - \theta) = K_\theta t + b \tag{4.2}$$

where, b = Constant (i.e., -ln$a$). Hence, the dynamic wetting process of water droplets on the modified surface obeys the first-order kinetic law (Wolstenholme and Schulman 1950):

$$\frac{d\theta}{dt} = K_\theta(\theta_0 - \theta) \tag{4.3}$$

Similarly, the droplet height (h) and volume (V) as a function of time follow the same process. Thus, Equations 4.1 to 4.3 apply to the decay process of h and V as well.

For the spreading process, *Boltzmann* equation (Devanne et al. 1997) was applied to simulate dimensional changes in base-diameter (ϕ), perimeter (ρ), and contact area (S) of a droplet profile during dynamic wetting. The equation has the following form:

$$\delta = \frac{\delta(+\infty) - \delta(-\infty)}{1 + \exp[(t_0 - t)/\Delta t]} + \delta(-\infty) \tag{4.4}$$

where, δ = Dimensional size in ϕ, ρ, or S, mm or mm^2 at time t,
$\delta(-\infty)$ = Initial value of dimension, mm or mm^2,
$\delta(+\infty)$ = Final value of dimension, mm or mm^2,
t_0 = The time at which δ is equal to the average of $\delta(-\infty)$ and $\delta(+\infty)$, seconds, and
Δt = Interval of time t, seconds,

In order to compare the influence of the exponential term on dynamic wetting process, Equation 4.4 can be rewritten as:

$$\delta = \frac{\delta(+\infty) - \delta(-\infty)}{1 + c \cdot \exp(-K_\delta t)} + \delta(-\infty) \tag{4.5}$$

where, c and K_δ = materials constants.

Slopes of curves for θ, h (or V), and ϕ (or ρ and S) against time, defined as wetting slopes (WS), are derived from Equations 4.1 and 4.5 by differentiation with time t. They are labeled as WS_θ for contact angle, WS_h for droplet height, and WS_ϕ for droplet base-diameter. The wetting slopes were used to evaluate kinetics of wetting for dynamic wetting process.

4.3 MATERIALS AND METHODS

4.3.1 Test Materials and Sample Preparations

Two MAPPs (Epolenes E-43 and G-3015, Eastman Chemical Company) and one copolymer of maleic anhydride and ethylene (PEMA, Polysciences, Inc.) were used in this study. The properties of these coupling agents are listed in Table 4.1. Benzoyl peroxide (BPO, Aldrich) was used as initiator. Toluene (Fisher Scientific) was used as solvent for both MAPPs and *n*-butanol (Fisher Scientific), for PEMA. Polyvinyl chloride (PVC) sheets (508 mm × 1270 mm × 0.0508 mm) were purchased from Curbell Plastics Company, Phoenix, AZ.

Sheets of commercial yellow poplar (*Liriodendron tulipifera*) and red oak (*Quercus rubra*) veneer (610 mm × 610 mm) were obtained from Columbia Forest Products Inc., Newport, VT. The nominal thickness for red oak and yellow poplar were 0.76 and 0.91 mm, respectively. The deviation of veneer thickness for both species was 0.127 mm. A total of 124 samples (50.8 mm × 25.4 mm × thickness) were cut from the veneer sheets for this study. Prior to coupling treatment, all veneer samples were conditioned to 5% MC in a conditioning chamber. All samples were numbered and kept in separate bags before testing.

Table 4.1. Properties of coupling agents.

Coupling Agent [a]	Shape and Appearance	Density (g/ml)	Molecular Weight		Acid Number (mgKOH/g)	Amount of MA Groups (%)	Viscosity (cp) [b]
			M_w (g/mol)	M_n (g/mol)			
E-43	Yellow pallet	0.930	9,100	3,900	47	4.4	400
G-3015	Light yellow pallet	0.913	47,000	24,800	15	1.3	25,000
PEMA	White flour	-	100,000	-	870	-	5

[a] The pH value of 5% PEMA solution at 20ºC is 5.2.
[b] The values of viscosity for E-43 and G-3015 were measured at 190ºC. The viscosity of PEMA was measured in a 2% solution.

4.3.2 Soxhlet Extraction

Soxhlet extraction was conducted on all wood specimens according to the ASTM standard D1105-96 to reduce the influence of extractives on chemical coupling. Wood samples were first extracted with a 120-ml mixing solution of toluene and ethyl alcohol for 4 hours. They sequentially underwent the second extraction with 120 ml ethyl alcohol for 4 hours. The extracted wood specimens were finally oven-dried at 70^{o}C for 24 hours to reach a constant weight. The oven-dried weight of each sample was measured. Secondary Soxhlet extraction was conducted to determine the graft rate of MAPP on wood specimens. All treated specimens were continuously extracted with toluene for 24 hours (Lu et al. 2002). The extracted specimens were then oven-dried at 70^{o}C for 24 hours to reach a constant weight.

4.3.3 Surface Treatments

Four kinds of surfaces from modified wood and wood-PVC composites were prepared for the wettability evaluation. They consisted of surfaces with coupling treatment (**S1**), surfaces with heat treatment (**S2**), PVC-coupling agent interphase (**S3**), and wood-coupling agent interphase (**S4**). For the last three kinds of surfaces, post treatments (e.g., heat treatment and tensile test) were performed after coupling treatment.

During coupling treatment (Lu et al. 2002), wood specimens were dipped in a coupling agent solution at 100^{o}C for 5 min under continuous stirring with a magnetic stirrer. The concentration levels of MAPP were designed to be 0, 12.5, 25, and 50 g/L. The weight ratio between BPO and MAPP was 0.5. The treated specimens were removed from the solution and cooled down to room temperature. All treated specimens were finally oven-dried at 70^{o}C for 24 hours to reach a constant weight.

Heat treatment for CA-treated specimens was conducted to simulate the interface in melt-blended composites from compression and injection molding. A specimen was hot-pressed with a miniature press during the treatment. The pressing cycle for each specimen was 3 min for heating and 1 min for cooling under a pressure of 0.138 MPa, similar to the procedure used for manufacturing wood-PVC laminates (Lu et al. 2002). The heating temperature was 210ºC. At the end of the heating period, the press platens were cooled with running tap water to 70ºC. After finishing, the specimen was removed and allowed to cool to room temperature.

Specimens for interface analysis were prepared as follows. A PVC film was first placed between two pieces of coupling agent-treated veneer to create a lap-joint specimen (Lu et al. 2002). The assembly was hot-pressed in a miniature press under a pressure of 0.276 MPa and heated at 178^{o}C for 3 min. At the end of the heating period, the press platens were cooled with running tap water to room temperature. The lap-joint of wood-PVC laminates was then tested with a Model 1125 INSTRON machine under a tensile load. Finally, fractured surfaces at the wood-PVC interface were randomly selected and used for contact angle analysis. All treated specimens were conditioned to reach about 5% MC.

4.3.4 Contact Angle Measurements and Water Droplet Morphology

An imaging system was used to measure contact angle and shape and size of water droplets for the prepared specimens. This system mainly consisted of a Meiji microscope, a Cole-Parmer CCD color video camera, a Cole-Parmer fiber optic illuminator, an Invedio signal capture card, a Panasonic monitor, and a computer (Figure 4.2). The magnification number of the microscope was 50 times.

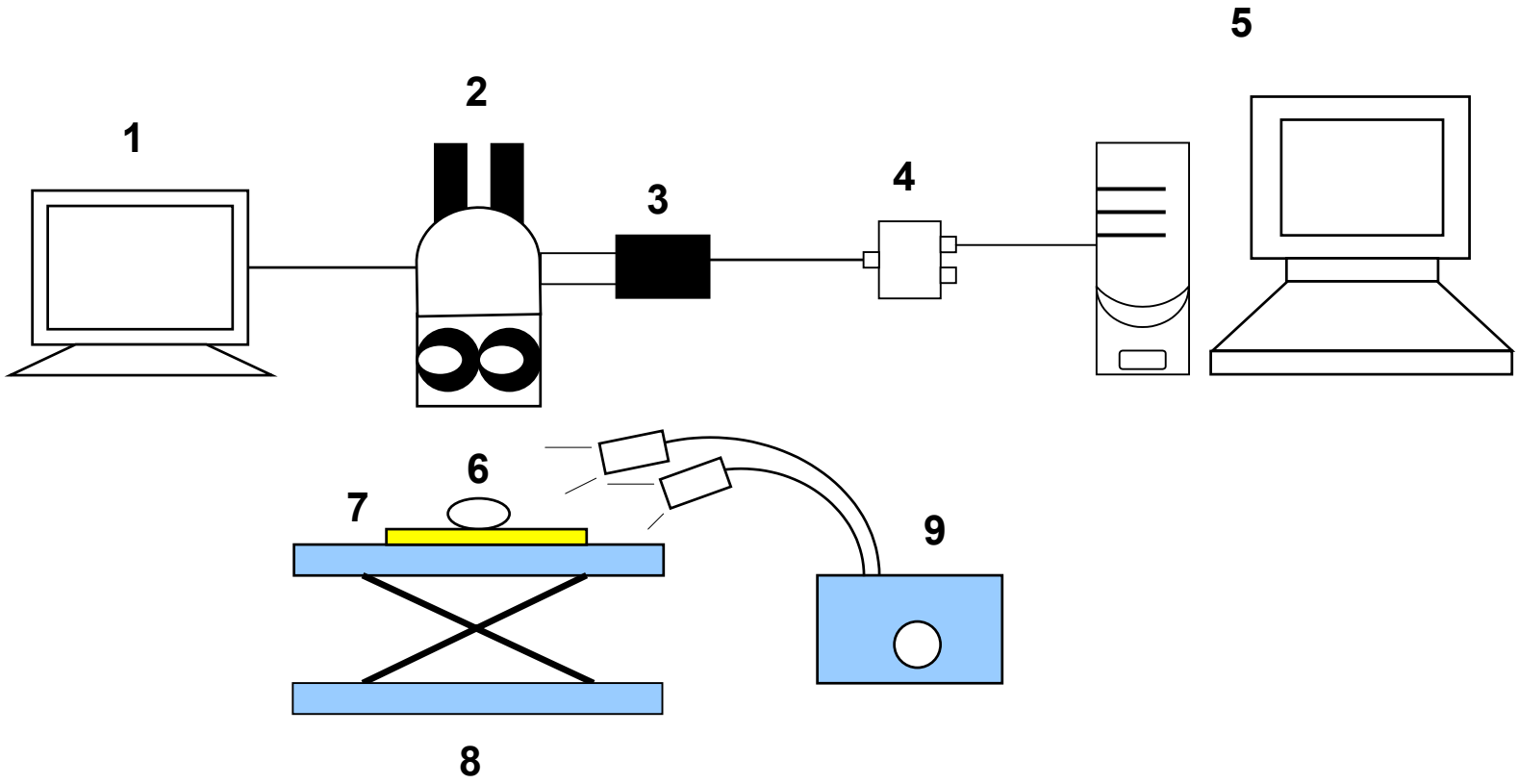

Figure 4.2. A schematic of the imaging system for dynamic wettability measurements. 1-monitor, 2-microscope, 3-CCD video camera, 4-signal capture card, 5-computer, 6-liquid droplet, 7-speciment, 8-adjustable view-station, and 9-optical illuminator.

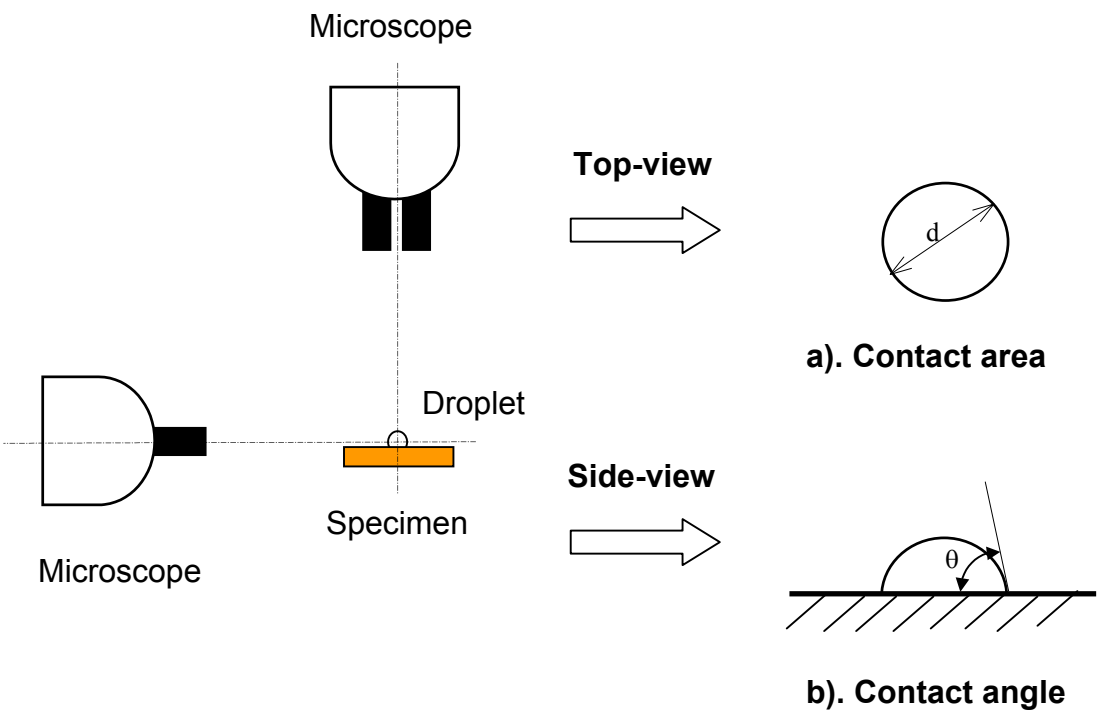

Figure 4.3. Two different setups of CCD video camera for measuring the profile of a sessile droplet on modified wood specimens and interphases. a) contact area and b) contact angle.

During measurement, a specimen was placed on the top of a miniature height adjustable view-station in front of or under the microscope (Figure 4.3). Static contact angles were measured in the horizontal direction, while the shape and size of a droplet were observed vertically under the microscope (Figure 4.3). The measurements were done in 15-second intervals from 0 to 45 seconds after the droplet was placed on sample surface.

The images were captured using the video camera. All captured images were stored as image files and measured for contact angle and profile dimension using SigmaScan software. A ratio (λ) of the minimum diameter to the maximum diameter of the contact area was calculated and used to evaluate the profile shape of water droplets. For dynamic wetting, base-diameter of a droplet on a specimen was measured at 0, 5, 15, 30, 60, 90, and 120 seconds after it was placed on wood surface. The contact angle and droplet height from the images were measured at 0, 3, 5, 10, 15, 20, 30, 45, 60, and 100 seconds (Figures 4.1 and 4.3).

4.3.5 Data Modeling

Experimental data were modeled using Equations 4.1 to 4.5. In order to describe the decay and spreading process more precisely, decay ratio (DR) for h or V and spreading ratio (SR) for ϕ, ρ, or S were defined as:

$$DR_h \text{ or } SR_\phi = \frac{\Gamma(t)}{\Gamma(0)} \tag{4.6}$$

where, $\Gamma = h$ or ϕ,

$\Gamma(t)$= dimensional size of a droplet profile at t seconds, and

$\Gamma(0)$= dimensional size of a droplet profile at 0 second.

During model fitting, DR and SR were calculated as a function of time. Similarly, the wetting slopes of DR and SR for h and ϕ are defined as WS_{hR} and $WS_{\phi R}$, respectively.

GrandPad Prism software (Motulsky 1999) was used to fit the data through nonlinear regression. The first-order exponential decay model (Equation 4.1) and the *Boltzmann* sigmoid (Equation 4.5) from the Prism equation library were selected with a 95% confidence interval to fit the data set. After fitting, a graph of residuals (i.e., the distances of each point from the curve) was plotted to check the goodness of fit. The maximum residual was made to be as small as possible for the best fit.

4.4 RESULTS AND DISCUSSION

4.4.1 Water Droplet Morphology

A water droplet on PVC film had a circular shape 15 seconds after it was placed on the surface ($\lambda = 1.0$, Figure 4.4a). The droplet diameter and λ value did not change even after 60 seconds' exposure (Table 4.2). This was due to the isotropic properties of PVC on wettability. Without coupling treatment, unextracted or extracted wood veneer showed its anisotropy with an elliptical water droplet ($\lambda = 0.65$ or 0.73, Table 4.2 and Figure 4.4b). After heat treatment, water droplets on unextracted wood had a circular shape ($\lambda = 0.93$, Table 4.3). They were, however, elliptical on extracted veneer ($\lambda = 0.93$, Figure 4.4c).

Water droplets on maleated wood veneer presented different profiles. For E-43 and PEMA-treated yellow poplar veneer, λ ratios were around 0.5 and smaller than those on untreated wood (Figures 4.4d, e and Table 4.2). However, λ ratios of G-3015-treated samples were equal to or close to 1 (Figure 4.4f and Table 4.2).

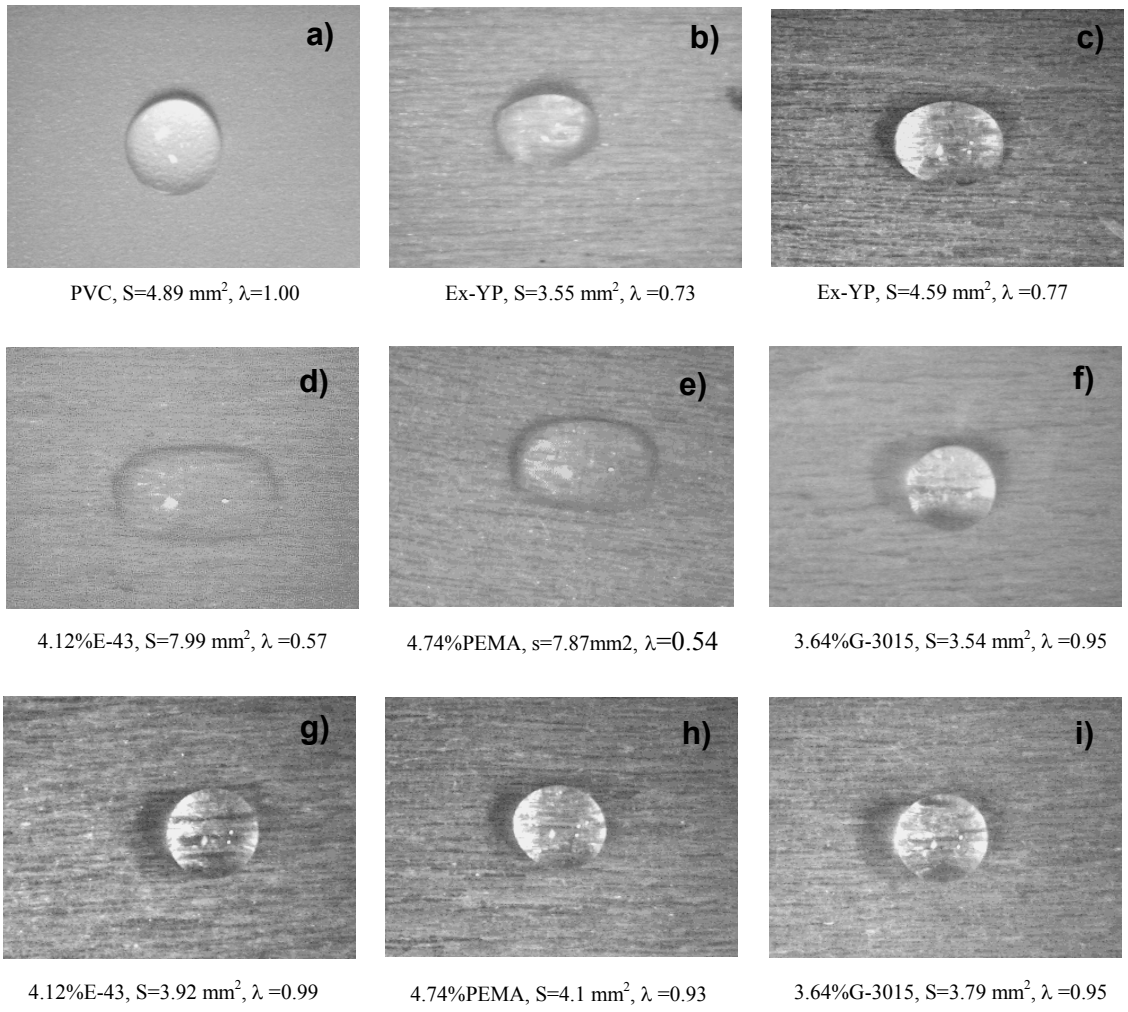

Figure 4.4. Morphology of water droplets on extracted yellow poplar veneer (Ex-YP) after 15 second exposure. a) PVC, b) unmaleated wood, c) wood with heat treatment, d)-f) maleated, and g)-i) heated after coupling treatment.

Table 4.2. Morphology of water droplets on maleated wood veneer after 15 second exposure.

Material	Wood species	Extraction before coupling	Coupling agent	Retention of coupling agent (%)	Diameter (mm)		λ ratio (d_{min}/d_{max})	Perimeter (mm)	Contact area (mm^2)
					d_{min}	d_{max}			
PVC	-	-	-	0.00	2.44	2.44	1.00	8.21	4.79
PVC [a]	-	-	-	0.00	2.44	2.44	1.00	8.11	4.66
Modified wood veneer (**S1**)	Yellow poplar	Unextracted	-	0.00	1.73	2.65	0.65	7.55	3.78
			E-43	3.64	1.79	2.83	0.63	7.98	4.23
			PEMA	5.21	1.55	2.78	0.56	7.92	4.03
			G-3015	3.49	1.81	1.81	1.00	6.09	2.68
		Extracted	-	0.00	1.79	2.44	0.73	7.25	3.55
			E-43	4.12	2.27	3.98	0.57	11.08	7.99
			PEMA	4.74	2.48	4.63	0.54	10.97	7.83
			G-3015	3.64	1.89	2.08	0.94	6.57	3.09
	Red oak	Extracted	-	0.00	1.53	2.03	0.75	7.32	3.59
			E-43	4.10	1.83	2.91	0.63	8.21	4.57
			PEMA	4.90	2.61	5.32	0.49	11.32	8.41
			G-3015	5.20	1.74	1.76	0.99	5.97	2.56

[a] Measured at 60 second exposure.

With heat treatment, E-43 and PEMA-treated specimens had lager λ ratios than those without heat treatment (Table 4.3 and Figures 4.4g and h). However, heat treatment did not have significant influence on wettability of G-3015-treated veneer (Figure 4.4i). At the wood-PVC interface, wood-coupling agent and polymer-coupling agent interphases presented high hydrophobicity compared with unmaleated wood specimens (Figure 4.5). All maleated interphases had a larger λ ratio than unmaleated wood surface (Table 4.3). Although there was no significant difference among these surface treatments for G-3015-treated veneer, interphases with E-43 and PEMA had larger λ ratios than E-43- and PEMA-treated veneer (Tables 4.2 and 4.3). For most maleated interphases, λ ratios were over 0.90 and close to 1 at the retention level close to 4% (Figure 4.5). It also clearly showed that the λ ratios of maleated interphases were close to those of maleated veneer with heat treatment (Table 4.3). However, interphases with PEMA had smaller λ ratios than those with E-43 and G-3015.

4.4.2 Static and Dynamic Contact Angles

For both maleated and unmaleated wood specimens, static contact angle was a decreasing function of wetting time (Figures 4.6 and 4.7). For unmaleated yellow poplar veneer, the contact angle change was larger than 20^{o} in a wetting period of 40 seconds (Figures 4.6a). At a similar retention level, initial contact angle (i.e., contact angle at zero second) on E-43- and PEMA-treated yellow poplar veneer decreased by over 70^{o} within 45 seconds (Figures 4.6b and c). For G-3015-treated veneer, however, initial contact angle deceased only by 3^{o} in the same interval (Figure 4.6d). Similar trends were also presented on maleated red oak veneer (Figure 4.7).

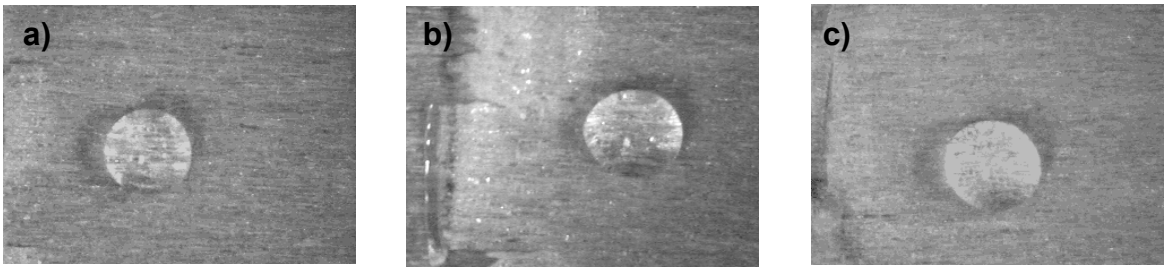

3.64%E-43, S=3.53mm^2, λ =0.99 | 5.21%PEMA, S=3.89mm^2, λ =0.93 | 3.49%G-3015, S=4.05mm^2, λ =0.96

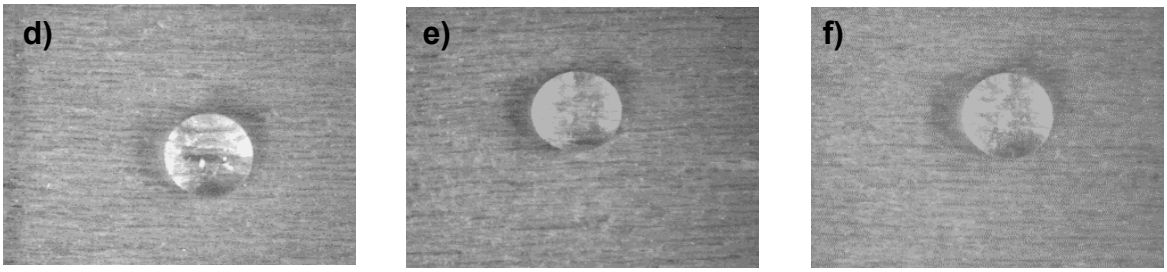

3.64%E-43, S=3.44mm^2, λ =0.93 | 5.21%PEMA, S=4.01mm^2, λ =0.95 | 3.49%G-3015, S=3.59mm^2, λ =0.94

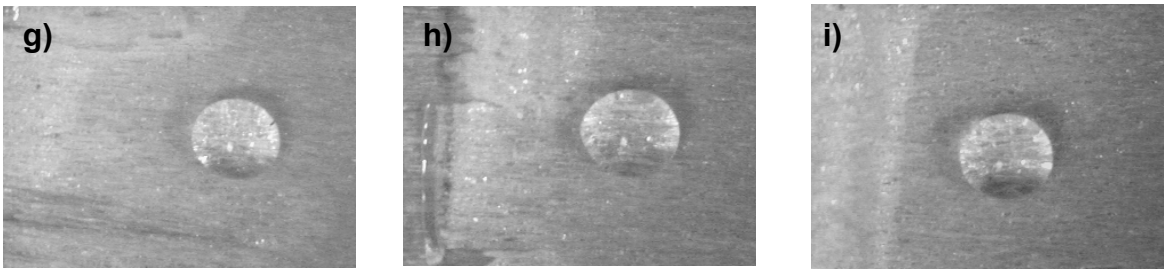

4.12%E-43, S=3.1mm^2, λ =0.90 | 4.74%PEMA, S=4.05 mm^2, λ =0.87 | 3.64%G-3015, S=3.64 mm^2, λ =0.91

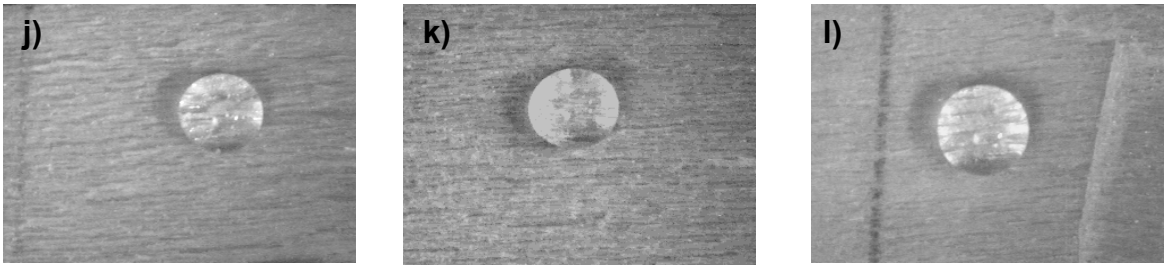

4.12%E-43, S=3.25 mm^2, λ =0.92 | 4.74%PEMA, S=3.46 mm^2, λ =0.89 | 3.64%G-3015, S=3.95 mm^2, λ =0.93

Figure 4.5. Morphology of water droplets on yellow poplar-PVC interface after 15 second exposure. a)-c) unextracted PVC-coupling agent interphases, d)-f) unextracted wood-coupling agent interphases, g)-i) extracted PVC-coupling agent interphases, and j)-l) extracted wood-coupling agent interphases.

Table 4.3. Morphology of water droplets on modified wood veneer and interphases of wood-PVC composites after 15 second exposure.

Material	Wood species	Extraction before coupling	Coupling agents	Retention of coupling agent (%)	Diameter (mm)		Ratio (d_{min}/d_{max})	Perimeter (mm)	Area (mm^2)
					d_{min}	d_{max}			
Modified wood with heat treatment (**S2**)	Yellow poplar	Unextracted	-	0.00	2.06	2.25	0.93	7.33	3.85
			E-43	3.64	2.02	2.16	0.94	7.17	3.70
			PEMA	5.21	1.99	2.11	0.94	6.91	3.45
			G-3015	3.49	2.11	2.17	0.97	7.34	3.87
		Extracted	-	0.00	2.06	2.68	0.77	8.18	4.59
			E-43	4.12	2.16	2.19	0.99	7.40	3.92
			PEMA	4.74	2.14	2.30	0.93	7.57	4.11
			G-3015	3.64	2.11	2.22	0.95	7.30	3.79
Thermoplastic-coupling agent Interphases (**S3**)	Yellow poplar	Unextracted	E-43	3.64	2.03	2.09	0.97	6.94	3.45
			PEMA	5.21	1.99	2.22	0.90	7.18	3.74
			G-3015	3.49	2.18	2.30	0.95	7.51	4.05
		Extracted	E-43	4.12	1.90	2.11	0.90	6.83	3.31
			PEMA	4.74	2.08	2.38	0.87	7.55	4.05
			G-3015	3.64	2.01	2.20	0.91	7.15	3.64
Wood-coupling agent Interphases (**S4**)	Yellow poplar	Unextracted	E-43	3.64	2.00	2.11	0.95	7.01	3.52
			PEMA	5.21	2.17	2.25	0.97	7.50	4.00
			G-3015	3.49	2.03	2.16	0.94	7.10	3.60
		Extracted	E-43	4.12	1.90	2.04	0.93	6.77	3.25
			PEMA	4.74	1.92	2.14	0.90	7.01	3.46
			G-3015	3.64	2.16	2.18	0.99	7.41	3.95

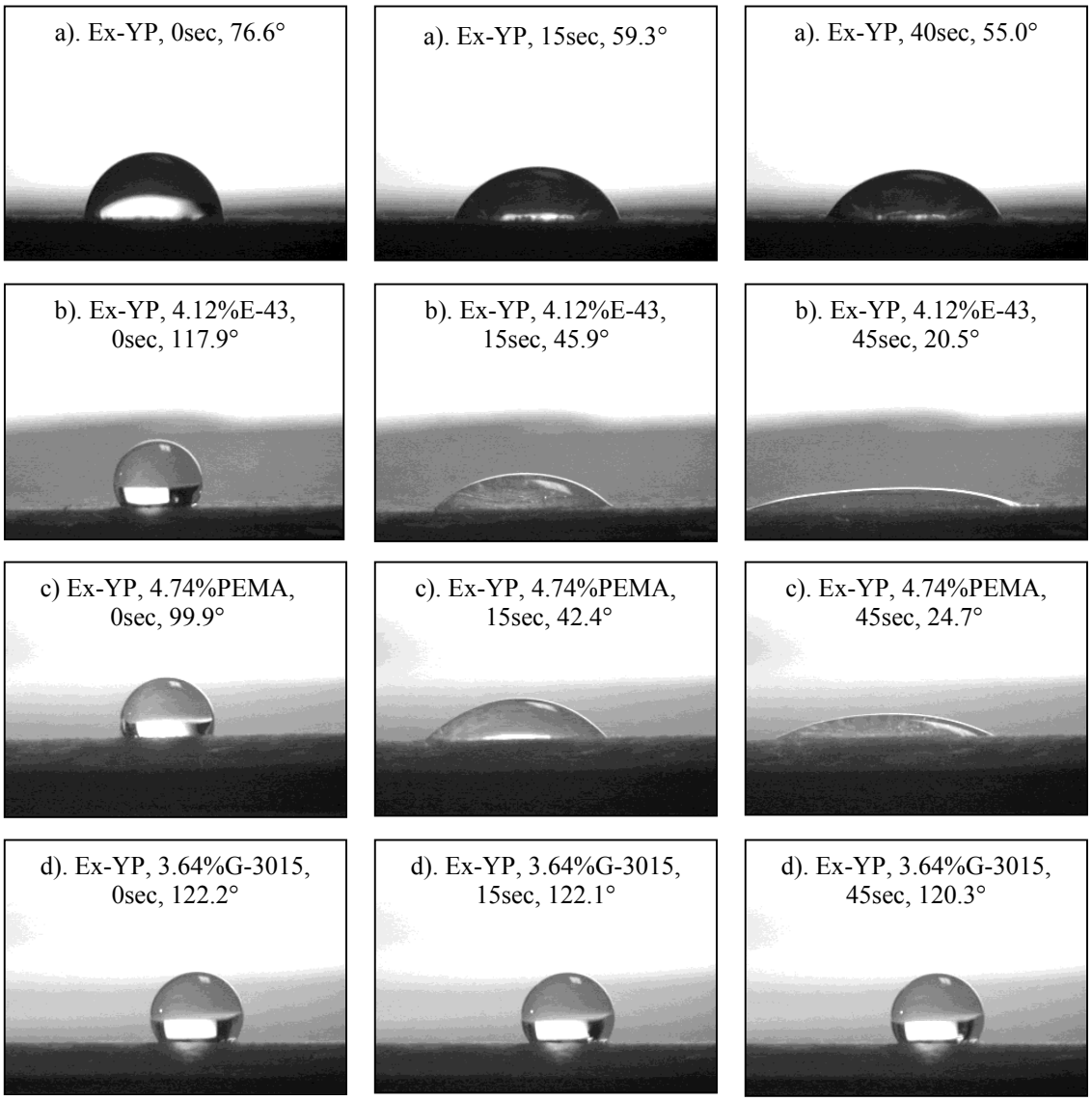

Figure 4.6. Contact angle changes on extracted yellow poplar specimens (Ex-YP) at different wetting periods. a) unmaleated veneer, b) 4.12% E-43 treated veneer, c) 4.74% PEMA treated veneer, and d) 3.64% G-3015 treated veneer.

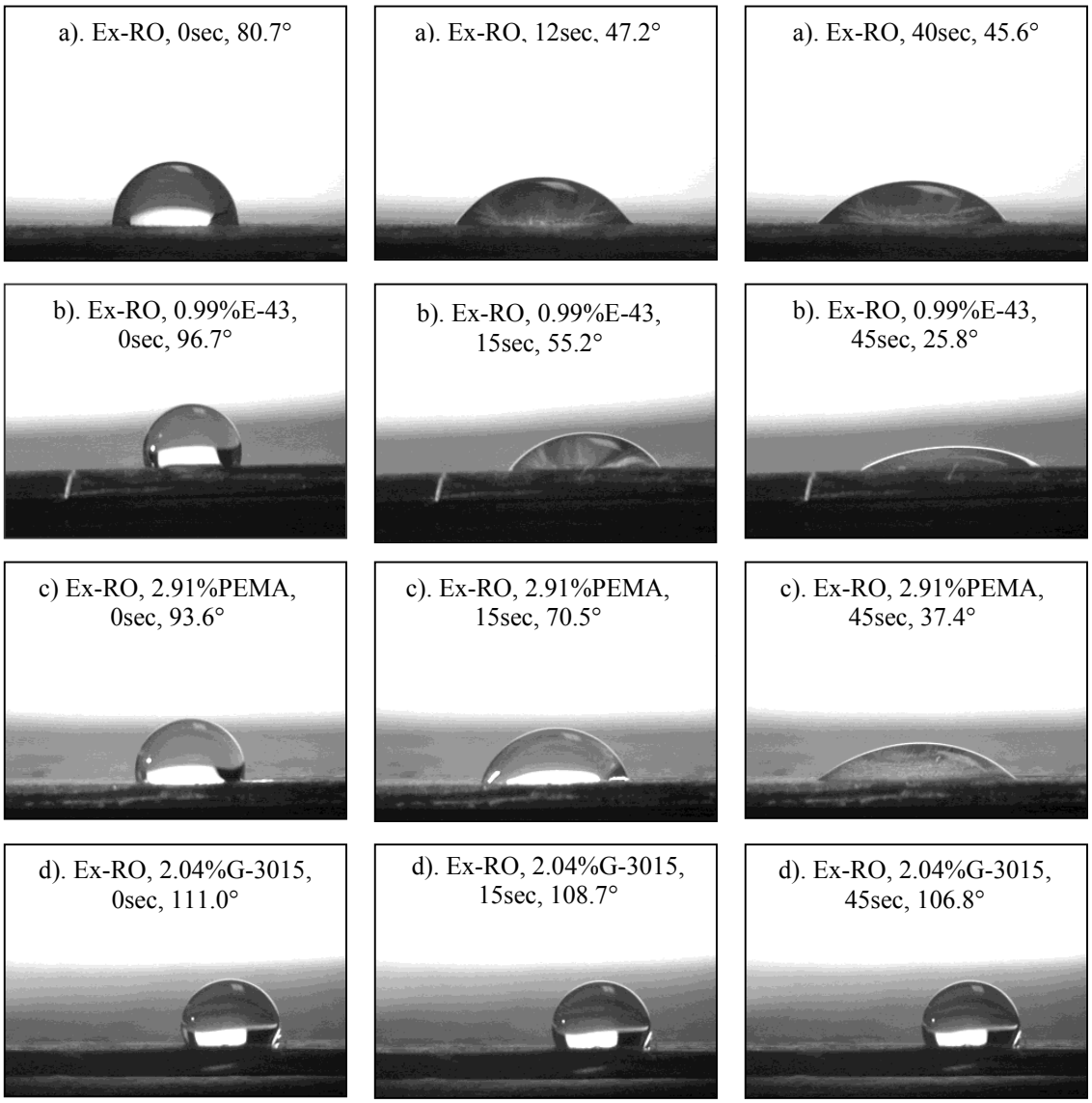

Figure 4.7. Contact angle changes on extracted red oak specimens (Ex-RO) at different wetting periods. a) unmaleated veneer, b) 0.99% E-43 treated veneer, c) 2.91% PEMA treated veneer, and d) 2.04% G-3015 treated veneer.

Measured contact angles as a function of wetting time for modified veneer are shown in Figure 4.8. Wood veneer modified with E-43, G-3015, and PEMA presented different dynamic wettability. The wetting process varied with coupling agent retention. For E-43 (Figure 4.8a), contact angle decreased with increase of retention and wetting time. Contact angle had a large drop at high retention but a smaller decrease at low retention. The largest contact drop occurred at the 6.83% retention level (Figure 4.8a). For PEMA-treated veneer, measured contact angle had a small drop at low retention but a larger drop at high retention. The angle decreased with the increase of coupling agent retention and wetting time (Figure 4.8b). At the 4.74% level, contact angle decreased by 80^{o} within around 40 seconds. At the 23.90% level, contact angles finally leveled off at around 85^{o}.

However, contact angle on G-3015-treated veneer was independent of retention levels and wetting time. At each retention level, contact angle on G-3015-treated surface was almost a constant in the wetting period between 0 and 100 seconds (Figure 4.8c).

4.4.3 Decay and Spreading Ratio

The wetting behaviors of wood veneer modified with different coupling agents at various retention levels were characterized with decay and spreading ratios (Figures 4.9 and 4.10). DR was a decreasing function of wetting time, whereas SR was an increasing function of the time. For E-43-treated specimens, DR_h at the 2.95% level decreased slowly, and it had a largest drop at the 6.84% level. DR_h at the 6.84% level decreased from 1 to 0.8 in about 100 seconds, but it decreased by 0.8 within 20 seconds at the 6.84% level. At the 7.41% level, DR_h gradually decreased and leveled off at 0.4 (Figure 4.9a).

a)

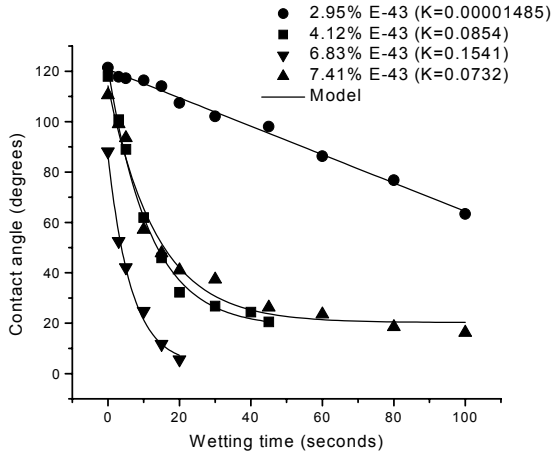

b)

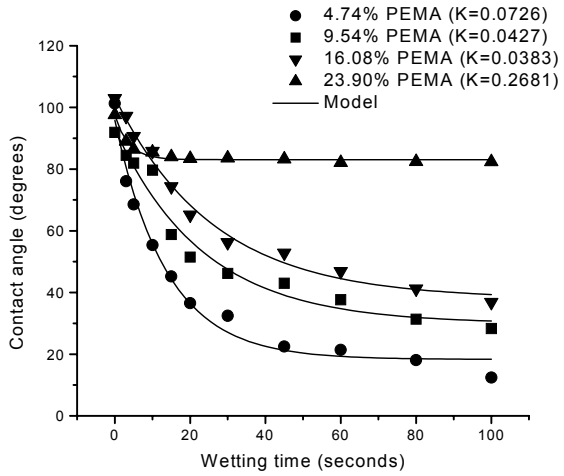

c)

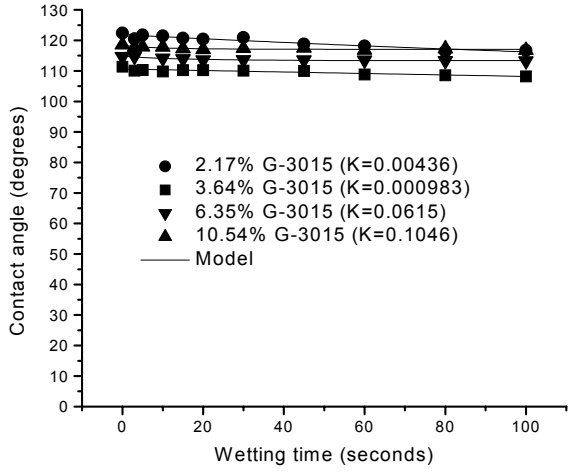

Figure 4.8. Effect of coupling agent retention on contact angle of water droplets on wood surfaces treated with a) E-43, b) PEMA, and c) G-3015.

a)

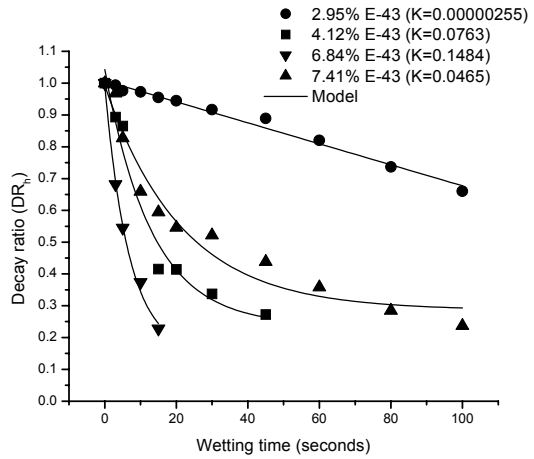

b)

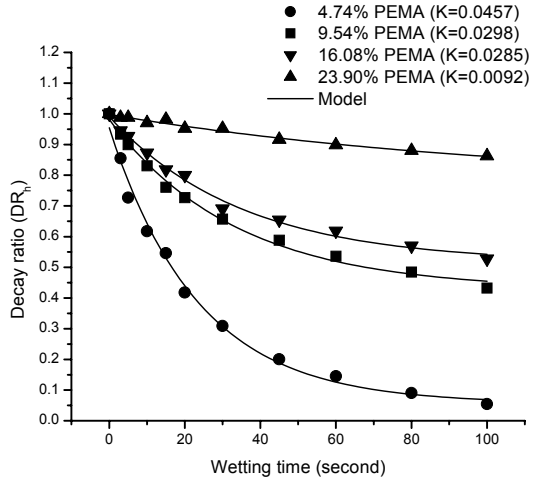

c)

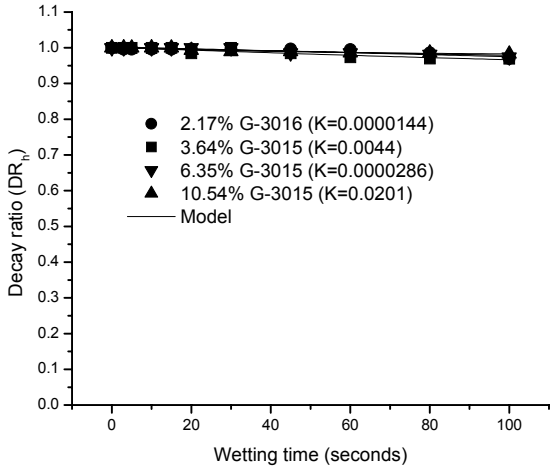

Figure 4.9. Effect of coupling agent retention on decay ratio of water droplets on wood surface treated with a) E-43, b), PEMA and c) G-3015.

a)

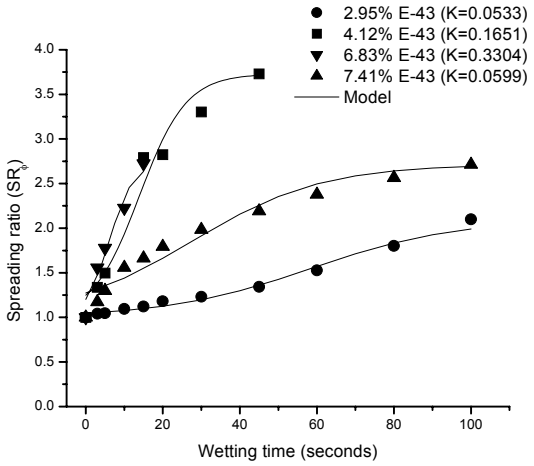

b)

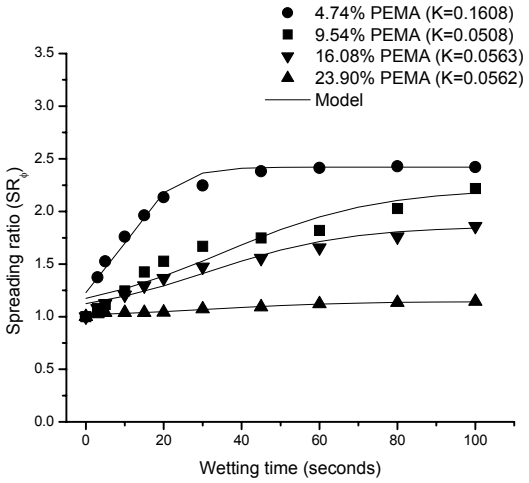

c)

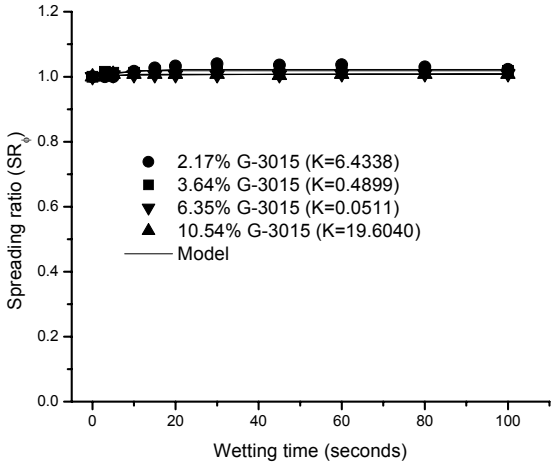

Figure 4.10. Effect of coupling agent retention on spreading ratio of water droplets on wood surface treated with a) E-43, b) PEMA, and c) G-3015.

The influence of coupling agent retention on PEMA-treated specimens was opposite to that on E-43-treated specimens. For PEMA, DR_h decreased with increase of retention. For example, DR_h at the 4.74% level had the largest drop. However, DR_h at high retention (e.g., larger than 9%) gradually decreased with increase of wetting time (Figure 4.9b). DR_h at the 23.90% level was between 0.9-1.0. However, G-3015 retention levels had no significant influence on DR_h. As shown in Figure 4.9c, DR_h was close to one and independent of wetting time and G-3015 retention.

For E-43-treated specimens, SR_ϕ increased with increase of coupling agent retention and wetting time. In 100 seconds, SR_ϕ at the 2.95% level increased from 1 to 1.84, but it increased from 1 to 3.74 within about 40 seconds at the 4.12% level. At the same wetting time (e.g., 10 seconds), SR_ϕ at the 2.95% level increased from 1.078 to around 2.5 at the 4.12% and 6.83% levels, but it dropped back to 1.5 at the 7.41% level (Figure 4.10a). For PEMA-treated specimens, SR_ϕ decreased with increase of coupling agent retention (Figure 4.10b). At the 23.90% level, however, SR_ϕ was around 1 and did not depend on wetting time. However, G-3015 retention also had no significant influence on SR_ϕ. For G-3015-treated specimens, all SR_ϕ values were around to one at each retention level, independent of retention and wetting time (Figure 4.10c).

Figure 4.11 shows the difference of dynamic wetting process on E-43-, G-3-15-, and PEMA-treated wood specimens at similar retention levels. E-43-treated specimens had the largest SR_ϕ, while SR_ϕ on PEMA-treated specimens was larger than those on G-3015-treated specimens. For both E-43 and PEMA-treated specimens, DR_h had almost the same values. At low retention levels, however, DR_h on PEMA-treated specimens had a larger drop than that on E-43-treated specimens (Figure 4.9). For G-3015-treated

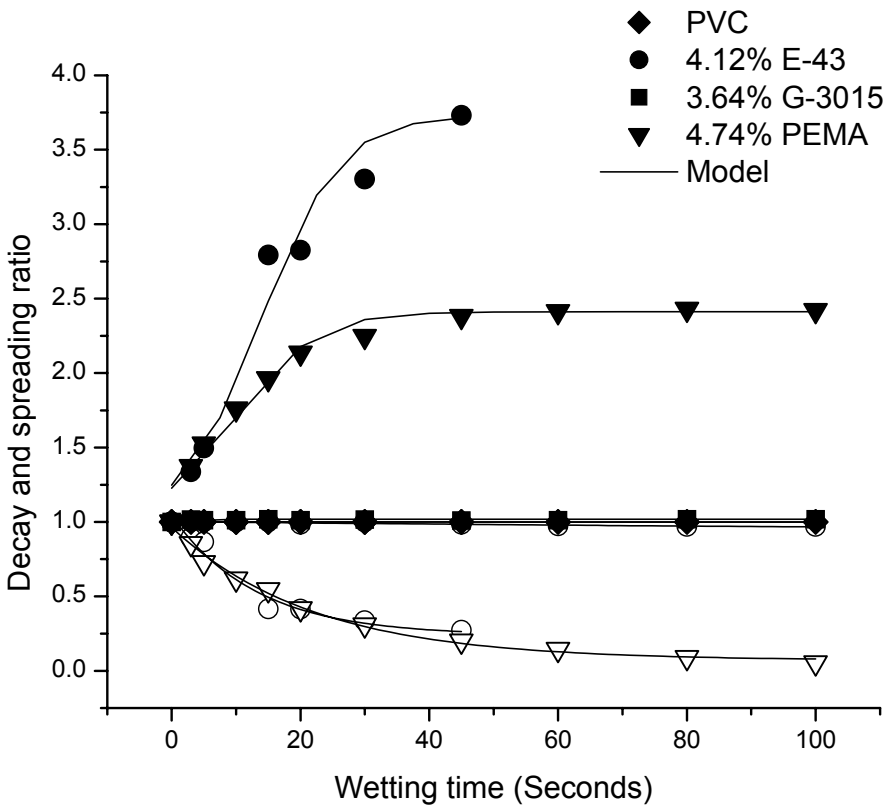

Figure 4.11. Dynamic wetting behaviors of E-43, PEMA, and G-3015. Solid symbols represent SR_{ϕ} and empty ones denote DR_h.

specimens, DR_h and SR_ϕ did not depend on wetting time and retention levels. They were stabilized at 1, similar to those of PVC (Figure 4.11).

The results clearly showed that DR_h had a dynamic wetting trend similar to contact angle (Figures 4.8 and 4.9). Contact angle is a function proportional to its decay height, but is the inverse of its base-diameter. Therefore, dynamic wetting process of chemically modified wood specimens is well represented with DR_h and SR_ϕ. Moreover, DR_h and SR_ϕ are easily compared for different coupling agents at different retention levels. Hence, they can be used to help better understand dynamic wetting process on treated veneer.

4.4.4 Wetting Slope

For all treated specimens, WS_θ varied with coupling agent type and retention (Table 4.4), and the slope converged into zero with increase of wetting time (Figures 4.8-4.10). E-43- and PEMA-treated specimens had larger WS_θ than G-3015-treated specimens. The initial wetting slope, $WS_\theta(0)$, on E-43-treated specimens increased with E-43 retention. The slope reached –12.84 at the 6.84% level, but it went back to –6.88 at the 7.41% level. For G-3015-treated specimens, initial wetting slope, $WS_\theta(0)$, increased with retention. However, the slope at 15 seconds, $WS_\theta(15)$, decreased with increase of retention. For PEMA-treated specimens, both $WS_\theta(0)$ and $WS_\theta(15)$ decreased with increase of retention.

E-43 and PEMA-treated specimens had larger $WS_{hR}(0)$ and $WS_{hR}(15)$ than G-3015 treated specimens. For E-43 treated specimens, the initial slope $WS_{\phi R}(0)$ and the slope at 15 seconds, $WS_{\phi R}(15)$, increased with increase of retention. $WS_{\phi R}(0)$ reached its

Table 4.4. Kinetics of wetting for water droplets on treated wood specimens. [a]

Coupling agent	Coupling agent retention (%)	Contact angle (θ) [b,c]			Decay ratio in height (DR_h) [b,c]			Spreading ratio in base-diameter (SR_ϕ) [b,c]		
		K_θ	$WS_\theta(0)$	WS_θ (15)	K_{hR}	$WS_{hR}(0)$	$WS_{hR}(15)$	$K_{\phi R}$	$WS_\phi(0)$	$WS_{\phi R}(15)$
E-43	2.95	1.49×10^{-5}	-0.5635	-0.5634	2.55×10^{-6}	-0.0033	-0.0033	0.0533	0.002364	0.004758
	4.12	0.0854	-8.7885	-2.4403	0.0763	-0.04234	-0.01348	0.1651	0.03724	0.005097
	6.84	0.1541	-12.8356	-1.272	0.1484	-0.1247	-0.01346	0.3304	0.05881	0.000833
	7.41	0.0732	-6.8753	-2.2949	0.0465	-0.03288	-0.01636	0.0599	0.01376	0.02557
PEMA	4.74	0.0726	-5.6287	-1.8937	0.0457	-0.04084	-0.02058	0.1608	0.03095	0.04955
	9.54	0.0427	-2.7003	-1.4238	0.0298	-0.01652	-0.01057	0.0508	0.0076	0.01202
	16.08	0.0383	-2.5047	-1.4100	0.0285	-0.01357	-0.00885	0.0563	0.005949	0.009767
	23.90	0.2681	-3.8445	-0.06896	0.0092	-0.00209	-0.00182	0.0562	0.000966	0.001605
G-3015	2.17	0.00436	-0.0697	-0.0653	1.44×10^{-5}	-0.000211	-0.000211	6.4338	0	0
	3.64	0.000983	-0.0243	-0.0243	0.00440	-0.00044	-0.000410	0.4899	0.00157	0
	6.35	0.0615	-0.0867	-0.0348	2.86×10^{-5}	-0.000277	-0.000277	0.0511	0.000109	0.000113
	10.54	0.1046	-0.133	-0.0277	0.0465	-0.001	-0.0005	19.604	0	0

[a] K_θ, K_{hR}, and $K_{\phi R}$ – constants related to contact angle, DR_h, and SR_ϕ, respectively
[b] WS_θ, WS_{hR}, and $WS_{\phi R}$ – wetting slopes of θ, DR_h, and SR_ϕ, respectively.
[c] Values in parentheses are the wetting time intervals. Negative wetting slopes mean decreasing, while positive ones, increasing.

maximum value at the 6.84% level, but $WS_{\phi R}(15)$ had a maximum value at the 4.12% level (Table 4.4). On G-3015-treated specimens, both $WS_{\phi R}(0)$ and $WS_{\phi R}(15)$ were equal to or close to zero, independent of retention and wetting time. However, they decreased with the increase of retention on PEMA-treated specimens. $WS_{\phi R}(0)$ at the 4.12% level was equal to 0.03095, but it was close to zero at the 23.90% level (Table 4.4).

As shown in Figure 4.12, the wetting slopes of contact angle on G-3015-treated specimens were equal to or close to zero. Also, E-43 and PEMA-treated specimens had larger wetting slopes. This indicated that E-43- and PEMA-treated wood veneer had higher surface energy than G-3015-treated specimens. The wetting slopes on E-43 treated specimens were larger than those on PEMA-treated specimens at the same retention level, because many free or ungrafted maleic anhydride groups on intra and intermolecular chains of PEMA molecules easily formed hydrogen bonding by dehydration during drying after coupling treatments, and thus decreasing the surface energy of treated specimens. Therefore, wood veneer treated with E-43 and PEMA had a polar surface, while that treated with G-3015 had a hydrophobic surface.

4.4.5 K Values

For E-43 and PEMA-treated specimens, K values for contact angle (K_θ), decay ratio (K_{hR}), and spreading ratio ($K_{\phi R}$) were proportional to initial wetting slope (Table 4.4). E-43-treated wood had smaller K values at low retention, but K values increased with the increase of E-43 retention. However, K values at high retention (e.g., 7.41%) decreased again. For PEMA-treated veneer, most K values decreased with the increase of retention. For the decay process, K_θ and K_{hR} on G-3015-treated specimens responded to the changes of initial wetting slopes. For the spreading process, however, $K_{\phi R}$ was

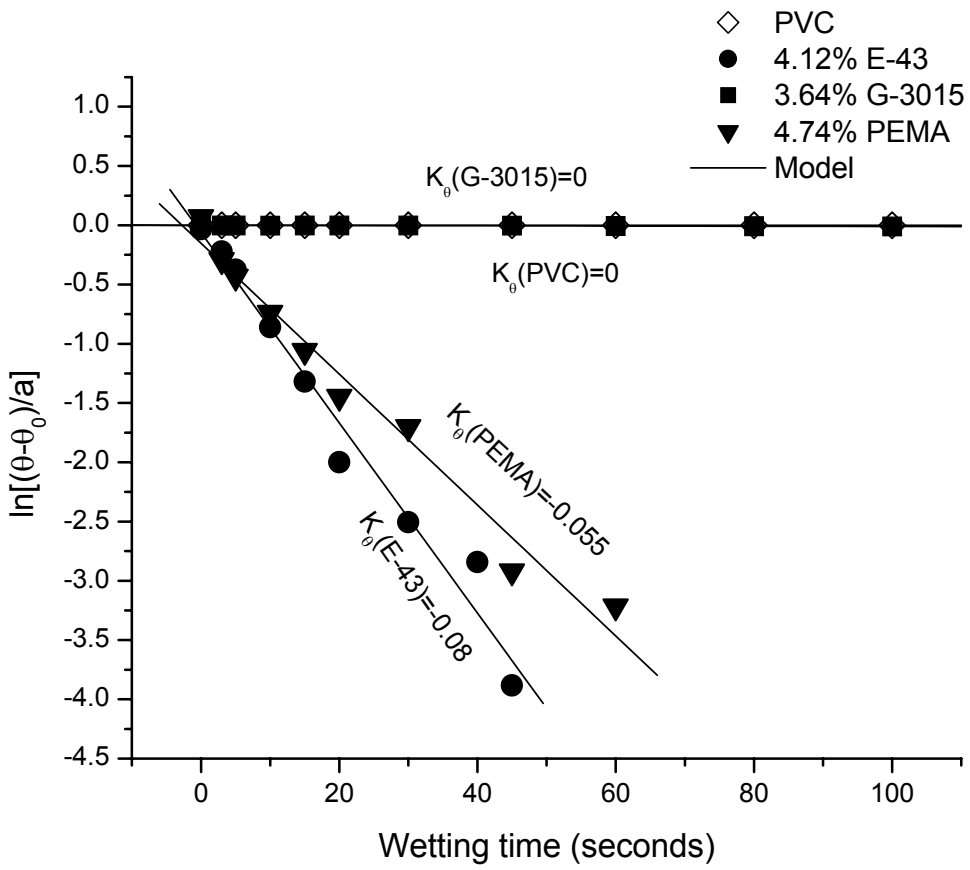

Figure 4.12. Comparison of wetting slopes WS_θ for E-43, G-3015, and PEMA treated wood veneer at similar retention levels.

independent of initial wetting slopes and retention levels. There was a big variation of $K_{\phi R}$ values on G-3015-treated veneer.

4.4.6 Factors Affecting Wetting Behaviors

Wood macroscopic properties greatly influenced its wetting behavior. Wood is a hygroscopic material. The porosity of wood varies with its species and microstructure. Yellow poplar and red oak have different vessel arrangement. Yellow poplar is diffuse-porous hardwood, while red oak is ring-porous hardwood. In the cross section, the pore size of vessel elements in yellow poplar is uniform and evenly distributed across the growth ring. However, vessels in early wood of red oak have much larger diameter than those in late wood. After rotary cutting, red oak veneer has a rougher surface than yellow poplar because of the scratchlike pattern of red oak after cutting (Vick 1999) and the significant difference between its early wood and late wood. Therefore, contact angle on red oak veneer early wood is larger than that on yellow poplar (Figures 4.6a and 4.7a).

However, capillary effects made red oak veneer with larger pore diameter on early wood to have faster wetting speed than yellow poplar with smaller pore diameter. Red oak has radially oriented rays that can allow excessive flow and overpenetration (Vick 1999). Also, red oak species usually has many open checks in the loose side during rotary cutting by a knife. This imperfection on red oak veneer also causes liquid overpenetration. As shown in Figures 4.6a and 4.7a, contact angle on red oak veneer decreased by 35^{o} but on yellow poplar, only by 20^{o} within 40 seconds.

In most situations, contact angle in the direction along wood grain was smaller than that in the cross direction (Table 4.5). For E-43-treated veneer, contact angle across the grain was 10 degrees larger than that along the grain. On wood veneer, capillary

Table 4.5. Initial contact angle on maleated wood veneer.

Material	Species	Coupling agent	Extraction before treatment	Orientation to wood grains [a]	Initial contact angle [b, c] (Degrees)			
Wood veneer	Yellow poplar	–	Unextracted	//	83.8(10.3)			
				⊥	-			
		–	Extracted	//	63.6 (6.3)			
				⊥	-			
Modified wood veneer (**S1**)	Yellow poplar	E-43	Unextracted		2.16%	3.64%	7.14%	8.05%
				//	103.1 (8.7)	84.2 (8.2)	89.8 (5.4)	64.8 (6.5)
				⊥	119.2 (11.4)	112.1 (3.1)	99.5 (5.3)	96.5 (6.0)
			Extracted		2.95%	4.12%	6.83%	7.41%
				//	114.8 (4.5)	104.7 (4.2)	89.6 (4.6)	93.0 (6.2)
				⊥	126.4 (5.8)	114.5 (5.1)	112.9 (2.8)	110.6 (4.4)
		PEMA	Unextracted		5.21%	9.67%	15.88%	25.00%
				//	83.2 (8.7)	92.2 (5.2)	104.6 (5.4)	104.7 (5.3)
				⊥	109.5 (5.5)	112.0 (7.3)	115.3 (7.8)	113.6 (5.9)
			Extracted		4.74%	9.54%	16.08%	23.90%
				//	81.0 (4.3)	90.1 (5.7)	91.5 (6.9)	92.8 (4.9)
				⊥	109.2 (2.5)	106.5 (7.4)	115.6 (4.0)	109.4 (7.2)
		G-3015	Unextracted		1.89%	3.49%	6.02%	9.48%
				//	123.0 (6.1)	118.5 (4.2)	118.4 (4.6)	116.6 (5.4)
				⊥	127.0 (7.1)	132.2 (5.6)	123.9 (4.3)	121.8 (5.6)
			Extracted		2.17%	3.64%	6.35%	10.54%
				//	125.8 (6.3)	113.5 (3.9)	117.3 (5.8)	119.2 (6.1)
				⊥	122.9 (5.0)	121.7 (3.8)	124.3 (4.0)	118.9 (8.4)
	Red oak	E-43	Extracted		0.25%	0.99%	4.10%	6.17%
				//	109.6 (6.3)	99.4 (5.4)	91.4 (7.5)	93.1 (7.5)
				⊥	109.2 (2.5)	98.6 (6.1)	90.8 (7.0)	83.2 (5.5)
		PEMA	Extracted		2.91%	4.90%	12.01%	17.44%
				//	78.0 (5.1)	80.8 (3.2)	85.8 (4.9)	93.2 (6.8)
				⊥	111.1 (7.8)	114.1 (6.1)	96.4 (7.1)	107.5 (4.2)
		G-3015	Extracted		0.45%	2.04%	5.20%	11.46%
				//	112.0 (3.8)	115.9 (7.0)	110.6 (4.9)	118.8 (7.7)
				⊥	115.0 (3.0)	115.4 (5.4)	125.1 (8.4)	121.2 (9.1)

[a] // and ⊥ indicate the direction parallel and perpendicular to the wood grain, respectively.
[b] The values underlined are retention levels of coupling agent.
[c] The values in parentheses are standard deviations.

effects on cut fiber tracheid and vessel lumens made wetting liquids to spread much easier along the grain direction than the cross direction (Shi and Gardner 2001). Also, the direction along wood grains is smoother than the cross direction. On the other hand, most molecular chains of coupling agents may be distributed along wood grain. Thus, the direction along the grain had larger surface tension than the cross direction.

Extracted wood veneer had higher polarity than unextracted veneer (Table 4.2 and Figures 4.4b and c). For yellow poplar veneer, contact angle along the wood grain on unextracted specimens was 20 degrees larger than that on extracted specimens (Table 4.5). This was due to the fact that more hydroxyl groups of lignocellulose freely exposed on wood surface and resulted in a more hydrophilic surface after extractives were removed (Lu et al. 2002).

Wtttability of modified wood veneer was influenced by different coupling agents. For E-43- and PEMA-modified veneer, their wetting behaviors were similar to that of wood surface (Figures 4.4b, d, and e). However, G-3015-modified veneer presented the wetting characteristics similar to PVC film (Figures 4.4a and f). As a result, G-3015-modified surface acted as thermoplastics, while E-43 and PEMA-modified surfaces were more like wood. The influence of coupling agent retention on initial contact angle of modified veneer is shown in Table 4.5 and Figure 4.13. For E-43, initial contact angle decreased with the increase of coupling agent retention, while initial contact angle increased with the increase of retention in the case of PEMA. For E-43 and PEMA, extractives influenced initial contact angle of modified veneer, especially at high retention. However, initial contact angle was independent of retention and extractives for

G-3015-treated wood veneer (Figure 4.13a). Similar wetting behavior was also presented for maleated red oak veneer treated (Figure 4.13b).

The difference in the wetting behavior of maleated wood specimens lies in the structure and coupling action of these coupling agents. E-43 has higher acid number but smaller molecular weight than G-3015. Compared with E-43 and G-3015, PEMA has larger molecular weight and higher acid number (Table 4.1). Due to the limitation of maleation at the interface (Lu et al. 2002), there were many free or ungrafted maleaic anhydride (MA) groups on surfaces of PEMA- and E-43-treated wood veneer. Consequently, wood specimens treated with E-43 and PEMA had higher polarity than those with G-3015.

For G-3015, some MA groups of G-3015 reacted with hydroxyl groups (-OH) through graft polymerization and formed ester linkage with wood. However, some free or ungrafted MA groups may be buried in the large G-3015 molecular chains. Therefore, G-3015 produced a less polar or non-polar structure at the interface.

PEMA has much more free MA groups on its molecular chains than E-43. These free MA groups can easily form hydrogen bonding through intra or inter molecular chains of PEMA and through their interaction with the hydroxyl groups of lignocellulose molecules by dehydration (Felix and Gatenholm 1991). The chemical structure of PEMA was preferred to produce hydrogen bonds between MA groups of its molecular chains and the hydroxyl groups of lingnocellulose and between MA groups of its intra molecular chains. The hydrogen bonding structure interfered with the wetting of water on wood surface and thus decreasing surface polarity of treated veneer. This may be the reason why the wetting behavior of PEMA was opposite to that of E-43 (Figure 4.13). Hence,

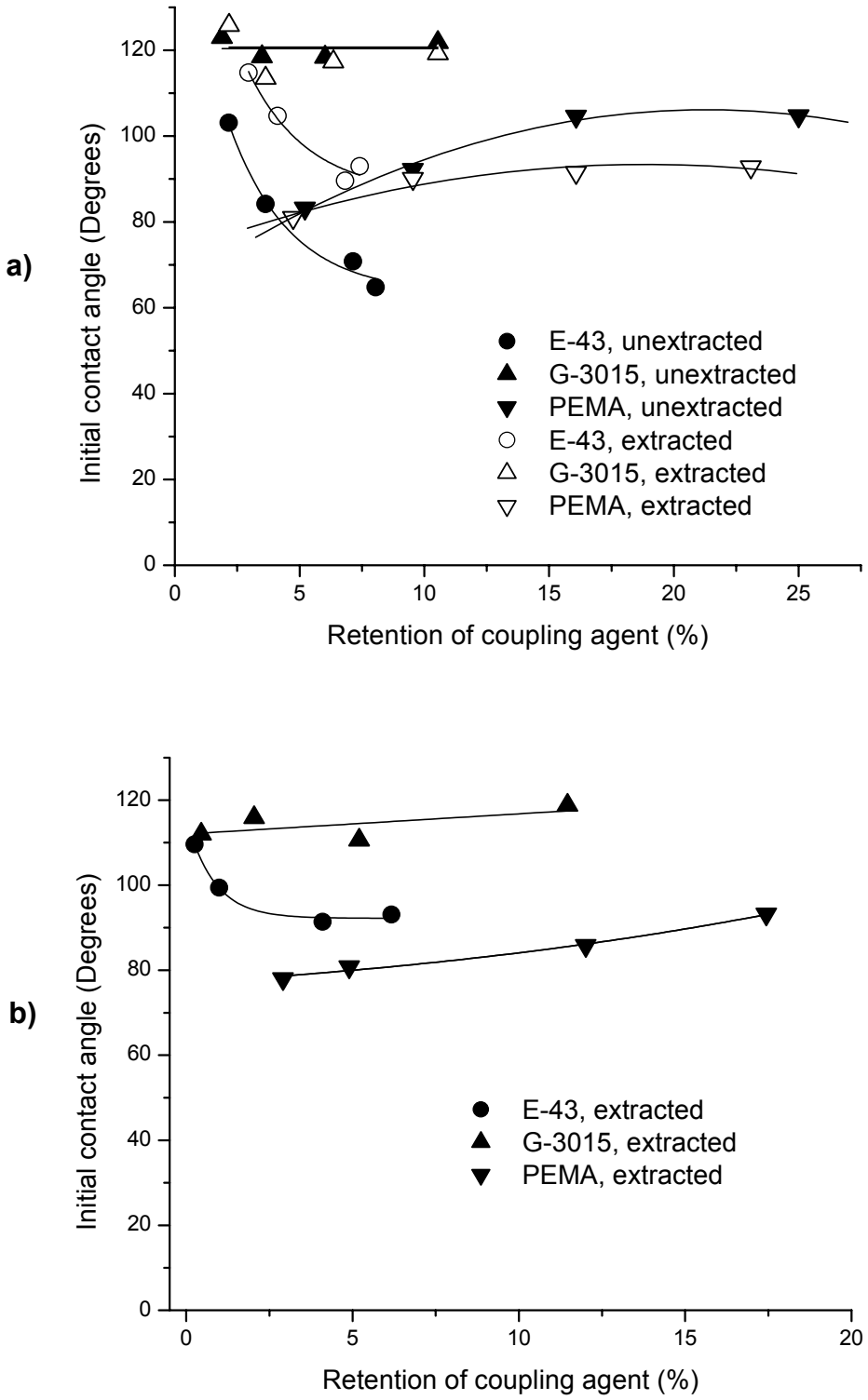

Figure 4.13. Effect of coupling agent retention on initial contact angle along wood grain on a) modified yellow poplar veneer and b) modified red oak veneer.

the wetting behavior of these two coupling agents with high acid number reflected their ability to form hydrogen bonding with the hydroxyl groups of lignocellulose.

The effects of most wood macroscopic properties on wettability of treated veneer were removed by maleation because coupling agents formed a relatively even and continuous film on wood surfaces. Except for directional effects, extractives, wood species, roughness and porosity, surface polarity, and other macroscopic properties had no significant influence on the wetting behavior of maleated specimens due to covering by this polymeric film (Tables 4.3 and 4, Figures 4.4, 4.6, 4.7, and 4.13). The wettability of maleated wood veneer was more related to molecular structure, acid number, and amount of free or ungrafted MA groups of coupling agents (Lu et al. 2002).

Heat treatment had an influence on the wetting behavior of maleated wood specimens. Heat treatment usually caused wood extractives to migrate to the surface and increased its hydrophobicity (Hemingway 1969). Heating wood veneer at 185ºC for 60 min resulted in poor wettability of wood and surface inactivation because of pyrolysis (Hancock 1963). Jordan and Wellons (1977) reported that the wettabillity of dipterocarp veneers decreased with the increase of heating temperature and time. Heated at higher temperatures (larger than 300ºC), wood generates volatile decomposition products from polysaccharides and a charred residue of lignin (Elder 1990).

In this study, the heating temperature (210ºC) for wood veneer was close to the decomposition temperatures of hemicellulose (225-325ºC) and lignin (250-500ºC), but much less than the decomposition temperature of cellulose (325-375ºC) (Shafizadeh and McGinnis 1971). Therefore, heating wood veneer for short time (3 min) lead to slight and slow pyrolytic degradation of xylan and surface dehydration and charring of lignin. These

pyrolytic products helped decrease surface polarity of wood veneer. On the other hand, di- and mono-carboxyl groups (i.e., hydrolyzed products of free or ungrafted MA groups of CAs) formed hydrogen bonding under heating (Felix and Gatenholm 1991), which helped reduce surface polarity of maleated veneer. Thus, surface polarity of treated specimens was decreased by heat treatment.

4.5 CONCLUSIONS

Wood veneer treated with three coupling agents containing MA presented different wetting behaviors. E-43 and PEMA-treated veneer had a hydrophilic surface, while G-3015-treated veneer had a hydrophobic surface. The surface polarity of treated veneer was related to molecular structure, acid number, and amount of free or ungrafted maleic anhydride groups of coupling agent. Because of coupling agent coating, extractives, wood species, roughness and porosity, surface polarity, and other macro properties of wood did not remarkably influence the wettability of maleated specimens.

The morphology of water droplets revealed their wetting behavior on modified surfaces. For E-43 and PEMA-treated veneer, a water droplet had an elliptical shape on the initial contact with wood veneer. However, a water droplet on a G-3015-treated specimen was more close to a circular shape. This indicated that wood veneer treated with E-43 and PEMA was more like wood, while wood veneer treated with G-3015 acted more like thermoplastics. According to water droplet morphology, surfaces with heat treatment were different from those with coupling treatment, but similar to fracture surfaces from shear test. Consequently, maleated surfaces were compatible to thermoplastics after heating. This also indicated that wood-PVC interface can be simulated with maleated wood surface with heat treatment for interfacial characteristics.

Initial contact angle was influenced by coupling agent type, acid number and retention of coupling agent, and direction of wood grains. Initial contact angles increased with increase of E-43 retention but decreased with increase of PEMA retention. However, they were independent of G-3015 retention. For E-43 and PEMA, contact angle cross wood grain was larger than that along the grain. There was no significant directional effect on contact angle on G-3015 treated surface.

Dynamic wetting process of water droplets on maleated wood surface was described with dynamic contact angle, decay ratio, and spreading ration, wetting slope, and K-values. For maleated wood veneer and wood-PVC interface, dynamic contact angle and DR in height followed the first-order exponential decay equation, while SR in droplet base-diameter obeyed the *Boltzmann* sigmoid model.

G-3015-treated wood had a smaller wetting slope than E-43 and PEMA-treated veneer. Wetting slope WS_{θ}, WS_{hR}, and $WS_{\phi R}$ increased with increase of E-43 retention, but they decreased with increase of retention on E-43-treated specimens. PEMA had a wetting process similar to E-43, but the effect of retention on wetting slope WS_{θ}, WS_{hR}, and $WS_{\phi R}$ of PEMA-treated specimens was opposite to that of E43-treated specimens. Wetting slope WS_{θ}, WS_{hR}, and $WS_{\phi R}$ of G-3015-treated veneer were independent of retention and wetting time. Therefore, G-3015-treated veneer presented a hydrophobic surface and acted as thermoplastics, while E-43 and PEMA treated veneer had a polar surface and was more like wood. For PEMA and E43-treated specimens, all *K*-values were related to initial wetting slopes. K_{θ} and K_{hR} on G-3015-treated specimens were proportional to initial wetting slope WS_{θ} (0) and $WS_{hR}(0)$. However, $K_{\phi R}$ on G-3015-treated wood was independent of $WS_{\phi R}(0)$.

4.6 REFERENCES

Bryant, B. S. 1968. Interaction of wood surface and adhesive variables. Forest Prod. J. 18(6): 57-62.

Chen, M. –J., J. J. Meister, D. W. Gunnells, and D. J. Gardner. 1995. A process for coupling wood to thermoplastic using graft copolymers. Adv. Polym. Tehcnol. 14(2): 97-109.

Devanne, H., B. A. Lavoie, and C. Capaday. 1997. Input-output properties and gain changes in the human corticospinal pathway. Exp. Brain Res. 114: 329-338.

Elder, T. 1990. Pyrolysis of wood. Pages 665-699 *in* D. N. –S. Hon and N. Shiraishi, eds. Wood and cellulosic chemistry. Marcel Dekker, Inc., New York, NY.

Elliott, T. A., and D. M. Ford. 1972. Dynamic contact angles. Part 7. –Impact spreading of water drops in air and aqueous solutions of surface active agents in vapor on smooth paraffin wax surfaces. Trans. Faraday Soc. 1: 1814-1823.

Feist, W. C. 1977. Wood surface treatments to prevent extractive staining of paints. Forest Prod. J. 27(5): 50-54.

Felix, J. M., and P. Gatenholm. 1991. The nature of adhesion in composites of modified cellulose fiber and polypropylene. J. Appl. Polm. Sci. 42: 609-620.

Freeman, H. A. 1959. Relation between physical and chemical properties of wood and adhesion. Forest Prod. J. 9(12): 451-458.

Gardner, D. J., F. P. Liu, M. P. Wolcott, and T.G. Rials. 1994. Improving interfacial adhesion between wood fibers and thermoplastics: A case study examining chemically modified wood and polystyrene. Pages 55-63 *in* P. R. Steiner, ed. Proceedings of Second Pacific Rim Bio-Based Composites Symposium. University of British Columbia, Vancouver, B.C., Canada.

Gray, V. R. 1962. The wettability of wood. Forest Prod. J. 12(9): 452-461.

Hancock, W. V. 1963. Effect of heat treatment on the surface of Douglas-fir veneer. Forest Prod. J. 13(2): 81-88.

Halliday, D. R., R. Rensick, and J. Walker. 1997. Fundamental of Physics. John Wiley & Sons, Inc., New York.

Hemingway, R. W. 1969. Thermal instability of fats relative to surface wettability of yellow birchwood (Betula lutea). TAPPI, 52(11): 2149-2155.

Herczerg, A. 1965. Wettability of wood. Forest Prod. J. 15(11): 499-505.

Hodgson. K. T., and J. C. Berg. 1988. Dynamic wettability properties of single wood pulp fibers and their relationship to absorbency. Wood Fiber Sci. 20(1): 3-17.

Jordan, D. L., and J. D. Wellons. 1977. Wettability of dipterocarp veneers. Wood Sci. 10(1): 22-27.

Kalnins, M. A., C. Katzenberger, S. A. Schmieding, and J. K. Brooks. 1988. Contact angle measurement on wood using videotape technique. J. Colloid Interface Sci. 125(1): 344-346.

Kleive, K. 1986. Weathered wood surfaces-Their influence on the durability of coating systems. J. Coating Technol. 58(740): 39-43.

Lee, S. B., and P. Luner. 1972. The wetting and interfacial properties of lignin. TAPPI 55(1): 116-121.

Liptáková, E., and J. Kúdela. 1994. Analysis of the wood-wetting process. Holzforschung 48: 139-144.

Liu, F.P., M. P. Wolcott, J. D. Gardner, and T. G. Rials. 1994. Characterization of the interface between cellulosic fibers and a thermoplastic matrix. Comp. Interfaces 2(60: 419-432.

Liu, F.P., J. D. Gardner, and M. P. Wolcott. 1995. A model for the description of polymer surface dynamic behavior. Contact angle vs. polymer surface properties. Langmuir 11: 2674-2681.

Lu, J. Z., Q. Wu, and I. I. Negulescu. 2002. The influence of maleation on polymer adsorption and fixation, wood surface wettability, and interfacial bonding strength in wood-PVC composites. Wood Fiber Sci. 34(3): 434-459.

Matuana, L. M., J. J. Balatinecz, and C. B. Park. 1998. Effect of surface properties on the adhesion between PVC and wood veneer laminates. Polym. Eng. Sci. 38(5): 765-773.

Motulsky, H. 1999. Analyzing data with GraphPad Prism. GraphPad Software, Inc., San Diego, CA, http://www.graphpad.com.

Nussbaum, R. M. 1999. Natural surface inactivation of Scots pine and Norway spruce by contact angle measurements. Holz Roh- Werkstoff 57: 419-424.

Oye, R, and T. Okayama. 1989. Ink absorption by cellulose paper in calligraphy. Pages 1443-1456 *in* C. Schuerch, ed. Cellulose and wood: chemistry and technology. John Wiley & Sons, Inc., New York.

Scheikl, M., and M. Dunky. 1996. Computerized static and dynamic contact-angle measuring methods in connection with the wettability of wood. Holz Roh- Werkst 54: 113-117.

Scheikl, M., and M. Dunky. 1998. Measurement of dynamic and static contact angles on wood for the determination of its surface tension and the penetration of liquids into the wood surface. Holzforschung 52: 89-94.

Shafizadeh, F., and G. D. McGinnis. 1971. Chemical composition and thermal analysis of cottonwood. Carbohyd. Res. 16: 273-277.

Shi, S. Q., and D. J. Gardner. 2001. Dynamic adhesive wettability of wood. Wood Fiber Sci. 33(1): 58-68.

Skinner, F. K., Y. Rotenberg, and A. W. Neumann. 1989. Contact angle measurements from the contact diameter of sessile drops by means of a modified axisymmetric drop shape analysis. J. Colloid Interface Sci. 30(1): 25-34.

Swanson, J. W., and J. J. Becher. 1966. The adhesion of polyethylene paper. TAPPI 49(5): 198-202.

Wilhelmy, J. 1863. Uber die Abhändigkeit der Capilaritats-Constanten des alkohols von Substanz und Gestalt des benetzten festen Köpers. Ann. Physik. 119: 177-217.

Wilkinson, M. C., and T. A. Elliott. 1974. Dynamic contact angles in Mercury/carbon tetrachloride/solution systems. III. The mechanism and kinetics of spreading. J. Colloid Inter. Sci. 48(2): 225-241.

Wolstenholme, G. A., and J. H. Schulman. 1950. Metal-monolayer interactions in aqueous systems. Part II. The adsorption of long-chain compounds from aqueous solution on to evaporation metal films. Trans. Far Soc. 46: 488-497.

Vick, C. B. 1999. Adhesive bonding of wood materials. Pages 9.1-9.25 *in* Wood handbook: Wood as an engineering material. Gen. Tech. Rep. FPL-GTR-113. U.S. Department of Agriculture, Forest Service, Forest Products Laboratory, Madison, WI.

Young, R. A. 1976. Wettability of wood pulp fibers : Applicability of methodology. Wood Fiber 8(2): 120-128.

Zhang, H.J., D. J. Gardner, J. Z. Wang, and Q. Shi. 1997. Surface tension, adhesive wettability, and bondability of artificially weathered CCA-treated southern pine. Forest Prod. J. 47(10): 69-72.

Zisman, W. A. 1976. Influence of constitution on adhesion. Pages 33-71 *in* Handbook of Adhesives. 2nd ed. Van Nostrand Reinhold Co., New York.

CHAPTER 5. SURFACE AND INTERFACIAL CHARACTERIZATION OF WOOD-PVC COMPOSITES. PART II. THERMAL AND DYNAMIC MECHANICAL PROPERTIES

5.1 INTRODUCTION

Chemical coupling agents usually act as bridge to link polar wood fiber and non-polar thermoplastics. This helps transfer the stresses between wood and thermoplastics, thus improving the interfacial bonding strength in wood fiber-polymer composites (WFPC) (Woodhams et al. 1984; Dalväg et al. 1985). The coupling forms include covalent bonds, secondary bonding (such as hydrogen bonding and van der Waals' forces), polymer molecular entanglement, and mechanical interblocking. Although the coupling action in wood-polymer composites is complicated, the primary forms of covalent bonds for coupling agents are esterification, etherification, carbamation, and carbon-carbon bonding (Lu et al. 2000). Coupling agents (such as maleated polypropylene) create a new structure at the interface, which influences morphology, crystallization, rheology, and mechanical, thermal, and other properties of wood-polymer composites (Rowell 1991; Kolosick et al. 1992; Quillin et al. 1993; Collier et al. 1995).

Thermal analysis has been extensively applied to investigate the thermal behavior of various materials as a function of temperature (Hatakeyama and Quinn 1994). A number of researches on thermal properties of WFPCs have been reported (Simenson and Rials 1996; Oksman and Lindberg 1995). Crystallization and morphology in WFPCs have been investigated with many thermal methods by a number of research workers (Felix and Gatenholm 1994; Ying et al. 1999). Weight or volume ratios of wood fiber greatly influenced glass transition temperatures (T_g) and storage moduli (E´) of the

resultant composites (Gatenholm et al. 1993). Effects of fiber content and dimensional size and interphase modified with MAPP on dynamic and mechanical behavior of wood flour/kenaf fiber-polypropylene composites have been reported (Sanadi et al. 1999). However, it is not clear how the interphase influences the thermal behaviors of resultant wood-polymer composites and whether there is any relationship between coupling agent performance and thermal properties.

As a continuation of our early paper on the influence of maleation on graft polymerization, wettability, and interfacial adhesion in wood-PVC composites (Lu et al. 2002), thermal properties of wood-PVC composites with chemical coupling were investigated in this work. The objectives of this study were to investigate thermal characteristics of wood-PVC composites with maleation and the relationship between thermal properties and coupling agent performance in resultant composites.

5.2 EXPERIMENTAL

5.2.1 Materials

Yellow poplar veneer (610 mm × 610 mm × 0.91mm) was obtained by Columbia Forest Products Co., VT. Wood veneer was cut into 50.8 mm by 25.4 mm in size. Moisture content of all wood specimens was between 5% and 6%. Clean and rigid polyvinyl chloride sheets (508 mm × 1270 mm × 0.0762 mm) with a density of 1,390 kg/m^3 were purchased from Curbell Plastics Co., AZ. The glass transition and melting temperatures of the PVC sheets are 81^oC and 175^oC, respectively. They have a tensile strength of 55 MPa and a tensile modulus of 2,800 MPa (Delassus and Whiteman 1999). Before manufacture of wood-PVC composites, PVC sheets were cut into a dimension of

25.4 mm by 12.7 mm for shear testing and 50.8 mm by 25.4 mm for DMA testing, respectively.

Two maleated polypropylenes (MAPPs), Epolene E-43 and Epolene G-3015, were used as coupling agents. E-43 has an average weight molar mass (M_w) of 9,100, and its acid number is between 40 and 55. G-3015 has a high molecular weight of 47,000 g/mol, but has a low acid number (between 12 and 18). E-43 contains more maleic anhydride groups than G-3015. Benzoyl peroxide (BPO) was used as initiator, and toluene was used as solvent for both MAPPs.

5.2.2 Soxhlet Extraction

Soxhlet extraction was conducted on all wood specimens according to the ASTM standard D1105-96 to reduce the influence of extractives on chemical coupling. The wood samples were first extracted with a 120-ml mixing solution of toluene and ethyl alcohol for 4 hours. They sequentially underwent the second extraction with 120 ml ethyl alcohol for 4 hours. The extracted wood specimens were finally oven-dried at 70^{o}C for 24 hours to reach a constant weight. The oven-dried weight of each sample was measured. Secondary Soxhlet extraction was conducted to determine the graft rate of MAPP on wood specimens. All treated specimens were continuously extracted with toluene for 24 hours (Lu et al. 2002). The extracted specimens were then oven-dried at 70^{o}C for 24 hours to reach a constant weight.

5.2.3 Coupling Treatments

The procedure of coupling treatment for wood specimens was described in the literature (Lu et al. 2002). Wood specimens were dipped in coupling solution at 100^{o}C for 5 min under continuous stirring with a magnetic stirrer. The concentration levels of

MAPP were designed to be 0, 12.5, 25, and 50 g/L. The weight ratio between BPO and MAPP was 0.5. The treated specimens were removed from the solution and cooled down to room temperature. All treated specimens were finally oven-dried at 70^{o}C for 24 hours to reach a constant weight.

Retention and graft rate of coupling agent for treated wood specimens were calculated according to the literature (Lu et al. 2002).

5.2.4 Manufacture of Wood-PVC Composites

The manufacture of wood-PVC composites followed the procedure given in Lu et al. (2002). To create a wood-PVC laminate, a piece of PVC sheet was inserted between two MAPP-treated wood specimens. The assembly was temporally fixed with two pieces of narrow Scotch tape on each side. The assembly was then hot-pressed with a small-scale press under a pressure of 0.276 MPa for a shear specimen and under a pressure of 0.552 MPa for a DMA specimen. The pressing cycle for the wood-PVC assembly consisted of a 3-min heating at 178^{o}C and a 1-min cooling under pressure. At the end of the heating period, the press platens were cooled with running tap water to 70^{o}C. The laminate was allowed to cool to room temperature (Lu et al. 2002).

5.2.5 Shear Strength Measurement

Shear tests were conducted with an INSTRON machine (Model 1125) according to ASTM standards D3163 and D3165. Two mechanical tensile grips were used to clamp the sample to the loading frame. The span between the two clamps was 50.8 mm. Each sample was tested to failure at a loading speed of 2.54 mm/min. Shear strength (Pa) was calculated as a ratio of the maximum failure load (N) to the bonding area (m^2).

5.2.6 Thermal Analysis

5.2.6.1 Dynamic Mechanical Analysis (DMA)

A DMA system (Seiko DMS 110) was used to conduct dynamic mechanical analysis for maleated wood-PVC composites. The specimen size was 50 mm by 12 mm. The DMA testing procedure consisted of three cycles: first heating, first cooling, and second heating (Table 5.1).

Table 5.1. DMA test cycles for wood, PVC, and wood-PVC composites.

Specimen	Test mode	Test cycle	Temperature (^{o}C)		Rate (°C/min)
			Start	Stop	
Wood	Bending	First heating	20	220	0.50
		First cooling	220	30	0.25
		Second heating	30	220	0.50
PVC	Bending	First heating	20	100	0.50
		First cooling	100	30	0.25
		Second heating	30	100	0.50
Woo-PVC composites	Bending	First heating	20	150	0.50
		First cooling	150	30	0.25
		Second heating	30	150	0.50

A test specimen was subjected to sinusoidal stress under a three-point bending mode. The span between the load and each supporting point was 20 mm. The oscillating frequencies of the load acting on the specimens were 0.01 Hz, 0.1 Hz, 1 Hz, 10 Hz, and 100 Hz. Testing temperatures changed according to test materials. Starting from room temperature, the maximum heating temperature was 220^{o}C for wood, 100^{o}C for PVC, and 150^{o}C for wood-PVC composites. The heating rate was 0.5^{o}C/min, while the cooling rate was 0.25^{o}C/min.

5.2.6.2 Thermogravimetric Analysis (TGA)

A modulated thermogravimetric analyzer (TA Instruments TGA2950) was used to characterize the decomposition and thermal stability of maleated wood-PVC composites. A specimen was first placed into a Seiko Al sample pan on the Pt basket in the furnace, and then heated from room temperature to 600^{o}C. The heating rate was 5^{o}C/min. During testing, the heating unit was flushed under a continuous nitrogen flow at a pressure of 8 KPa. To separate possible overlapping reactions during measurements, derivative thermogravimetric (DTG) analysis was also conducted to measure the mass change of a specimen with respect to temperature (dm/dT) using the same TGA system.

5.2.6.3 Differential Scanning Calorimetry (DSC)

A modulated DSC analyzer (TA Instruments DSC Q100) was used to determine the thermal complex transitions of maleated wood-PVC composites. A specimen pressed into an aluminum sample pan was placed into the heating chamber for DSC. For comparisons of wood, PVC, and resultant composites, the maximum temperature was controlled at 150^{o}C for all composite specimens. The heating rate was 5^{o}C/min. During measurements, the heating chamber was flushed with a continuous nitrogen flow at a pressure of 8 KPa. Each specimen was measured twice. For separating possible overlapping brands, a derivative DSC (DDSC) was applied to help analyze DSC spectra.

In order to remove the blocking effect of wood veneer on DSC spectra, a wood-PVC composite sample was delaminated with a sharp knife into a PVC film and two pieces of wood veneer to help investigate characteristics of esterification in DSC spectra. The maximum testing temperature for PVC-coupling agent interphases was less than

220°C, while the maximum testing temperature for wood-coupling agent interphases was controlled to be 400°C.

5.3 RESULTS AND DISCUSSION

Primary thermal and mechanical properties of wood-PVC composites are summarized in Table 5.2. Retention and graft rate of MAPP on wood after coupling treatment are listed in Table 3.2.

5.3.1 Dynamic Mechanical Analysis

Wood-PVC composites treated with coupling agents presented thermal behaviors different from wood and PVC. As shown in Table 5.2 and Figure 5.1, the glass transition (T_g) of PVC was about 80°C, while T_g of yellow poplar was close to 150°C. From the first heating, T_g of wood-PVC composites was around 89°C at the frequency of 1 Hz. Therefore, T_g of wood-PVC composites was between those of wood and PVC.

Frequency of the oscillating load greatly influenced T_g of wood-PVC composites (Figure 5.2). From the second heating, the glass transition of wood-PVC composites with 6.83% E-43 shifted about 20°C from 0.01 Hz to 100 Hz. Similar trends also occurred in wood-PVC composites with other retention levels of MAPP in the same heating procedure and with all retentions in other two procedures. Thus, the larger the frequency used, the higher the glass transition of wood-PVC composites.

Storage modulus E′ increased with the increase of MAPP retention (Table 5.2). At low retention levels, E′ of maleated wood-PVC composites was lower than or close to the value from composites without maleation (Figure 5.2). When retention levels were over 3%, E′ was as high as 9 GPa. The modulus was lower than 9 GPa after the retention level was larger than 6% for both MAPPs. However, retention did not significantly

Table 5.2. Thermal and mechanical properties of wood-PVC composites.

Material	Shear strength (MPa)	E′ (GPa) [a]	E″ (GPa) [a]	tanδ [a]	T_m of MAPP (^oC) [b]	T_g of wood (^oC) [b]	Enthalpy at MAPP T_m (J/g)	Enthalpy at wood T_g (J/g)	TG at 600^{o}C (%)
PVC	-	5.73	0.44	0.39	-	77	0	0	10.3
Wood veneer	-	10.43	0.41	0.05	-	151	0	0.003025	18.8
WPC with									
0% E-43	3.14	7.85	1.04	0.22	-	151	0	0.003025	16.8
2.95% E-43	2.90	7.96	0.97	0.22	153	141	0.08328	0.01684	17.9
4.12% E-43	3.03	9.45	1.23	0.24	152	140	0.2322	0.07899	18.2
6.83% E-43	3.32	9.16	1.15	0.23	146	133	0.2840	0.05358	16.5
7.41% E-43	3.71	-	-	-	147	134	0.3499	0.1009	-
0% G-3015	3.14	7.85	1.04	0.22	-	151	0	0.003025	16.8
2.17% G-3015	2.90	7.08	0.8	0.23	159	149	0.04766	0.01867	16.5
3.86% G-3015	2.94	8.98	1.16	0.24	157	148	0.07654	0.01561	15.4
6.35% G-3015	3.61	8.56	1.09	0.24	151	141	0.1204	0.1041	17.0
10.54% G-3015	3.85	-	-	-	152	141	0.4917	0.3300	-

[a] All values were measured in first heating at 1 Hz.;
[b] The values were based on interphases.

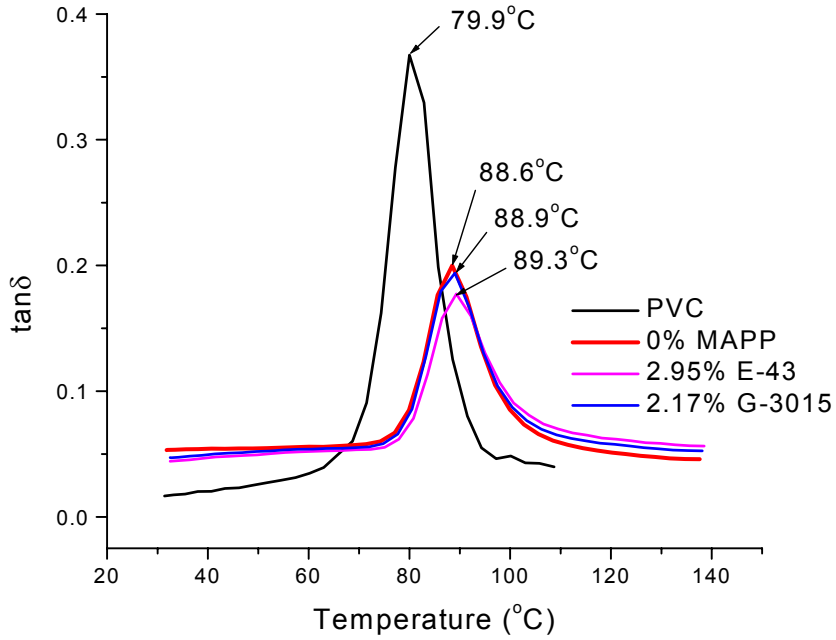

Figure 5.1. Glass transitions of wood-PVC composites in comparison with PVC in the second heating at a frequency of 1 Hz.

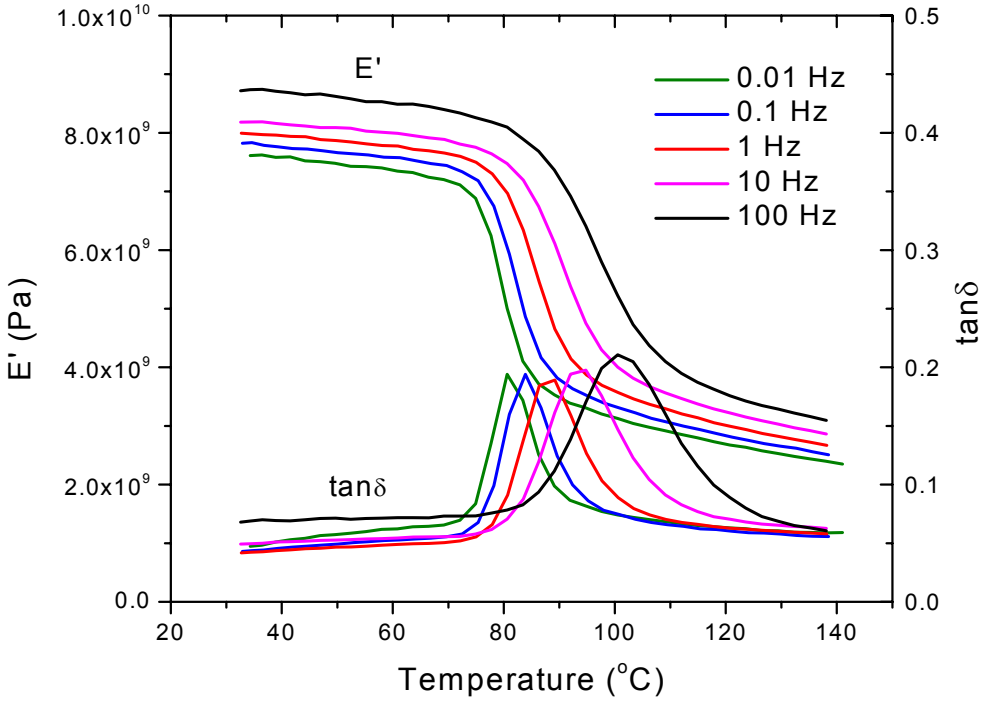

Figure 5.2. Influence of frequency on the storage modulus *E´* and *tan*δ of wood-PVC composites with 6.83%E-43 at the second heating.

influence the glass transition of wood-PVC composites. Composites treated with MAPP had almost the same glass transition temperature (Figure 5.3). The value of tanδ for wood-PVC composites was about half that of PVC and much larger than that of wood (Table 5.2). There was no significant difference in tanδ for composites with and without maleation. Therefore, tanδ was independent of MAPP retention and graft rate.

Interfacial bonding strength of wood-PVC composites increased with the increase of storage modulus E′ and complex modulus E* at low retention levels and graft rate. However, interfacial bonding strength was not so sensitive to these moduli at high retention levels and graft rate. This indicated that interfacial adhesion was more closely related to MAPP retention, graft rate, and the interfacial structure (Lu et al. 2002).

5.3.2 Thermogravimetric Analysis

According to the TG spectra (Figure 5.4a), PVC underwent two separate degradation steps under heating. PVC was stable at low temperatures. At about 250^{o}C, its thermogravimetric percentage (TG%) drastically dropped to 50%. It gradually decreased before 400^{o}C. There was another drastic drop at around 410^{o}C. TG% of PVC decreased to about 15% and was stable until the temperature reached 600^{o}C. Wood also presented two separate decomposition procedures. The first decomposition occurred below and at 80^{o}C. This was because of water evaporation from wood. The moisture content of wood accounted for about 5-6% based on weight. Wood started degrading at 250^{o}C. The second procedure was slow and gradual. TG% of wood finally dropped to about 17% at 600^{o}C.

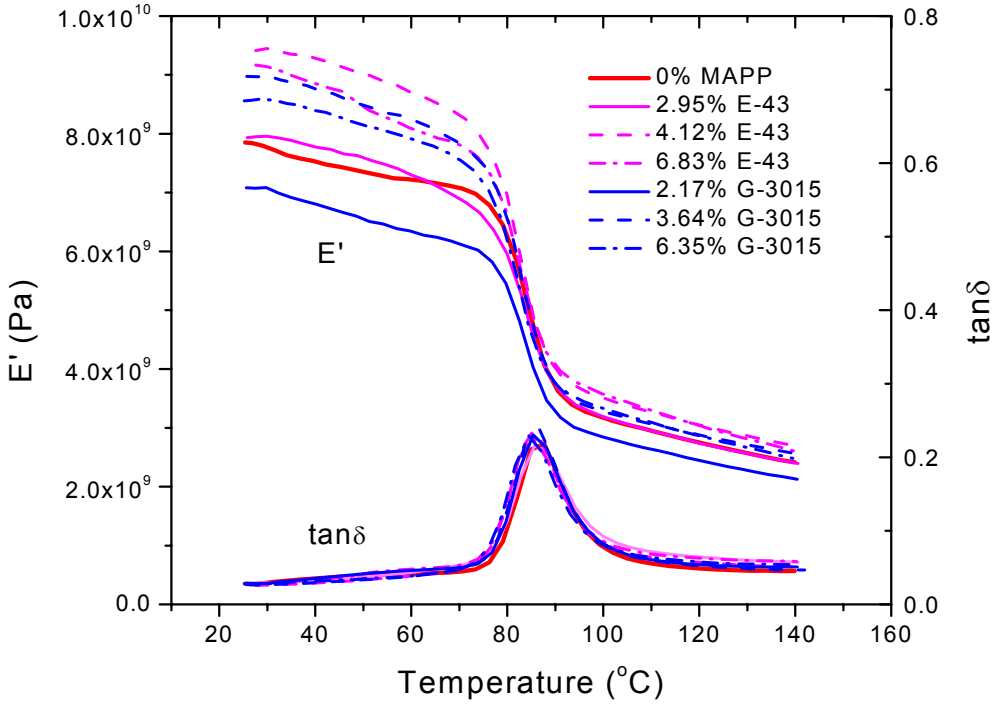

Figure 5.3. Influence of meleation on storage modulus *E´* and phase angle *tan*δ of wood-PVC composites in the first heating at a frequency of 1 Hz.

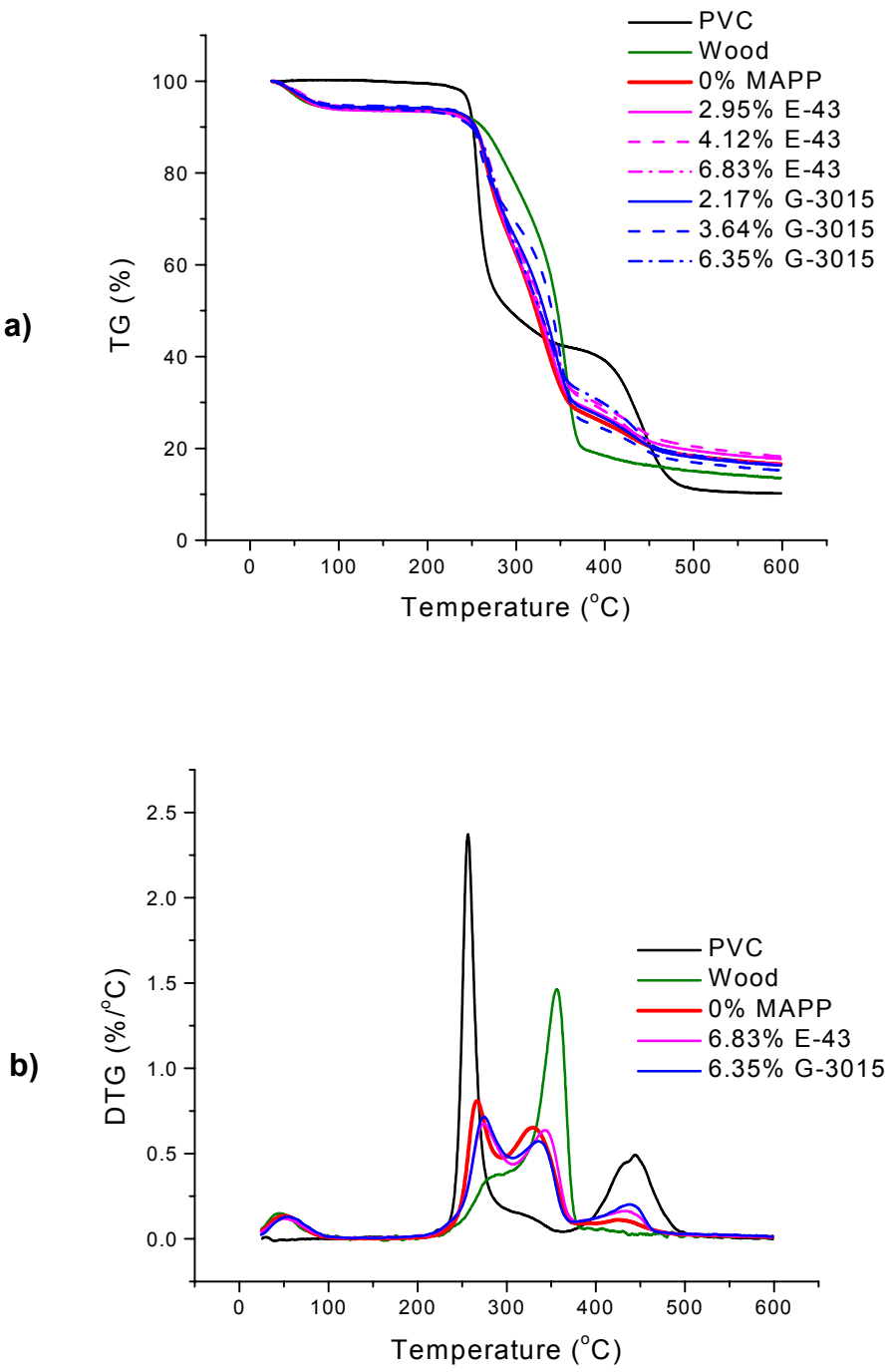

Figure 5.4. Influence of maleation on decomposition of wood-PVC composites. a) TG and b) DTG.

Thermal decomposition behavior of wood-PVC composites was more close to that of wood (Figure 5.4a). Since PVC accounted for a very small weight proportion (<5%) in composites, wood-PVC composites acted more like wood. Similar to wood, wood-PVC composites also had a gradual decomposition procedure. The decomposition behavior of maleated wood-PVC composites was close to that without maleation at low temperatures (<250^{o}C). However, TG curves of maleated composites deviated from those without maleation after temperatures were greater than 300^{o}C. Particularly, composites with 3.64% G-3015 presented a distinguished deviation compared with G-3015-maleated composites at other retention levels and composites with all E-43-maleated composites.

According to the DTG spectra (Figure 5.4b), PVC had a large and sharp DTG peak at 250^{o}C and a small and broad peak at about 450^{o}C. For wood, a small and broad peak occurred at 50^{o}C, and a big and sharp peak at 350^{o}C. The latter peak had a broad base, indicating that another peak at around 275^{o}C overlapped with it. These four composite peaks of wood and PVC were all presented in wood-PVC composites, but the second and the third peaks overlapped. The first and the third peaks were the characteristics of wood, while the second and the forth were from PVC. These two overlapping peaks shifted somewhat compared with those feature peaks of wood and PVC, respectively. It was clearly shown that maleation caused shifts to the right on these two overlapping peaks (Figure 5.4b). Also, the second peak of PVC was very weak in the DTG spectra of wood-PVC composites. This indicated that maleated wood-PVC composites had improved thermal stability compared to PVC.

5.3.3 Differential Scanning Calorimetry

As shown in Figure 5.5, the glass transition of PVC was 77^{o}C, close to the result from DMA. For wood, a broad endothermal peak appeared at 80^{o}C because of water evaporation from wood. For wood-PVC composites with maleation, a similar peak also occurred in the DSC spectra. However, the spectra of composites with E-43 had a significant shift to the right side compared with those with G-3015. Because E-43 has more anhydride groups in its molecular backbone than G-3015, many ungrafted or non-reacted maleic anhydride (MA) groups may exist at the interface after manufacture (Lu et al. 2002). This shifting may be caused by these ungrafted or non-reacted MA groups at the interface. Therefore, the glass transition of wood-PVC composites cannot be easily detected due to the interference of water evaporation in wood and the presence of single and double carboxylic acids from ungrafted MA groups at the interface.

On the DDSC spectra, composites with E-43 and G-3015 presented similar thermal behavior (Figure 5.6). Maleated composites had a small peak in the range of around 50^{o}C to 60^{o}C. Tm(IV) is the melting temperature (T_m) of maleaic anhydride groups (CRC Press 2000). This indicated that there were ungrafted or free maleaic anhydride groups at the interface after coupling treatment. Also, a weak band was presented at around 77^{o}C and Tg(I) was the glass transition (T_g) temperature of PVC. Tg(II) was presented at around 157^{o}C for composites with G-3015. It was the glass transition of wood. Composites with E-43 had a left shifting Tg(II) (i.e., T_g of lignin) to around 150^{o}C. T_m of PVC appearred as Tm(I) at around 125^{o}C, but it shifted left to the

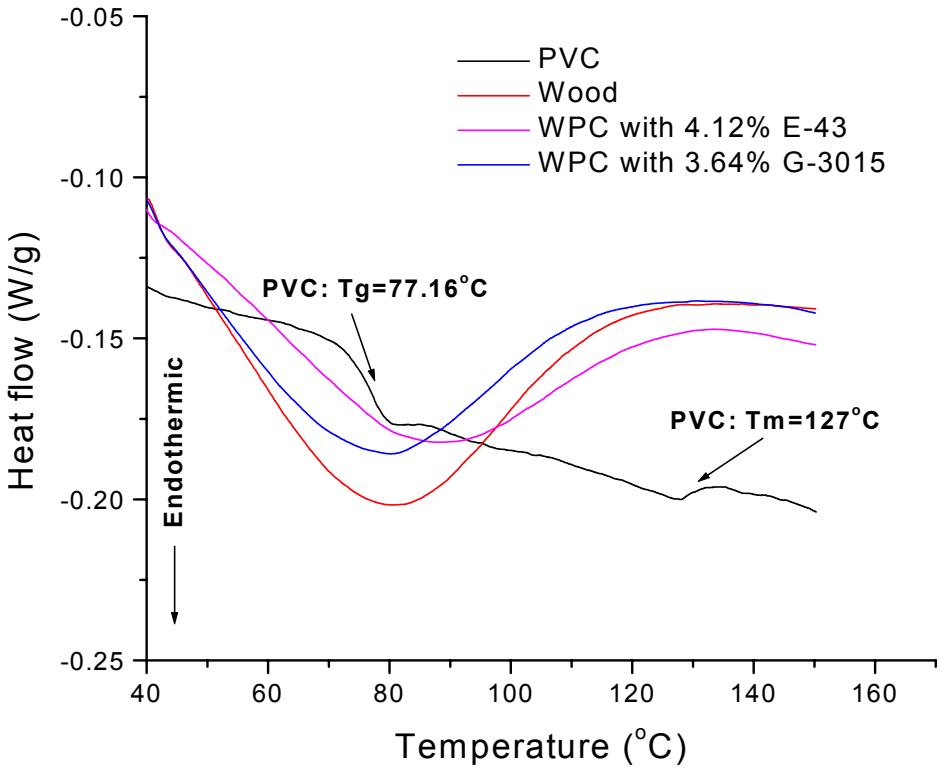

Figure 5.5. Influence of wood and its moisture content on DSC spectra of wood-PVC composites.

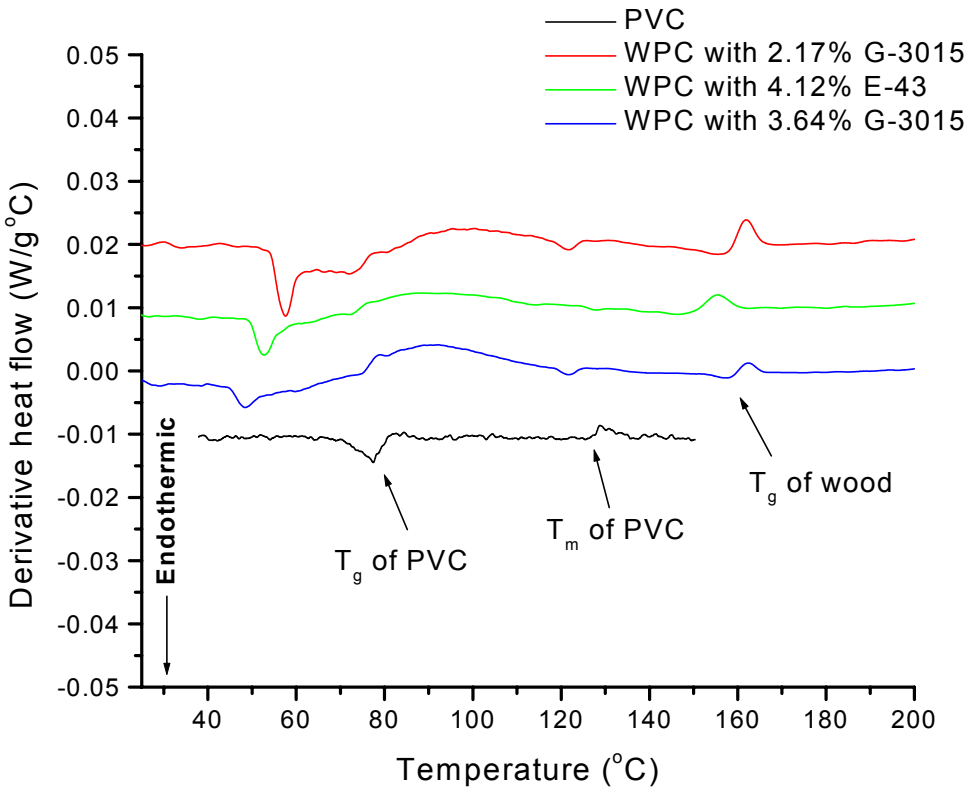

Figure 5.6. DDSC spectra of maleated wood-PVC composites.

value of around 123°C on the spectra of maleated composites. This denoted that maleation had significant influence on thermal behavior of resultant composites.

PVC film separated from composites presented the DSC spectra of PVC-coupling agent interphases (Figure 5.7). T_g and T_m of PVC were 77°C and 123°C, respectively. For E-43, an endothermal peak appeared at around 70°C, perhaps because single and double carboxyl groups on the molecular chains of E-43 were transferred as anhydride groups by dehydration. All composites with E-43 presented T_g of PVC at around 80°C. However, T_m of PVC shifted left, and the larger the MAPP retention, the larger the shifting (Figure 5.7). Although E-43 had a strong band of melting temperature at around 160°C, composites with low E-43 retention did not present this feature. This peak was still weak even when E-43 concentration levels were as high as over 4%. This might indicate that there were few coupling reactions between MAPP and PVC.

DSC spetra of wood-coupling interphases with E-43 and G-3015 were presented in Figure 5.8. On DSC curves, a coupling agent-wood interphase had four endothermic peaks and three exothermix peaks. The composite peaks at around 150°C were signals from T_g of wood and T_m of MAPP. The broad peaks at around 250°C were due to the pyrolyzation of hemicellulose and lignin (White and Dietenberger 2001). The small bands at around 320°C might be responsible for the chain sissor of MAPP under high temperatures, while the big and sharp peaks at around 360°C were due to depolymerization of cellulose. The first two exothermal peaks were mainly attributed to exothermic reaction of exposed char and volatiles with environmental oxgyen. The third exothermic peak was due to the cleavage of carbon-carbon linkage between lignin. structural units (White and Dietenberger 2001). Peak areas at 150 °C and 350 °C varied

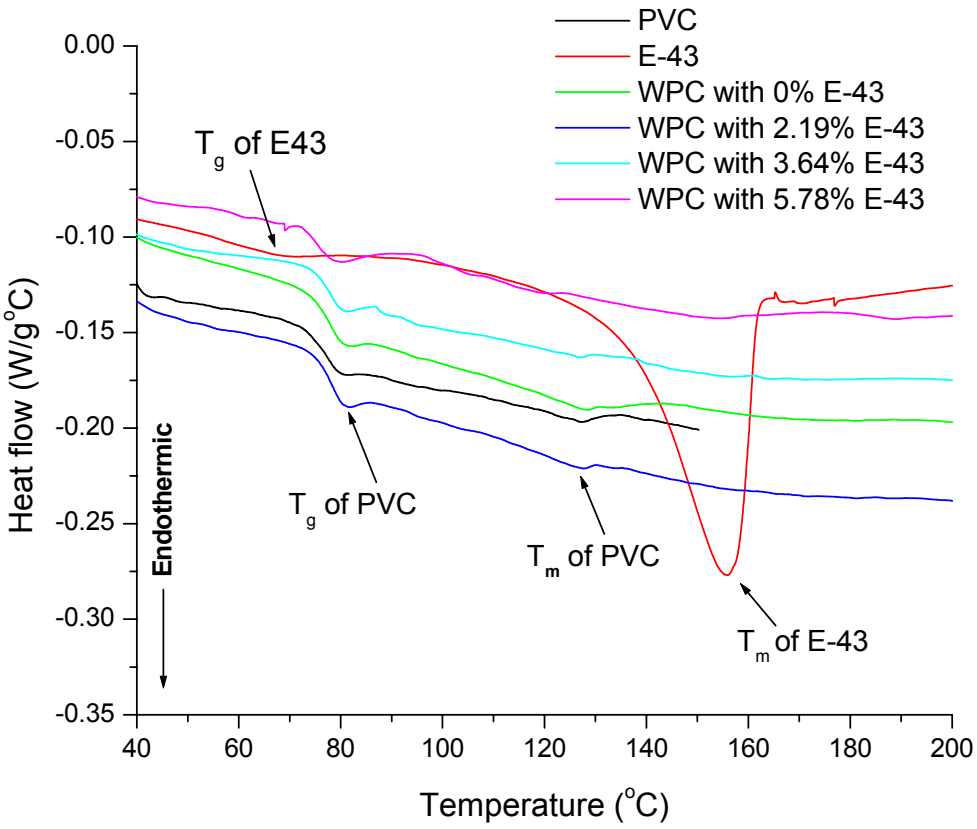

Figure 5.7. DSC spectra of PVC-MAPP interphases.

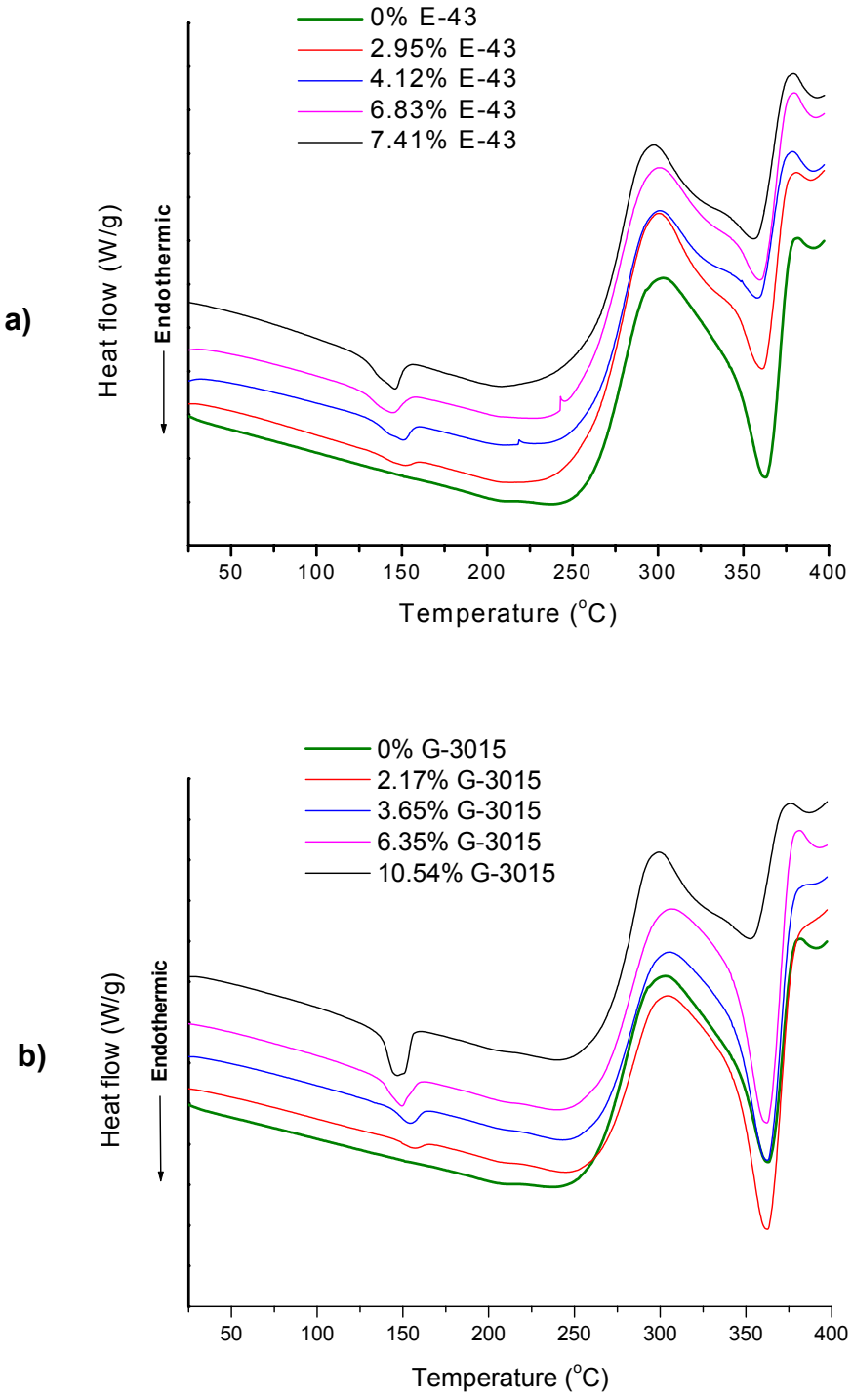

Figure 5.8. DSC curves of wood-MAPP interphases. a) wood-E-43 interphases and b) wood-G-3015 interphases.

with MAPP retention, but those at 200 ^{o}C and 250 ^{o}C were almost independent of MAPP retention. The peak area at 150^{o}C increased with the increase of MAPP retention, but that at 350^{o}C decreased with the increase of MAPP retention levels. For both E-43 and G-3015, the bands at round 150^{o}C shifted left with the increase of MAPP retention (Figure 5.8)

According to DDSC spectra of wood-coupling interphases, composites with E-43 and G-3015 had five endothermic bands in the temperature range between 25^{o}C and 375^{o}C (Figure 5.9). The first band on DSC spectra was divided into two peaks on DDSC curves. By enlarging these DSC and DDSC spectra, overlapped regions at around 140^{o}C-160^{o}C were separated into two individual peaks (Figure 5.10). Tg(II) at the first peak between 140^{o}C and 150^{o}C was T_g of wood, but Tm(III) at the second peak between 150^{o}C and 160^{o}C, T_m of MAPP. For both E-43 and G-3015, Tg(II) and Tm(III) had a left shift with the increase of coupling agent retention. For example, Tg(II) decreased from 141^{o}C to 134^{o}C as E-43 retention increased from 2.95% to 7.41%. For G-3015-wood interphases, Tg(II) had a smaller decrease with increase of G-3015 retention (Table 5.2). Enthalpy (ΔH) values at Tg(II) and Tm(III) increased with the increase of coupling agent retention. For wood-E-43 interphases, ΔH values at Tg(II) increased from 0.003025 to 0.1009 J/g, and ΔH values at Tm(III) increased from 0 to 0.3449 J/g as E-43 retention increased from 0% to 7.41%. At Tg(II), wood-G-3015 interphases had higher enthalpy than wood-E-43 interphases at the same retention level (Table 5.2). However, wood-G-3015 interphases had lower enthalpy values at Tm(III) than wood-E-43 interphases at the

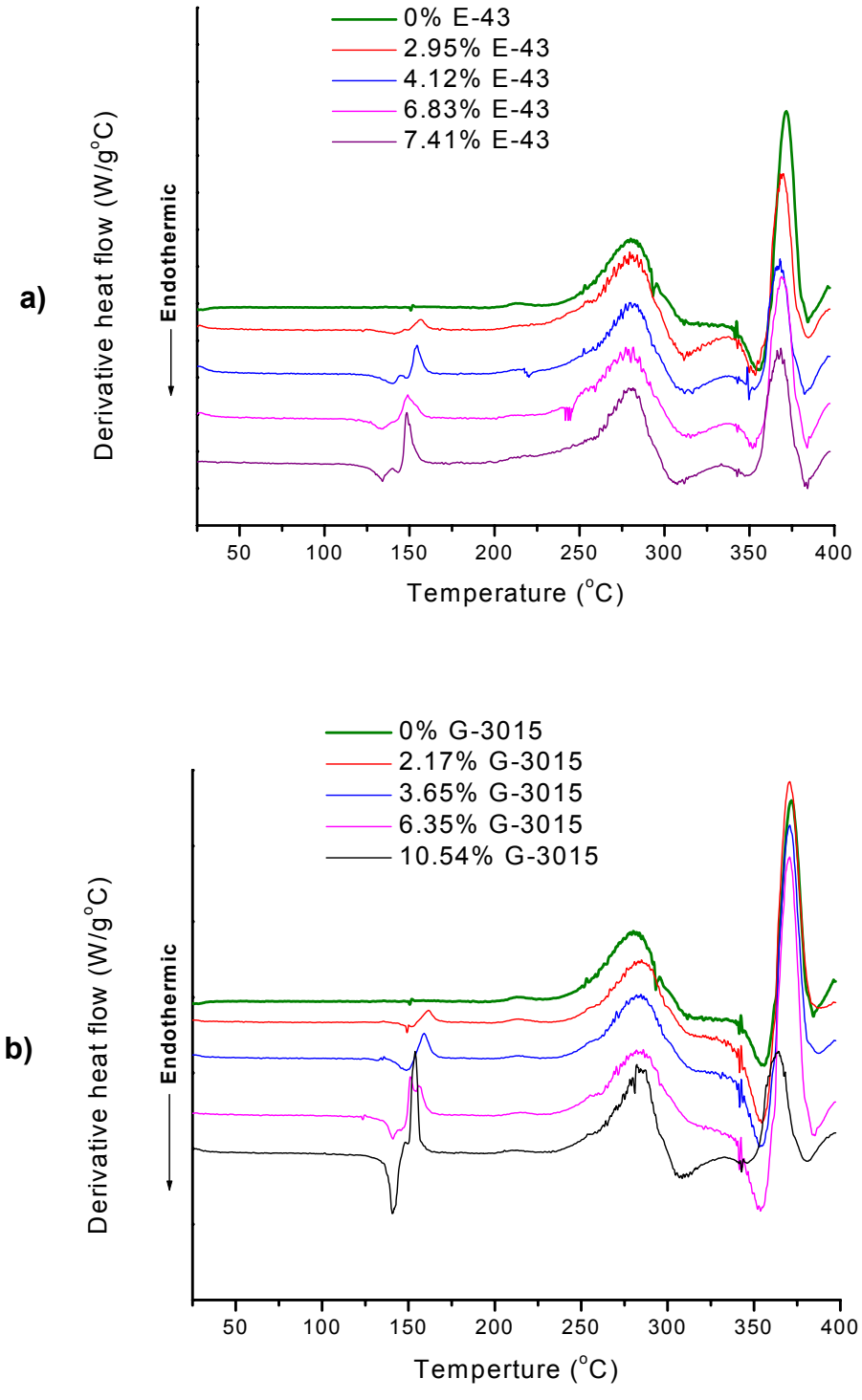

Figure 5.9. DDSC spectra of wood-MAPP interphases. a) wood-E-43 interphases and b) wood-G-3015 interphases.

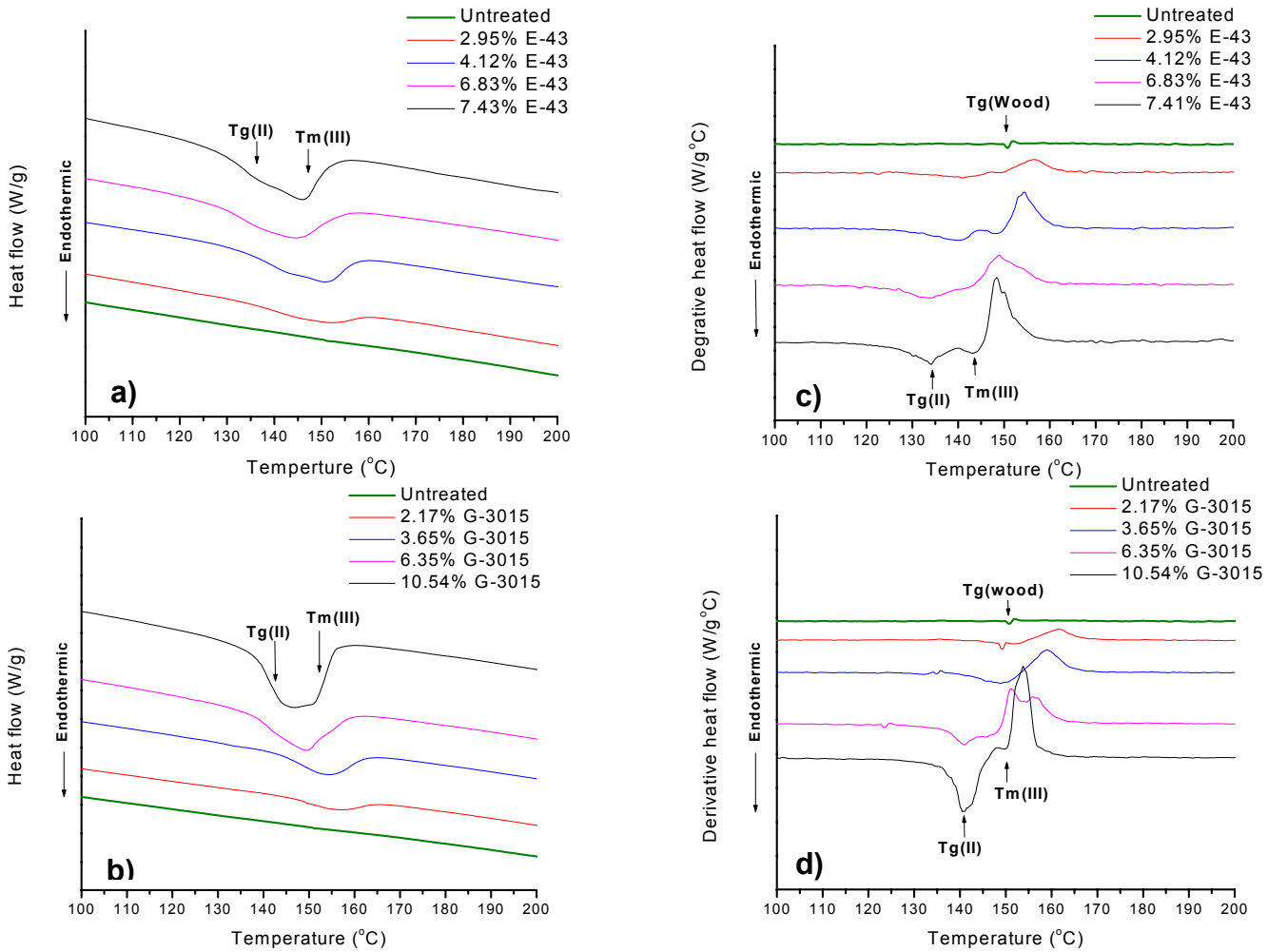

Figure 5.10. DSC and DDSC curves of wood-MAPP interphases in a temperature range between 100°C and 200°C. a) and c) wood-E-43 interphases and b) and d) wood-G-3015 interphases.

same retention level. Therefore, the molecular structure of coupling agents influenced the thermal behavior of the resulting composites.

5.4 CONCLUSIONS

Maleation significantly influenced thermal and dynamic mechanical properties of wood-PVC composites. Storage modulus E′ and complex modulus E* of maleated wood-PVC composites increased with the increase of MAPP retention. There was a small decrease of E′ and E* at high retention levels. However, tanδ was independent of MAPP retention. Interfacial bonding strength was related to these moduli at low retention levels. However, the correlation between the strength and moduli was not so significant at high retention levels. T_g of maleated composites was around 89^{o}C, between T_g values of PVC and wood.

Maleated wood-PVC composites had a larger TG% at 600^{o}C than PVC and wood. In the temperture range between 100^{o}C and 600^{o}C, maleated wood-PVC composites had lower DTG% compared with wood and PVC. Therefore, maleated wood-PVC composites had better thermal stability than wood and PVC under high temperatures.

Compared with wood, PVC, and untreated wood–PVC composites, maleated wood-PVC composites had significant shifts in most DMA, TGA, and DSC spectra. On most DSC spectra, T_g of wood and T_m of MAPP for maleated wood-PVC composites had a left shift at coupling agent-wood interphases with the increase of coupling agent retention compared with wood veneer. However, T_g of PVC was almost independent of coupling agent retention. This shift was mainly due to chemical coupling by MAPP at the

interface. Therefore, maleated wood-PVC composites had thermal behavior different from wood, PVC, and untreated wood-PVC composites.

5.5 REFERENCES

Collier, J. R., M. Lu, M. Fahrurrozi, and B. J. Collier. 1996. Cellulosic reinforcement in reactive composite systems. J. Appl. Polym. Sci. 61: 1423-1430.

CRC Press. 2000. CRC handbook of chemistry and physics. D. R. Lide ed., 81st edition, CRC Press, New York.

Dalväg, H., C. Klason, and H. –E. Strömvall. 1985. The efficiency of cellulosic fillers in common thermoplastics, part II. Filling with processing aids and coupling agents. Inter. J. Polym. Mater. 11: 9-38.

Delassus, P. T., and N. F. Whiteman. 1999. Physical and mechanical properties of some important polymers. Pages V159-V169 *in* J. Brandrup, E. H. Immergut, E. A. Grulke, A. Abe, and D. R. Bloch, eds. Polymer handbook. John Wiley & Sons, New York.

Felix, J. M., and P. Gatenholm. 1994. Effect of transcrystalline morphology on interfacial adhesion in cellulose/polypropylene composites. J. Mater. Sci. 29: 3043-3049.

Gatenholm, P., H. Bertilsson, and A. Mathiasson. 1993. The effect of chemical composition of interphase on dispersion of cellulose fibers in polymers. I. PVC-coated cellulose in polystyrene. J. Appl. Polym. Sci. 49: 197-208.

Hatakeyama, T., and , F. X. Quinn. 1994, Thermal analysis: Fundamentals and applications to polymer science, John Wiley & Sons, New York.

Kolosick, P. C., G. E. Myers, and J. A. Koutsky. 1992. Polypropylene crystallization on maleated polypropylene-treated wood surface: Effects on interfacial adhesion in wood polypropylene composites. Pages 137-154 *in* R. M. Rowell, T. L. Laufenberg, and J. K. Rowell, eds. Materials Interactions relevant to recycling of wood-based materials, vol. 266. Materials Research Society, Pittsburgh, PA.

Lu, J. Z., Q., Wu, and H. S., McNabb. 2000. Chemical coupling in wood fiber and polymer composites: A review of coupling agents and treatments. Wood Fiber Sci. 32 (1): 88-104.

Lu, J. Z., Q., Wu, and I. I. Negulescu. 2002. The influence of maleation on polymer adsorption and fixation, wood surface wettability, and interfacial bonding strength in wood-PVC composites. Wood Fiber Sci. 34 (3): 434-459.

Oksman, K., and H. Lindberg. 1995. Interaction between wood and synthetic polymers. Holzforschung 49(3): 249-254.

Quillin, D.T., D. F. Caulfield, and J. A. Koutsky. 1993. Crystallinity in the polypropylene/cellulose system. I. Nucleation and crystalline morphology. J. Appl. Polym. Sci. 50: 1187-1194.

Rowell, R.. 1991. Chemical modification of wood. Pages 703-756 *in* D. N. –S. Hon, and N. Shiraishi, eds. Wood and cellulosic chemistry. Marcel Dekker, Inc., New York.

Sanadi, A. R., D. F. Caulfield, N. M. Stark, and C. C. Clemons. 1999. Thermal and mechanical analysis of lignocellulosic-polypropylene composites. Pages 67-78 *in* Proc. of Fifth International Conference on Woodfiber-Plastic Composites. Forest Products Society, Madison, WI.

Simonsen, J., and T. G. Rials. 1996. Morphology and properties of wood-fiber reinforced blends of recycled polystyrene and polyethylene. J. Thermo. Comp. Mater. 9: 292-302.

White, R. H., and M. A. Dietenberger. 2001. Wood products: Thermal degradation and fire. Pages 9712-9716 *in* K. H. J. Buschow, R. W. Cahn, M. C. Flemings, B. Ilschner, E. J. Kramer, and S. Mahajan. eds. Encyclopedia of materials: Science and technology. Elsevier Science Ltd., New York.

Woodhams, R. T., G. Thomas, and D. K. Rodgers. 1984. Wood fiber as reinforcing fillers for polyolefins. Polym. Eng. Sci. 24(15): 1166-1171.

Ying, S., T. G. Rials, and M. P. Wolcott. 1999. Crystallization behavior of polypropylene and its effect on wood fiber composites properties. Pages 139-146 *in* Proc. of Fifth International Conference on Woodfiber-Plastic Composites, Forest Products Society, Madison, WI.

CHAPTER 6. IMPROVING MECHANICAL PROPERTIES OF WOOD FIBER-HIGH DENSITY POLYETHYLENE COMPOSITES BY CHEMCIAL COUPLING WITH MALEATED POLYETHYLENE

6.1 INTRODUCTION

A number of studies on wood fiber-polymer composites (WFPC) have been reported in the last two decades (Woodham et al. 1984). Polyethylene (PE) is one of the four most popular thermoplastics in the world. PE is generally divided into high-density polyethylene (HDPE), low-density polyethylene (LDPE), and linear low-density polyethylene (LLDPE). It is reported that HDPE accounts for about 47% of the total PE products in 2000 in the United States (C&EN 2002). HDPE is usually produced as bottles, containers, film or sheet, inject molding, pipe, conduit, and other products. Over 50% of HDPE products are manufactured with blow and injection molding (Chenier 1992). Since the 1970s, significant effort has been made to recycle the out-of-service thermoplastic products and plastic wastes in the world (Thompson Publishing Group 2001).

Wood fiber-polyethylene composites have been studied by a number of research workers (Xanthos 1983; Woodhams et al. 1984; Kokta and Daneault 1986; Raj et al. 1990). More efforts have been made to improve interfacial bonding strength between polar wood fiber and the non-polar polyolefin matrix. So far, various bonding agents have been used in wood fiber-PE composites. These agents include acetic anhydride (Chtourou et al. 1992), silanes (Beshay et al. 1985; Raj et al. 1989; Raj et al. 1990; Raj. and Kokta 1991; Rozman et al. 1998a), isocyanates (Raj et al. 1988; Raj et al. 1989; Raj et al. 1990; Raj and Kokta 1991; Joseph et al. 1996), maleated polypropylene (MAPP) (Raj and Kokta 1991; Gonzalez et al. 1992), maleic anhydride and styrene copolymers or

styrene-butadiene-styrene block copolymers (Oksman and Lindberg 1998; Simonsen et al. 1998; Ha et al. 1999), titanates (Liao et al. 1997), polymethacrylate (Razi et al. 1999), zircoaluminate (Freischmidt and Michell 1991), poly[methylene(polyphenol isocynate)] (Maldas and Kokta 1990), urea-formaldehyde resin (Hwang 1997), phenolformaldehyde resin (Chtourou et al. 1992; Simonsen and Rials 1992) and so on. Recycled polyethylene has been extensively used in WFPC (Yam et al. 1990; Chtourou et al. 1992; Simenson and Rials 1992; Ha et al. 1999). Recycled wood materials such as wood wastes and newspaper fiber have also been used in wood fiber-PE composites (Gonzalez et al. 1992; Simonsen et al. 1998). Recently, more attention has been paid to the application of agro-fibers (or biofibers) such as kenaf, jute, flax, pineapple leaf, and sisal fibers as fillers in HDPE or other thermoplastic polymers (Schneider et al. 1995; Joseph et al. 1996; George et al. 1998).

Compounding process directly influence compounding quality of wood-polymer blends and coupling agent performance in resultant composites (Xanthos 1983; Takase and Shiraishi 1989; Maldas and Kokta 1990). For wood fiber-polymer composites, compounding process was normally divided into one-step process and two-step process (Lu et al. 2000). The former is appropriate to continuous mixers (such as extruder and injection molding), whereas the latter is preferred to batch mixers (such as roll mills and rotor mixers). Krzysik et al. (1991) reported that the two-step process was preferred for the manufacture of air-formed wood fiber-polymer composites.

For refiner ground pulp (RGP) and PP composites, the optimum mixing conditions are 10 minutes under a mixing temperature of 180ºC and a rotation speed of 50 rpm (Takase and Shiraishi 1989). Takase and Shiraishi (1989) also reported that

rotation speed had similar influence on the coupling effectiveness as did mixing time and moderate mixing speeds were preferred for better fiber length distribution and coupling effectiveness. Usually, mixing temperature is controlled at less than 200°C for most coupling treatments to avoid decomposition and degradation of wood fibers and some thermoplastic matrices (Woodhams et al. 1984; Maldas et al. 1989; Takase and Shiraishi 1989; Myers et al. 1993).

Maldas and Kokta (1990) reported that with a two-roll mill system the maximum improvement in mechanical properties of chemithermomechanical pulp (CTMP) and PS composites was achieved when the mixing time was 15 min at 175ºC. The blends were required to re-mix 5 and 10 times (about 6-8 min) during compounding. Hence, the two-step process resulted in a better distribution of coupling agents at the interface by mixing coupling agents with polymer and wood fiber (Maldas et al. 1989).

Coutinho et al. (1997) investigated the effect of treatment and mixing conditions on mechanical properties of wood fiber-polypropylene composites with silane coupling agents. They reported that the optimal mixture conditions of wood fiber-polypropylene composites were 180^{o}C for the mixture temperature and 10 min for the time of mixture under rotation speed of 60 rpm. By pretreating wood fiber with silane A172, mechanical properties of resultant composites were optimized under above-mentioned compounding conditions.

Rozman et al. (1998b) compared effects of two different blending systems (an internal mixer and a single-screw extruder) on mechanical properties of oil palm empty fruit bunch-polypropylene composites. For the internal mixer, mixing was conducted at 180^{o}C with rotation speed of 25 rpm. The single-screw extruder was operated at rotation

speed of 20 rpm and with increasing temperature zones of 160, 170, and 180^{o}C. They reported that composites produced by the internal mixer had higher tensile strength, tensile modulus, and impact strength than those by extrusion because the internal mixer produced better filler dispersion and improved the wetting of the filler surface.

Blending wood fiber with a polymer is the key step of composite production, because compounding process help uniformly distribute wood fiber and coupling and modifying agents in the thermoplastic matrix, decrease pore ratio, and stabilize the filler/matrix interaction (Berlin et al. 1986). However, there has been no criterion to determine optimum compounding conditions. Usually, compounding conditions vary with mixing machine type, compounding steps, weight ratio of wood fiber and the polymeric matrix, moisture content of wood fiber, and species of thermoplastics and wood fiber. Sometimes, it may be difficult to isolate these factors. In this study, a statistical method was introduced to explore the relationship among rotation speed, mixing temperature, and compounding time in an inner mixer and their influence on the mechanical properties of resultant wood-polymer blends.

Although a number of studies have been done on coupling mechanisms of wood-polymer composites (Gaylord 1972; Zadorecki and Flodin 1985), the mechanism of coupling reactions at the interface is still not well understood. Esterification on MAPP-treated wood fiber has been reported by a number of researchers (Kishi et al. 1988, Felix and Gatenholm 1991). Kishi et al. (1988) used xylene to extract radiata pine fiber-polypropylene composites for 48 hrs and analyzed xylene-extracted remains with FTIR. It was reported that acid anhydride groups appeared at 1860 cm^{-1} and 1780 cm^{-1}. Based on FTIR results, a half-ester linkage model was proposed (Kishi et al. 1988).

Felix and Gatenholm (1991) made a fundamental research on interfacial adhesion in maleated cellulose fibers-polypropylene composites with chemical analyses. MAPP-treated wood fibers were extracted with toluene for 48 hrs to remove ungrafted MAPP, and extracted fibers were analyzed with FTIR. MAPP with heat treatment had a peak at 1717 cm^{-1}. It indicated that MAPP was transferred from a hydrolyzed form to an anhydride form by heating. By FTIR, MAPP-treated wood fibers were extracted with toluene for 24 hrs. The peak at 1739 cm^{-1} was from the monomeric form of the dicarboxylic acid, whereas the peak at 1746 cm^{-1} arose from ester bonds between the copolymer and the fibers. Based on these findings, two models, including half-ester and diester structures were suggested to illustrate interfacial adhesion in maleated wood fiber-polymer composites (Felix and Gatenholm 1991). It was also reported the characteristic of esterification at 1729-1748 cm^{-1} on MAPP-treated Kraft pulp and cellulosic fibers (Kazayawoko et al. 1997; Matuana et al. 2001). However, this characteristic band was not direct evidence that an esterification reaction was obtained between thermo-mechanical pulp and MAPP (Kazayawoko et al. 1997).

Electron spectroscopy for chemical analysis (ESCA) or X-ray photoelectron spectroscopy (XPS) has been applied to determine chemical components and function groups at the interface. Felix and Gatenholm (1991) reported that compared with untreated fibers, MAPP-treated fibers had a dramatic increase at the peak of 285 eV characteristic for C-C bonding. However, maleation decreased O/C ratio and O/(O-C=O) ratio of treated fibers. Hence, treated fibers had hydrophobic surface. Kazayawoko et al. (1999) studied wood fibers treated with E-43 and G-3002 using XPS techniques. For maleated fibers, there was a dramatic increase in the proportion of C-C/C-H bonding, but

the contributions of C-O, C=O/O-C-O, and O-C=O groups were decreased. Moreover, maleated fibers had smaller oxygen-carbon (O/C) ratio than untreated wood fibers. The increase in proportion of C-C/C-H bonding and decrease in O/C ratio was attributed to the attachment of MAPP to wood fiber surface by graft polymerization. Mutuana et al. (2001) also reported similar XPS results of E-43-treated cellulosic fibers.

Maleated polyethylene (MAPE) has been used as a compatibilizer in starch/protein-polymer composites (Bikaris and Panayiotou 1997). However, there have been few reports on application of MAPE in wood-polymer composites (Sanadi et al. 1992). According to the interfacial similarity rule (Lu et al. 2000), MAPE maybe effectively improve interfacial bonding between polar wood and non-polar polyethylene. Therefore, it is necessary to investigate chemical reaction and interfacial structure of MAPEs with advanced chemical analysis techniques and to understand coupling action of MAPEs at the interface in wood fiber-polyethylene composites.

Much effort has been made to improve interfacial bonding strength between polar wood fiber and the non-polar polyethylene matrix (Xanthos 1983; Raj et al. 1988). Recycled polyethylene and wood wastes have been extensively used in WFPC (Chtourou et al. 1992). Recently, more attention has been paid to the application of agro-fibers such as kenaf, jute, flax, pineapple leaf, and sisal fibers as fillers in HDPE or other thermoplastic polymers (Schneider et al. 1995; Joseph et al. 1996).

Kokta and coworkers (1990) investigated the influence of four different isocyanate coupling agents on mechanical properties of wood fiber-polystyrene composites. They reported that chemical structure and molecular weight of coupling agents had an important impact on mechanical properties of the resultant composites.

With longer molecular chains and more function groups per mole, poly[methylene (polyphenol isocynate)] (PMPPIC) had better coupling effectiveness than other isocyante coupling agents. More recently, Snijder and Bos (2000) investigated the coupling efficiency of nine different maleated polypropylene (MAPP) copolymers in agrofiber-polypropylene (PP) composites by injection molding. It was found that the molecular weight of MAPP was a more important parameter than MA content in MAPP for coupling efficiency. The backbone structure of MAPP influenced the interfacial adhesion in the resultant composites because of miscibility in the PP matrix (Snijder and Bos 2000). In another paper (Snijder et al. 1997), they reported that the mechanical properties of the resultant composites increased with the amount of MAPP, but the effect leveled off or decreased at high MAPP concentration levels.

Most effective coupling forms at the interface in WFPC are usually created through the interfacial similarity rule (Lu et al. 2000). Coupling agents (such as maleic anhydride and dichlorotriazine) create a crosslinking structure on wood surface and some polymer is grafted onto wood by coupling agents. Thus, modified wood has a surface similar to the matrix. Alternately, coupling agents with a structure similar to the matrix are grafted onto wood, which is helpful to improve interfacial adhesion. The wood fiber-MAPP-PP structure belongs to the latter coupling form. A similar coupling structure at the interface may exist in wood fiber-PE composites. Maleated polyethylene (MAPE) or maleic anhydride-grafted polyethylene (PE-*g*-MA) has been extensively used as a compatiblizer in HDPE/LDPE-starch composites (Bikiaris and Panayiotou 1997; Sailaja and Chanda 2001). However, there have been few reports on using MAPE as a coupling

agent in WFPC (Sanadi et al. 1992). Therefore, it is necessary to investigate whether MAPE is effective in improving interfacial bonding strength in WFPC.

In this study, several MAPE copolymers were used as coupling agents in wood fiber-HDPE composites. The objectives of this study were 1) to investigate the influences of compounding conditions on mechanical properties of resultant composites, 2) to compare the difference between one-step and two-step process, 3) to determine the best compounding conditions for compounding quality and mechanical properties of resultant composites, 4) to investigate the relationship among rotation speed, mixing temperature, and compounding time using statistical analysis, 5) to investigate interfacial structure and characterization of maleated wood fiber-HDPE composites by chemical analyses, 6) to observe the interfacial morphology of fracture surface and distribution of coupling agent, and 7) to study the coupling mechanisms of MAPEs at the interface, 8) to examine the interfacial similarity rule with the wood fiber-MAPE-HDPE structure, 9) to investigate the effects of coupling agent type and structure on mechanical properties of resultant composites, and 10) to search for the best MAPEs for wood fiber-HDPE interface in terms of coupling performance.

6.2 MATERIALS AND METHODS

6.2.1 Materials

6.2.1.1 Wood Fiber

Mixed thermomechanical pulp (TMP) fibers were obtained from Temple-Inland Company, Diboll, TX. Before compounding process, TMP fibers were dried in an oven at 100^{o}C for 24 hours. Moisture content of dried TMP fibers was between 2% and 3%.

6.2.1.2 Thermoplastics

HDPE pellets (PE10462N, Dow Chemical) were obtained from a plastic company. The density of HDPE is 962.5 kg/m^3. Its melting temperature and melt index are 134^{o}C and 10 g/10min, respectively. HDPE has a tensile strength between 19-30 MPa and a flexural modulus between 0.7-1.7 GPa (Delassus and Whiteman 1999).

6.2.1.3 Coupling Agents and Initiator

Four MAPEs (C10, C16, E17, and E20) were obtained from Eastman Chemical Company, Longview, Texas. Other two kinds of MAPE (100D and 226D) were obtained from Dupont Canada Inc., Ontario, Canada. Epolene E-43 (a product of MAPP, Eastman Chemical) was used as a reference for MAPEs in this study. Basic properties of these coupling agents were listed in Table 6.1. The concentration levels of coupling agent were 0, 1%, 3%, 5%, and 10% based on the weight of oven-dried wood fiber.

Dicumyl peroxide (DCP) was used as an initiator. The amount of DCP was controlled to be 1% of the weight percentage of coupling agent.

6.2.2 Compounding Process

The melt-molding process for manufacturing wood fiber-polymer composites followed the one-step and the two-step blending processes (Lu et al. 2000). The weight ratio of wood fiber and HDPE was 50:50. For the one-step process, wood fibers, thermoplastics, coupling agent, and initiator were sequentially fed into a Haake blender (Model Rheomix 600). Both blending torque and compounding temperature were measured during compounding. After mixing, melts were removed from the blender and

Table 6.1. Properties of MAPE and MAPP.

Coupling agent	Molecular weight (g/mol)		Backbone structure	Density (kg/m^3)	Acid number (mg KOH/g) [a]	Amount of maleic anhydride groups (wt%) [b]	Viscosity (cp)
	M_w	M_n					
C10	35,000	7,700	LDPE	906	<0.05	<0.05	7,800 (at 190°C)
C16	26,000	5,600	LDPE	908	5	0.5	8,500 (at 190°C)
E17	4,200	1,050	LDPE	908	25	2.3	550 (at 125°C)
E20	7,500	1,600	HDPE	960	17	1.6	800 (at 150°C)
226D	-	-	LLDPE	930	-	-	-
100D	-	-	HDPE	960	-	-	-
E-43	9,100	3,900	PP	930	47	4.4	400 (at 190°C)

[a] 100D and 226D have high graft ratios on wood fiber.

[b] wt% is weight percentage of backbone polymer.

cooled down to room temperature. The melts were ground with a Thomas-Wiley miller (Model 3383L10) to pass through a 20 mesh screen. For the one-step process, a 3×3×2 random completely randomized design (CRD) factorial experiment was used to identify the optimum blending conditions for wood fiber-HDPE composites (Table 6.1).

For the two-step process, a small amount of thermoplastics were firstly grafted onto wood fiber with coupling agent during compounding and then ground into powders (20 meshes). Secondly, the pretreated blends were further mixed with wood fibers and thermoplastics. After compounding, all resulting blends were ground again into powder (20 meshes).

6.2.3 Manufacture of Wood Fiber-HDPE Composites

Ground powder with a required weight was placed into a two-piece aluminum molding set. The mold was pressed with a miniature hot press at 168°C for 3 min and cooled down to room temperature at the same pressure for 1 min. The pressure for heating and cooling was controlled to be 0.16 MPa. Specimens were made with this molding set for tensile testing and dynamic mechanical analysis. Density of all specimens was controlled to be 1,000 ± 50 kg/m^3.

6.2.4 Soxhlet Extraction of Maleated Composites

Before chemical analyses (e.g., infrared analysis and ESCA in next subsections), all composites samples were Soxhlet-extracted. A small amount of composite samples were placed into the Soxhlet thimble and continuously fluxed with a hot solution of xylene for 48 hrs. Extracted samples were then oven-dried at 70°C for 24 hrs to reach a constant weight.

6.2.5 Measurement of Mechanical Properties of the Resultant Composites

Dynamical mechanical properties of resultant composites were analyzed with a Seiko DMS 110 dynamic mechanical analysis system. After DMA analysis, all tension-testing specimens were cut into a dog-bone shape with a cutting tool by following the ASTM standard ASTM D638. Tensile strength was tested according to ASTM D638 using an INSTRON (Model 1125) test machine.

6.2.6 Interfacial Morphology Analysis

Fracture surface after tensile testing was observed with a scanning electronic microscope (Model Cambridge 260) under a voltage of 15 KV. Before scanning, each sample was coated with gold to improve its surface conductivity.

6.2.7 Chemical Component Analysis

Chemical information at the interface was analyzed with an electrical spectroscopy for chemical analysis (ESCA AXIS 165). ESCA was operated under a high vacuum pressure between 10^{-8} – 10^{-7} torr. For each composite specimen after tensile test, a scanning survey on fracture surface was run in a low-resolution between 0 to 1200 eV with a passing energy of 89.45 eV. Carbon (C1s) and oxygen (O1s) atomic compositions were evaluated and binding energy values were recalibrated based on the known binding energy of C1s peaks with a Scienta ESCA 300 database (Negulescu et al. 2000). Interactions between wood fiber and HDPE with and without maleation were compared.

6.2.8 Fourier Transform Infrared Analysis

Functional groups at the interface in maleated wood fiber-polymer composites were analyzed using a FTIR spectroscopy (Model Perkin-Elmer 1760X). Two methods for sample preparation were employed in this study.

For HDPE and maleaded polyolefin pellets, a cast film method was used. A xylene solution of maleated polyolefins was prepared in a beaker and dropped with a pipette on a NaCl disk. A uniform and continuous film was formed on this disk until the solvent was completely evaporated (Smith 1996).

A potassium bromide (KBr) pellet technique was used for maleated composite samples. A milligram of the finely ground sample was mixed with about 100 mg of dried KBr powder within a sample set. A pressure of 69-103 MPa was applied to yield a transparent disk (Smith 1996). The scanning range of FTIR was between 4000 and 500 cm^{-1} with a resolution of 4 cm^{-1}.

6.2.9 Data Analysis

For the one-step blending process, a three-way ANOVA was conducted to investigate the main effects and interaction effects of these three factors on flexural moduli of the resulting composites. The difference among each level of these three factors was compared using Duncan's multiple range tests.

A 7×5 completely randomized design factorial experiment was conducted to investigate the influence of coupling agent type (seven maleated copolymers) and concentration (0%, 1%, 3%, 5%, and 10%) on the mechanical properties of wood fiber-HDPE composites. Based on this factorial experiment, a two-way ANOVA was conducted to determine main and interaction effects of these two factors. The coupling effectiveness of maleated copolymers was compared using Tukey's studentized range test.

6.3 EXPERIMENTAL DESIGN

6.3.1 Compounding Parameters

For the one-step process, a random completely randomized design (CRD) with a 3×3×2 factorial experiment was used to find out the optimum blending conditions for wood fiber-HDPE composites (Table 6.2). There were three factors, including compounding temperature, mixing time, and rotation speed.

Table 6.2. Experimental design for compounding conditions in a one-step process. [a, b]

Experiment	Rotation Speed (rpm)	Temperature (^{o}C)	Time (Min)
Mix 1	60	150	10
Mix 2	60	165	15
Mix 3	60	180	20
Mix 4	60	150	10
Mix 5	60	165	15
Mix 6	60	180	20
Mix 7	60	150	10
Mix 8	60	165	15
Mix 9	60	180	20
Mix 10	90	150	10
Mix 11	90	165	15
Mix 12	90	180	20
Mix 13	90	150	10
Mix 14	90	165	15
Mix 15	90	180	20
Mix 16	90	150	10
Mix 17	90	165	15
Mix 18	90	180	20

[a] The weight ratio of wood fiber and HDPE was 50%:50%.
[b] The concentration of E20 was 5 wt% of oven-dried wood fiber.

6.3.2 Coupling Effectiveness and Best Coupling Agents

A 7×4 CRD factorial experiment was conducted to investigate the influence of coupling agent type (seven maleated copolymers) and concentration (1%, 3%, 5%, and

10%) on mechanical properties of wood fiber-HDPE composites. Based on this factorial experiment, an ANOVA was conducted to determine main effects and interaction effects of these three factors. A principal components analysis (PCA) was applied to investigate coupling agent performance for these coupling agents. The best MAPE coupling agents for wood fiber-HDPE composites were identified through PCA and biplot analysis.

6.4 RESULTS AND DISCUSSION

6.4.1 Compounding Process

6.4.1.1 Characterization of Wood Fiber-HDPE Blending Process

During compounding, wood fiber-HDPE blends mainly underwent A and B stages in the one-step process (Figure 6.1). On stage A, blend torque sharply increased as HDPE pellets were added. At the same time, mixing temperature sharply decreased because inner temperature dropped by feeding cold thermoplastics into the mixing chamber. After HDPE was melted, torque decreased to around 50-100 Nm/kg and temperature back to the setting point. The actual torque values varied with the amount of HDPE as expected. The more HDPE pellets were added, the larger the torque needed. After adding wood fibers on stage B, there were rapid increases in machine torque and mixing temperature because of surface friction between wood fiber and HDPE. With continued compounding, melt torque of wood-HDPE blends gradually decreased and mixing temperature was stabilized to around 170^{o}C.

During compounding, fillers were dispersed into the matrix by shear stress, which was significantly influenced by the loading ratio of fillers (Matthews 1982). For wood-HDPE blends with a weight ratio of 50:50, there was an increase in melt torque and mixing temperature at stage C, respectively (Figure 6.1). Melt torque increased with At

a)

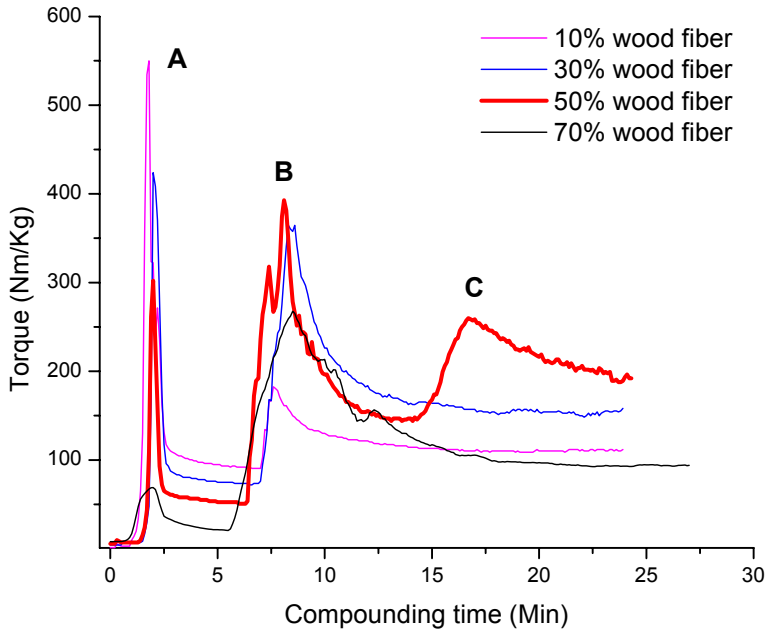

b)

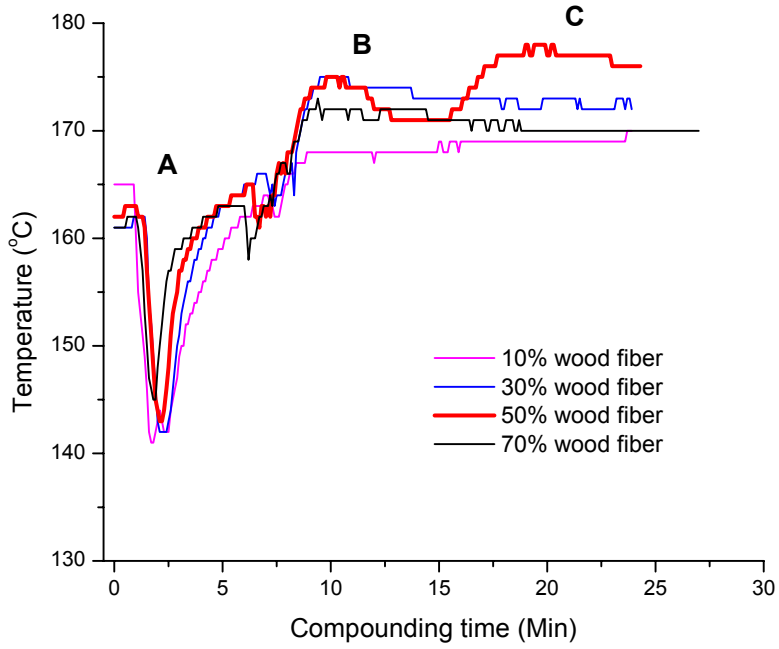

Figure 6.1. Effect of wood loading in wood fiber-HDPE blends on a) blending torque and b) temperature. The blends were mixed at 165°C and 60 rpm for 15 min.

increase of weight percentage of wood fibers, and it dramatically increased to around 260 Nm/kg as the loading ratio of wood fiber was as high as 50%. However, torque decreased to around 100 Nm/kg at 70% wood fiber (Figure 6.2). This was due to that the total surface contact area of individual fibers with the matrix was close to the maximum value at around 50% wood fiber, and the dispersion resistance reached the maximum value. 50% wood fiber, therefore, a large torque was built up by shear stress (Figure 6.1a). The shear stress also caused a larger temperature increase by about 8^{o}C (Figures 6.2).

Maleated wood fiber-HDPE blends presented compounding characterization similar to unmaleated blends. There were four different compounding stages for maleated wood fiber-HDPE blends (50:50) (Figure 6.3). After adding coupling agent on stage B, torque had a small drop (around 50 Nm/kg) and then back to 50 Nm/kg. On stage C (Figure 6.3a), torque had a large jump after adding wood fibers because surface friction was produced at the interface. This friction also caused a large increase in blend temperature (Figure 6.3b). However, the torque value of maleated blends decreased by 50 Nm/kg compared with that of unmaleated blends. This implied that adding coupling agent improved flow ability of thermoplastics.

On stage D, a large jump of torque and temperature appeared for maleated blends due to dispersion (Figure 6.3). Melt torque gradually reduced on stage D for maleated blends, but its decreasing slope was smaller than that of unmaleated blends. There was a small temperature increase after adding initiator, which was related to the graft reaction at the interface. Torque was finally stable to around 220 Nm/kg for maleated blends (50:50). Therefore, stage D presented the significant difference between modified blends and unmodified blends. For unmodified blends, temperatures were stable and

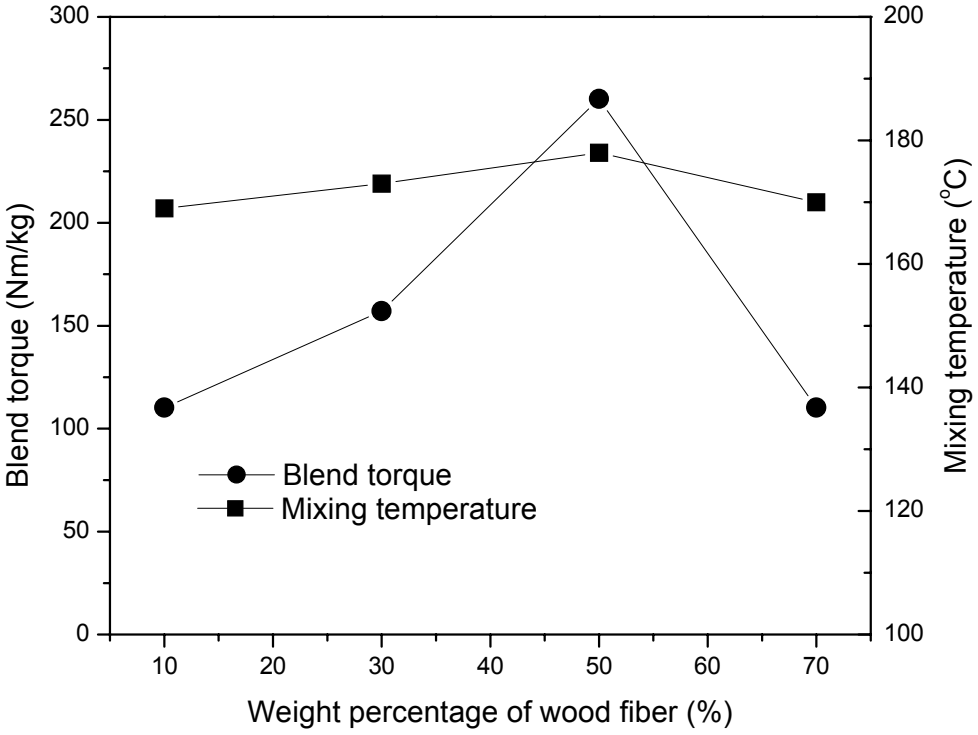

Figure 6.2. Torque and temperature changes of wood-polymer blends at 10 min and 13 min after adding wood fiber, respectively.

a)

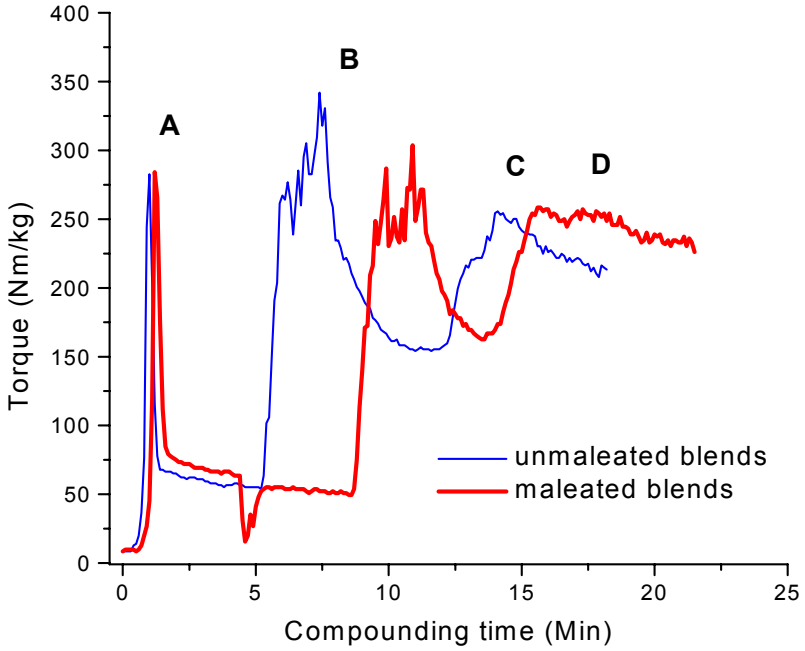

b)

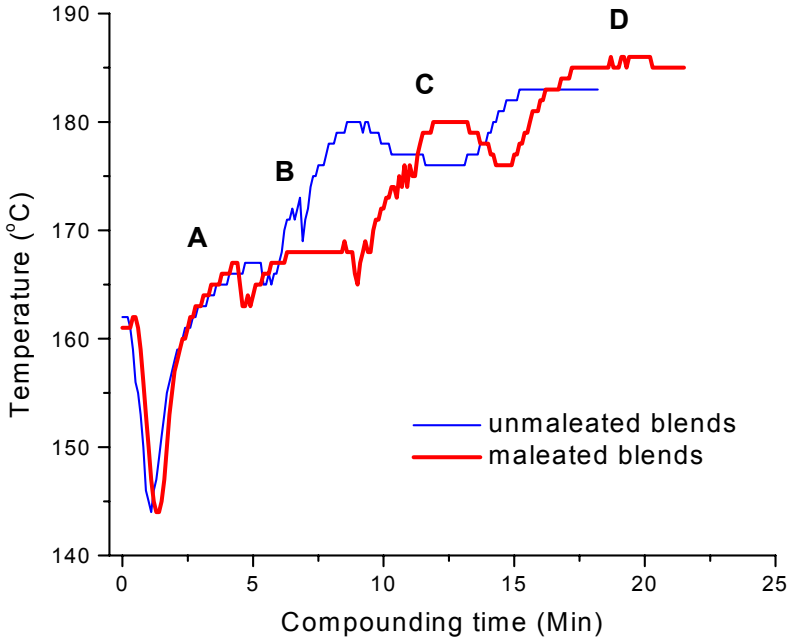

Figure 6.3. Compounding characterization of maleated wood fiber-HDPE blends on a) Torque and b) Temperature. Unmaleated and maleated blends (50%wood:50%HDPE) were mixed at 165°C and 90 rpm for 10 min, respectively. The concentration of E-20 was 5 wt% of oven-dried wood fiber.

independent of compounding time, whereas there was a temperature increase for modified blends because of graft reaction at the interface by coupling agent.

6.4.1.2 Effect of Coupling Agent Concentration

For untreated wood fiber-HDPE blends (50%:50%), melt torque by surface friction and dispersion was around 330 Nm/kg and 250 Nm/kg, respectively (Figure 6.4). Themelt torque decreased by 50 Nm/kg as E-20 concentration was 5%. However, surface friction and dispersion stress had significant changes as coupling agent concentration was lager than 10%. Melt torque decreased to around 220 Nm/kg when coupling agent concentration was 20%. It was equal to 130 Nm/kg, around one third of that of unmaleated blends, as concentration level of E-20 was high up to 50%. During dispersion, melt torque of all maleated blends converged into about 130 Nm/kg, which was one half for untreated blends (Figure 6.4). Consequently, coupling treatment helped improve the compatibility between wood fiber and thermoplastics.

6.4.1.3 Effect of Compounding Conditions on Torque and Temperature

In general, torque decreased with increase of mixing time and temperature, and increased with increase of rotation speed. For surface friction, melt torque and mixing temperature at 90 rpm were larger than those at 60 rpm, but torque and temperature related to dispersion at 90 rpm was smaller than those at 60 rpm (Table 6.3). At 90 rpm, there were large melt torque and mixing temperature increases (ΔQ and ΔT) generated by surface friction (Table 6.3).

At the same rotation speed and compounding temperature, ΔQ and ΔT by dispersion decreased with increase of compounding time and mixing temperature, but those by surface friction were independent of compounding time and mixing temperature.

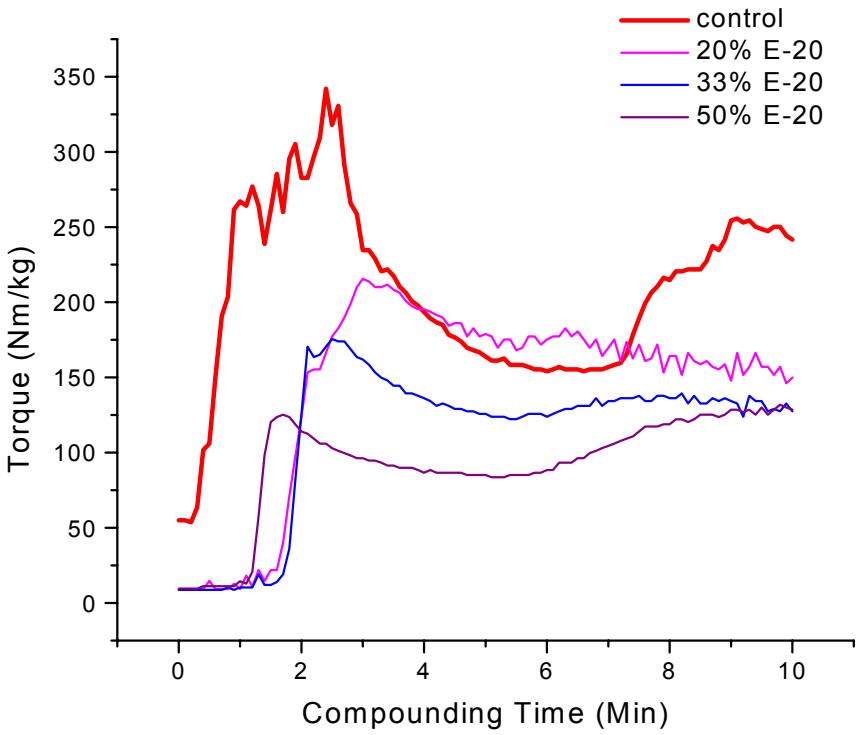

Figure 6.4. Effect of coupling agent concentration on melt torque of wood-HDPE blends (50%:50%). Wood-HDPE blends were mixed with a) no coupling agent (control), b) 20% E20, c) 33% E20 and d) 50% E20 at 165^{o}C and 90 rpm for 10 min.

Table 6.3. Melt torque and mixing temperature changes in different compounding conditions for the one-step process. [a, b]

Rotation Speed (rpm)	Temperature (°C)	Time (Min)	Melt torque of blends Q (Nm/kg)				Torque increase ΔQ (Nm/kg)		Temperature increase ΔT (°C)	
			Add HDPE	Add E-20	Add Fiber	Add DCP	Friction	Dispersion	Friction	Dispersion
60	150	10	55.4	48.1	153.7	253.4	105.6	99.7	11	5
	150	15	59.7	48.9	153.5	215.9	104.6	62.4	12	6
	150	20	48.1	39.7	143.5	212.3	103.7	68.9	11	7
	165	10	51.6	46.2	148.1	236.1	101.9	88.1	12	7
	165	15	48.9	43.5	141.0	220.7	97.8	80.0	10	7
	165	20	44.9	38.1	138.6	194.3	100.5	55.7	12	6
	180	10	40.0	36.2	142.7	241.3	106.5	98.9	11	5
	180	15	42.4	35.9	143.5	210.5	105.6	67.0	8	6
	180	20	40.0	35.1	142.4	196.2	107.0	54.0	8	7
90	150	10	62.7	54.0	171.3	227.8	117.3	56.5	14	4
	150	15	63.8	48.9	165.6	201.6	116.7	36.7	13	6
	150	20	55.4	42.2	161.6	199.7	119.4	38.1	14	7
	165	10	62.7	48.9	164.3	229.9	114.0	65.9	12	10
	165	15	62.1	54.0	157.5	208.0	103.5	50.5	13	8
	165	20	56.5	45.1	152.7	195.9	107.5	43.2	12	10
	180	10	77.5	48.1	167.0	216.4	118.9	49.4	12	3
	180	15	55.4	45.9	165.6	208.0	120.0	42.4	13	5
	180	20	55.1	45.7	166.2	195.3	120.5	29.5	12	5

[a] The weight ratio of wood fiber and HDPE was 50:50.
[b] The concentration of E20 was 5% of oven-dried weight of wood fiber.

At both rotation speeds, torque was not so sensitive to surface friction, but it was sensitive to dispersion (Table 6.3). Therefore, surface friction was more related to rotation speed, but dispersion was more related to compounding time and mixing temperature. By adding initiator, ΔQ and ΔT at 90rpm were smaller than those at 60 rpm. This may imply that high rotation speed and long mixing time interfered with dispersion of wood fiber in the matrix and graft reaction by coupling agent during compounding.

As shown in Figure 6.5, rotation speed influenced melt torque and mixing temperature of maleated blends. For all these four stages, melt torques were almost the same at both rotation speeds under the same mixing temperature and compounding time. On stage C and D, however, mixing temperature at 90 rpm increased by 10-11^{o}C compared with that at 60 rpm.

6.4.1.4 Effect of Compounding Conditions on Dynamic Mechanical Properties

Compounding conditions had a significant influence on most dynamic mechanical properties of resultant composites (Table 6.4). At 60 rpm, complex modulus, E*, increased with increase of mixing time at low mixing temperatures, but it decreased with increase of time at high mixing temperatures (Figure 6.6). E* also showed this decreasing trend at high temperatures when the rotation speed was 90 rpm. This was attributed to the fact that high rotation speed increased the dispersion of length distribution for wood fiber (Takase and Shiraishi 1989). Also, this decreasing trend was due to decomposition and degradation of wood fiber, coupling agents, and even HDPE under high temperatures (Maldas et al. 1989; Takase and Shiraishi 1989). At high rotation speed and a high mixing temperature, the inner temperature in the mixing chamber was high up to 195^{o}C because of friction and graft reaction. This high temperature may cause chain scission of

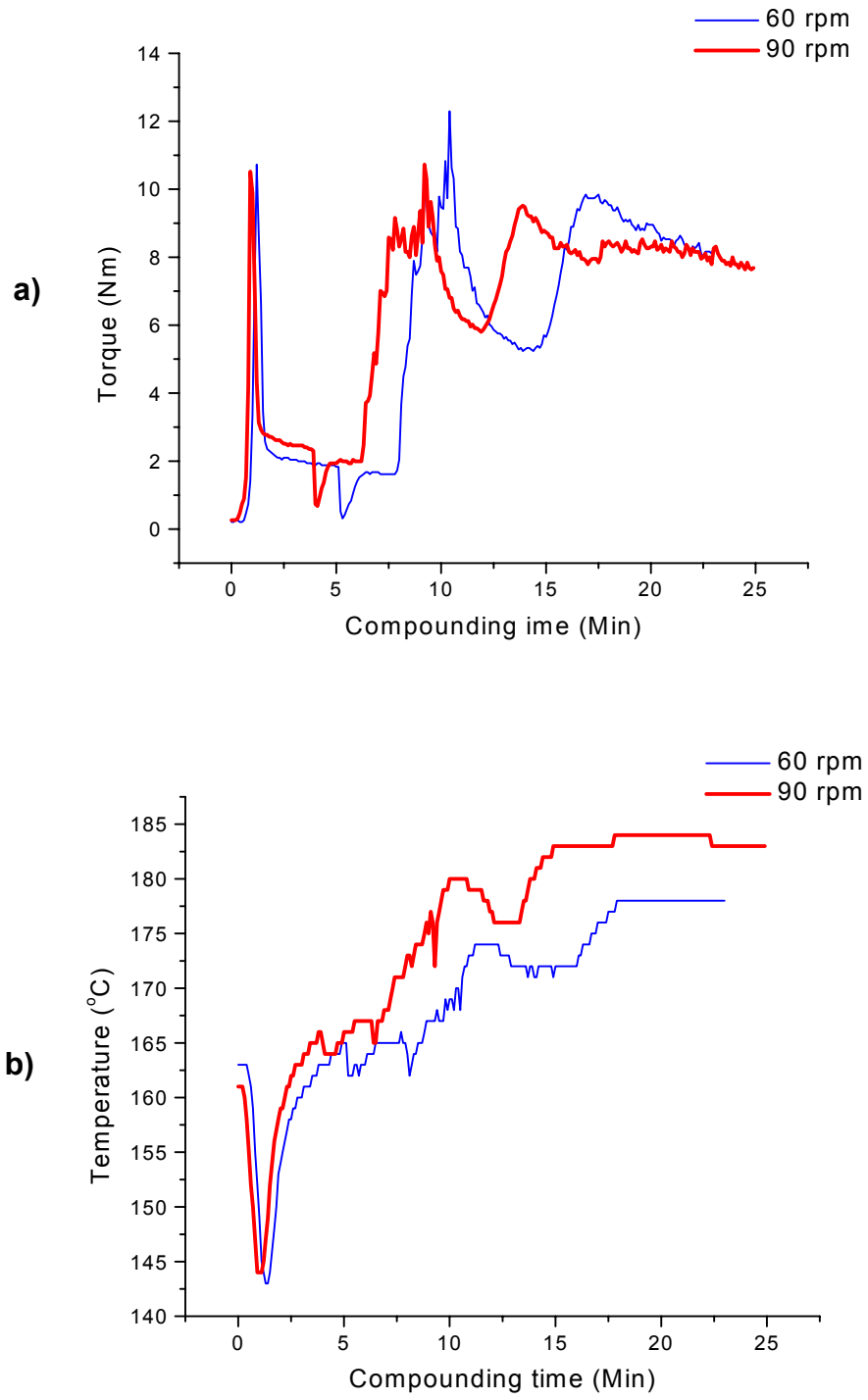

Figure 6.5. Influence of rotation speed on a) torque and b) mixing temperature for wood-HDPE blends with 5% E20. The compounding temperature and mixing time were 165°C and 15 min, respectively.

Table 6.4. Influence of different compounding conditions in the one-step process on dynamic mechanical properties of maleated wood fiber-HDPE composites at 25°C. [a]

Compounding condition [b, c]						Dynamic mechanical properties of resultant composites [d]			
Rotation speed (rpm)		Mixing temperature (°C)		Compounding time (Min)		E^*_{int} (GPa)	E′ (GPa)	E″ (GPa)	tanδ ($\times 10^{-2}$)
Level	Duncan's grouping	Level	Duncan's grouping	Level	Duncan's grouping				
60		150		10	A	2.91 (0.23)	3.11 (0.33)	0.21 (0.03)	6.7 (0.3)
60	A	150	A	15	A	3.82 (0.63)	3.26 (0.59)	0.20 (0.03)	6.1 (0.2)
60		150		20	A	3.92 (0.73)	3.63 (0.51)	0.22 (0.03)	6.0 (0.1)
60		165		10	A	3.96 (0.46)	4.25 (0.42)	0.26 (0.03)	6.3 (0.1)
60	A	165	B	15	A	4.30 (0.64)	4.13 (0.45)	0.24 (0.03)	5.8 (0.1)
60		165		20	A	3.99 (0.25)	3.80 (0.12)	0.22 (0.01)	5.9 (0.2)
60		180		10	A	4.68 (0.37)	4.50 (0.23)	0.26 (0.01)	5.8 (0.1)
60	A	180	B	15	A	4.23 (0.43)	4.21 (0.38)	0.26 (0.02)	6.1 (0.2)
60		180		20	A	3.92 (0.55)	3.90 (0.39)	0.24 (0.03)	6.2 (0.3)
90		150		10	A	3.90 (0.24)	3.73 (0.18)	0.22 (0.01)	6.0 (0.1)
90	B	150	A	15	A	4.35 (0.61)	4.14 (0.42)	0.26 (0.03)	6.2 (0.0)
90		150		20	A	4.19 (0.43)	4.12 (0.19)	0.26 (0.01)	6.2 (0.1)
90		165		10	A	5.00 (0.79)	4.84 (0.64)	0.30 (0.05)	6.2 (0.1)
90	B	165	B	15	A	4.64 (0.62)	4.45 (0.37)	0.27 (0.01)	6.1 (0.2)
90		165		20	A	4.37 (0.38)	4.21 (0.26)	0.26 (0.02)	6.1 (0.1)
90		180		10	A	4.30 (0.41)	4.42 (0.18)	0.26 (0.01)	5.9 (0.1)
90	B	180	B	15	A	4.19 (0.45)	4.12 (0.29)	0.25 (0.01)	6.1 (0.3)
90		180		20	A	4.13 (0.62)	4.04 (0.34)	0.29 (0.02)	6.4 (0.2)

[a] The weight ratio of wood fiber and HDPE was 50:50.
[b] Levels with the same letter have no significantly different.
[c] Duncan's grouping was based on E^*_{int}.
[d] The values in parentheses are standard deviation.

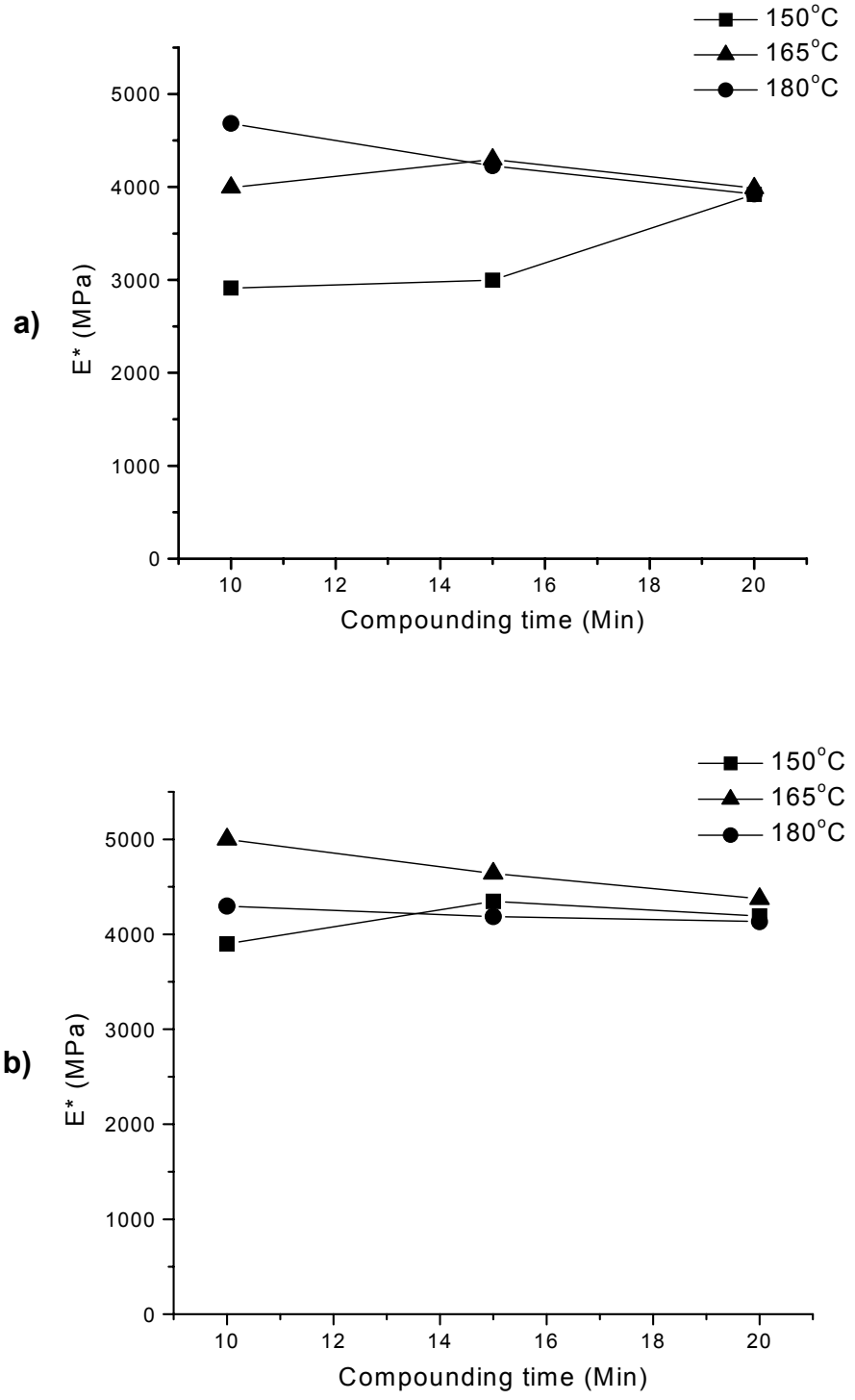

Figure 6.6. Influence of different compounding conditions on complex modulus of wood fiber-HDPE composites. a) 60 rpm and b) 90 rpm. The weight ratio of wood fiber and HDPE was 50%:50% and the concentration of E20 was 5 wt% of oven-dried wood fiber.

cellulose and polymer molecules. It was interested that E* converged to a value around 4.0 GPa with the increase of mixing time (Figure 6.6).

Storage (or elastic) modulus E′ also presented a trend similar to complex modulus E*. Better strength properties occurred when mixing temperature and mixing time were 165^{o}C and 10 min at 90 rpm, while the optimum compounding condition at 60 rpm was 180^{o}C and 10 min (Table 6.4). Hence, short mixing time is helpful to improve mechanical properties of the resultant composites.

Loss (or viscous) modulus E″ was between 0.2 and 0.3 GPa for maleated wood fiber-HDPE composites. Composites with high E′ values also had high E″ values. Moreover, composites with high modulus had small tanδ values at 25^{o}C, compared with those with low modulus (Table 6.4). According to experimental results, tanδ values were between 0.058 and 0.067.

According to statistical analysis, the main effects of rotation speed and mixing temperature and the interaction effect between speed and temperature were significant. However, the main effect of compounding time and other interaction effects were not significant (Table 6.5). By Duncan's multiple range test (Table 6.4), the effect of mixing temperature at 150^{o}C on E* means was significantly different from that at 165^{o}C and 180^{o}C. The effect of rotation speed at 60 rpm on E* means was also significantly different from that at 90 rpm. Although E* means decrease with increase of compounding time, there was no significant difference among the compounding time levels.

Based on above discussion, the optimal compounding parameters at 60 rpm were with a mixing temperature of 180^{o}C and a compounding time of 10 min. The optimum compounding condition at 90 rpm was at a temperature of 165^{o}C and a compounding

time of 10min. Therefore, short mixing time, appropriate rotation speed, and high temperatures were suitable to improve compounding quality of modified blends and dynamic mechanical properties of resultant composites.

Table 6.5. Three-way ANOVA of complex modulus E* of the resultant composites by the one-step process. [a]

Source	DF	Type III sum of square	Mean square	F value	Pr > F
Model	17	13.317	0.783	3.13	0.0020
Speed	1	2.843	2.843	11.35	0.0018
Temp	2	4.496	2.248	8.98	0.0007
Speed*Temp	2	2.095	1.047	4.18	0.0233
Time	2	0.0169	0.008	0.03	0.9669
Speed*Time	2	0.193	0.0965	0.39	0.6829
Temp*Time	4	2.284	0.571	2.28	0.0796
Speed*Temp*Time	4	1.389	0.347	1.39	0.2579
Error	36	9.015	0.250		

[a] Speed- rotation speed, Temp- mixing temperature, and Time- compounding time.

6.4.1.5 Two-step Process versus One-step Process

At the same concentration level of coupling agent, mixing time for dispersion in a two-step process was smaller than in a one-step process and a control (Figure 6.7). For untreated blends, the maximum dispersion torque occurred at about 9 min after adding wood fiber. For maleated blends with the one-step and the two-step processes, it was decreased to 7 min and 5 min, respectively. Therefore, maleation forced the dispersion range shift left. The two-step process shortened the dispersion period by 2 min compared

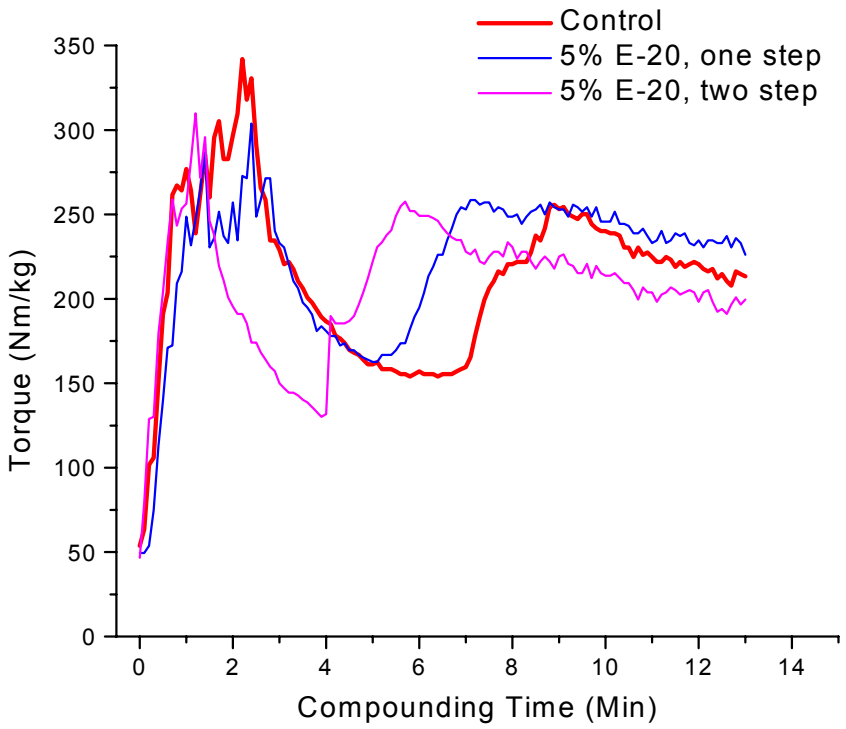

Figure 6.7. Comparison of two-step process and one-step process for wood-HDPE blends (50%:50%). The kneading process was conducted at 165°C and 90 rpm for 10 min. The concentration of E20 was 5 wt% of oven-dried wood fiber.

with the one-step process, and by 4 min compared with the control (untreated blends), although the values of maximum dispersion torque were almost the same (Figure 6.7). This was due to that pretreated wood fiber was more easily dispersed in the polymeric matrix. Therefore, a two-step process was usually better than a one-step process because pretreated wood fiber more effectively improve the interfacial compatibility and miscibility (Štepek and Daoust 1983).

6.4.2 Coupling Mechanisms of MAPE

MAPEs presented clear feature peaks of their backbone chain at three regions (Figure 6.8a). The backbone molecule, polyethylene, had a strong peak of (-C-H) at about 2923 and 1466 cm^{-1}, respectively and a moderate peak of ($-CH_2-$) at around 720 cm^{-1}. Methyl groups ($C-CH_3$) also presented a significant peak at around 2850 cm^{-1}. Polypropylene had the peaks similar to polyethylene, but it had a moderate feature peak of propyl groups at 1160 cm^{-1} and a strong peak at around 1370 cm^{-1}.

Different from HDPE, MAPEs had characteristic peaks in the range between 1800 and 1650 cm^{-1} (Figure 6.8b). Within the range between 1800 and 1700 cm^{-1}, two bands separated by about 60 cm^{-1} were the characteristic of cyclic anhydrides (Colthup 1950; Smith 1991). The peak at low frequency of 1717 cm^{-1} was more intense than that at high frequency of 1790 cm^{-1}. For 100D, 226D, and C16, these two bands were significant. However, E20 and E17 had a strong low band but a weak high band, while C16 had an intense high band (which was significantly shifted to right) but its low band was weak or disappeared. Except for E17 and C10, most MAPE coupling agents also presented a weak peak at 1651 cm^{-1}. E43 had a pair of bands similar to MAPEs, but both shifted to lower frequency due to the influence of propyl groups.

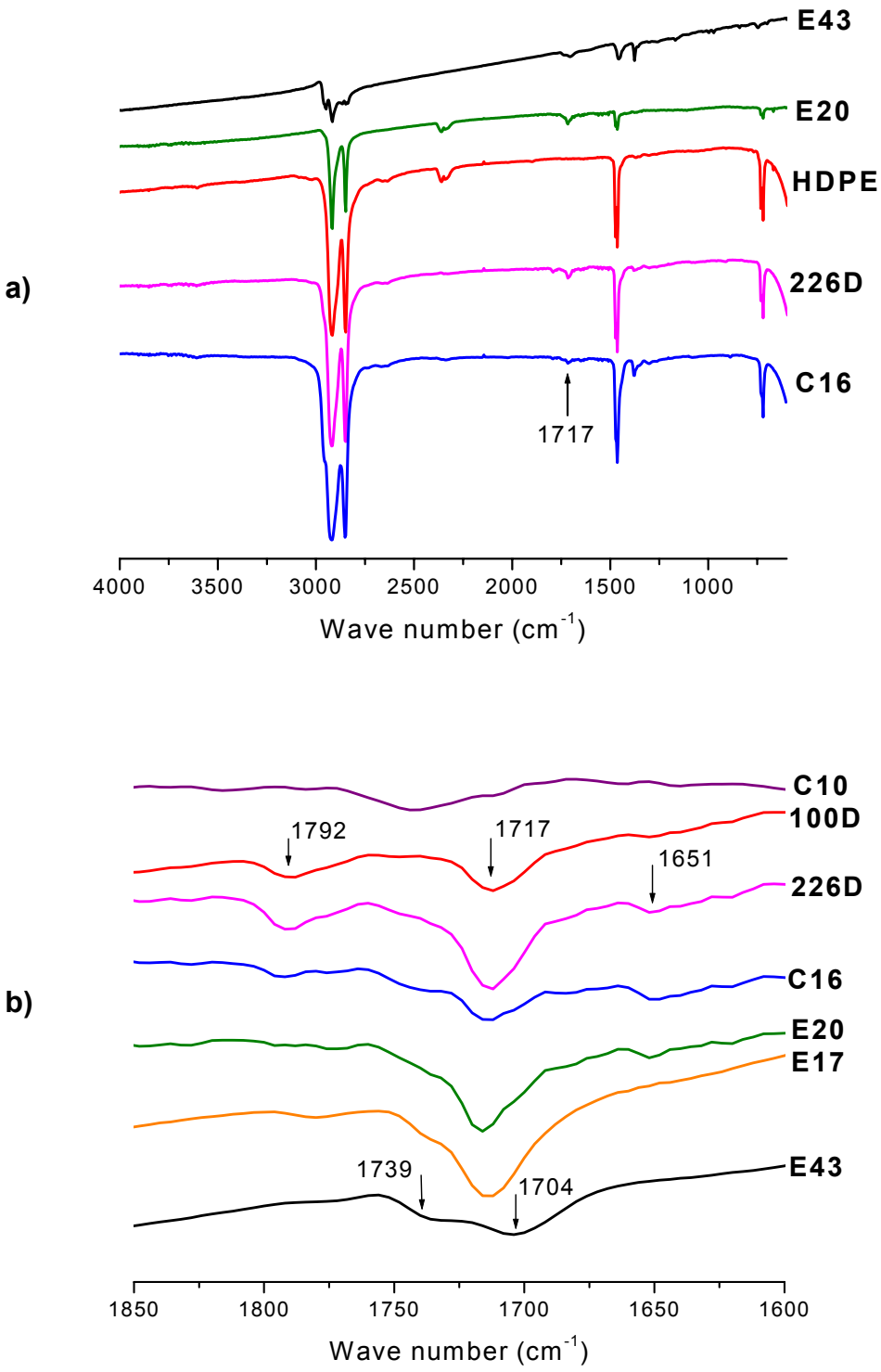

Figure 6.8. FTIR spectra of MAPE and MAPP coupling agents. a) Selected coupling agents and b) Characteristic peaks of maleated polyolefins.

For untreated composites, the peak at around 3400 cm^{-1} was due to absorbed water in wood fiber. Composites with E43 and C16 also showed this strong peak. Composites with E43 and C16 had a strong peak at 2923 and 2840 cm^{-1}, respectively, which were the characteristic IR spectra of PE and PP. Compared with untreated composites, composites with C16 and with E43 presented a feature peak of esterification at 1751 cm^{-1} and 1678 cm^{-1}, respectively (Figures 6.9 and 10). In the range between 1900 and 1400 cm^{-1}, composites with C16 and E43 had a broad band at round 1640 cm^{-1}. Composites with C16 also had a peak at 1457 cm^{-1}. For both maleated composites, the feature peak of cyclic anhydrides appeared at 1717 cm^{-1} (Figure 6.9). This agreed with the report that there existed free or ungrafted maleaic anhydride groups at the interface because of limitation on graft polymerization (Lu et al. 2002).

ESCA spectra were obtained by scanning fractural surface of wood fiber-HDPE composites after tensile testing (Figure 6.11). Carbon and oxygen were the two primary components of composites with and without coupling treatment. For wood fiber-HDPE composites, carbon (>90% in weight) had a stronger signal than oxygen (<10%), because it mostly came from HDPE and most wood surfaces were covered by the polymeric matrix.

Compared with untreated composites, composites with coupling agent had higher concentration of carbon but lower concentration of oxygen (Table 6.6). For composites with 100D, oxygen concentration was about 1-2% and almost independent of coupling agent concentration. For composites with C16 and E20, oxygen ratio decreased with increase of coupling agent concentration. However, it increased with increase of coupling agent concentration for composites with 226D. This indicated that chemical compositions

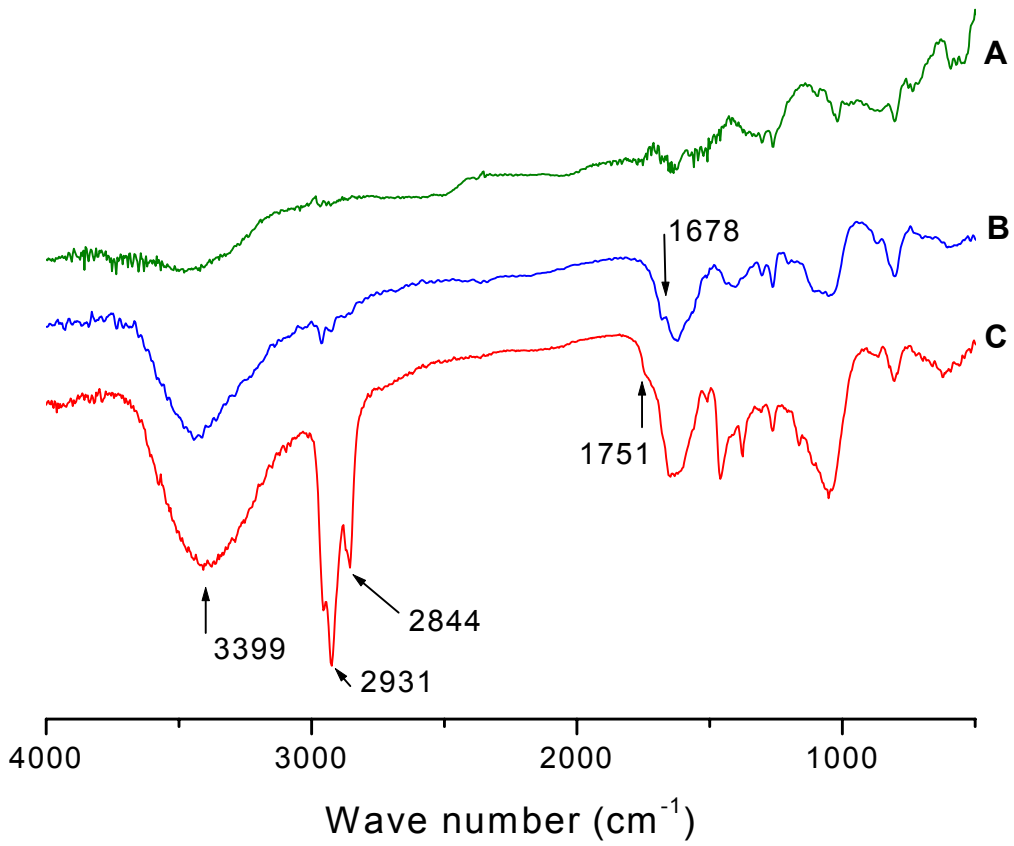

Figure 6.9. FTIR spectra of xylene-unextractable composite samples in a region between 4000 and 500 cm^{-1}. A- untreated composites, B- Composites with 3% E43, and C- Composites with 3% C16.

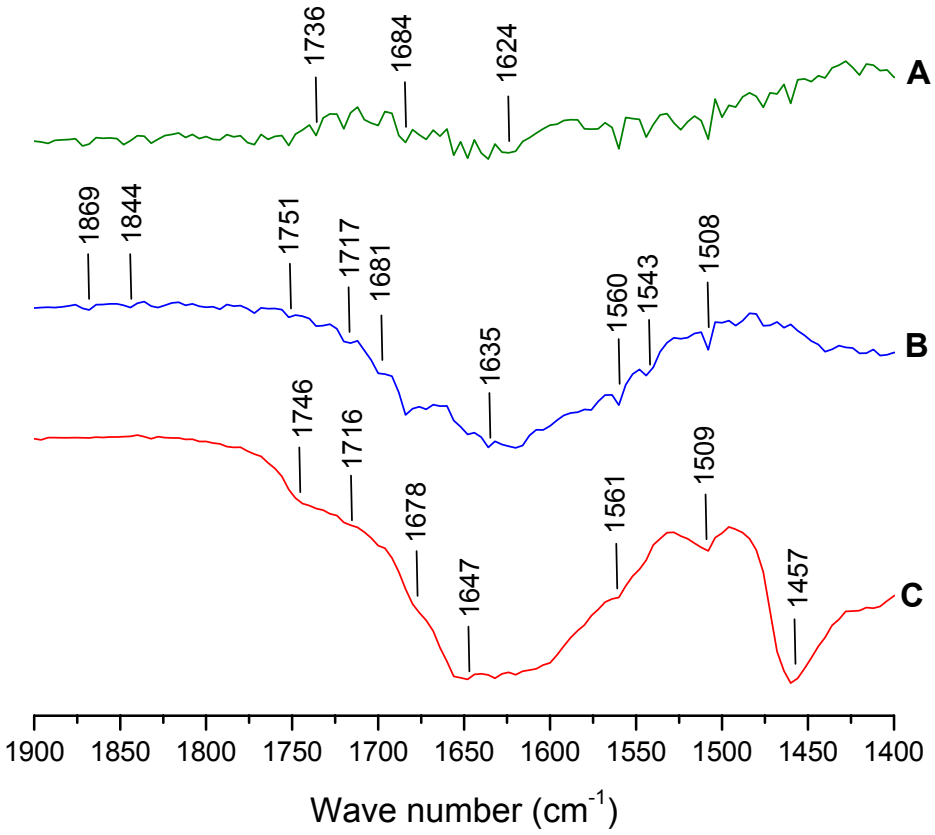

Figure 6.10. FTIR spectra of xylene-unextractable composite samples in a region between 1850 and 1400 cm^{-1}. A- untreated composites, B- composites with 3% E43, and C- composites with 3% C16.

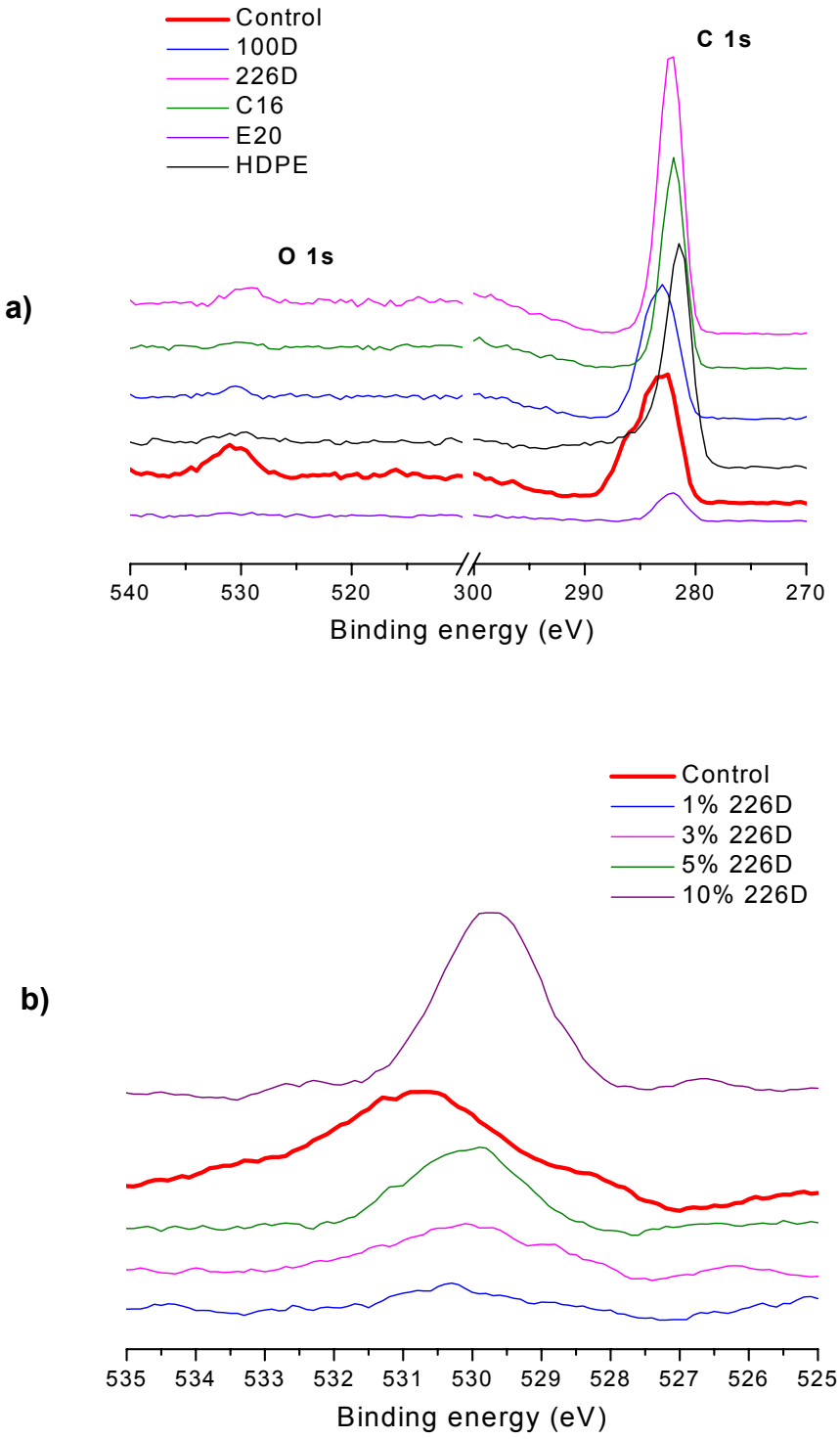

Figure 6.11. ESCA spectra for fracture surface of wood fiber-HDPE composites after tensile failure. a) Survey spectra of selected coupling agents with a concentration level of 3% and b) O 1s spectra of composites with 226D.

Table 6.6. Chemical compositions on fracture surface of wood fiber-HDPE composites.

Composite sample	Concentration of coupling agent [a]	Binding energy (eV)		Mass concentration (%)	
		C 1s	O 1s	C	O
Untreated	0%	282.5	531.0	93.75	6.25
100D	1%	282.5	529.5	98.56	1.44
	3%	282.0	530.5	98.88	1.12
	5%	282.0	532.0	98.85	1.18
	10%	282.5	529.5	98.34	1.66
	100%	282.0	529.5	94.45	5.55
226D	1%	282.0	529.5	98.43	1.57
	3%	282.0	529.0	97.43	2.57
	5%	282.0	530.5	97.36	2.64
	10%	282.0	529.5	92.31	7.69
	100%	282.0	529.5	91.95	8.05
C16	1%	282.0	529.5	95.10	4.90
	3%	282.0	529.5	98.53	1.47
	10%	282.5	529.0	98.58	1.42
	100%	282.0	529.5	94.66	5.34
E20	1%	282.0	529.5	97.60	2.40
	3%	282.0	529.0	94.46	5.54
	10%	282.0	529.0	97.13	2.87
	100%	282.0	529.5	89.34	10.66

[a] 100% means pure coupling agent.

at the interface were influenced by coupling agent type and structure, coupling agent concentration, and its coupling reaction with wood and the polymer matrix.

For untreated composites, the binding energy at C 1s and O 1s was around 282 and 530 eV, respectively. Compared with untreated composites, composites with MAPEs had right-shifting peaks at C 1s spectra but had a left shift compared with HDPE. They also had right-shifting peaks at O 1s spectra compared with untreated composites (Figure 6.11a). This indicated that chemical covalent bonding took place at the interface. As shown in Figure 6.11b, composites with 226D had a significant right-shifting peak compared with untreated composites. Composites with 226D at different concentrations had almost the same peak of about 529 eV at O 1s spectra. Intensity of these peaks was related to oxygen ratio at the interface (Table 6.6). The results agreed with that the amount of free single and double carboxyl acids increased with the increase of coupling agent concentration (Lu et al. 2002).

Based on above results and previous reports (Gaylord et al. 1989, 1992), coupling mechanisms of MAPE in wood fiber-HDPE composites are proposed in Figure 6.12. Through dehydration, double acids on MAPE are transferred as maleaic anhydride groups with a close ring, but this reaction is reversible. With an initiator, some polyethylene and MAPE molecules become free radicals. Non-radicals may switch with free radicals to form new radicals. Two polyethylene radicals may combine together and become a new polyethylene molecule with larger molecular weight. One polyethylene radical may react with one MAPE radical to form a maleaic anhydride grafted polyethylene molecule. A MAPE radical may also react with a double carbon-carbon bond at the end or on the branch of a polyethylene molecular chain. This coupling reaction is preferred for LLDPE molecules. Two MAPE radicals may react each other to form saturated and unsaturated MAPE molecules.

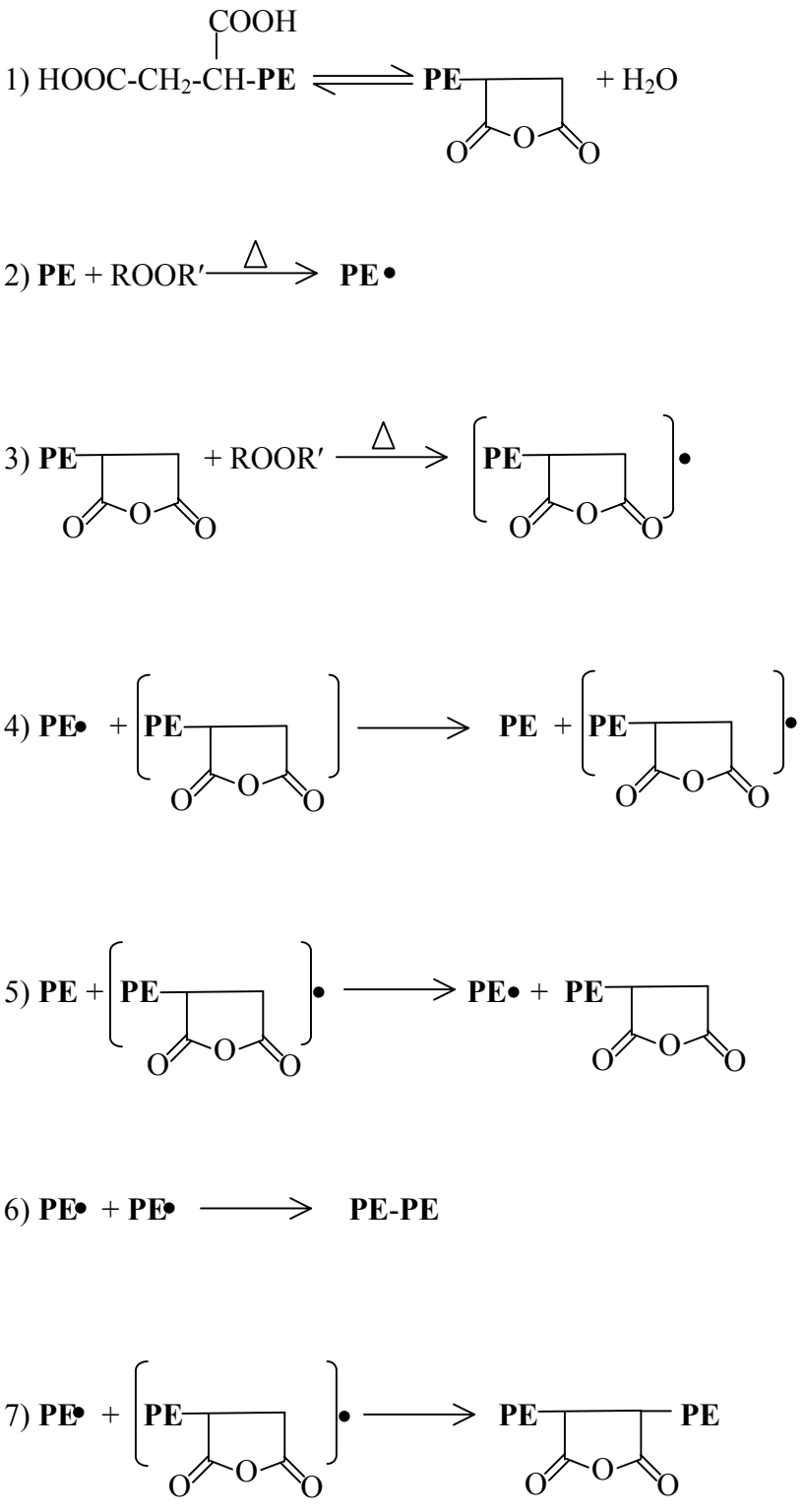

Figure 6.12. Chemical coupling mechanisms in maleated wood fiber-HDPE composites.

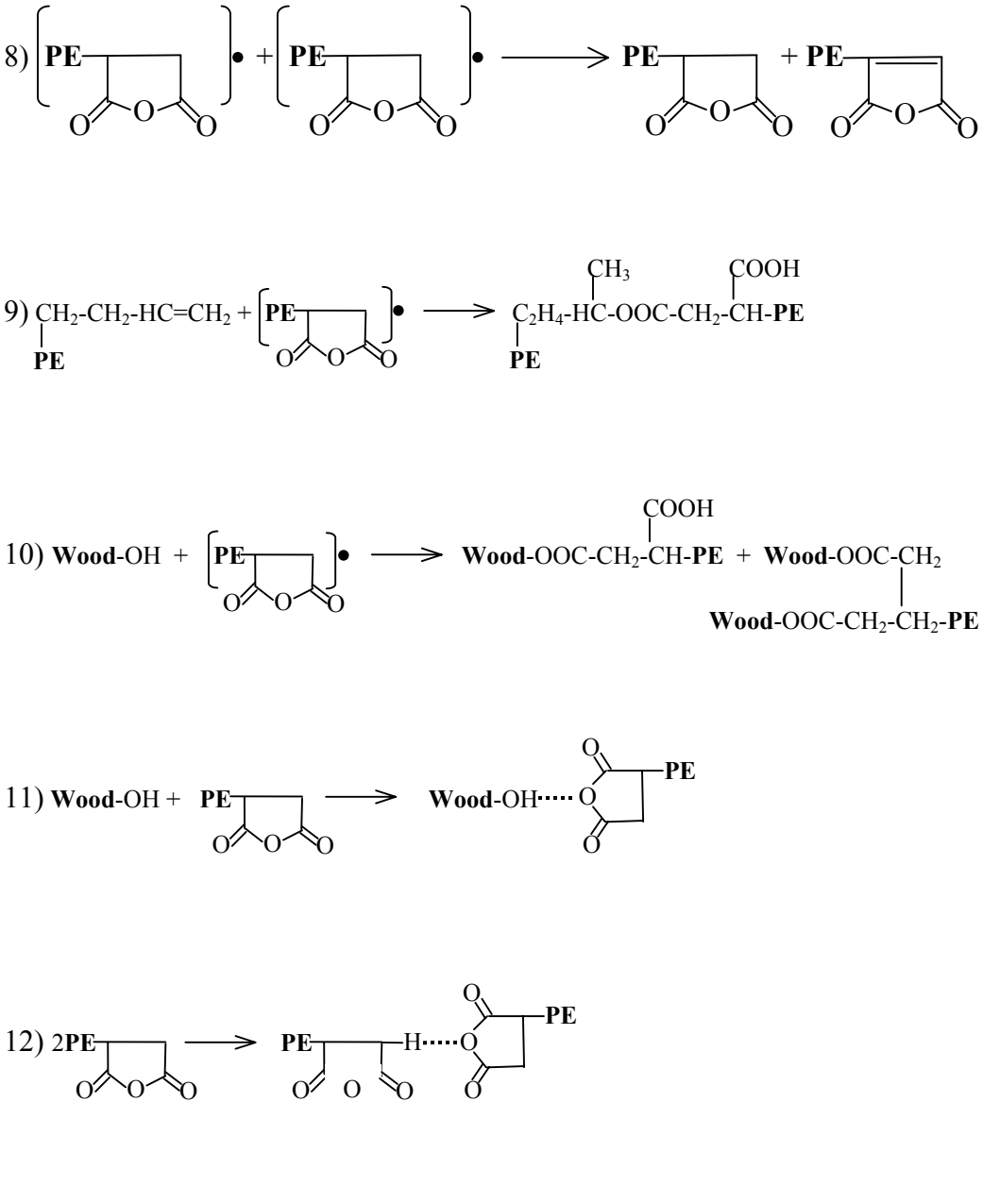

Figure 6.12. Continued.

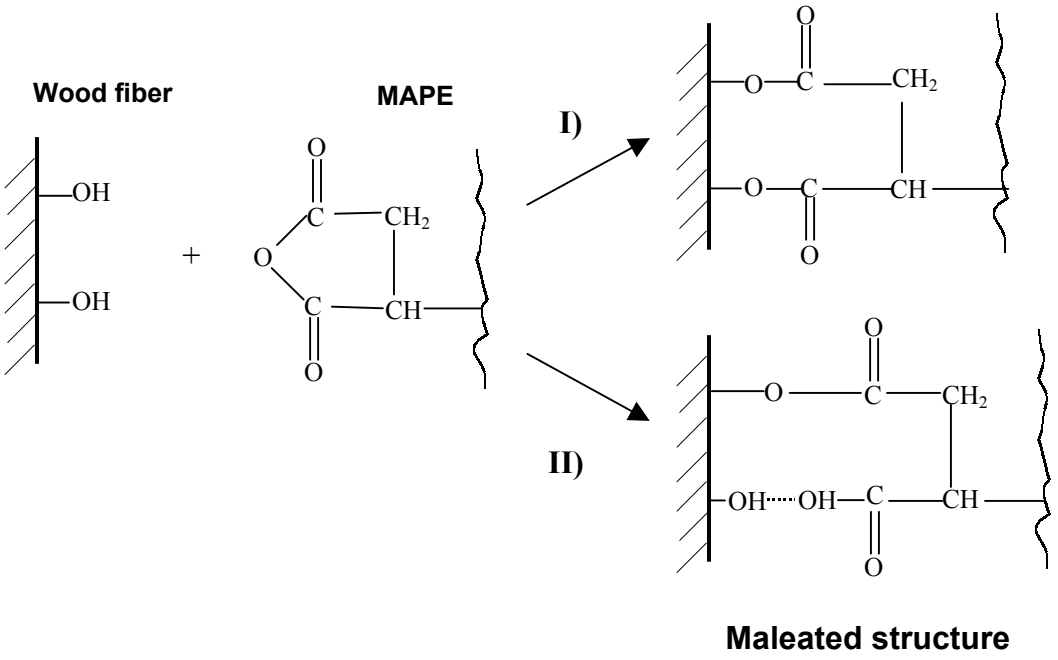

Figure 6.13. Hypothetical grafting structure at the interface in maleated wood fiber-PE composites. I) succinic bridge structure and II) half succinic bridge structure.

MAPE radicals react with hydroxyl groups of wood to form a graft polymerization structure. The reaction between wood and MAPE may result in two products (Figure 6.13). One is the copolymer with diester bonds, whereas another has the half-ester structure (Kishi et al. 1988, Felix and Gatenholm 1991). Secondary bonding is also involved in wood-polymer composites. As shown in Figure 6.12, a hydrogen atom of a hydroxyl group on wood may form hydrogen bonding with the oxygen atom of a maleaic anhydride group. Also, a hydrogen atom on the maleaic anhydride group of a MAPE molecule may form the hydrogen bonding with the oxygen atom on the maleaic anhydride group of another MAPE molecule (Figure 6.12).

6.4.3 Interfacial Morphology and Coupling Agent Distribution

For high concentration of wood fibers (e.g., 70% in weight), the polymer matrix was not continuously distributed and most wood fibers directly contacted one another, thus resulting in poor adhesion at the interface (Figure 6.14a). This situation was improved when the amount of thermoplastics was equal to or larger than that of wood fibers in weight (Figure 6.14b). Most wood fibers were enveloped by the polymer matrix when polymer phases were abundant in composites (i.e., the weight ratio of polymer and wood was larger than one). Hence, wood fibers and thermoplastics were mainly linked through mechanical connection for untreated composites.

For untreated wood fiber-HDPE composites, wood surfaces were usually smooth and individual fibers had clear profiles on fractural surface (Figure 6.14c). Thermo-plastics penetrated into pit lumens (Figures 6.14c and d), cracks, and other void parts on wood fiber and gaps between fibers to form mechanical connection. Under tensile loading, composites with 70% fiber were damaged along the direction parallel to fiber

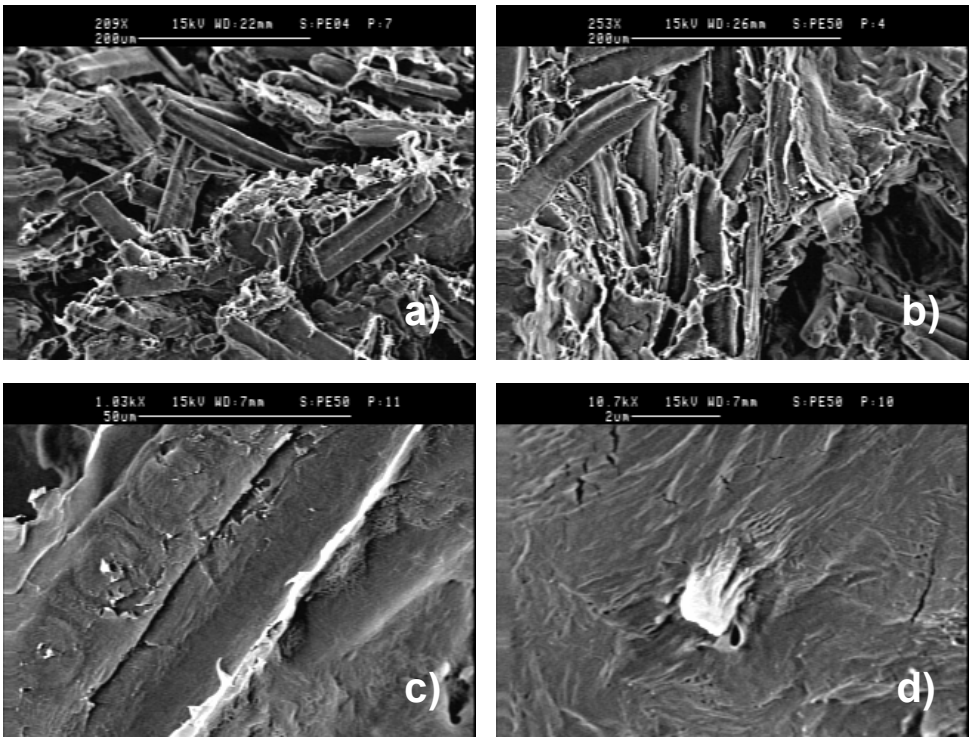

Figure 6.14. SEM micrographs for fracture surface of untreated wood fiber-HDPE composites. a) 70% fibers, b) 50% fibers, and c) and d) with HDPE-filled pit lumens (containing 50% fibers).

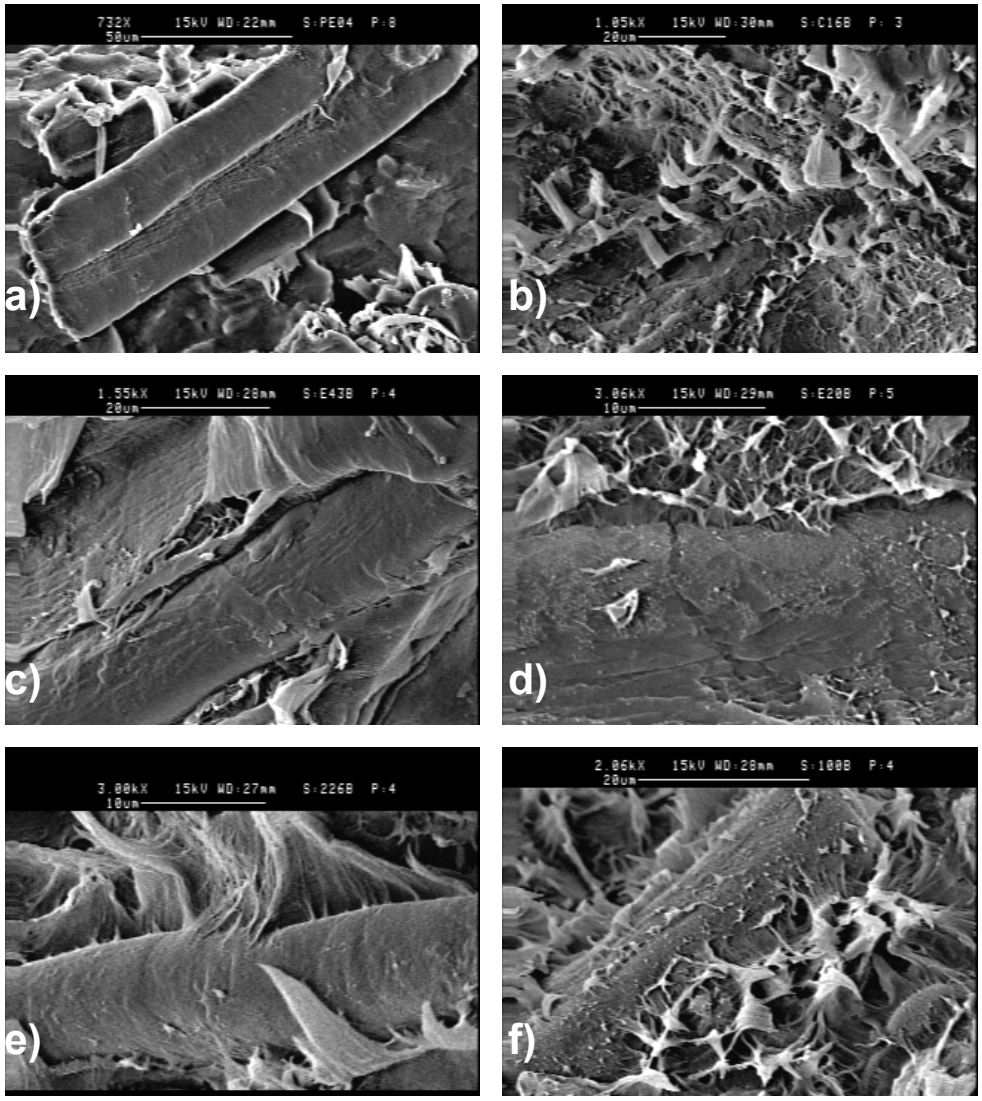

Figure 6.15. SEM micrographs for fracture surface of maleated wood fiber-HDPE composites with 50% wood fibers. a) untreated composites, b) with 3% C16, c) with 3% E43, and d) with 3% E20, and e) and f) with 3% 100D.

length due to shearing failure between fiber bundles (Figure 6.14a). When the weight ratio of wood fiber was equal to or larger than that of thermoplastics, tensile failure was mainly due to fiber separation (Figure 6.14a) and peel-off (Figure 6.14b) of wood fiber from the matrix. However, pullout damage was dominant on fractural surfaces of composites and produced holes or grooves with smooth wall when the amount of thermoplastics in weight was larger than that of wood fiber (Figures 6.14b and c).

Different from untreated composites, fibers in maleated composites had a rougher fractural surface (Figures 6.14a, 6.14b, 6.15a, and 6.15b). Wood fibers were peeled off (Figures 6.14a) and pulled out from the matrix (Figures 6.14b and c) or embedding in the matrix (Figures 6.15b, c, d, e, and f). The latter two cases seemed to be dominant for most composites with coupling agent because of chemical coupling at the interface. Composites with coupling agent presented strong interfacial adhesion (Figure 6.15b, c, d, e, and f). Some polymer molecules were still grafted on wood surfaces by coupling agent after tensile failure (Figures 6.15e and f). It indicated that a maleated copolymer indeed strengthened the interfacial adhesion through chemical bonding.

In general, coupling agents are randomly distributed in composites. A coupling agent randomly reacted with wood fiber and the matrix to form graft polymerization. Its grafting sites were randomly distributed on wood. Therefore, a network of coupling agent was formed at the interface. However, there was a limit for chemical coupling reaction and only part of coupling agent was grafted onto wood surface and even cross-linked at the interface (Lu et al. 2002). Furthermore, esterification of maleated polyolefins was usually limited to the surface layer (Felix and Gatenholm 1991).

Based on above observations by SEM, *pinwheel* models are proposed to illustrate coupling agent distribution in the resultant composites (Figure 6.16). A symmetric structure applies to Structure I when the amount of wood fiber is equal to that of thermoplastics in weight. In this model, wood fiber is evenly separated in the polymer matrix. A coupling agent is distributed at the interface to form the following four modes: polymer-wood, polymer-coupling agent-polymer, polymer-coupling agent-wood, and wood-coupling agent-wood interphases. Asymmetric structures (such as Structure II and III) are suitable for maleated composites when the amount of wood fiber is unequal to that of polymer. In Structure II, wood fibers are enveloped in the matrix, while most fibers form bundles and the polymer matrix is not continuous in Structure III. Structure II has four interphases: polymer-polymer, polymer-wood, wood-coupling agent-polymer, and polymer-coupling agent-polymer. Similarly, wood-wood, wood-polymer, wood-coupling agent-polymer and wood-coupling agent-wood interphases exist in Structure III.

6.4.4 Coupling Agent Performance

6.4.4.1 Mechanical Properties of the Resultant Composites

Figure 6.17 shows measured flexural modulus and tensile strength of the untreated wood-HDPE composites as a function of wood fiber weight percentage in relation to total composite weight. Flexural modulus of the composites increased with the increase of wood fiber at low wood fiber weight ratio ranges (Figure 6.17). The modulus reached its maximum value at the 35% wood fiber weight and gradually decreased with further increase of wood fiber. Tensile strength of the resultant composites increased slightly at the low weight ratio and reached its maximum at the 15% fiber weight and

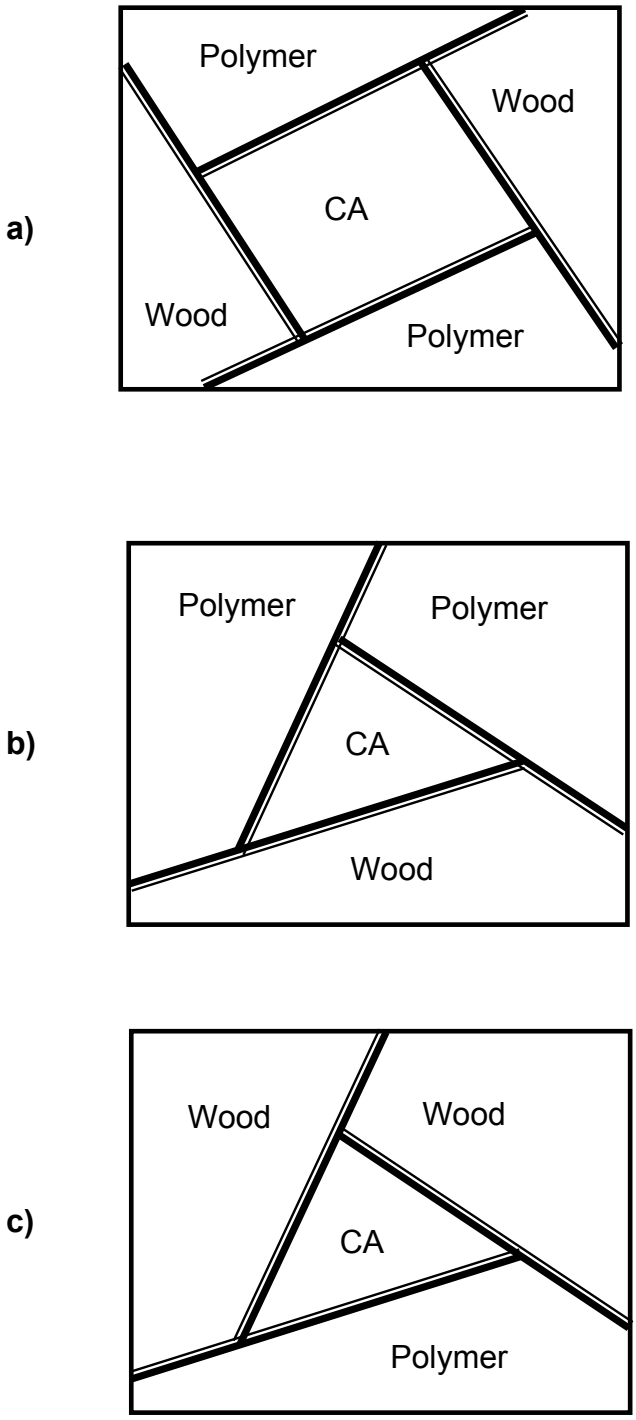

Figure 6.16. Hypothetical structures of wood-polymer interface for melt-blended wood fiber-polymer composites with a coupling agent (CA). a) Structure I- wood-polymer weight ratio=1, b) Structure II-wood-polymer weight ratio<1, and c) Structure III- wood-polymer weight ratio>1.

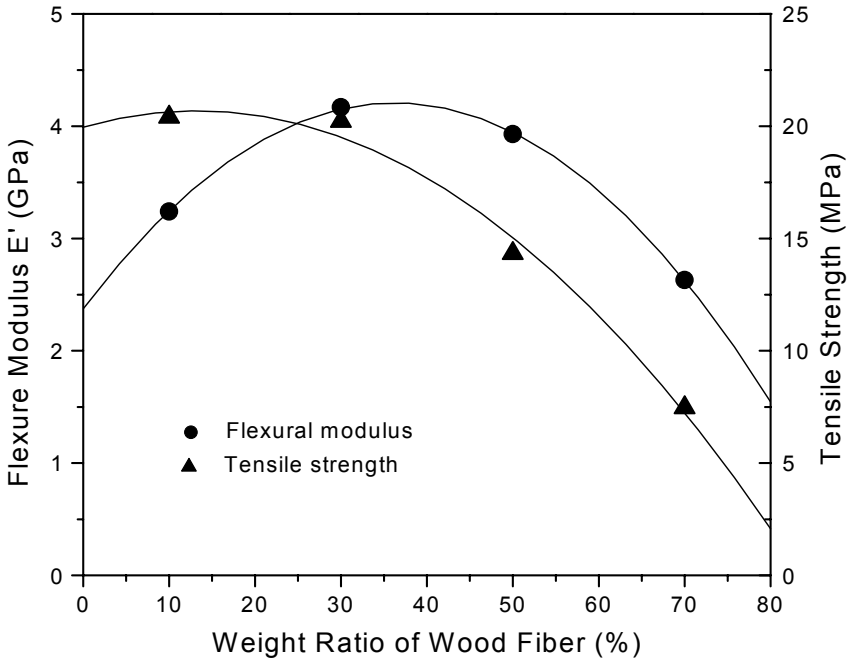

Figure 6.17. Influence of wood fiber weight percentage on mechanical properties of wood fiber-HDPE composites.

Table 6.7. Coupling performance of MAPEs in wood fiber-HDPE composites. [a]

Coupling agent	Concentration of coupling agent (wt%)	Density (kg/m^3)	Tensile strength (MPa)	Flexural modulus at 1Hz and 27°C (GPa)			tanδ at 1Hz and 27°C ($\times 10^{-2}$)
				E′	E″	E*	
Control	0	1069	10.53 (0.67)	3.54 (0.15)	0.245 (0.009)	3.55 (0.15)	6.91 (0.07)
E43	1	1033	16.06 (0.76)	3.64 (0.09)	0.231 (0.004)	3.64 (0.09)	6.35 (0.09)
	3	1019	18.85 (1.02)	3.39 (0.33)	0.217 (0.021)	3.39 (0.33)	6.39 (0.11)
	5	1018	15.15 (1.23)	3.40 (0.14)	0.222 (0.009)	3.40 (0.14)	6.53 (0.06)
	10	1025	18.87 (4.10)	3.59 (0.26)	0.233 (0.017)	3.60 (0.26)	6.49 (0.08)
E20	1	1011	22.11 (2.74)	3.61 (0.39)	0.228 (0.005)	3.61 (0.40)	6.32 (0.10)
	3	1027	20.34 (0.52)	3.38 (0.12)	0.222 (0.008)	3.34 (0.12)	6.56 (0.05)
	5	1041	19.40 (0.99)	3.36 (0.24)	0.225 (0.016)	3.37 (0.24)	6.71 (0.04)
	10	1021	16.00 (1.17)	3.21 (0.45)	0.217 (0.006)	3.22 (0.44)	6.75 (0.10)
E17	1	998	19.35 (1.18)	3.64 (0.49)	0.230 (0.027)	3.64 (0.50)	6.33 (0.10)
	3	1014	18.55 (2.57)	3.32 (0.31)	0.220 (0.031)	3.33 (0.48)	6.61 (0.13)
	5	992	17.35 (0.72)	3.13 (0.19)	0.209 (0.013)	3.14 (0.19)	6.68 (0.11)
	10	998	17.54 (1.83)	3.04 (0.27)	0.215 (0.017)	3.05 (0.27)	7.05 (0.11)
C10	1	1030	20.13 (0.90)	3.47 (0.25)	0.220 (0.014)	3.48 (0.26)	6.35 (0.11)
	3	1034	22.84 (1.88)	3.50 (0.38)	0.225 (0.024)	3.51 (0.39)	6.41 (0.07)
	5	1025	19.26 (1.56)	3.15 (0.34)	0.207 (0.022)	3.16 (0.34)	6.57 (0.10)
	10	1006	20.36 (3.28)	2.99 (0.30)	0.196 (0.020)	3.00 (0.30)	6.56 (0.09)
C16	1	1017	20.39 (2.98)	4.22 (0.37)	0.268 (0.023)	4.22 (0.37)	6.37 (0.12)
	3	1021	23.97 (0.49)	4.42 (0.35)	0.277 (0.018)	4.43 (0.35)	6.28 (0.13)
	5	975	21.83 (2.33)	4.11 (0.14)	0.268 (0.009)	4.12 (0.15)	6.51 (0.04)
	10	1008	19.24 (3.14)	3.89 (0.42)	0.253 (0.003)	3.90 (0.42)	6.51 (0.05)
100D	1	1039	21.17 (1.03)	4.51 (0.39)	0.277 (0.024)	4.52 (0.39)	6.14 (0.09)
	3	1063	22.29 (0.83)	4.11 (0.47)	0.249 (0.030)	4.11 (0.47)	6.06 (0.15)
	5	1045	22.34 (0.18)	3.66 (0.31)	0.225 (0.018)	3.66 (0.32)	6.14 (0.06)
	10	1056	24.41 (3.30)	4.05 (0.29)	0.253 (0.019)	4.06 (0.29)	6.25 (0.07)
226D	1	1050	22.82 (2.57)	3.89 (0.49)	0.243 (0.031)	3.90 (0.49)	6.23 (0.05)
	3	1038	25.33 (3.32)	3.97 (0.29)	0.240 (0.015)	3.98 (0.29)	6.06 (0.17)
	5	1047	23.33 (0.42)	4.04 (0.17)	0.251 (0.010)	4.05 (0.17)	6.21 (0.04)
	10	1068	23.30 (3.54)	4.56 (0.45)	0.285 (0.026)	4.57 (0.45)	6.24 (0.07)

[a] The weight ratio between oven-dried wood fiber and HDPE was 50%:50%.

decreased with the increase of wood fiber. The results agreed with those reported by Kishi et al. (1988).

All maleated composites had better mechanical properties than untreated composites. Compared with composites without maleation, maleated composites were improved on interfacial bonding strength by 140% on maximum and flexural modulus by 29% (Table 6.7). Based on the storage modulus E′, MAPE and MAPP coupling agents were divided into two groups. The first group included C16, 226D and 100D, and the second group consisted of C10, E17, E20, and E43. Within each group, coupling agents had similar performance. In the first group, E′ of the composites treated with 226D increased with increase of coupling agent concentration. Composites with 100D had a larger E′ at low concentration levels, but E′ decreased or leveled off at the high levels. C16 had a trend similar to 100D (Figure 6.18). For the second group, coupling agents did not significantly influence E′ of the composites. Coupling agent C10 had large molecular weight. However, it did not have significant influence on E′. E′ of the composites with these four coupling agents decreased with the increase of the coupling agent concentration (Figure 6.18).

Loss modulus (E″) varied with coupling agent type and concentration. Composites with E17, E20, E43, and C10 had lower E″ than the composites without coupling treatment (Table 6.7). For these four agents, E″ also decreased with the increase of coupling agent concentration. Compared with the untreated composites, composites with C16, 100D, and 226D had higher E″. For composites with 226D and C16, E″ decreased at high concentration. However, composites with 100D increased with the

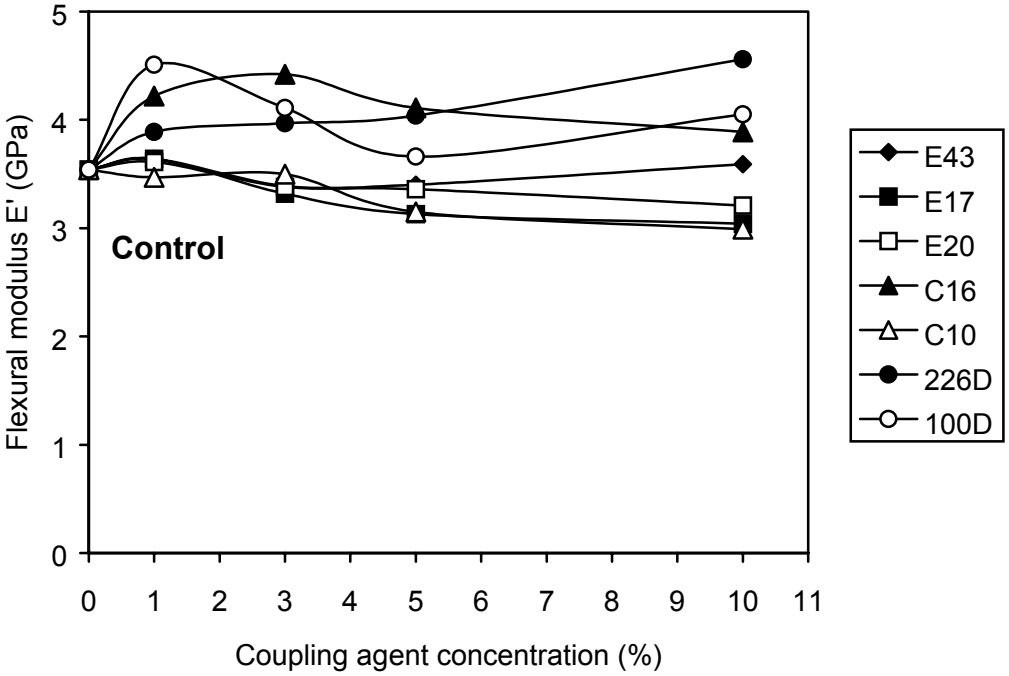

Figure 6.18. Influence of coupling agent concentration on flexural modulus E′ of wood fiber-HDPE composites.

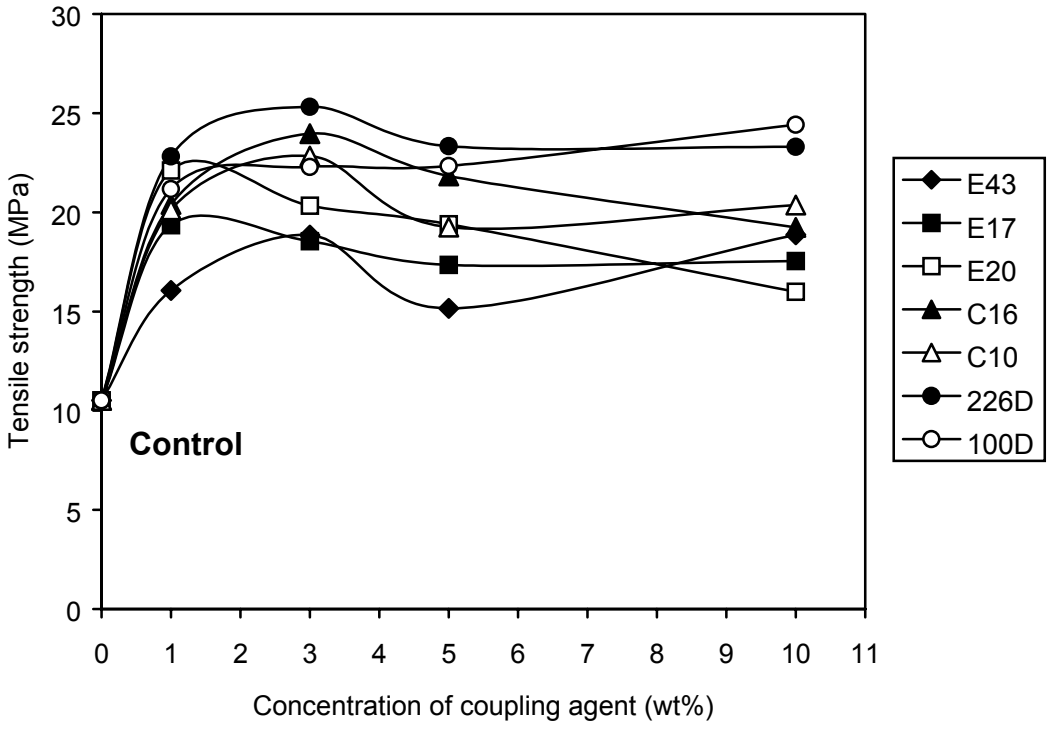

Figure 6.19. Influence of coupling agent concentration on tensile strength of wood fiber-HDPE composites.

increase of the coupling agent concentration. Phase angle of composites was also influenced by coupling agent concentration. Since tanδ is equal to the ratio of E″ and E′, it is an inverse function of E′. Phase angle of the composites increased with the increase of the coupling agent concentration (Table 6.7). For composites with E20, E17, E43, C10, and C16, tanδ had large increase. However, tanδ had small changes for composites with 100D and 226D.

As shown in Figure 6.19, composites with 226D had the highest tensile strength among the seven coupling agents. The tensile strength was 25.33 MPa at the 3% concentration level. For 100D, tensile strength of the composites increased with the increase of the coupling agent concentration. The strength reached the maximum value of 24.4 MPa at the 10% level. C16 also had better performance, similar to 100D and 226D at the low concentration levels. However, it had low flexural modulus at the high concentration levels (Table 6.7).

For composites treated with E17, E20, E43, and C10, tensile strength increased at the low concentration levels, but it decreased at the high concentration level (Figure 6.19). At the 1% concentration level, tensile strength of the composites with E20 and E17 was around 20 MPa. Its performance was better than that of both 100D and 226D. Compared with other coupling agents, E43 had the lowest tensile strength of 16.1 MPa at the 1% concentration level. Even at the 3% concentration level, C10 was still competitive with 226D, 100D, and C16 in terms of tensile strength (Figure 6.19). However, E-20, E43, C16, and C10 had low tensile strength at the high concentration levels (>3%).

According to the two-way ANOVA on storage modulus (Table 6.8), the main effects of coupling agent type and concentration and the interaction effect between

Table 6.8. Statistical analysis for storage modulus of wood fiber-HDPE composites.

Source [a]	DF	Sum of squares	Mean square	F value	Pr>F
Model	28	28.890	1.032	9.35	<0.0001
CA	7	20.787	2.970	26.89	<0.0001
CAconcen	3	2.592	0.864	7.82	<0.0001
CA*CAconcen	18	5.520	0.307	2.78	0.0005
Error	147	13.140	0.110		

Tukey's grouping [b]	100D	C16	226D	Control	E43	E20	E17	C16
		A				**B**		

[a] CA-coupling agent type, CAconcen-coupling agent concentration.
[b] Coupling agents with the same letter are not significantly different.

coupling agent type and concentration were significant. The main effect of coupling agent type and the interaction effect were significant on interfacial bonding strength. However, the main effect of coupling agent concentration on the bonding strength was not significant (Table 6.9).

6.4.4.2 Coupling Models

Based on mechanical properties of the wood fiber-HDPE composites treated with different coupling agents, three models were proposed to illustrate coupling agent performance at the interface (Figure 6.20). As shown, wood fiber-polymer interactions at the interface may include: **a)** *brush* structure (Gatenholm and Felix 1993), **b)** *switch* structure (Lu et al. 2002), and **c)** *amorphous* structure with primary interphases of **1**) wood fiber (boxes), **2**) coupling agent or polymer (solid or dashed scribbles), and **3**) the

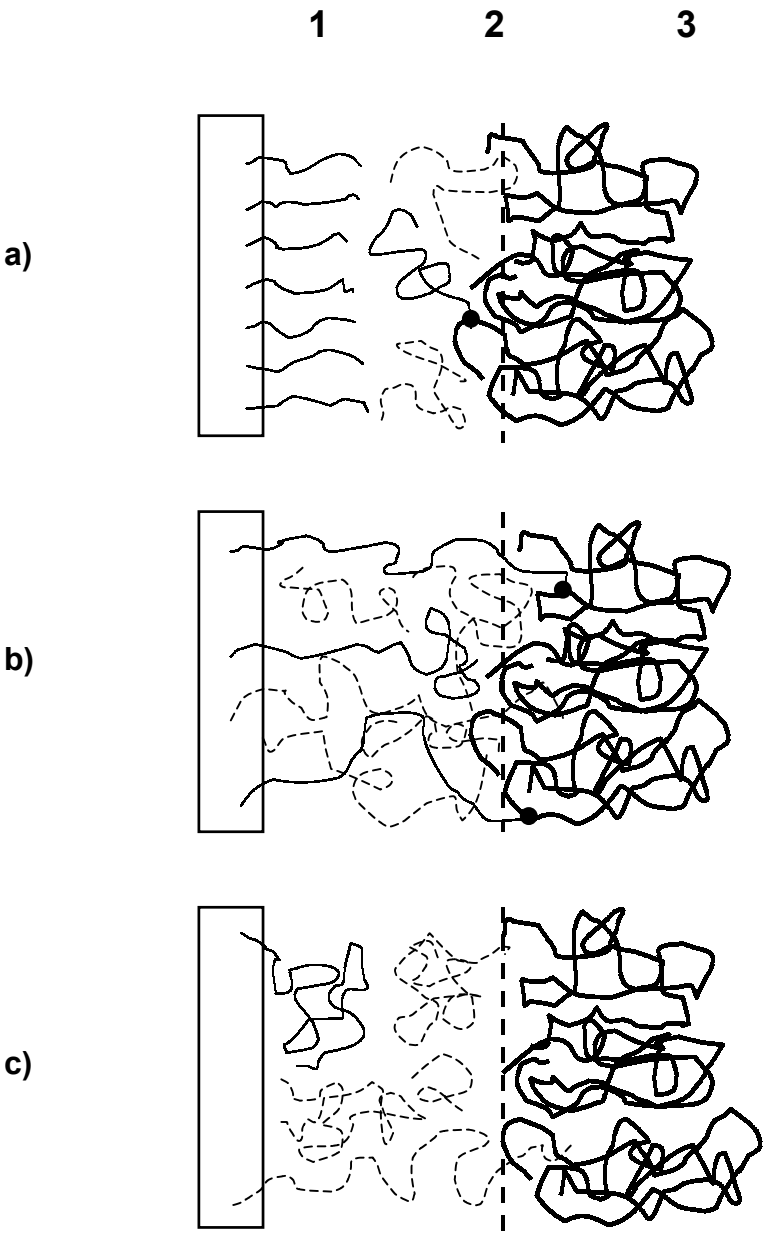

Figure 6.20. Schematic of wood fiber-polymer interactions at the interface between wood fiber and the thermoplastic matrix.

Table 6.9. Statistical analysis for interfacial bonding strength of wood fiber-HDPE composites.

Source [a]	DF	Sum of squares	Mean square	F value	Pr>F
Model	28	845.483	30.196	6.23	<0.0001
CA	7	468.693	66.956	13.81	<0.0001
CAconcen	3	24.640	8.213	1.69	0.1784
CA*CAconcen	18	352.150	19.564	4.03	<0.0001
Error	58	281.304	4.850		

Tukey's grouping [b]	100D	226D	C16	C10	E43	E20	E17	Control
	A		**B**					**C**

[a] CA-coupling agent type, CAconcen-coupling agent concentration.
[b] Coupling agents with the same letter are not significantly different.

polymer matrix (bold scribbles). Dashed curves present free chains of polymers or ungrafted coupling agents. Coupling agents grafted on wood (with solid ends) may be cross-linked with the polymer matrix (with nodes). Coupling agents or polymers may be fixed on wood by mechanical interblocking (with dashed ends). Also, coupling agents may be grafted on polymer molecular chains (with nodes). Free ends of polymers and coupling agents may be linked together through molecular chain entanglement.

Coupling agents with high acid number and low molecular weight easily resulted in a *brush* structure at the interface. E-43, E-17 and E-20 had small molecular weight (less than 10,000) but high acid number (larger than 15). These agents had negative influence on flexural modulus and tensile strength. The molecular chains of these agents were so short that they were not effective for strengthening the interfacial bonding

(Maldas et al. 1990), although these agents easily generated graft polymerization structure at the interface.

Coupling agents (such as 100D and 226D) with high acid number and large molecular weight were preferred to the *switch* structure. For both 100D and 226D, interfacial-bonding strength was greatly improved compared with those without coupling treatment (Figure 6.19). C16 probably helped form the *switch* structure at the interface, although it did not have many maleic anhydride groups on its molecular backbone. Without effective graft polymerization, coupling agents (such as C10) with high molecular weight usually formed the *amorphous* structure at the interface. They helped strengthen the interface through molecular chain entanglement and mechanical interblocking. There were a few chances for them to react with wood fiber and thermoplastics because they had few maleic groups on their molecular chains.

6.4.4.3 Coupling Effectiveness

Unlike the continuous interface of wood veneer-polymer laminate composites (Lu et al. 2002), wood fiber was randomly distributed and separated in a continuous thermoplastic matrix. It was encapsulated or enveloped by the thermoplastic matrix mainly with mechanical connection. Without the coupling treatment, the interfacial region was weakly linked. Under loading, composites were mainly damaged along the loose and weak interfacial connections between wood fiber and thermoplastics (Figure 6.14a) and followed a cohesive mode. For composites with coupling treatment, most wood fibers were combined with thermoplastics through covalent bonding or strong interfacial bonding and the interface was strengthened with coupling agents, thus resulting in a stronger interfacial structure (Figure 6.15b). For this coupling structure,

interfacial fracture usually accompanied with cross-section damage of wood fibers. After tensile failure, the fiber surface in untreated composites was smooth (Figure 6.15a), whereas the fiber in maleated composites had a rough surface and it was embedded in the matrix with chemical link (Figures 6.15b-f). Consequently, this adhesion mode effectively improved mechanical properties of wood fiber-polymer composites (Table 6.7).

Interfacial bonding strength was related to coupling agent concentration. Among the seven coupling agents, coupling agent performance was improved at low concentration. However, coupling effectiveness was poor at high concentration (Figures 6.18 and 19). This was due to the fact that an excess of coupling agents generated many by-products and interfered with coupling reaction, and thus resultes in low bonding strength at the interface (John 1982; Beshay et al. 1985). On the other hand, the existence of excessive coupling agents might enlarge the gap between wood fiber and thermoplastics, thus weakening the interface.

Coupling agent type also influenced interfacial bonding of the resultant composites. Acid number and molecular weight of coupling agent were the most important indexes for coupling agent performance. As shown in Figure 6.21, interfacial-bonding strength followed 3D paraboloid models with concentration, molecular weight, and acid number of coupling agent. In general, interfacial-bonding strength decreased with the increase of coupling agent concentration and acid number but increased with increase of the molecular weight (Figures 6.21a and b).

Acid number and molecular weight had different impacts on coupling agent performance at a given concentration level (Figure 6.22). Acid number had a negative

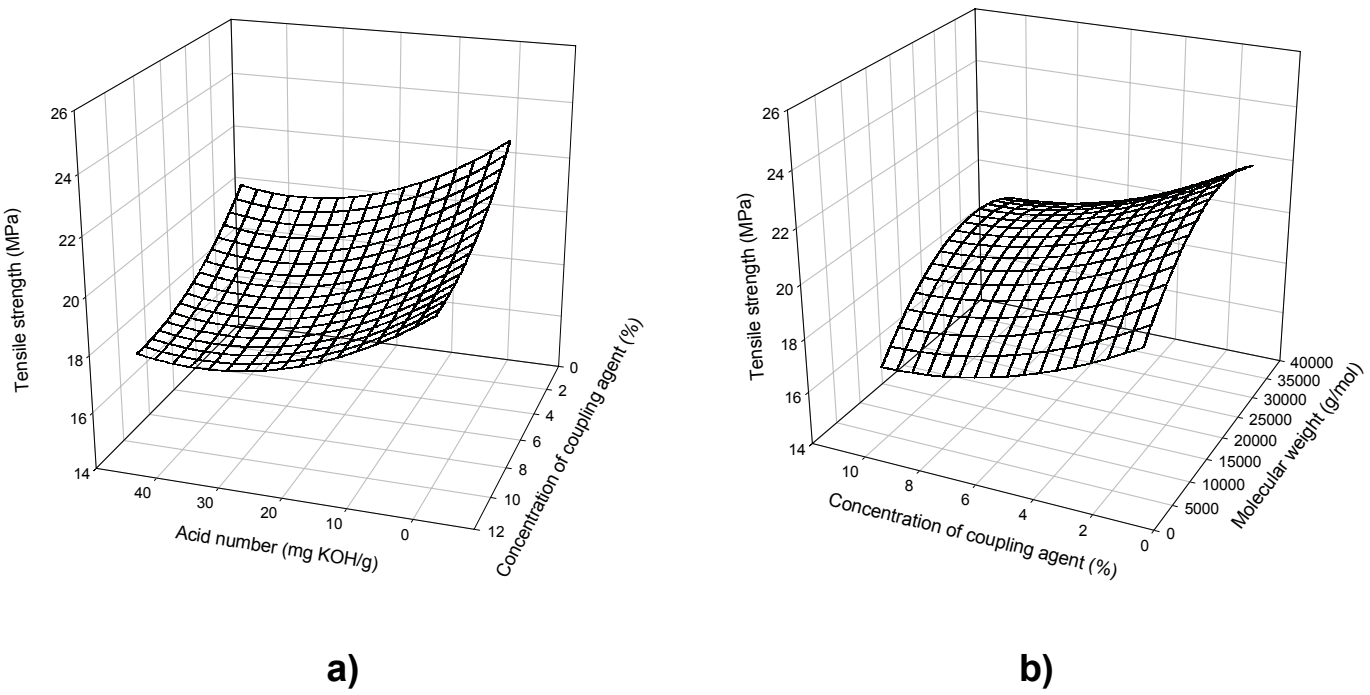

Figure 6.21. Relationship among coupling agent type, coupling agent concentration, and interfacial bonding strength of wood fiber-HDPE composites. a) acid number and b) molecular weight.

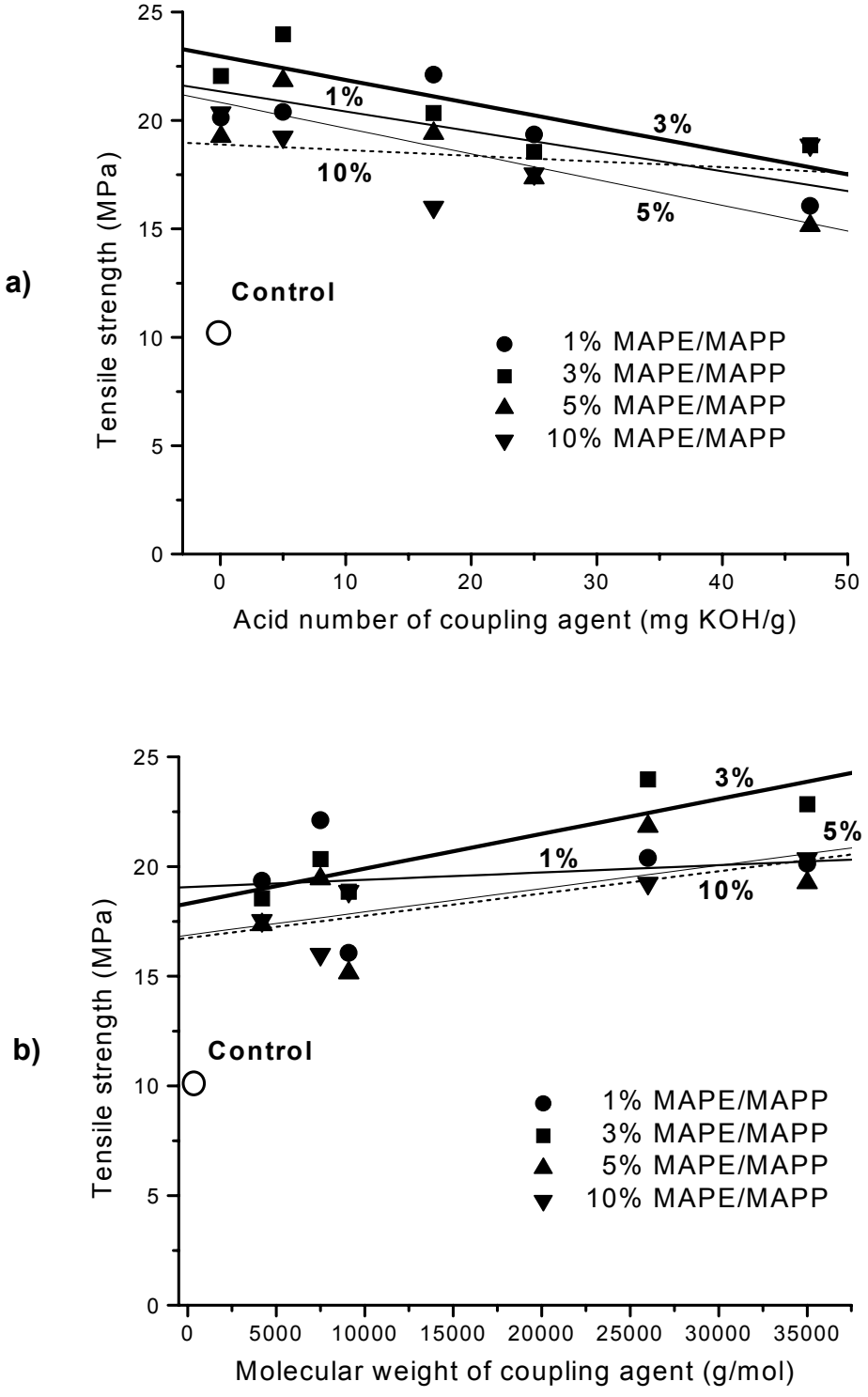

Figure 6.22. Influence of coupling agent on tensile strength of wood fiber-HDPE composites under different concentration levels. a) acid number and b) molecular weight.

impact on interfacial bonding strength (Figure 6.22a). At concentration levels between 1% and 5%, tensile strength dropped quickly at high acid numbers. However, tensile strength was almost independent of acid numbers at high concentration levels (≥10%).

At low concentration level (≤1%), interfacial-bonding strength was not so sensitive to the changes of molecular weight (Figure 6.22b). This indicated that coupling agents with low molecular weight but high acid number competed with coupling agents with high molecular weight but low acid number at low concentration. Interfacial-bonding strength increased with increase of coupling agent molecular weight, at moderate and high concentration levels (≥3%). Therefore, molecular weight had a positive impact on interfacial adhesion.

Backbone structure of coupling agents also affected interfacial bonding strength of the resultant composites. There seemed to be no significant difference between coupling agents with LDPE or with HDPE. For example, the value of coupling performance coefficient [i.e., tensile strength/(acid number × molecular weight)] for E20 was 0.172 MPa/mg KOH·mol and 0.184 MPa/mg KOH·mol for E17. Compared with E-43, E20 had only two thirds of its molecular weight and around one third of its acid number. However, composites with E20 had better interfacial bonding strength than those with E43 at the concentration levels less than 5%. This was due to the fact that E43 had a smaller coupling performance coefficient than E20. Although composites with E43 had higher interfacial-bonding strength than untreated composites and composites with E17, E43 had poorer performance than 100D, 226D, C16, and C10 (Figures 6.18 and 19). This may indicate that coupling agents with HDPE backbone were feasible at the wood fiber-HDPE interface.

Coupling agents with a LLDPE backbone structure were better than those with a HDPE or LDPE backbone structure at low concentration (Table 6.7). Composites with 226D had higher tensile strength than those with 100D at low concentration. LLDPE is composed of copolymers of ethylene with modest amounts of butene, hexene, or octene linear α–olefins (Delassus and Whiteman 2000). As shown in reaction 9 in Figure 6.12, these linear olefin structures were helpful to graft copolymerization through carbon-carbon bonding. Coupling agents with LLDPE backbone also improved interfacial adhesion by molecular chain entanglement.

According to Tukey's studentized range test, composites with seven coupling agents were significantly different from untreated composites (Tables 6.8 and 9). For storage modulus, 100D, C16, and 226D were significantly from other coupling agents. However, E43, E20, E17, and C16 were not significant from control (Table 6.8). For interfacial bonding strength, 100D, 226D, and C16 were the best among these seven coupling agents (Table 6.9). Although it was difficult to separate 226D and 100D from C16 and C10, they were better than coupling agents with small molecular weight (e.g., E17, E20, and E43). Composites with E17 had a different mean response from composites with other coupling agents and the control. However, there was no significant difference between C16, C10, E43, and E20 (Table 6.9). Based on the above statistical analysis, coupling effectiveness for these agents was ranked as follows: 100D>226D> C16>C10>E43>E20>E17.

6.5 CONCLUSIONS

Compounding conditions directly influenced compounding quality of wood fiber and polymer blends and finally affected interfacial bonding and flexural modulus of

resultant composites. At the amount of 50% wood fiber in weight, the optimum compounding parameters at 60 rpm for wood fiber-HDPE blends were with a temperature of 180^{o}C and mixing time of 10 min for the one-step process. The optimum compounding condition at 90 rpm was at a temperature of 165^{o}C and mixing time of 10 min. Therefore, short mixing time, appropriate temperatures, and moderate rotation speed helped improve compounding quality of modified blends and dynamic mechanical properties of resultant composites.

For the one-step process, statistical analysis indicated that the main effects of rotation speed and mixing temperature and the interaction effect between speed and temperature were significant. However, the main effect of compounding time and other interaction effects were not significant. By Duncan's multiple range tests, there was significant difference among the levels of temperature and rotation speed. However, there was no significant difference among the levels of compounding time. The two-step process was better than the one-step process, because coupling agents were more evenly distributed at the interface with the two-step process.

In this study, FTIR and ESCA analyses indicated that esterification was the primary covalent bonding at the interface for maleated copolymers. Eesterification occurred in the range between 1800 and 1650 cm^{-1} at FTIR spectra. It caused a shift at most O 1s and C 1s spectra of composites with coupling agent compared with those of wood, HDPE, and untreated composites. Based on these analyses, chemical coupling mechanisms of MAPEs were proposed. Succinic and half succinic esters were the two primary covalent bonding products to cross-link wood fibers and the polymer matrix at the interface. Although most FTIR and ESCA spectra of MAPE were different from those

of MAPP, composites with MAPE had an interfacial structure similar to those with MAPP. There, MAPEs were also effective at the interface.

Maleated copolymers were randomly distributed at the interface. Observations by SEM indicated that for untreated composites the polymer matrix and wood fibers were mainly linked with mechanical connection, while the network structure at the interface in maleated wood fiber-HDPE composites was the evidence of chemical bridge between wood fibers and polymer through esterification. The interfacial morphology was illustrated with the *pinwheel* models.

For MAPE and MAPP coupling agents, interfacial-bonding strength, flexural modulus, and other mechanical properties of the resultant composites were related to coupling agent type, molecular weight and acid number of coupling agent, and concentration. In general, interfacial-bonding strength of wood fiber-HDPE composites reached maximum value at relatively low concentration of coupling agent, and the strength decreased or leveled off at high concentration. Coupling agent performance in maleated wood fiber-HDPE composites was illustrated with a) *brush* structure, b) *switch* structure, and 3) *amorphous* structure. In this study, the maximum value of interfacial adhesion was achieved at the concentration level of around 3% for most maleated composites.

Acid number and molecular weight of coupling agent were the two most important parameters for interfacial-bonding strength. At low concentration, acid number and molecular weight had a negative effect on interface-bonding strength and flexural modulus. With a modest or large amount of coupling agent (e.g., 3%-5%), interfacial-bonding strength decreased with the increase of acid number but increase of molecular

weight. However, acid number and molecular weight of coupling agent were not independent of each other. Mechanical properties of maleated composites were usually influenced by the interaction effect between these two indexes.

Backbone structure of coupling agents also affected interfacial-bonding strength. At the same acid number and molecular weight, there was no significant difference between MAPEs with LDPE backbone and those with HDPE backbone. However, MAPEs with LLDPE backbone seemed to be better than those with HDPE and LDPE, because the linear α-olefin structure of LLDPE helped improve interfacial adhesion. It was shown that MAPEs were feasible at the interface between wood fiber and HDPE. Based on statistical analysis, maleated copolymers 100D, 226D, and C16 were the best coupling agents for wood fiber-HDPE composites.

6.6 REFERENCES

Anonymous. 2001. Environmental packaging: U. S. guide to green labeling, packaging, and recycling. Thompson Publishing Group, Washington, D. C.

Anonymous. 2002. Facts and figures for the chemical industry. C&EN 80(25): 42-82.

Beshay, A. D., B. V. Kokta, and C. Daneault. 1985. Use of wood fibers in thermoplastic composites II: Polyethylene. Polym. Comp. 6(4): 261-271.

Bikiaris, D., and C. Panayiotou. 1997. LDPE/starch blends compatibilized with PE-g-MA copolymers. J. Appl. Polym. Sci. 70: 1503-1521.

Berlin, A. A., S. A. Volfson, N. S. Enikolopian, and S. S. Negmatov. 1986. Principles of polymer composites. Spring-Verlag, Berlin, Germany. 123 pp.

Chenier, P. J. 1992. Survey of Industrial Chemistry. 2nd edition. Wiley-VCH, Inc., New York.

Chtourou, H., B. Riedl, and A. Ait-Kadi. 1992. Reinforcement of recycled polyolefins with wood fibers. J. Reinf. Plast. Comp. 11: 372-394.

Colthup, N. B. 1950. Spectra-structure correlation in the infra-red region. J. Opt. Soc. Am. 40: 397-400.

Coutinho, F. M. B., T. H. S. Costa, and D. L. Carvalho. 1997. Polypropylene-wood fiber composites: Effect of treatment and mixing conditions on mechanical properties. J. Appl. Polym. Sci. 65: 1227-1235.

Delassus, P. T., and N. F. Whiteman. 1999. Physical and mechanical properties of some important polymers. Pages V159-V169 *in* J. Brandrup, E. H. Immergut, E. A. Grulke, A. Abe, and D. R. Bloch, eds. Polymer handbook. John Wiley & Sons, New York.

Filex, J. M., and P. Gatenholm. 1991. The nature of adhesion in composites of modified cellulose fibers and polypropylene. J. Appl. Polym. Sci. 42: 609-620.

Freischmidt, G., and A. J. Michell. 1991. Performance of zircoaluminate coupling agents in wood flour/fibre-polyolefin composites. Polym. Inter. 24: 241-247.

Gatenholm, P., and J. M. Felix. 1993. Interphase design in cellulose fiber/polypropylene composites. Pages 237-244 *in* T. C. Chung, ed. New advances in polyolefins. Plenum Press, New York, NY.

Gaylord, N. G. 1972. US Patent 3,645,939.

Gaylord, N. G., R. Metha, V. Kumar, and M. Tazi. 1989. High density polyethylene-g-maleic anhydride preparation in presence of electron donors. J. Appl. Polym. Sci. 38: 359-371.

Gaylord, N. G., R. Metha, D. R. Mohan, and V. Kumar. 1992. Maleation of linear low-density polyethylene by reactive processing. J. Appl. Polym. Sci. 44: 1941-1949.

George, J., S. S. Bhagawan, and S. Thomas. 1998. Improved interactions in chemically modified pineapple leaf fiber reinforced polyethylene composites. Comp. Interfaces, 5(3): 201-223.

Gonzalez, C., C. M. Clemons, G. E. Myers, and T. M. Harten. 1992. Effects of several ingredient variables on mechanical properties of wood fiber-polyolefin composites blended in a thermokinetic mixer. Pages 127-136 *in* R. M. Rowell, T. L. Laufenberg, and J. K. Rowell, eds. Materials interactions relevant to recycling of wood-based materials, vol. 266, Materials Research Society, Pittsburgh, PA.

Ha, C. -S, H. –D. Park, and W. -J. Cho. 1999. Recycling of commingled plastics by cellulosic reinforcement. J. Appl. Polym. Sci. 74: 1531-1538.

Hwang, G.-S. 1997. Manufacturing of plastic/wood composite boards with waste polyethylene and wood particles. Taiwan J. For. Sci. 12(4): 443-450.

John, W. E. 1982. Isocyanate as wood binders: A review. J. Adhes. 15: 59-67.

Joseph, K., S. Thomas, and C. Pavithran. 1996. Effect of chemical treatment on the tensile properties of short sisal fibre-reinforced polyethylene composites. Polymer 37 (23): 5139-5149.

Kazayawoko, M., J. J. Balatinecz, and R. T. Woodhams. 1997. Effect of ester linkage on the mechanical properties of wood fiber-polypropylene composites. J. Reinf. Plast. Comp. 16(15): 1383-1406.

Kazyawoko, M., J. J. Balatinecz, and R. N. S. Sodhi. 1999. X-ray photoelectro spectroscopy of maleatd polypropylene treated wood fibers in a high-intensity thermokinetic mixer. Wood Sci. Technol. 33: 359-372.

Kishi, H., M. Yoshioka, A. Yamanoi, and N. Shiraishi. 1988. Composites of wood and polypropylenes I. Mokuzai Gakkaishi 34(2): 133-139.

Kokta, B. V., and C. Daneault. 1986. Use of grafted aspen fibers in thermoplastic composites: IV. Effect of extreme conditions on mechanical properties of polyethylene composites. Polym. Eng. Sci. 7(5): 337-348.

Kokta, B. V., D. Maldas, C. Daneault, and P. Beland. 1990. Composites of polyvinyl chloride-wood fibers. I. Effect of isocyanate as a bonding agent. Polym. –Plast. Technol. Eng. 29(1&2): 87-118.

Krzysik, A. M., and J. A. Younquist. 1991. Bonding of air-formed wood fiber/polypropylene composites. Int. J. Adhes. Adhesives 11(4): 235-240.

Liao, B. Y. Huang, G. Cong. 1997. Influence of modified wood fibers on the mechanical properties of wood fiber-reinforced polyethylene. J. Appl. Polym. Sci. 66: 1561-1568.

Lu, J. Z., Q. Wu, and H. S. McNabb. 2000. Chemical coupling in wood fiber and polymer composites: A review of coupling agents and treatments. Wood Fiber Sci. 32(1): 88-104.

Lu, J. Z., Q., Wu, and I. I. Negulescu. 2002. The influence of maleation on polymer adsorption and fixation, wood surface wettability, and interfacial bonding strength in wood-PVC composites. Wood Fiber Sci. 34 (3): 434-459.

Maldas, D., and B. V. Kokta. 1990. Influence of polar monomers on the performance of wood fiber reinforced polystyrene composites. I. Evaluation of critical conditions. Int. J. Polym. Mater. 14(3-4): 165-189.

Maldas, D., B. V. Kokta, and C. Daneault. 1989. Influence of coupling agents and treatments on the mechanical properties of cellulose fiber-polystyrene composites. J. Appl. Polym. Sci. 37: 751-775.

Matuana, L. M., J. J. Balatinecz, R. N. S. Sodhi, and C. B. Park. 2001. Surface characterization of esterified cellulosic fibers by XPS and FTIR spectroscopy. Wood Sci. Technol. 35: 191-201.

Matthews, G. 1982. Polymer Mixing Technology. Applied Science Publishers, New York, NY.

Myers, G. E., I. S. Chahyadi, and C. A., Coberly. 1993. Wood flour and polypropylene or high-density polyethylene composites: Influence of maleated polypropylene concentration and extrusion temperature on properties. Pages 49-56 *in* M. P. Wolcott ed. Wood fiber/polymer composites: Fundamental concepts, process, and materials options. Proc. 1st Wood Fiber-Plastic Composites Conference, Madison, WI.

Negulescu, I. I., S. Despa, J. Chen, and B. J. Collier. 2000. Characterizing polyester fabrics treated in electrical discharges of radio-frequency plasma. Textile Res. J. 70(1): 1-7.

Oksman, K., and H. Lindberg. 1998. The influence of a SBS compatiblizer in polyethylene-wood flour composites. J. Appl. Polym. Sci. 68: 1845-1855.

Raj, R. G., and B. V. Kokta. 1991. Improving the mechanical properties of HDPE-wood fiber composites with additives/coupling agents. Pages 1883-1885 *in* ANTEC, Proc. of 49th Annual Technical Conference, Montreal, Canada, May 5-9, 1991. Society of Plastics Engineers, Brookfield, CT. 1883-1885 pp.

Raj, R. G., B. V. Kokta, D. Maldas, and C. Daneault. 1988. Use of wood fibers in thermoplastic composites: VI. Isocyanate as a bonding agent for polyethylene-wood fiber composites. Polym. Comp. 9(6): 404-411.

Raj, R. G., B. V. Kokta, D. Maldas, and C. Daneault. 1989. Use of wood fibers in thermoplastics. VII. The effect of coupling agents in polyethylene-wood fiber composites. J. Appl. Polym. Sci. 37: 1089-1103.

Raj, R. G., B. V. Kokta, G. Grouleau, and C. Daneault. 1990. The influence of coupling agents on mechanical properties of composites containing cellulosic fillers. Polym.-Plast. Technol. Eng. 29(4): 339-353.

Razi, P. S., R. Portier, and A. Raman. 1999. Studies on polymer-wood interface bonding: Effect of coupling agents and surface modification. J. Comp. Mater. 33(12): 1064-1079.

Rozman, H. D., G. B. Peng, and Z. A. M. Ishak. 1998a. The effect of compounding techniques on the mechanical properties of oil palm empty fruit bunch-polypropylene composites. J. Appl. Polym. Sci. 70: 2647-2655.

Rozman, H. D., G. B. Peng, and Z. A. M. Ishak. 1998b. The effect of compounding techniques on the mechanical properties of oil palm empty fruit bunch-polypropylene composites. J. Appl. Polym. Sci. 70: 2647-2655.

Sailaja, R. R. N., and M. Chanda. 2001. Use of maleic anhydride-grafted polyethylene as compatibilizer for HDPE-tapioca starch blends: Effects on mechanical properties. J. Appl. Polym. Sci. 80(6): 863-872.

Sanadi, A. R., R. M. Rowell, and R. A. Young. 1992. Estimation of fiber-matrix interfacial shear strengths in lignocellulosic-thermoplastic composites. Pages 81-92 *in* R. M. Rowell, T. L. Laufenberg, and J. K. Rowell, eds. Materials interactions relevant to recycling of wood-based materials, Vol. 266. Materials Research Society, Pittsburgh, PA.

Schneider, J. P., G. E. Myers, C. M. Clemons, and B. W. English. 1995. Biofibres as reinforcing fillers in thermoplastic composites. Eng. Plast. 8(3): 207-222.

Simonsen, J., and T. Rials. 1992. Enhancing the interfacial bond strength of lignocellulosic fiber dispersed in synthetic polymer matrices. Pages 105-111 *in* R. M. Rowell, T. L. Laufenberg, and J. K. Rowell, eds. Materials interactions relevant to recycling of wood-based materials, vol. 266. Materials Research Society, Pittsburgh, PA.

Simonsen, J., R. Jacobson, and R. Rowell. 1998. Properties of styrene-maleic anhydride copolymers containing wood-based fillers. For. Prod. J. 48(1): 89-92.

Smith, A. L. 1991. Infrared spectroscopy. *in* J. W. Robinson ed. Practical handbook of spectroscopy. CRC Press, Boca Raton, FL.

Smith, B. C. 1996. Fundament of Fourier transform infrared spectroscopy. CRC press, New York, NY.

Snijder, M. H. B., E. Wissing, and J. F. Modder. 1997. Polyolefins and engineering plastics renforced with annual plant fibers. Pages 181-191 *in* Proc. of 4th Internaltional Conference on Woodfiber-Plastic Composites, Forest Products Society, Madison, WI.

Snijder, M. H. B., and H. L. Bos. 2000. Reinforcement of polypropylene by annual plant fibers: Optimisation of the coupling agent efficiency. Comp. Interfaces 7(2): 69-72.

Štepek, J., and H. Daoust .1983. Additives for Plastics. Polymer/properties and Applications 5. Springer-Verlag, New York, NY.

Takase, S., and N. Shiraishi. 1989. Studies on composites from wood and polypropylene. Part I. J. Appl. Polym. Sci. 37: 645-659.

Woodhams, R. T., G. Thomas, and D. K. Rodgers. 1984. Wood fibers as reinforcing fillers for polyolefins. Polym. Eng. Sci. 24(15): 1166-1171.

Xanthos, M. 1983. Processing conditions and coupling effects in polypropylene/wood flour composites. Plast. Rubber Process. Appl. 3(3): 223-228.

Yam, K. L., B. K. Gogoi, C. C. Lai, and S. E. Selke. 1990. Composites from compounding wood fibers with recycled high density polyethylene. Polym. Eng. Sci. 30(11): 693-699.

Zadorecki, P., and P. Flodin. 1985. Surface modification of cellulose fibers. II. The effect of cellulose fiber treatment on the performance of cellulose-polyester composites. J. Appl. Polym. Sci. 30: 3971-3983.

CHAPTER 7. CONCLUSIONS AND RECOMMENDATIONS

Coupling agents play an important role in improving interfacial affinity and adhesion between polar wood fiber and non-polar polymer matrixes. Over forty coupling agents have been extensively used in research and production. Among them, the most popular are isocyanates, anhydrides, silanes, and anhydride-modified polymers, such as PMPPIC and MAPP.

At the interface, primary bonding forces include covalent bonding, secondary bonding (such as van der Waals's forces and hydrogen bonding), macromolecular chain entanglement, and mechanical interblocking. Covalent bonding between coupling agent and the polymer matrix is mainly carbon-carbon bonding (such as MA and dichlorotriazines). Main forms of covalent bonding between wood and coupling agent are carbamation (such as PMPPIC), esterification (such as MA, MAPP, and MAPE), and etherification (such as silanes and dichlorotriazines). Sometimes, wood fiber and the polymer matrix may be strongly connected with crosslinking structure. However, graft polymerization at the interfaced is usually limited. Ungrafted coupling agents may strengthen the interface through secondary bonding and macromolecular chain entanglement. Some free ends of the matrix may penetrate into cracks on wood surface and gaps or cell lumens in wood, resulting in an interblocking (or glue nail) structure. Therefore, the interface is strengthened with these mechanisms (Table 7.1).

Chemical coupling in wood-polymer composites follows the interfacial similarity rule. Coupling agents either crosslink part of the polymer matrix to the wood surface to form a non-polar copolymer, or modify polarity of the polymer matrix by grafting it with

Table 7.1. Coupling mechanisms in wood-polymer composites.

Coupling type	Structure at the interface			
Covalent bonding (>50 Kcal/mol)	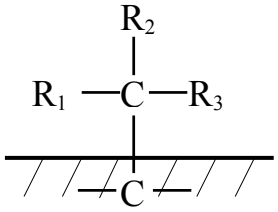	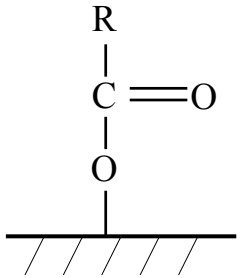	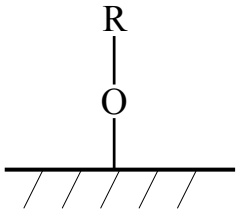	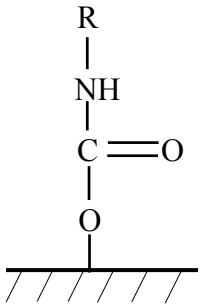
	Carbon-carbon bonding	**Esterification**	**Etherfication**	**Carbamation**
Secondary bonding (<10 Kcal/mol)	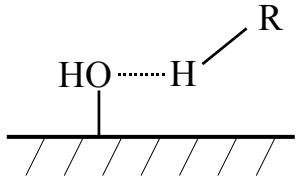	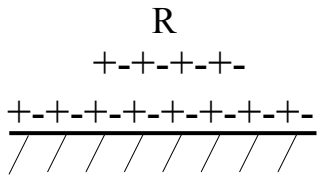		
	Hydrogen bonding (~5 Kcal/mol)	**van der Waals forces (<4 Kcal/mol)**		
Mechanical adhesion	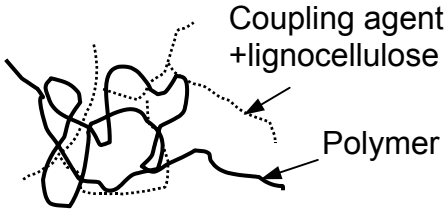	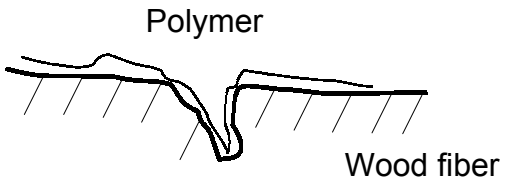		
	Molecular chain entanglement	**Mechanical interlocking**		

polar monomers to form a graft copolymer. As one of the most effective methods, wood fiber is usually grafted with coupling agents with a backbone structure identical or similar to the polymer matrix. Then, the other end of coupling agent is connected with the matrix through van der Waals's forces or macromolecular chain entanglement. Thus, coupling agent performance is effectively improved.

7.1 CONCLUSIONS

According to the studies on maleation in wood-polymer composites, conclusions are made as follows:

1. In general, graft copolymerization by maleation is limited. At low concentration, graft efficiency is as high as 90%, while graft efficiency is as low as 30% at high concentration. For maleated wood veneer, the relationship among graft rate, concentration, and retention of coupling agent follows three-dimensional *parabloid* models.
2. Wettability of maleated wood surface is significantly influenced by acid number, amount of free or ungrafted maleic anhydride, and concentration of coupling agent. Wood veneer treated with E43 and PEMA has a more polar surface than wood and it acts like wood, whereas G-3015-treated wood specimens are hydrophobic and act more like thermoplastics.
3. Dynamic contact angle and height of a droplet on maleated wood follows the natural decay process, while the spreading process of the droplet fits the *Boltzmann* sigmoid model. Therefore, dynamic wetting process can be illustrated with time-dependent changes of spreading ratio and decay ratio. Wetting slopes of contact angle, decay ratio, and spreading ratio on G-3015-

treated specimens follow the first order law, while those of E43- and PEMA-treated veneer vary with coupling agent type and retention.

4. Maleation affects thermal behavior of maleated wood and resultant wood-polymer composites. Compared with untreated composites, maleated wood-PVC composites have a remarkable shift in most TGA, DSC, and DMA spectra. Maleated wood-polymer composites have larger TG% but smaller DTG% than wood, PVC and untreated composites. MAPP presented its characterization at bands around 50^{o}C, 150^{o}C, and 320^{o}C, respectively.
5. For melt-blending process, compounding conditions have significant effects on compounding quality of wood-polymer blends and mechanical properties of resultant composites. The best interfacial bonding strength is achieved at short compounding time, appropriate mixing temperatures, and moderate rotation speed. For wood fiber-HDPE composites, optimal compounding parameters are suggested as a condition with a temperature of 180^{o}C (or 165^{o}C) and a rotation speed of 90 rpm (or 60 rpm) for a compounding period of 10 min.
6. Based on fractural surface analysis by SEM, coupling agents are randomly distributed at the interface. Observation by SEM indicated that the polymer matrix and wood fibers are mainly linked with mechanical connections, while the network structure at the interface in maleated wood fiber-HDPE composites presents the evidence of chemical bridge between wood fibers and polymer through a maleated copolymer. The interfacial morphology is illustrated with the *pinwheel* models.

7. Esterification is the effective covalent bonding at the wood-coupling agent interphase in wood fiber-polymer composites, while carbon-carbon bonding takes place at the interface between coupling agent and the polymer matrix. Sometimes, wood and the matrix may be cross-linked with maleated copolymers. There are also secondary bonding such as hydrogen bonding and van der Waals forces at the interface. In addition, mechanical connections between wood fiber and the polymer matrix such as mechanical interblocking and molecular chain entanglement make contributions to interfacial adhesion.
8. For wood-plastic laminates, interfacial adhesion followed the *monolayer* models. For melt-blended composites, coupling mechanisms can be explained with 1) *brush*, 2) *switch*, and 3) *amorphous* structures. Therefore, the interface is strengthened with covalent bonding, secondary bonding, polymer chain entanglement, and mechanical interblocking. Based on FTIR and ESCA analyses, chemical mechanisms for wood fiber-HDPE composites are proposed in this study.
9. Coupling agent performance is mainly influenced by acid number, molecular weight, backbone structure, and concentration of maleated copolymer. In general, coupling agents with large molecular weight, moderate acid number, and appropriate concentration are preferred to have better performance at the interface. For wood fiber-polymer composites, the best interfacial bonding strength is achieved at the concentration level of 3% for most maleated polyolefin coupling agents.

10. Based on the experimental results, 226D, 100D, and C16 are the best coupling agents among the maleated copolymers used in this study. Compared with composites without maleation, maleated composites increase interfacial bonding strength by 140% and flexural modulus, by 29% at the concentration level of 3%.

7.2 RECOMMENDATIONS FOR FUTURE WORK

Based on limitations in this study, future work is suggested as follows:

1) For compounding process, traditional research methods are not satisfactory to determine compounding conditions. Advanced statistical techniques (such as response surface and mixture experiment) are required to investigate optimum ingredient weight ratios, and correlation among these parameters, as well as influence of compounding conditions (mixing temperature, compounding time, and rotation speed) on these parameters.

2) Although it is assumed that coupling agents are randomly distributed at the interface, actual location and distribution of coupling agents at the interface are not completely understood. Therefore, it is necessary to apply advanced techniques for coupling agent distribution in the future.

3) So far, there has not been a feasible and reliable method to evaluate and compare coupling effectiveness of different coupling agents. Therefore, it is necessary to develop a new evaluation system for coupling effectiveness in wood-polymer composites.

4) Due to the blocking effect of the polymer matrix, it is difficult to analyze interfacial characterization of wood-polymer composites. In the future, it is useful to

introduce some advance surface analytical techniques (such as micro thermal analysis) to reveal interfacial characterization and chemical coupling mechanisms.

5) For most coupling agents currently used, there are still many ungrafted coupling agent molecules at the interface in resultant composites. These free and polar molecules may weaken interfacial bonding strength. Accordingly, it is helpful to remove these by-products. It is necessary to develop new coupling agents and treatments to more effectively improve interfacial adhesion.

6) Wood-polymer composites with multifunctions are required to meet customer's requirements on interfacial bonding strength, impact strength, fire and decay resistance, dimensional stability, and durability and degradability under natural environment. More fundamental work in this aspect will be required in the future.

APPENDIX. LETTERS OF PERMISSION

LSU AgCenter
Research & Extension

SCHOOL OF RENEWABLE NATURAL RESOURCES
Louisiana Forest Products Development Center
227 Renewable Natural Resources Building - LSU
Baton Rouge, Louisiana 70803-6202
(225)578-4255
Fax: (225)578-4251
Web site: www.lsuagcenter.com

Research and Extension Programs
Agriculture
Economic/Community Development
Environment/Natural Resources
Families/Nutrition/Health
4-H Youth Programs

Date: September 26, 2003

Dr. Gaza Ifju

Editor of Wood and Fiber Science
Department of Wood Science and Forest Products
Brooks Forest Products Center
Virginia Tech
Blacksburg, VA 24061-0503

Dear Dr. Ifju:

I am writing to obtain the permission for the use of two articles published in Wood Fiber and Science. I am a doctoral candidate in the School of Renewable Natural Resources at Louisiana State University. I am the first author and would include these articles in my dissertation. These articles are:

1). Chemical coupling in wood fiber and polymer composites: A review of coupling agents and treatments. J. Z. Lu, Q. Wu, and H. S. McNabb, Jr. Vol. 32, No. 1, 2000, pp. 88-104, and

2). The influence of maleation on polymer adsorption and fixation, wood surface wettability, and interfacial bonding strength in wood-PVC composites. J. Z. Lu, Q. Wu, and I. I. Negulescu. Vol. 34, No. 3, 2002, pp.434-459.

Thank you for your consideration of my request.

Sincerely yours,

Ziqiang Lu

School of Renewable Natural Resources
Louisiana State University Agricultural Center
Baton Rouge, LA 70803
Tel.: (225)578-4358; Fax: (225)578-4251
Email: zlu1@lsu.edu

Wood and Fiber Science
Wood Science & Forest Products, Virginia Tech (Mail Code 0503),
Brooks Forest Products Center, Blacksburg, VA 24061
Telephone: 540/231-8215; Fax: 540/231-8868; E-mail: ifju@vt.edu

October 27, 2003

Ziqiang Lu
Graduate student
227 School of Renewable Natural Resources
Louisiana State University
Baton Rouge, LA 70803

Dear Mr. Lu:

In response to your request we hereby grant permission to reprint the following articles at no charge in your dissertation:

J.Z. Lu, Q. Wu, and H.S. McNabb, jr., 2000. Chemical coupling in wood fiber and polymer composites: A review of coupling agents and Treatments. Wood and Fiber Science, 32(1): 88-104.

J.Z. Lu, Q. Wu, and I.I. Negulescu, 2002. The influence of maleation on polymer adsorption and fixation, wood surface wettability and interfacial bonding strength in wood-PVC composites. Wood and Fiber Science, 34(3):434-459.

This permission is subject to the following conditions:

1. Reproduction of these articles is confined to the purpose for which permission hereby granted.
2. Suitable acknowledgement to the source must be made in a reference list at the end of your dissertation with a note: "Reprinted with the permission of Wood and Fiber Science".
3. This permission includes for LSU to supply single copies, on demand, of the complete dissertation.
4. In case the above articles are planned to be reprinted in languages other than English, please reapply separately for each one. Permission excludes use in electronic form. The electronic forms of the above articles will be posted in the future exclusively on the website of the Society of Wood Science and Technology.

Sincerely,

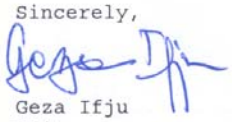

Geza Ifju
Editor

VITA

John Ziqiang Lu was born in Guangdong, China. In 1983, he graduated with a bachelor science degree in engineering from Nanjing Forestry University, Nanjing, China. After graduation, he worked as an assistant engineer at Hengyang Wood Composites Company in China from 1983 to 1988. He was promoted to an engineer in 1988. He came back to the Nanjing Forestry University in August 1988 and received his master's degree in engineering in 1991. From 1991 to 1994, he worked as an instructor and then as an assistant professor at the Nanjing Forestry University.

He came to the United States to pursue advanced degrees in 1994. He received his second master's degree from Iowa State University in 1997. He was honored as a member of *Xi Sigma Pi* (Forestry Honor Society) and *Gamma Sigma Delta* (The Honor Society of Agriculture) in 1996 and 1997, respectively.

He transferred to Louisiana State University for his doctoral program in wood-polymer composites in 1998. Since then, he has been a doctoral candidate in the School of Renewable Natural Resources. Currently, he is an active member of American Chemical Society, Society of Plastic Engineers, Forest Products Society, and Society of Wood Science and Technology. He will receive his doctoral degree in forestry in December 2003.